



PEOPLE'S DEMOCRATIC REPUBLIC OF ALGERIA
MINISTRY OF HIGHER EDUCATION AND SCIENTIFIC RESEARCH
IBN KHALDOUN UNIVERSITY OF TIARET
FACULTY OF APPLIED SCIENCES



THESIS

Presented by:

Miss. BOUZEKRI AMINA

Thesis Submitted in Fulfillment of the Requirements for:
Degree of DOCTORAT (L.M.D) in Renewable Energies

THEME

*Hybrid algorithms for the intelligent management of a
renewable production system: Power Quality
Enhancement and service continuity contribution*

Presented on July 2018

Under Board of Examiners composed of:

President	Prof. Cheikh BELFEDAL	University Ibn Khaldoun, Tiaret
Examiner	Prof. Youcef Meslem	University Ibn Khaldoun, Tiaret
Examiner	Prof. Said Hassaine	University Ibn Khaldoun, Tiaret
Examiner	Prof. Mohamed Tadjine	National Polytechnic School, Alger
Supervision	Prof. Tayeb Allaoui	University Ibn Khaldoun, Tiaret



PEOPLE'S DEMOCRATIC REPUBLIC OF ALGERIA
MINISTRY OF HIGHER EDUCATION AND SCIENTIFIC RESEARCH
IBN KHALDOUN UNIVERSITY OF TIARET
FACULTY OF APPLIED SCIENCES
ELECTRICAL ENGINEERING DEPARTMENT



THESIS

Presented by:

Miss. BOUZEKRI AMINA

Thesis Submitted in Fulfillment of the Requirements for:

Degree of DOCTORAT (L.M.D) in Renewable Energies

THEME

*Hybrid algorithms for the intelligent management of a
renewable production system: Power Quality
Enhancement and service continuity contribution*

Presented on July 2018

Under Board of Examiners composed of:

President	Prof. Cheikh Belfdal	University Ibn Khaldoun, Tiaret
Examiner	Prof. Youcef Meslem	University Ibn Khaldoun, Tiaret
Examiner	Prof. Said Hassaine	University Ibn Khaldoun, Tiaret
Examiner	Prof. Mohamed Tadjine	National Polytechnic School, Alger
Supervision	Prof. Tayeb Allaoui	University Ibn Khaldoun, Tiaret

قال الله تعالى:

بِسْمِ اللَّهِ الرَّحْمَنِ الرَّحِيمِ

" اقرأ باسم ربك الذي خلق (1) خلق الإنسان من علقه (2)
اقرأ وربك الأكرم (3) الذي علم بالقلم (4) علم الإنسان ما
لم يعلم (5) "

سورة العلق

قال الله تعالى:

بِسْمِ اللَّهِ الرَّحْمَنِ الرَّحِيمِ

" اقرأ باسم ربك الذي خلق (1) خلق الإنسان من علقه (2)
اقرأ وربك الأكرم (3) الذي علم بالقلم (4) علم الإنسان ما
لم يعلم (5) "

سورة العلق

Acknowledgements

First of all, all praise and thanks are due to the Almighty Allah who always guides me to the right path and has helped me to complete this thesis.

There are many people whom I have to acknowledge for their support, help and encouragement during the journey of preparing this thesis. So, I will attempt to give them their due here, and I sincerely apologize for any omissions.

I am indeed grateful to my supervisor, Prof. Allaoui Tayeb, whose encouragement, guidance, and support helped me throughout my course of study in Laboratory of Electrical and Computer Engineering (L2GEGI).

I am also grateful to Messrs. Denai Mouloud and Mihoub Youcef for their comments, insights, and advice in publishing articles during my research.

I am equally grateful to the Board of Examiners; Prof. Cheikh Beldhal as a president and the examiners: Prof. Said Hassaine, Prof. Youcef Meslem, and Prof. Mohamed Tadjine

I am thankful to my entire family members for their motivation and support especially my mother.

My special thanks also go to all the teachers of the Department of Electrical engineering particularly those who taught us during my studying.

Lastly; I am thankful also my friends: Aggad Fatima Samia, Tamer Amina, Abid Mimouna, Sihem and master graduation friends for their support and understanding throughout my studying.

DEDICATION

*I dedicate this work to my family especially my parents, brothers and
sisters*

شهد العالم خلال السنوات القليلة الماضية تطورا سريعا في استخدام الطاقة المتجددة في استهلاك الكهرباء. فقد بلغ إجمالي إنتاج لطاقة الرياح عام 2015 إلى 432,83 ميغاواط بارتفاع نسبته % 17 مقارنة بالعام الذي قبله. ومن جهة أخرى، فإن تغير طبيعة الأحمال بالمنشآت الصناعية والتجارية والسكنية التي تعتمد خصوصا على الكترونييات القوى، أدى إلى تدهور جودة التغذية التي أصبحت تعاني من عدة مشاكل والتي تعتبر ذات أهمية خاصة لكلا من مرفق الكهرباء والمستهلكين. من أجل هذا السياق، تم تقديم هذه الأطروحة تحت عنوان: إستراتيجية الخوارزميات الذكاء الاصطناعي الهجينة للتحكم في نظام إنتاج الطاقة المتجددة لغرض تحسين جودة التغذية وتحقيق استمرارية إنتاجها.

ولههدف تحقيق ذلك، يتناول هذا العمل بداية بتقديم إستراتيجية تحكم لنظام إنتاج الطاقة الكهربائية من خلال طاقة الرياح والتي تعتمد على مولد ثنائي التغذية ذات نظام تحكم متغير، الذي يسمح بالاتصال بشبكة الكهرباء من جهتي: باتصال مباشر عبر ثابت المولد واتصال غير مباشر بالعضو الدوار عبر محول قدرة رجعي. تسمح هذه التركيبة بالتحكم في الطاقة المنتجة للشبكة من خلال ثلاث وحدات للتحكم وهي كالأتي: وحدة التحكم للمحول الجانبي للدوار والذي يسمح بالتحكم في الطاقة الفعالة والغير فعالة المنتجة من طرف العضو الثابت للمولد، وحدة التحكم للمحور الجانبي للشبكة والذي يسمح بالتحكم بالتوتر المستمر المتمركز بين المحولين (AC/DC/AC) ووحدة التحكم MPPT والتي تسمح باستخلاص التوربينات أقصى طاقة حركية ممكنة من الرياح. تضمن هذه الوحدات للتحكم في إنتاج طاقة كهربائية جيبية شبه مثالية للشبكة، إلا أن هذه الطاقة تتعرض للكثير من الاضطرابات بسبب تزايد المعدات والأجهزة ذات الخصائص الغير خطية والتي تتغذى من شبكة التوزيع كهربائية معقدة. تتمثل هذه الاضطرابات في تشوه موجتي الجهد والتيار، تقلب وارتعاش الجهد، انخفاض وارتفاع الجهد، عدم اتزان الجهد والتيار، تقلب التواتر والتوافقيات... الخ. قد تؤدي هذه الاضطرابات إلى اختلال عمليات تشغيل المعدات أو انهيار بعض المعدات. وقد تم معالجة نوعين من هذه الاضطرابات في هذه الأطروحة أولهما: التوافقيات واختلال أو انقطاع الجهد نتيجة عطل في احد المحولات وذلك باستعمال استراتيجيات الذكاء الاصطناعي.

لحذف أو التخفيض من التوافقيات والتشويش تستخدم عدة حلول منها المرشحات الفعالة، كالمرشح الفعال المتوازي والذي يعمل على فكرة مراقبة الإشارة الكهربائية المشوهة بالتوافقيات ويحدد تردد وقيمة هذه التوافقيات ثم حذفها عن طريق حقن ديناميكي لتيار معاكس لها. ولتحقيق ذلك بدون تكلفة زائدة للنظام، يقترح هذا العمل إستراتيجية تحت اسم نظام الأولية، والتي تسمح بتسيير الأولية بين التحكم في الطاقة الفعالة وغير فعالة المنتجة وتخفيض التوافقيات. تبين نتائج المحاكاة في بيئة ماتلاب على فاعلية هذه الإستراتيجية والتي سمحت بانخفاض التوافقيات في الشبكة من % 16 إلى % 1,98، والتي تعبر في الحدود العالمية المسموح بها.

ولههدف ضمان استمرارية إنتاج الطاقة في حالة تعطل أحد الترونزستورات الثنائية أحادية القطبية للمحول الجانبي للعضو الدوار، تم تطبيق إستراتيجية تعتمد على الذكاء الاصطناعي الهجين لمجالين منه إلا وهما: النظام الخبير والضباب المنطقي. تعمل هذه الإستراتيجية على تشخيص وتحديد العطل للترونزستور ثم عزله على النظام واستبداله بأخر سليم من أجل ضمان استمرارية الانتاج دون انقطاع. وبينت نتائج المحاكاة في بيئة ماتلاب كذلك فاعلية وسرعة هذه الاستراتيجية في تشخيص وعزل واستبدال الترونزستور المعطوب في زمن أقل من دور واحد.

Abstract

Over the recent years, the world has witnessed a rapid development in the use of renewable energy in electricity consumption. Where, in 2015 the Total wind power production was reached to 432.83 MW, i.e. an increase of 17% from the previous year. In other side, the changing in the nature of loads in industrial, commercial and residential establishments connecting to the grid, led the disturbances in quality of energy which must be as a pure sinusoidal waveform with specific phases and frequency.

This thesis investigates and proposes new solutions to enhance the power quality and reliability of electricity supply of wind turbine energy based on Doubly Fed Induction Generator (DFIG) system using hybrid artificial intelligence algorithms. The control scheme of the overall system consists of three controls blocks namely the Rotor Side Converter (RSC), Grid Side Converter (GSC) and the Maximum Power Point Tacking (MPPT) control which permits energy exchange between the wind energy conversion system and the grid. The problems of power quality including harmonic distortion are discussed in details and mitigation techniques based on shunt active power filtering are presented. An efficient and economical solution based on the concept of priority control is proposed. This priority control method permits to manage the priority among the previous system production controls and the harmonics currents suppression using Synchronous Reference Frame (SRF) harmonic extraction current method. In addition, and to ensure service continuity, a hybrid-intelligent Fault Tolerant Control (FTC) strategy of IGBT open-circuit for Rotor Side Converter (RSC) has been presented. The FTC strategy is based on Expert Systems and combines a simple fault detection method based on fuzzy logic inference and uses rotor current average values to detect the faulty switch in a very short period. Furthermore, to improve the performance of the closed-loop system during transients and faulty conditions, different currents controllers like conventional PI, hysteresis, PI fuzzy-adaptive controllers and PI controller optimized using Genetic Algorithms have been used.

The simulation model was developed in Matlab/Simulink environment and the results demonstrate that the proposed techniques can effectively reduce the Total Harmonic Distortion (THD) in the grid currents and maintain the quality of energy within the international standards and ensure service continuity of the system during open switch IGBT fault.

Résumé

Au cours des dernières années, le monde a connu un développement rapide dans l'utilisation des énergies renouvelables pour la production d'électricité. En 2015, la capacité éolienne totale a atteint 432,83 MW, avec une augmentation de 17% par rapport à l'année précédente. Les charges des clients y compris industrielles, commerciales et résidentielles raccordées au réseau de distribution sont la principale source de perturbations affectant la qualité de l'énergie qui doit être une forme d'onde sinusoïdale pure d'amplitude et de fréquence spécifiques.

Cette thèse propose de nouvelles solutions pour améliorer la qualité et la fiabilité de l'alimentation électrique des éoliennes à partir d'un système de générateur d'induction à double alimentation (GADA) utilisant des algorithmes hybrides basés sur l'intelligence artificielle. Le système de contrôle du système global se compose de trois blocs de contrôle, à savoir le convertisseur côté rotor (RSC), le convertisseur côté réseau électrique (GSC) et le contrôle MPPT (Maximum Power Point Tracking) permettant l'échange d'énergie entre le système de conversion d'énergie éolienne et le réseau. Les problèmes de qualité de puissance y compris la distorsion harmonique sont discutés en détail et des techniques d'atténuation basées sur le filtrage actif parallèle sont présentées. Une solution efficace et économique basée sur le concept de contrôle prioritaire est proposée. Cette méthode de contrôle de priorité permet de gérer la priorité parmi les contrôles de production du système précédents et la suppression des courants harmoniques à l'aide de la méthode d'extraction d'harmoniques à base de référence synchrone (SRF). En outre, et pour assurer la continuité du service, une stratégie de commande hybride intelligente qui tolère aux défauts (FTC) du circuit ouvert de l'IGBT du convertisseur côté de rotor (RSC) a été présentée. La stratégie FTC est basée sur des systèmes experts combine une méthode simple de détection de défaut basée sur l'inférence de logique floue et utilise les valeurs moyennes du courant du rotor pour détecter le commutateur défectueux sur une période très courte. En outre, pour améliorer les performances du système en boucle fermée pendant les transitoires et les conditions défectueuses, différents contrôleurs de courants comme PI, hystérésis, contrôleurs PI flou-adaptatifs et un contrôleur PI optimisé utilisant des algorithmes génétiques ont été utilisés.

Le modèle de simulation a été développé dans l'environnement Matlab / Simulink et les résultats démontrent que les techniques proposées peuvent réduire efficacement la distorsion harmonique totale (THD) dans les courants de réseau et maintenir la qualité de l'énergie et la continuité des services dans les normes internationales.

Contents

<i>Dedication</i>	<i>i</i>
<i>Acknowledgement</i>	<i>ii</i>
<i>ملخص</i>	<i>iii</i>
<i>Abstract</i>	<i>iv</i>
<i>Résumé</i>	<i>v</i>
<i>Contents</i>	<i>vi</i>
<i>Liste of Tables</i>	<i>xii</i>
<i>Liste of Figures</i>	<i>xiii</i>
<i>Liste of Principal Symbols</i>	<i>xviii</i>
<i>Liste of Abbreviations</i>	<i>xx</i>

General Introduction

<i>1. Overview</i>	<i>1</i>
<i>2. Thesis objectives and organization</i>	<i>3</i>
<i>3. References</i>	<i>5</i>

Chapter I: Control Strategy a DFIG-based on Wind Turbine System

<i>1.1. Introduction</i>	<i>7</i>
<i>1.1.1. Overview</i>	<i>7</i>
<i>1.1.2. Objectives and organesation</i>	<i>8</i>
<i>1.2. Renewable and non-renewable energies</i>	<i>9</i>
<i>1.2.1. Non-renewable energy</i>	<i>9</i>
<i>1.2.2. Renewable energy</i>	<i>11</i>
<i>1.2.2.1. Solar energy</i>	<i>11</i>
<i>1.2.2.2. Hydro-energy</i>	<i>11</i>
<i>1.2.2.3. Biomass energy</i>	<i>12</i>
<i>1.2.2.4. Geothermal energy</i>	<i>12</i>
<i>1.2.2.5. Wind energy</i>	<i>12</i>
<i>1.2.2.6. Wind energy statistics</i>	<i>13</i>
<i>1.3. Wind turbine system</i>	<i>15</i>
<i>1.3.1. History</i>	<i>15</i>
<i>1.3.2. Types of Wind Turbines</i>	<i>15</i>
<i>1.3.2.1. Wind turbines axis types</i>	<i>16</i>
<i>1.3.2.2. Wind turbine capacity type</i>	<i>17</i>
<i>1.3.2.3. Direct drive and geared drive wind turbines</i>	<i>17</i>
<i>1.3.2.4. Fixed speed and variable speed wind turbines</i>	<i>17</i>

Contents

1.3.2.5. Onshore and offshore wind turbines	18
1.3.3. Wind turbine configuration and work	18
1.3.4. Wind Power and Wind Power Density (WPD).....	20
1.3.5. Betz limit.....	20
1.4. Variable-Speed Wind Turbine based on Doubly-Fed Induction Generator system modeling	21
1.4.1. Wind turbine modeling	21
1.4.1.1. Power content of free flowing wind stream.....	21
1.4.2. Doubly-Fed Induction Machines Modeling	22
1.4.2.1. Principle operation of DFIG.....	23
1.4.2.1.1. Sub-synchronous and Super-synchronous	24
1.4.2.2. Mathematical models of the DFIG system.....	24
1.4.2.2.1. Equivalent representation and vectors formulation in a, b c frame	25
1.4.2.2.2. Moving from phase frame to bi-phase frame	28
1.4.2.2.3. Modeling of DFIG in dq reference frame	28
1.4.3. Grid side converter and machine side converter modeling.....	34
1.4.3.1. Machine-side converter modeling.....	34
1.4.3.2. Grid-side converter modeling	38
1.5. Control of variable speed wind turbine Based on Doubly-Fed Induction Generator System.....	39
1.5.1. Modeling in dq reference frame with stator-flux orientation.....	40
1.5.2. DFIG-Based Wind Power System control goal.....	43
1.5.3. Maximum power point tracking (MPPT) control.....	43
1.5.3.1. Tip Speed Rotor (TSR) control.....	44
1.5.3.2. MPPT-PI regulator control.....	44
1.5.4. Rotor-Side Converter Control (RSC).....	45
1.5.4.1. Stator powers control loop.....	46
1.5.4.2. Rotor currents control loop.....	47
1.5.5. Grid-Side Converter (GSC) control	49
1.5.5.1. Control of the DC-link voltage.....	50
1.5.5.2. Hysteresis voltage source currents controlled PWM for GSC.....	51
1.6. Simulation resultants	52
1.7. Conclusion.....	56
1.8. References	57

Chapter II: Artificial Intelligence

2.1. Introduction.....	61
2.1.1. Overview	61
2.1.2. Chapter goal and organesation.....	61

Contents

2.2. Artificial Intelligence (AI)	62
2.2.1. Intelligence definition.....	62
2.2.2. Type of Intelligence	62
2.2.3. Philosophy of AI.....	62
2.2.4. Artificial Intelligence definition	62
2.2.5. Goals of AI	64
2.2.6. Applications of AI.....	64
2.2.7. Research areas of AI	65
2.3. Expert system.....	65
2.3.1. Definition.....	65
2.3.2. Expert system & Expert human.....	66
2.3.3. Components of Expert system	66
2.3.4. Rules Creation.....	67
2.3.5. Types of inference engine.....	69
2.3.6. Expert system applications.....	69
2.4. Fuzzy Logic	69
2.4.1. Definition.....	70
2.4.2. Fuzzy sets	70
2.4.2.1. Membership fucntions	70
2.4.2.2. Membership fucntions types.....	71
2.4.3. Fuzzy sets	70
2.4.4. Fuzzy logic system.....	74
2.4.5. Fuzzy logic applications.....	75
2.5. Algorithm Genetic	76
2.5.1. Definition.....	76
2.5.2. Basic Terminology.....	76
2.5.3. Basic stucture	77
2.5.4. Population initialization.....	77
2.5.5. GA encoding.....	78
2.5.6. Fitness function	79
2.5.7. Genetic operations	79
2.5.7.1. crossover or recombination	79
2.5.7.2. Mutation.....	80
2.5.7.3. Selection.....	80
2.5.8. Genetic algorithm application area.....	80
2.6. Conclusion.....	80
2.7. Refeneces.....	82

Chapter III: Power Quality Enhancement of DFIG Based Wind Energy System

3.1. Introduction.....	85
3.1.1. Overview	85
3.1.2. Chapter objectives and organesation.....	85
3.2. Power Quality (PQ) problems	86
3.2.1. Power quality definition.....	86
3.2.2. Types of power disturbances.....	86
3.2.2.1. Transients.....	87
3.2.2.2. Interruptions.....	87
3.2.2.3. Voltage variation.....	88
3.2.2.4. Voltage fluctuations	89
3.2.2.5. Voltage unbalance.....	89
3.2.2.6. power freaquency variations.....	90
3.2.2.7. Waveform distortions	90
3.2.3. Sources of disturbances.....	92
3.2.3.1. Disturbances resulting from the electric utility.....	92
3.2.3.2. Disturbances resulting from grid and consumer's equipments.....	92
3.2.4. Compatibility levels of power quality disturbances	93
3.2.5. Mitigation power disturbances.....	93
3.3. Harmonic	94
3.3.1. Linear and non-linear loads.....	94
3.3.2. Harmonics mathematical analysis	95
3.3.3. Harmonics consequences	95
3.3.4. Harmonics mitigation.....	95
3.4. Active Power Filters (APF).....	99
3.4.1. Shunt active power filters (Shunt APF).....	99
3.4.2. Series active power filters (Series APF).....	100
3.4.3. Hybrid active power filters.....	100
3.4.4. Unified Power Quality Conditioner (UPQC).....	101
3.5. Active Power Filters (APF).....	102
3.5.1. THD global system calculation without filter	102
3.5.2. Global schematic with shunt active power filter	103
3.5.3. Shunt-Active power filter block.....	104
3.5.4. Harmonic currents extraction method	104
3.5.4.1. Active and reactive powers method (PQ).....	105
3.5.4.2. Synchronous Reference Frame (SRF) method	106

Contents

3.5.5. <i>Modified rotor side converter control</i>	107
3.5.5.1. <i>Priority method</i>	107
3.5.5.1.1. <i>The priority control method</i>	107
3.5.5.2. <i>Rotor currents control methods</i>	109
3.5.5.2.1. <i>Hysteresis rotor currents control</i>	109
3.5.5.2.2. <i>Conventional PI rotor currents control</i>	114
3.5.5.2.3. <i>PI-adaptive fuzzy logic rotor currents control</i>	117
3.5.5.2.4. <i>Comparison rotor current controller's methods</i>	124
3.6. <i>Conclusion</i>	126
2.7. <i>Refeneces</i>	127

Chapter VI: Hybrid-Intelligent Fault Tolerant Control Strategy of Open-circuit IGBT for RSC Power Converter in Wind Turbine System

4.1. <i>Introduction</i>	131
4.1.1. <i>Overview</i>	131
4.1.2. <i>Chapter objectives and organesation</i>	132
4.2. <i>Electronic devices</i>	133
4.2.1. <i>Definition</i>	133
4.2.2. <i>Classification of power electronic devices</i>	133
4.2.3. <i>Transistor</i>	133
4.2.3.1. <i>Definition</i>	133
4.2.3.2. <i>Solid-state material devices</i>	134
4.2.3.3. <i>Transistor's Types</i>	134
4.2.3.3.1. <i>Bipolar Junction Transistor (BJT)</i>	137
4.2.3.3.2. <i>Field Effect Transistor (FET)</i>	137
4.2.3.4. <i>Field Effect Transistor (FET) types</i>	138
4.2.3.4.1. <i>Junction Field Effect Transistor (JFET)</i>	138
4.2.3.4.2. <i>Metal Oxide Semiconductor Field Effect Transistor (MOSFET)</i>	138
4.3. <i>Insulated-Gate Bipolar Transistor (IGBT)</i>	139
4.3.1. <i>Definition</i>	139
4.3.2. <i>Characteristics and applications</i>	140
4.3.3. <i>Technical IGBT work</i>	141
4.3.3.1. <i>Fault description</i>	141
4.3.3.2. <i>IGBT switch fault classification</i>	142
4.4. <i>Open-circuit IGBT switch fault mechanisms</i>	143
4.4.1. <i>Bond wire lift-off or rupture</i>	143
4.4.2. <i>Gate driver failure</i>	144

Contents

4.5. Open-circuit IGBT switch fault detection methods	144
4.5.1. Park's Vector Method	145
4.5.2. AC Current Space Vector Instantaneous Frequency	145
4.5.3. Diagnosis by Sensing Voltage Across Lower Switch	145
4.5.4. Centroid-Based Fault Detection	145
4.5.5. Diagnosis by Sensing Voltage Across Lower Switch	145
4.5.6. Centroid-Based Fault Detection	145
4.5.7. Neural Network Method	145
4.5.8. ANFI System method	146
4.6. Open-circuit IGBT switch fault detection methods	146
4.6.1. Definition	146
4.6.2. Fault tolerant control classification	146
4.6.3. Phase redundancy (Redundancy leg).....	147
4.6.4. Triac	147
4.7. Open-circuit IGBT fault switch affects	148
4.8. Algorithm Genetic-Fuzzy-Expert system of Open-circuit IGBT switch fault tolerant strategy for RSC in wind turbine system	150
4.8.1. Fuzzy-Expert system Fault tolerant control for RSC open switch fault	150
4.8.2. Fuzzy open switch fault detection method	150
4.8.3. Expert system Fault tolerant control RSC	154
4.8.4. GA-PI rotor currents control	154
4.9. Simulation results.....	156
4.10. Conclusion.....	161
4.11. References	163

IV. General Conclusion

5.1. Conclusion.....	167
5.2. Future work.....	168

List of Tables

Chapter I

<i>Table 1.1. Wind Power Density.....</i>	<i>20</i>
<i>Table 1.2. Possible interruption states for RSC.....</i>	<i>36</i>
<i>Table 1.3. System parameters.....</i>	<i>53</i>

Chapter II

<i>Table 2.1. Psychologiste Howard Gardner Intelligence type</i>	<i>63</i>
<i>Table 2.2. Some definitions of AI</i>	<i>64</i>
<i>Table 2.3. Comparisons between an expert system and that of a human expert.....</i>	<i>66</i>
<i>Table 2.4. Expert system applications domain.....</i>	<i>70</i>
<i>Table 2.5. Others lows operations of fuzzy sets.....</i>	<i>74</i>
<i>Table 2.6. Fuzzy logic applications.....</i>	<i>75</i>
<i>Table 2.7. Genetic Algorithms application area</i>	<i>81</i>

Chapter III

<i>Table 3.1. Compatibility levels of power quality disturbances</i>	<i>39</i>
<i>Table 3.2. Fuzzy rules for ΔKp-i gain</i>	<i>119</i>
<i>Table 3.3. Fuzzy rules for ΔKi-i gian</i>	<i>119</i>

Chapter IV

<i>Table 4.1 Average values of three-phase currents under different open switch fault.....</i>	<i>152</i>
<i>Table 4.2. Rules of the fuzzy logic-based open switch FDM.....</i>	<i>152</i>
<i>Table 4.2. GA parameters used in the model</i>	<i>156</i>

Chapter I

<i>Figure.1.1 Petroleum and gas formation</i>	<i>9</i>
<i>Figure.1.2 Fossil fuels formation of energy consumed in 2014</i>	<i>9</i>
<i>Figure1.3 Petroleum and gas existing in the world.</i>	<i>10</i>
<i>Figure.1.4 prevailing winds over the surface of the earth</i>	<i>13</i>
<i>Figure 1.5. The best places of the air circulation in the earth</i>	<i>14</i>
<i>Figure 1.6 The best places of the air circulation in Algeria</i>	<i>14</i>
<i>Figure 1.7. Global Cumulative Installed Capacity 2001-2016</i>	<i>15</i>
<i>Figure 1.8. Axis wind turbine types.....</i>	<i>16</i>
<i>Figure 1.9. Fixed-speed wind turbine with an induction generator.....</i>	<i>18</i>
<i>Figure 1.10. Variable-speed wind turbine with a synchronous/induction generator.....</i>	<i>18</i>
<i>Figure 1.11. Wind turbine configuration.....</i>	<i>19</i>
<i>Figure 1.12. Wind turbine foundation types.....</i>	<i>19</i>
<i>Figure 1.13. Variable-speed wind turbine with a doubly-fed induction generator.....</i>	<i>21</i>
<i>Figure 1.14. DFIG with its converters</i>	<i>23</i>
<i>Figure 1.15. stator and rotor windings of DFIG in a, b, c frame reference.....</i>	<i>26</i>
<i>Figure 1.16. DFIG equivalent circuit</i>	<i>26</i>
<i>Figure 1.17. reference frames</i>	<i>29</i>
<i>Figure.1.18. Combined vector representation.....</i>	<i>30</i>
<i>Figure 1.19. stator and rotor windings of DFIG in dq frame reference rotates with ω_k.....</i>	<i>32</i>
<i>Figure 1.20. DFIG equivalent circuit in dq frame</i>	<i>32</i>
<i>Figure.1.21. Back-to-back converter.....</i>	<i>34</i>
<i>Figure 1.22. Circuit configuration of two-level back-to-back converter</i>	<i>35</i>
<i>Figure 1.23. Rotor side converter circuit diagram.....</i>	<i>35</i>
<i>Figure 1.24. Rotor side converter model.....</i>	<i>37</i>
<i>Figure 1.25. Rotor side converter diagram block in dq reference frame.....</i>	<i>38</i>
<i>Figure 1.26. Grid Side Converter modeling</i>	<i>39</i>
<i>Figure 1.27. Voltages currents and flux vectors in dq Synchronously Rotating Reference Frame.....</i>	<i>40</i>
<i>Figure 1.28. Schematic block diagram of the inner system.....</i>	<i>42</i>
<i>Figure 1.29. DFIG-Based Wind Power System Model control.....</i>	<i>43</i>
<i>Figure 1.30. MPPT control</i>	<i>44</i>
<i>Figure 1.31. Block diagram for the RSC control</i>	<i>46</i>
<i>Figure 1.32. Block diagram of the rotor current control of the d-axis reference frame</i>	<i>48</i>
<i>Figure 1.33. block diagram of the rotor current control of the q-axis reference frame.....</i>	<i>48</i>
<i>Figure 1.34. Principal block diagram of Grid-Side Converter (GSC) control</i>	<i>49</i>
<i>Figure 1.35. Block diagram of stator currents and direct voltage GSC control.....</i>	<i>50</i>

Liste of Figures

Figure 1.36. DC-link voltage feedback control loop.....	50
Figure 1.37. block diagram of current hysteresis control.....	52
Figure. 1.38. (a) I_{rq} current,(b) I_{rd} Current ; (c) active stator power P_s (d) reactive stator power Q_s ; (e) Torque C_{em} (f)DC-voltage V_{dc} ; (g) Wind speed (h)Speed of DFIG with MPPT.....	54
Figure 1.39. Three-phase stator currents.....	55
Figure 1.40. Three-phase stator currents zoom	55

Chapter II

Figure 2.1. Expert System components	66
Figure 2.2. Different types of membership functions	72
Figure 2.3. Logical operations (a) Fuzzy sets, (b) Crisp sets.....	73
Figure 2.4. Fuzzy Logic System (FLS)	75
Figure 2.5.. Flowchart of the GA optimization technique.....	77
Figure 2.6. Chromosomes using tree encoding	79

Chapter III

Figure 3.1. Impulsive and oscillatory transients.....	87
Figure 3.2. Supply voltage short and long interruption.....	88
Figure 3.3. Short-duration voltage variations: sag.....	88
Figure 3.4. Short-duration voltage variations: swell.....	88
Figure 3.5. Long duration voltage variations	89
Figure 3.6. Voltage fluctuation.....	89
Figure 3.7. Voltage unbalance	90
Figure 3.8. Power frequency variations.....	90
Figure 3.9. Direct current offset.....	91
Figure 3.10. Harmonic current distortion.....	91
Figure 3.11. Notching voltage variation	91
Figure 3.12. Noise voltage variation.....	92
Figure 3.13. Voltage and current waveforms for linear loads.....	95
Figure 3.14. Effect of Harmonics in the waveform of the power of non-linear loads.....	95
Figure 3.15. Harmonic spectrum	98
Figure 3.16. Subdivision of active power filter	99
Figure 3.17. Shunt active power filter.....	100
Figure 3.18. Series active power filters.....	100
Figure 3.19. Hybrid filter	101

Liste of Figures

Figure 3.20. Unified Power Quality Conditioner (UPQC) structure.....	101
Figure 3.21. Point power common coupling wind turbine system connection.....	102
Figure 3.22. Current waveforms and their FFT (a) non-linear load, (b) grid, (c) generator.....	103
Figure 2.23 Global schema of Active filter of DFIG based wind turbine system.....	104
Figure 3.24. Active and reactive powers method (PQ) block.....	106
Figure 3.25. Block diagram of SRF method.....	107
Figure 3.26. Modified Rotor-Side Converter Control (MRSC).....	108
Figure 3.27. Priority control method	108
Figure 3.28. Hysteresis rotor currents control.....	110
Figure 3.29. Hysteresis band.....	110
Figure 3.30. Hysteresis currents control: (a) quadrature rotor current with its Zoom I_{rd} ; (b) direct rotor current with its Zoom I_{rq} , (c) a phase rotor current with its Zoom I_{ra}	111
Figure 3.31. Direct and quadrature rotor currents injected in hysteresis rotor currents control	112
Figure 3.32. (a) quadrature and direct stator powers; (b)DC-link voltage and Torque machine, (c) a phase stator current for grid and machine (DFIG).....	112
Figure 3.33. Non-linear load current.....	113
Figure 3.34. (a) Wind speed (b) Speed of DFIG with MPPT.....	113
Figure 3.35. Current waveforms and their FFT for (a) non-linear load, (b) grid, (c) generator	114
Figure 3.36. Close loop conventional PI rotor currents control.....	114
Figure 3.37. Conventional PI rotor currents control: (a) quadrature rotor current with its Zoom I_{rd} ; (b) direct rotor current with its Zoom I_{rq}	115
Figure 3.38. Direct and quadrature rotor currents injected in Conventional PI rotor currents control..	115
Figure 3.39. Non-linear load current.....	115
Figure 3.40. (a) quadrature and direct stator powers; (b)DC-link voltage and Torque machine, (c) a phase stator current for grid and machine (DFIG) for Conventional PI rotor currents control	116
Figure 3.41. Current waveforms and their FFT for (a) non-linear load, (b) grid, (c) generator for Conventional PI rotor currents control.....	117
Figure 3.42. PI-adaptive fuzzy logic rotor currents control Bloc diagram.....	118
Figure 3.43. Fuzzy logic bloc diagram controller.....	118
Figure 3.44. Fuzzy Inference System (FIS) plot diagram.....	119
Figure 3.45. Membership functions for (a) inputs variables err , Δerr (b) and outputs $\Delta Kp-i$ and $\Delta Ki-i$.	120
Figure 3.46. Output variables surface of $\Delta Kp-i$ and $\Delta Ki-I$	120
Figure 3.47. PI-adaptive fuzzy logic rotor currents control: (a) quadrature rotor current with its Zoom I_{rd} ; (b) direct rotor current with its Zoom I_{rq}	121
Figure 3.48. Direct and quadrature rotor currents injected in Conventional PI rotor currents control..	121
Figure 3.49. Non-linear load current.....	121
Figure 3.50. $\Delta Kp-i$ and $\Delta Ki-i$ Variation gains for direct rotor current PI-adaptive fuzzy logic controller.....	122
Figure 3.51. $\Delta Kp-i$ and $\Delta Ki-i$ Variation gains for quadrature rotor current PI-adaptive fuzzy logic	

Liste of Figures

Controller	122
Figure 3.52. (a) quadrature and direct stator powers; (b)DC-link voltage and Torque machine, (c) a phase stator current for grid and machine (DFIG) for PI-adaptive fuzzy logic rotor currents control.....	123
Figure 3.53. Current waveforms and their FFT for (a) non-linear load, (b) grid, (c) generator for PI-adaptive fuzzy logic rotor currents control.....	124
Figure 3.54. Comparison direct rotor current controller's methods	125
Figure 3.55. Comparison quadrature rotor current controller's methods.....	125

Chapter IV

Figure 4.1 Block diagram of a power processor.....	133
Figure 4. 2. Semiconductor materials	134
Figure 4.3. Silicon of Germanium atoms	135
Figure 4.4. N-Type and P-Type semiconductors.....	135
Figure 4.5 P-N junction.....	136
Figure 4.6. PN-junction principal work.....	136
Figure 4.7. Transistor type's classification.....	137
Figure 4.8. PNP and NPN Bipolar Junction Transistor	137
Figure 4.9. PNP Junction Field Effect Transistor.....	138
Figure 4.10. NPN Junction Field Effect Transistor	138
Figure 4.11. Circuit Symbols for Depletion Mode MOSFETs (IGFETs).....	139
Figure 4.12. Circuit Symbols for Enhancement Mode MOSFETs (IGFETs).....	139
Figure 4.13. Insulated-Gate Bipolar Transistor (IGBT) structure.....	140
Figure 4.14. Electronic power switches classification.....	141
Figure 4.15. IGBT switch faults classification	143
Figure 4.16. FDI classification	144
Figure 4.17. FTC classification	146
Figure 4.18. Fault-tolerant designs for IGBT power electronics	147
Figure 4.19. Typical phase redundant circuit	148
Figure .4.20. RSC topology	148
Figure 4.21. Currents affect: (a) direct and quadrature rotor currents, (b) continuous current, (c) three-phase stator currents and rotor current phase.....	149
Figure 4.22. Fuzzy-Expert system Fault tolerant control for RSC open switch fault scheme.....	151
Figure 4.23. Three-phase rotor side converter currents mean values	151
Figure 4.24. Flowchart of the expert system-based open switch FDM.....	153
Figure 4.25. (a) Membership functions of the input variables (b) Output surface (c) Rule viewer	153
Figure 4.26. Redundancy leg of the FTC strategy.....	154
Figure 4.27. Flowchart of the FTC strategy	155

Liste of Figures

<i>Figure 4.28. Rotor side converter control system</i>	155
<i>Figure 4.29. Flowchart of the GA optimization technique</i>	156
<i>Figure 4.30. (a) Wind speed (b) Speed of DFIG with MPPT, (c) P_s (d) Q_s, (e) I_{rd} current (f) I_{rq} current, (g) Torque, (h) V_{dc} voltage</i>	158
<i>Figure 4.31. Direct rotor current: Comparison of GA-tuned PI controller and conventional PI Controller</i>	159
<i>Figure 4.32. Quadrature rotor current: Comparison of GA-tuned PI controller and conventional PI controller</i>	159
<i>Figure 4.33. GA-based PI controllers gains K_p and K_i</i>	159
<i>Figure 4.34. Fuzzy logic open switch fault detection (second switch fault S_2)</i>	160
<i>Figure 4.35. Indices $ind1$, $idn2$ and $ind3$</i>	160
<i>Figure 4.36. Redundant leg switching signals</i>	160
<i>Figure 4.37. Time detection for three switches: (a) S_1 , (b) S_2 , (c) S_3</i>	160
<i>Figure 4.38 Three -phase RSC currents average values</i>	160

List of Principal Symbols

List of principal symbols used in this thesis is given below:

I_{rd}	<i>d_axis rotor current</i>
I_{rq}	<i>q_axis rotor current</i>
I_{sd}	<i>d_axis stator current</i>
I_{sq}	<i>q_axis stator current</i>
I_{DC}	<i>DC current</i>
V_{rd}	<i>d_axis rotor voltage</i>
V_{rq}	<i>q_axis rotor voltage</i>
V_{sd}	<i>d_axis stator voltage</i>
V_{sq}	<i>q_axis stator voltage</i>
T_{em}	<i>Electromagnetic torque</i>
T_m	<i>Mechanical torque</i>
φ_s	<i>Stator flux linkage</i>
φ_r	<i>Rotor flux linkage</i>
φ_{sd}	<i>d_axis Stator flux linkage</i>
φ_{sq}	<i>q_axis Stator flux linkage</i>
φ_{rd}	<i>d_axis rotor flux linkage</i>
φ_{rq}	<i>q_axis rotor flux linkage</i>
P_s	<i>Active stator power</i>
Q_s	<i>Reactive stator power</i>
f_s	<i>Stator frequency</i>
f_r	<i>Rotor frequency</i>
R_s	<i>Stator resistance</i>

List of Principal Symbols

R_r	<i>Rotor resistance</i>
L_s	<i>Stator inductance</i>
L_r	<i>Rotor inductance</i>
M_{sr}	<i>Mutual inductance</i>
s	<i>Slip</i>
θ_s	<i>Stator angle</i>
θ_r	<i>Rotor angle</i>
θ_m	<i>Mechanical angle</i>
ω_s	<i>Stator angular speed</i>
ω_r	<i>Rotor angular speed</i>
ω_m	<i>Mechanical angular speed</i>
E	<i>Kinetic wind energy</i>
V	<i>Wind speed</i>
C_p	<i>Coefficient power of wind turbine</i>
J	<i>Moment of inertia</i>
F	<i>Friction coefficient</i>

List of general abbreviations

List of general abbreviations used in this thesis is given below:

<i>DFIG</i>	<i>Doubly Fed Induction Generator</i>
<i>RSC</i>	<i>Rotor Side Converter</i>
<i>GSC</i>	<i>Grid Side Converter</i>
<i>MPPT</i>	<i>Maximum Power Point Tracking</i>
<i>DC</i>	<i>Direct Current</i>
<i>AC</i>	<i>Alternative Current</i>
<i>FSIG</i>	<i>Fixed Speed Wind Turbine</i>
<i>VSWT</i>	<i>Variable Speed Wind Turbine</i>
<i>PWM</i>	<i>Pulse Width Modulation</i>
<i>HAWT</i>	<i>Horizontal Axis Wind Turbine</i>
<i>VAWT</i>	<i>Vertical Axis Wind Turbine</i>
<i>WPD</i>	<i>Wind Power Density</i>
<i>AI</i>	<i>Artificial Intelligence</i>
<i>ES</i>	<i>Expert System</i>
<i>FL</i>	<i>Fuzzy Logic</i>
<i>AG</i>	<i>Algorithm Genetic</i>
<i>PQ</i>	<i>Power Quality</i>
<i>SRF</i>	<i>Synchronous Reference Frame</i>
<i>THD</i>	<i>Total Harmonic Distortion</i>
<i>APF</i>	<i>Active Power Filter</i>
<i>PCC</i>	<i>Point of Common Coupling</i>
<i>RSM</i>	<i>Root Mean Square</i>
<i>LPF</i>	<i>Low Pass Filter</i>
<i>MRSC</i>	<i>Modified Rotor Side Converter</i>
<i>err</i>	<i>error</i>
<i>FIS</i>	<i>Fuzzy Inference System</i>

List of general abbreviations

<i>PI</i>	<i>Proportional-Integral</i>
<i>IGBT</i>	<i>Insulated Gate Bipolar Transistor</i>
<i>FTC</i>	<i>Fault Tolerant Control</i>
<i>FDI</i>	<i>Fault Detection and Isolation</i>
<i>BJT</i>	<i>Bipolar Junction Transistor</i>
<i>FET</i>	<i>Field Effect Transistor</i>
<i>STPWM</i>	<i>Sinusoidal Triangular Pulse Width Modulation</i>

General Introduction

Introduction

1. Overview

Wind energy technology has experienced huge progress during the last decade. This was encouraged by the need to develop ambient friendly clean and renewable forms of energy and the continuously rise of oil price. Large-size wind turbine farms are nowadays producing electricity at great scale throughout the world. Where in 2015, increase in wind generation was equal to almost half of global electricity growth [1]; the worldwide total cumulative installed electricity generation capacity from wind power amounted to 432,883 MW, an increase of 17% compared to the previous year [2].

Various wind turbine configurations using different generator topologies have been extensively studied, developed and built. There are two main types of wind turbines systems: the Fixed-Speed Wind Turbine (FSWT) and the Variable-Speed Wind Turbine (VSWT). The FSWT uses a multistage gearbox and a squirrel cage induction generator (SCIG) and is directly connected to the grid. The VSWT uses a multistage gearbox and a synchronous generator or Doubly-Fed Induction Generator (DFIG) and is connected to the grid via a power electronic converter. VSWT has become the most popular type of wind turbine system. There are several reasons for using variable-speed operation of wind turbines; among those are possibilities to reduce stresses of the mechanical structure, acoustic noise reduction and the possibility to control active and reactive powers injected in the grid [3]. Most of the major wind turbine manufactures are developing new larger wind turbines in the 3-to-5-MW range [4]. These large wind turbines are all based on variable-speed operation with pitch control using a direct-driven synchronous generator or a doubly-fed induction generator (DFIG).

The use of the doubly fed induction machines was subject of many investigations in research and especially in generator mode for the wind turbine [4, 5]. The major advantage of this machine, which has made it popular, is that the power electronic equipment only has to handle a fraction (20–30%) of the total system power using back-to-back converters which are controlled by pulse width modulation (PWM). Therefore, the losses in the power electronic converter and its cost can be reduced, compared to a synchronous generator wind turbine system where the converter has to handle the total power [6, 7]. The wind energy conversion system using DFIG is connected directly to the grid via stator and via back-to-back PWM converter (AC/DC/AC) commonly divided into grid-side converter (GSC) and rotor side converter (RSC). The RSC has been controlled in order to ensure the decoupled between the two stator powers (reactive and active powers) using the electromagnetic torque delivered by the maximum power point tacking control (MPPT). The GSC controls the power flow exchange with the grid via the rotor, by maintaining the DC bus at the constant voltage level [8]. The main goals of these controls are; to optimize use of the wind turbine capacity (optimal extraction of electric energy from the kinetic energy contained in the incident wind) and to improve power quality to approach the habitual performances met in the classical forms of energy.

A good power quality can be defined as pure sinusoidal voltage/current waveform with 1 p.u magnitude and 1 p.u frequency and the phase shift of 120 degree between the adjacent phases in the three phase system of voltage/current, these are the important characteristics which is aimed by the system to produce and delivered to the customers [9]. Therefore, any changing in this power waveform (voltage/current) is generally defined as a power quality disturbance or problem which can results a failure or mal-operation of equipments user's or a complete shutdown [10]. The power quality problems are classified as a seven eight categories which are: transients, long-duration voltage variations, short-duration voltage variations, waveform distortions; voltage imbalance; voltage fluctuations and frequency variations; each type of these problems has different categories that define by their proper consequences from the less to the most dangerous. The most severe problems of power quality are interruptions and harmonics distortion. These two power quality problems must be eliminated or reduced.

Particularly, the increasing penetration of power electronics-based loads (non-linear loads) is creating a growing concern for harmonic distortion in the grid. The negative impact of harmonics may not be immediately evident, but over time can result in increased power demand, system loss, and shorter equipment lifetimes [11]. In order to suppress or at least reduce the influence of harmonics, several possible ways have been previously proposed among of those are the passive and active filters. The performance of passive filters is strongly dependent on the system impedance at the harmonic frequencies. The system impedance depends on the distribution network configuration and the loads. Therefore, design of passive filters involves thorough system analysis in order to obtain adequate filtering performance of the filter. Whereas; the active filters measure the harmonic currents present in the system and generate opposite harmonics to cancel those produced by the harmonic sources [12].

When the supply voltage has been zero for a long or a short time; it's named as an interruption power quality problem. This problem is often permanent and requires human intervention to repair the system for restoration and it can be caused by the failures of one or many components of the system. According to a survey, semiconductor failure and soldering joints failure in power devices take up 34% of power electronic system failures [13]. Another survey shows that around 38% of the faults in variable-speed ac drives are due to failure of power devices [14]. A recent questionnaire on industrial power electronic systems also showed that all the responders regard power electronic reliability as an important issue, and 31% of the responders selected the "semiconductor power device" as the most fragile component [14]. The most used power devices for industrial applications are IGBTs [15]. Therefore it is worth investigating IGBT's failure and exploring the solutions to improve the reliability of IGBT power electronic converters. The failure of IGBTs can be generally classified as catastrophic failure and wear out failure. IGBT wear out failure is mainly induced by accumulated degradation with time, while catastrophic failure is triggered by single-event overstress, such as overvoltage, over current, overheat and so on [16, 17].

Switching device faults can be classified into short switch fault and open switch fault. A short switch fault not only generates an abnormal over-current in the power conversion system and in the generator but also causes some secondary problems like the demagnetization of the generator. Therefore; in case of a short switch fault, the entire system should be shut down immediately for safety [18]. An open switch fault does

not require halting operation, but the noise, over-current and the vibrations can be induced in the generator and the system. Furthermore, the over-current can flow into healthy switches and can cause additional faults in these switches. However, if an open switch fault is not handled immediately, it can cause also secondary problems in the generator and other devices. In a results; various switching device fault diagnostic and protection methods have been developed during the last decade especially for an IGBT switch faults [19, 20].

2. Thesis objectives and organization

In this work, a wind turbine system based-on doubly fed induction generator connected to the grid has been studied in a goal to improve a power quality by reducing the harmonics in the grid and realize its service continuity during any fault of an open circuit IGBT switch for a rotor side converter.

In a first chapter, we have talked firstly about the revolution of renewable energies in the world and their advantages compared with non-renewable one, then we have concentrated our studying in the wind turbine energy based on DFIG where we talk about: wind kinetic energy, betz limit, wind turbine types, the composition of DFIG and its mathematical models in a dq reference and back-to-back converter modeling...etc.

In a second part, we have presented the modulation and the control for each part of the global system (Turbine, generator and the two converters). The DFIG is simulated as an induction machine having 3-phase supply in the stator and 3-phase supply in the rotor. The rotor coupled via two powers converters: the rotor-side converter (RSC) and the grid-side converter (GSC). The RSC ensures a decoupled active and reactive stator power control, P and Q according to the reference torque delivered by the maximum power point tacking control (MPPT), this last permit to extract optimal electric energy from wind with high quality specifications. The GSC controls the power flow exchange with the grid via the rotor, by maintaining the DC bus at a constant voltage level.

In the second chapter, we have talked about the artificial intelligent theories and its applications in the technology field and we concentrate our studying in three types among them which are: fuzzy logic, expert system and genetic algorithm.

In the third chapter, we have presented a system model including Shunt Active Power Filter (SAPF) in order to improve the power quality by reducing the currents harmonics in the grid. Therefore, we have reminded firstly the different power quality problems existing in the grid then we were detailed especially in the currents harmonics, their caused, their consequences and their solutions and finally the SAPF was used among the several harmonics mitigations. The active filter using here is based on a priority method which permits to filtering the harmonics in the grid via the system converter's (GSC and RSC), the aim of this method is to manage the priority among three different controls: active stator power control; reactive stator power control and harmonic rotor currents control; by using the active shunt filter with Synchronous Reference Frame (SRF) method harmonic extraction. In other side, and in order to have a high performance and robustness; an adaptive-fuzzy PI control are including for currents rotor control and compared with hysteresis and conventional PI controllers.

In the last chapter, we have presented an open circuit IGBT switch fault tolerant control strategy for rotor side converter. In the first part, we have talked briefly about semiconductors technology especially the transistors and their types like JBT, FET and IGBT and we concentrate our studies in the IGBT one, where we have talked about their advantages, its function, their characteristics and their faults (open and short faults). Then an IGBT open circuit switch fault for rotor side converter is studying in this part and detected using a fuzzy logic fault detection method which permits to detect the faulty switch among the other healthy switches using the expert system concept. After the detection; a four-leg redundant topology is used which permit to change the level contain the faulty switch with a healthy one in order to realize service continuity and reliability of the system.

3. References

- [1] International Energy Agency (IEA), Medium-Term Renewable Energy Market Report 2015 (MTRMR), Market Analysis and Forecasts to 2020.
- [2] David, A. 2015. Wind energy outlook 2015: Could total installed wind capacity reach 2,000 GW by 2030? The World's #1 Renewable Energy Network for News, Information, and Companies. <http://www.renewableenergyworld.com/articles/2015/02/wind-energy-outlook-2015-could-total-installed-wind-capacity-reach-2000-gw-by-2030.html>.
- [3] R. Pena, J. Clare, and C. Asher, "*Double fed induction generator using back-to-back PWM converter and its application to variable-speed wind-energy generation*", IEE Proceedings - Electric Power Applications , vol.143, pp.231–241. 1996.
- [4] S. Muller, M. Deicke, and R. Doncker, "*Doubly fed induction generator systems for wind turbines*", IEEE Industry Applications Magazine, vol. 17, pp. 26–33, 2002.
- [5] Brekken; TKA. Mohan, N. "*Control of a doubly fed induction wind generator under unbalanced grid voltage conditions*". IEEE Transactions.
- [6] Abhijeet Awasthi and al, "*Study for Performance Comparison of SFIG and DFIG Based Wind Turbines*", International Journal of Latest Trends in Engineering and Technology (IJLTET); Vol. 2 Issue 4 July 2013.
- [7] A. kumar agrawal and al, "*Study of wind turbine driven DFIG using AC/DC/AC converter*", Electrical Engineering.
- [8] Lie, Xu., "*Direct Active and Reactive Power Control of DFIG for Wind Energy Generation*". IEEE Transactions on Energy conversion, September 2006.
- [9] Camelia Youcef .M, "*Power Quality*", book, Dar eldjamiain Iltibaa, 1995.
- [10] Joseph Seymour, "*The Seven Types of Power Problems*", Electric Power Research Institute, The Cost of Power Disturbances to Industrial & Digital Economy Companies, 2001.
- [11] Camelia Youcef .M, "*The Harmonics in Electrical Networks*", book, Dar eldjamiain Iltibaa, 2005.
- [12] E. Forehand E. Mc. William, "*An Evaluation of Harmonic Mitigation Techniques A Major Qualifying Project*", Bachelor of Science in Electrical and Computer Engineering.

- [13] F. W. Fuchs. “*Some Diagnosis Methods for Voltage Source Inverters In Variable Speed Drives with Induction Machines A Survey*”. IEEE Industrial Electronics Conference, Roanoke, Virginia, USA, 2002. CD-ROM Paper.
- [14] Friedrich W. Fuchs, “*Some Diagnosis Methods for Voltage Source Inverters In Variable Speed Drives with Induction Machines A Survey*”, Conference: Conference: Industrial Electronics Society, 2003. IECON '03. The 29th Annual Conference of the IEEE, Volume: 2.
- [15] Bimal K. Bose, “*Bose-Modern power electronics and AC drives*”, book, Prentice Hall PTR (2002).
- [16] B.C. Kok, M.S. Looi, H.H. Goh, “*Insulated Gate Bipolar Transistor Failure Analysis in Overvoltage Condition*”, International Conference on Renewable Energies and Power Quality (ICREPQ'12), Santiago de Compostela (Spain), 28th to 30th March, 2012.
- [17] M. Trivedi and al. "Failure mechanisms of IGBTs under short-circuit and clamped inductive switching stress", IEEE Transaction on Power Electronics, vol. 14, Issue: 1, Jan. 1999, pp: 108 – 116.
- [18] B.C. Kok, M.S. Looi, H.H. Goh, “*Insulated Gate Bipolar Transistor Failure Analysis in Overvoltage Condition*”, International Conference on Renewable Energies and Power Quality (ICREPQ'12), Santiago de Compostela (Spain), 28th to 30th March, 2012.
- [19] B. Lu and S. K. Sharma, “*A Literature Review of I BT Fault Diagnostic and Protection Methods for Power Inverters*” IEEE Trans. on Ind. Appl., vol. 45, no. 5, pp 1770-1777, 2009.
- [20] Wu, Rui; Blaabjerg, Frede; Wang, Huai; Liserre, Marco; Iannuzzo, Francesco, “*Catastrophic Failure and Fault-Tolerant Design of IGBT Power Electronic Converters -An Overview*”, In Proceedings of the 39th Annual Conference of the IEEE Industrial Electronics Society, IECON 2013 (pp. 507-513).

Chapter I: Control Strategy for Doubly Fed Induction Generator Based Wind Energy System

Abstract: *Wind power is the fastest growing renewable energy and is promising as the number one source of clean energy in the near future. Among various generators used to convert wind energy, the doubly fed induction generator (DFIG) has attracted more attention due to its lower cost, lower requirement of maintenance, variable speed, higher energy capture efficiency, and improved power quality. The DFIG is simulated as an induction machine having 3-phase supply in the stator and 3-phase supply in the rotor. The rotor coupled via two power converters: the rotor-side converter (RSC) and the grid-side converter (GSC). The RSC ensures a decoupled active and reactive stator power control, P and Q according to the reference torque delivered by the maximum power point tracking control (MPPT). The GSC controls the power flow exchange with the grid via the rotor, by maintaining the DC bus at a constant voltage level. The simulation model was developed in Matlab/Simulink environment. The results were showed that the control strategy can effectively produce a maximum power extracted from the wind energy with unity power factor to the grid.*

1.1 Introduction

1.1.1 Overview

Wind energy conversion systems have been attracting wide attention as a renewable energy source, commonly recognized to be a clean and environmentally friendly renewable energy resource that can reduce our dependency on fossil fuels, has developed rapidly in recent years. Wind power has a history more than 3000 years old, and people began to use it to generate electrical power about 120 years ago. The development of wind power has always fluctuated with oil prices. The technology of wind power was first boosted during the 1970s oil crisis, but damped down afterwards. During the last decade, due to the concessionary policy towards the wind power industry adopted by many countries, the wind market has developed rapidly, and the wind turbine technology has experienced an important evolution over time [1, 2, 3].

One of limiting factors in wind turbines lies in their generator technology. There is no consensus among academics and industry on the best wind turbine generator technology. Traditionally, there are three main types of wind turbine generators which can be considered for the various wind turbine systems, these being direct current (DC), alternating current (AC) synchronous and AC asynchronous generators. In principle, each can be run at fixed or variable speed. These induction (asynchronous) generators fall into two types: fixed speed induction generators (FSIGs) with squirrel cage rotors and doubly-fed induction generators (DFIGs) with wound rotors [4]. It is important that the generator can function at variable speed but the presence of converters between the generator and the network harms the global efficiency of the installation. Therefore, the use of doubly fed induction machines was subject of many investigations in research and especially in generator mode for the wind turbine, nowadays; over 85% of the installed wind turbines utilize DFIGs [4, 5] and the largest capacity for the commercial wind turbine product with DFIG has increased towards 5MW in industry.

The DFIG proposes a good compromise between the variation speed range which it authorizes and the converters size compared to the machine nominal power. In addition of that, it can be suitable for the variable nature of wind speed and it can be operated in any desired power factor through power electronic converter control. Moreover, the special connection of rotor windings results in a lower converter cost and also a lower loss [4, 5]. In the DFIG topology, the stator is directly connected to the grid through transformers and the rotor is connected to the grid through PWM power converters while the rotor is indirectly connected to the grid through back-to-back converter. The converters can control the stator power which permits to provide around 10 to 40% of the generators rated power.

Several control strategies were established to control the power exchange between the machine and the network via the back-to-back converter (two-level AC-DC-AC converter). A two-level AC-DC-AC converter is divided into rectifier and inverter and it is used with the DFIG in order to control the global system, where; it is possible to control both of active and reactive stator power through the changing of the

rotor currents and thus the changing of frequency and magnitude voltage of AC-DC-AC converter using pulse width modulation (PWM) strategy [6].

1.1.2 Objectives and organization

This chapter starts with a brief background about the disadvantages of non-renewable energies and the advantages and development of the renewable energies in the word especially the wind energy (section 2). In the third section, a wind turbine system history, construction, types and its principal work has been discussed with their main expressions which mainly using in this domain.

In the section follow (fourth), variable-speed wind turbine based on doubly-fed induction generator system modeling has been derived. This section firstly introduces the mathematical model of wind turbine with its simulation block diagram following by the mathematical models of the two converters (RSC and GSC).

Then, DFIG machine description, principal work, equivalent circuit and model equations have been discussed. In the mathematical machine model, we trait the model equations in three phases frame and bi-phase frame with a brief view about transformations technique.

In section five, the decoupled method is introduced for DFIG system control-based on which, the active and reactive power can be controlled independently. Where, the control strategy is divided into three blocks diagram which are: RCC control block, GSC control block and MPPT control block. The main objective of RSC is to control the stator powers to suit the variation of the wind speed and the last ensure the DC-link voltage constant.

The objective of the GSC is to ensure regulation of the dc-voltage bus, and thereby indirectly control the stator terminal voltage. Moreover, the DFIG characteristics can be adjusted so as to achieve maximum of effective power conversion or capturing capability for a wind turbine using MPPT block control.

A simulation study is performed to examine the power characteristic of the DFIG wind turbine system control and finally the chapter is summarized in the conclusion section.

1.2 Renewable and non-renewable energies

1.2.1 Non-renewable energy

Non renewable energy is energy from fossil fuels (coal, petroleum and natural gas) and uranium; it is called also: a finite resources. All fossil fuels formed in a similar way. Hundreds of millions of years ago, earth had different landscape. It was covered with wide, shallow seas and swampy forests. When the living organisms (plants and animals) died; they fell in to the water or swamps. Due to the lack of oxygen under water the dead living organisms did not decay completely, they turned into layers of earth changed under the heat pressure, physical and chemical changes permit transfer these layers into coal; oil and natural gas [7, 14].

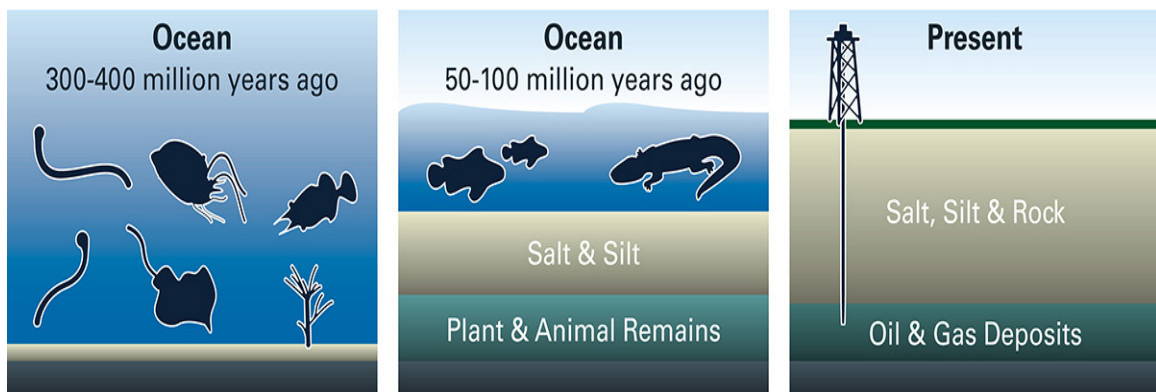


Figure 1.1. Petroleum and gas formation [49].

During the industrial revolution, fossil fuels seemed to be the ideal energy source. They are used to fuel cars and airplanes, power electricity and a huge of products that we use every day. So; there are of great importance in our life. Figure 1.2 shows the energy consumed in 2014 [8].

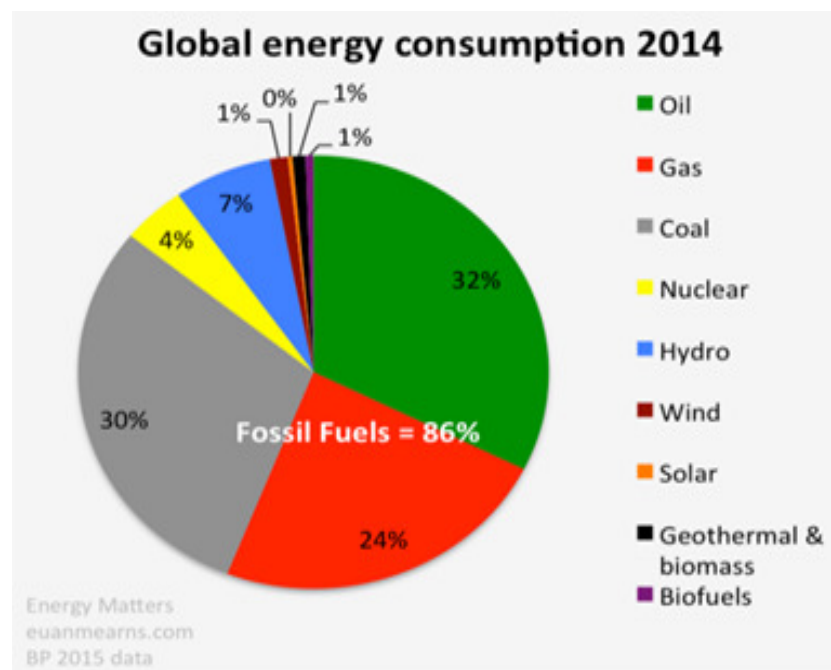


Figure 1.2. Fossil fuels formation of energy consumed in 2014 [8].

a) Advantages [14]:

- Fossil fuels are a valuable source of energy. They are relatively inexpensive to extract in addition of that; they are very easy to find.
- It has a capacity to generate huge amounts of electricity in just single location.
- Transporting oil or gas to the power station can be made through the use of pipes making it an easy task.

b) Disadvantages [14]:

- Burning of fossil fuels is harmful for the environment. When coal and oil are burned; they release particles that can pollute the air water and lands. Pollution is a major disadvantage of fossil fuels, this is because they give off carbon dioxide when burned thereby causing a green house effect.
- Over exploration of fuels has already resulted in their depletion and it would take millions of years to replace them.

Therefore, the use of fossil fuels has both its benefits and drawbacks. In any case, it is time to look for alternative sources of energy to ensure safe and healthy life for the generations to come.

The philosophical motivation to use less fossil fuel became much more enticing after the oil crisis which events in October 1973, when the OPEC countries quadrupled the price of oil from 3 to 12 V.S dollars from one day to another [9].

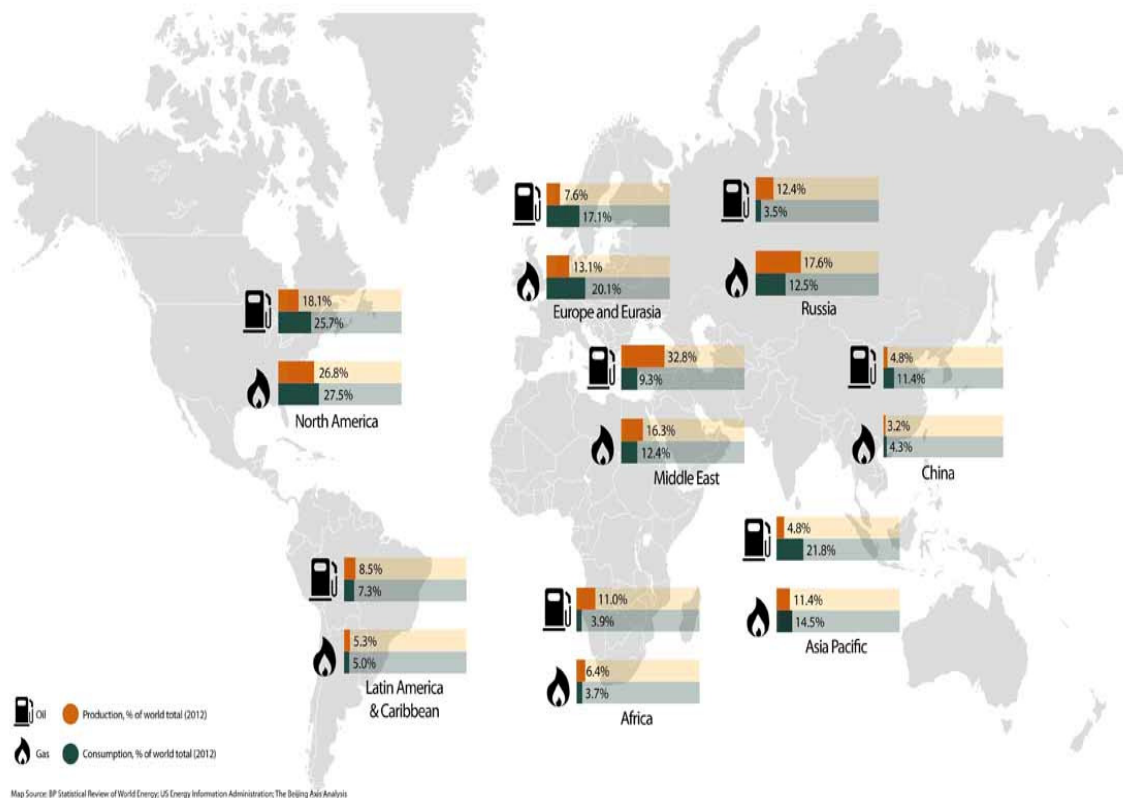


Figure 1.3. Petroleum and gas existing in the world [10].

1.2.2. Renewable energy

Renewable energy source is energy that is generated from sunlight, wind, water, biomass and geothermal heat sources. These sources are naturally and constantly replenished, which are why they are deemed as renewable. The solar energy deemed as the principal generation source of the other sources, without solar there would be no wind, no wave and no plants...[11, 12]

Depending to their source, there are many forms of renewable energy named: solar energy, wind energy, hydro energy, biomass energy and geothermal energy [11, 12, 13].

1.2.2.1. Solar energy

This energy based on the conversion of the sunlight; which are used either to generate electricity directly using photovoltaic cells (Solar Photovoltaic (PV)) or mirrors to produce heat to warm water (solar thermal) [11, 12, 13].

- *Advantages*
 - Its advantages and disadvantages
 - It is clean, silent and non-polluting source.
 - It is a free source and available every day.
 - It has a low maintenance cost.
- *Disadvantages*
 - Cost of solar panels is still relatively high compared to other forms of energy.
 - Usually, a solar panel can convert 22% of the energy it gets from the sun into electrical energy, meaning it need a big surface area to produce the desired amount of energy.
 - Storage cell; battery technology needs to advance to hold electricity to cover of little to no sunshine.
 - Solar energy is not available at night and in raining season.
 - The pollution in the atmosphere can also degrade the quality and efficiency of photovoltaic cells.

1.2.2.2 Hydro-energy

Hydro-energy is energy derived from the force of moving water Most hydroelectric energy comes from the potential energy of dammed water driving a water turbine and generator. The power extracted from the water depends on the volume and on the difference in height between the source and the water's outflow. This height difference is called the head. The amount of potential energy in water is proportional to the head [13, 14].

There are four broad hydro-power topologies which are: run of river hydro-power, storage hydro-power, pumped storage hydro-power; offshore hydro-power and tidal hydropower.

One of the major advantages of hydroelectricity is the elimination of fuel. Because there is no

fuel combustion, there is little air pollution in comparison with fossil fuel plants and limited thermal pollution compared with nuclear plants.

1.2.2.3 Biomass energy

Biomass considered as an energy resource is fundamentally different from carbon free energy sources. It could generate energy and material products similar to the traditional ones produced by existing fossil fuel uses.

Biomass energy refers to fuels made from plants and animal wastes. The Biomass resource is organic matter in which the energy of sunlight is stored in chemical bonds. When the bonds between carbon, hydrogen and oxygen molecules are broken by digestion, combustion (or) decomposition these substances release stored energy [12, 13, 14].

1.2.2.4 Geothermal energy

Geothermal energy is the heat from the Earth. It's clean and sustainable. Resources of geothermal energy range from the shallow ground to hot water and hot rock found a few miles beneath the Earth's surface, and down even deeper to the extremely high temperatures of molten rock called magma. Geothermal heat pumps can tap into this resource to heat and cool buildings. A geothermal heat pump system consists of a heat pump, an air delivery system (ductwork), and a heat exchanger-a system of pipes buried in the shallow ground near the building [12,13, 14].

1.2.2.5 Wind energy

Wind is a form of solar energy; where it caused by the uneven heating of the atmosphere by the sun. The irregularities of earth's surface, and rotation of the natural movement of the air, especially is the form of a current of air bellowing from a particular direction; where the air flows from regions of higher pressure to regions of lower pressure. This wind flow or motion energy can be used to generate electricity using turbines [12, 13, 14].

Ever since the days of sailing ships, it has been recognized that some areas of the earth's surface have higher wind speeds than others. Terms like doldrums, horse latitudes, and trade winds are well established in literature. A very general picture of prevailing winds over the surface of the earth is shown in Figure 1.4. In some large areas or at some seasons, the actual pattern differs strongly from this idealized picture. These variations are due primarily to the irregular heating of the earth's surface in both time and position [15].

Wind flow patterns are modified by the earth's terrain, bodies of water, and vegetative cover. The best places to built wind farms are in coastal areas, where the wind is strong and stables. These places include round hills, open plains and gaps in mountains. Sometimes the best place to put wind turbines is off shore, on the ocean's surface [16].

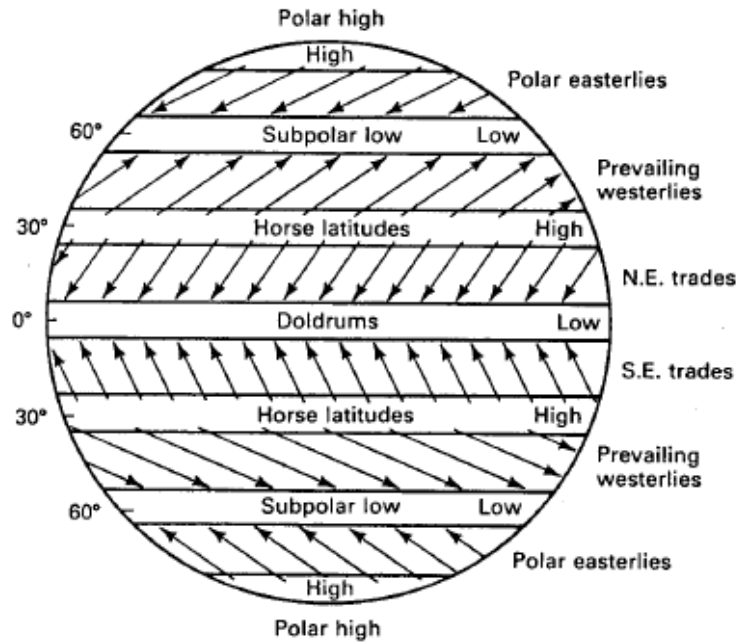


Figure 1.4. prevailing winds over the surface of the earth [15].

Figure 1.5 and Figure 1.6 show the best places of the air circulation in the earth and in Algeria respectively. The most promising sites are in Algeria are situated in the region of Adrar in the south with wind speed around 6 to 7 m/s, and Tiaret in the north-west of the country with wind speed equal around 5 to 6 m/s (as shown Figure 1.6) [17].

1.2.2.6 Wind power Statistics

Wind Energy is the most mature and developed renewable energy. In 2016, increase in wind generation was equal to almost half of global electricity growth; the worldwide total cumulative installed electricity generation capacity from wind power amounted to 496,790 MW, an increase of 12% compared to the previous year [18]; as shown Figure 1.7.

In most parts of the world wind energy supplies only a fraction of the total power demand, if there is any wind power production at all. In other regions, for example in China, USA, Germany, India, Spain and other some countries; wind energy supplies a significant amount of the total energy demand. In 2015, wind energy supplied around 145,362 MW of the total system demand by energy penetration of 33.6 % in China. Where, in USA; it supplied around 74,174 MW of the total system demand by energy penetration of 17.2% [18].

In Algeria the most promising sites are situated in the region of Adrar in the south where Sonalgaz commissioned 12 turbines to the Spanish manufacturer Gamesa totaling 10 MW in 2014. The program for development of renewable energies 2011-2030 adopted by the government in February 2011, renewable energies is placed at the heart of energy and economy policies led. The renewable consistency of the program to realize for national market needs over the period 2015-2030 is 22 000 MW, among whom more than 4500 MW will be realized before 2020, with 5010 MW for the wind energy installation [19, 20].

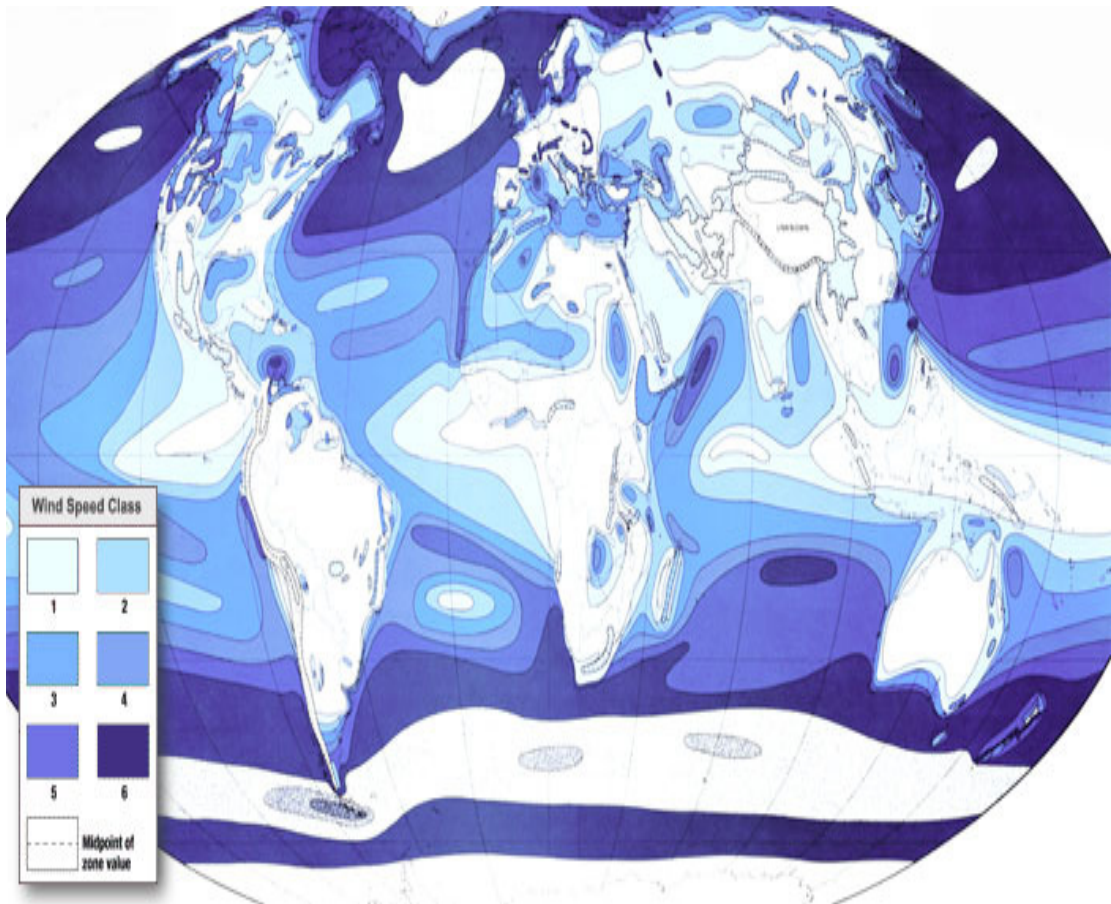


Figure 1.5. The best places of the air circulation in the earth [16].

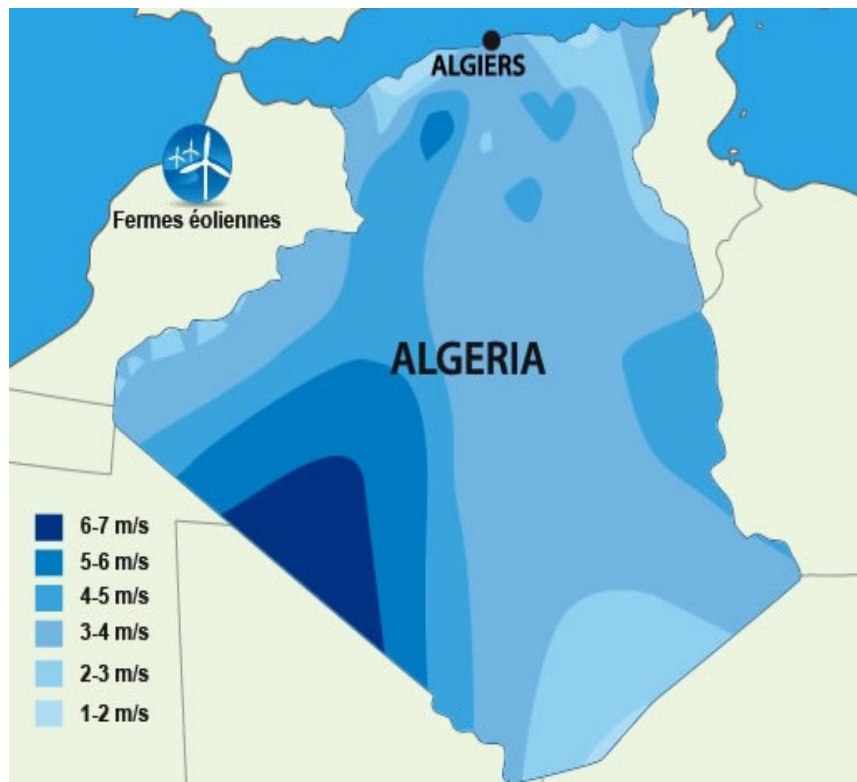


Figure 1.6 The best places of the air circulation in Algeria [17].

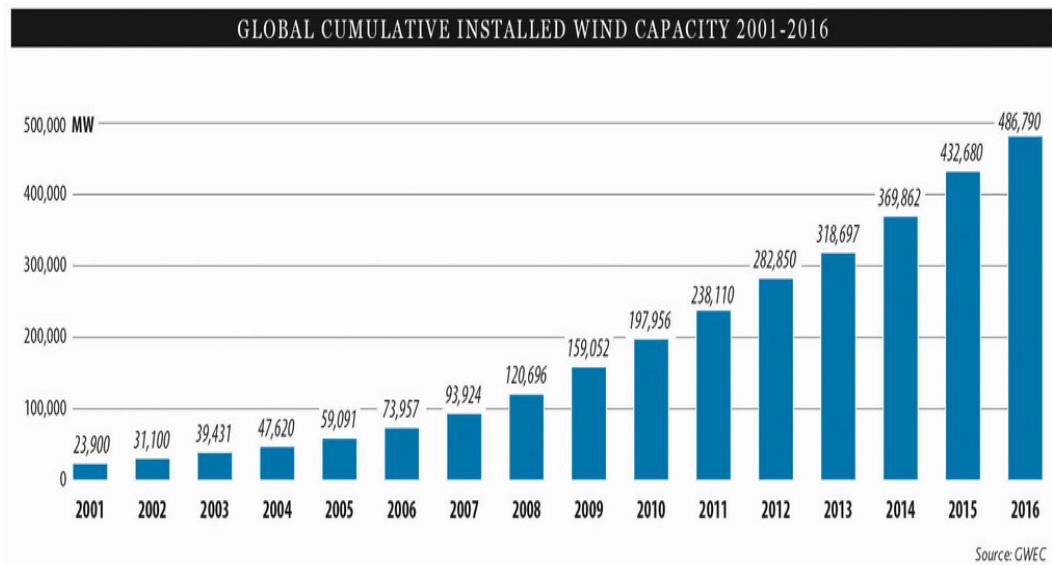


Figure 1.7. Global Cumulative Installed Capacity 2001-2016 [18].

1.3. Wind turbine system

Wind power has been used since antiquity to move boats powered by sails or to operate the machinery of mills to move their blades. Since the early twentieth century, it produces energy through wind turbines which permit to transmit the wind energy into electricity. These wind turbines are often grouped together in wind farms to make better use of energy, reducing environmental impact. They are especially useful in places where it's hard to transport fuel.

1.3.1. History

Denmark was the first country to use the wind for generation of electricity. The Danes were using a 23 m diameter wind turbine in 1890 to generate electricity. By 1910, several hundred units with capacities of 5 to 25 kW were in operation in Denmark. About 1925, commercial wind-electric plants using two- and three-bladed propellers appeared on the American market. The most common brands were Wincharger (200 to 1200W) and Jacobs (1.5 to 3 kW). These were used on farms to charge storage batteries which were then used to operate radios, lights, and small appliances with voltage ratings of 12, 32, or 110 volts. A good selection of 32 Vdc appliances was developed by industry to meet this demand. Then the Rural Electric Administration (REA) was established by Congress in 1936. Low interest loans were provided so the necessary transmission and distribution lines could be constructed to supply farmers with electricity. In the early days of the REA, around 1940, electricity could be supplied to the rural customer at a cost of 3 to 6 cents per kWh. The corresponding cost of wind generated electricity was 12 to 30 cents per kWh when interest, depreciation, and maintenance were included. The lower cost of electricity produced by a central utility plus the greater reliability led to the rapid demise of the home wind electric generator [21, 22,].

1.3.2. Types of Wind Turbines

In the different weather of the world; wind turbines must be built to withstand and operate under any strong storms whether: coast or deserts, cold polar or hot tropical conditions. Therefore, various wind turbine

concepts have been developed and built for maximizing the wind energy output, minimizing the turbine cost, and increasing the turbine efficiency and reliability. They can be classified according to the turbine generator configuration, airflow path relatively to the turbine rotor, turbine capacity, the generator-driving pattern, the power supply mode, and the location of turbine installation.

1.3.2.1. Wind turbines axis types

There are mainly two types of wind turbine: The horizontal axis wind turbine (HAWT) and the vertical axis wind turbine (VAWT) are classified or differentiated by the axis of rotation the rotor shafts.

a) Horizontal Axis Wind Turbines

HAWTs have a horizontal rotor shaft and an electrical generator which is both located at the top of a tower and can be further classified as upwind and downwind wind turbines as shown figure. The majority of horizontal-axis wind turbines being used today are upwind turbines, in which the wind rotors face the wind. The main advantage of upwind designs is to avoid the distortion of the flow field as the wind passes through the wind tower and nacelle.

For a downwind turbine, wind blows first through the nacelle and tower and then the rotor blades. This configuration enables the rotor blades to be made more flexible without considering tower strike. However, because of the influence of the distorted unstable wakes behind the tower and nacelle, the wind power output generated from a downwind turbine fluctuates greatly.

b) Vertical Axis Wind Turbines

VAWTs are designed with a vertical rotor shaft and generator and gearbox are placed at the bottom of the turbine, and a uniquely shaped rotor blade that is designed to harvest the power of the wind no matter which direction is it blowing like: Rotor Darrieus, Rotor Darrieus H and Rotor Hélicoïdale as shown Figure 1.8.

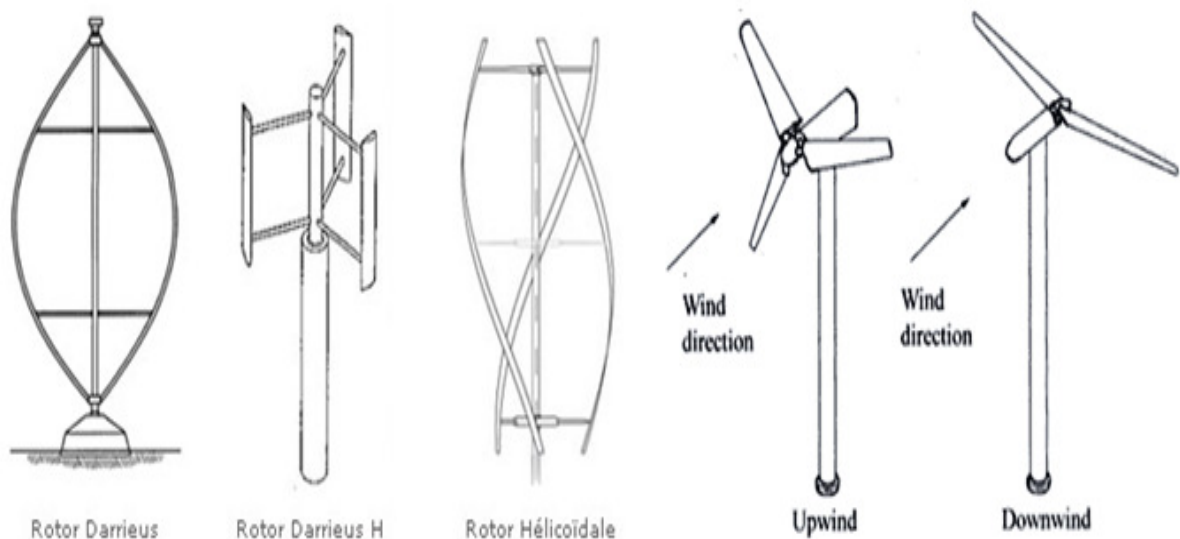


Figure 1.8. Axis wind turbine types [54, 55].

1.3.2.2. Wind turbine capacity types

Wind turbines can be divided into a number of broad categories in view of their rated capacities: micro, small, medium, large, and ultra-large wind turbines.

- Micro wind turbines: with the rated power less than several kilowatts.
- Small wind turbines: with the output power less than 100 KW.
- Medium wind turbines: sizes with power ratings from 100 kW to 1 MW.
- Large wind turbines: with the output power up to 10 MW.
- Ultra-large wind turbines: with the capacity more than 10 MW.

1.3.2.3. Direct drive and geared drive wind turbine types

Wind turbines can be classified as either direct drive or geared drive groups. To increase the generator rotor rotating speed to gain a higher power output, a regular geared drive wind turbine typically uses a multi-stage gearbox to take the rotational speed from the low-speed shaft of the blade rotor and transform it into a fast rotation on the high-speed shaft of the generator rotor.

The advantages of geared generator systems include lower cost and smaller size and weight. However, utilization of a gearbox can significantly lower wind turbine reliability and increase turbine noise level and mechanical losses. As the contrast, most of small wind turbines are off-grid for residential homes, farms, telecommunications, and other applications.

1.3.2.4. Fixed speed and variable speed wind turbine types

Wind turbines can operate either with a fixed speed or a variable speed. In the early 1990s the standard installed wind turbines operated at fixed speed. That means that the turbine is directly connected to the electrical grid according to Figure 1.9 which shows a Fixed-speed wind turbine with an induction generator; and regardless of the wind speed, the wind turbine's rotor speed is fixed and determined by the frequency of the supply grid, the gear ratio and the generator design. During the past few years the variable-speed wind turbine has become the dominant type among the installed wind turbines. In the variable-speed wind turbine, the generator is controlled by power electronic equipment, which makes it possible to control the rotor speed as shown Figure 1.10. In this way the power fluctuations caused by wind variations can be more or less absorbed by changing the rotor speed. Hence, the power quality impact caused by the wind turbine can be improved compared to a fixed-speed turbine [37].

There are various constructions for variable speed wind turbine will be presented as follow:

- Variable-speed wind turbine equipped with a cage-bar induction generator or synchronous generator.
- Variable-speed wind turbine equipped with multiple-pole synchronous generator or multiple-pole permanent-magnet synchronous generator.
- Variable-speed wind turbine equipped with a doubly-fed induction generator.

There are also other existing wind turbine concepts; a description of some of these systems can be found in [37].

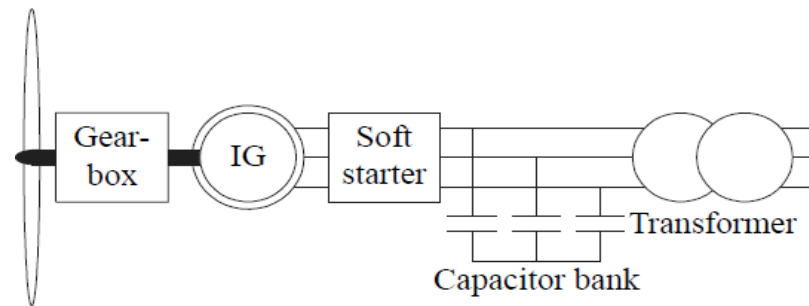


Figure 1.9. Fixed-speed wind turbine with an induction generator.

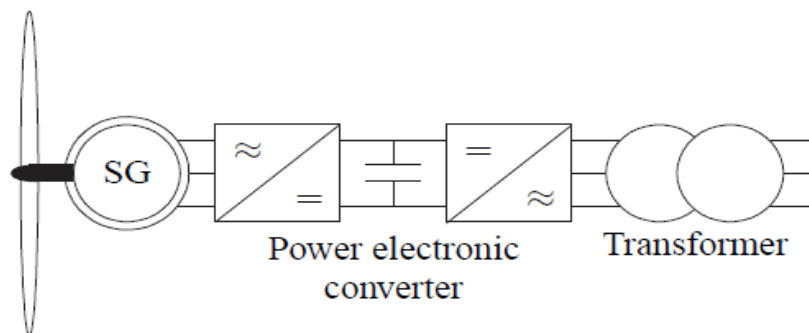


Figure 1.10. Variable-speed wind turbine with a synchronous/induction generator.

1.3.2.5. Onshore and offshore wind turbine types

A large wind farm may consist of several hundred individual wind turbines which are connected to the electric power transmission network and can be located either in-land which named: onshore wind turbine farm or in bodies of water which named: offshore wind turbine farm.

There are a number of advantages of onshore turbines, including lower cost of foundations, easier integration with the electrical-grid network, lower cost in tower building and turbine installation, and more convenient access for operation and maintenance. However, offshore wind turbines can make higher power output and operate more hours each year compared with the same turbine installed onshore.

1.3.3. Wind turbine configuration and work

Most of the modern large wind turbines are horizontal-axis turbines with typically three blades. As shown in Figure 1.11, a wind turbine is comprised of a nacelle, foundation, tower and blades. It operates on a simple principle. The energy in the wind turns three propeller-like blades around a rotor. The rotor is connected to the main shaft, which spins a generator to create electricity [23, 24, 25, 26].

a) Foundation

The foundation holds the turbine in place in the ground. A wind turbine has to have a strong foundation to handle strong winds and support the overall height and the length of the blades. As shown figure, it's

classified as follow: (a) Mono-pile; (b) tri-pod; (c) jackets; (d) Gravity foundation [23, 24, 25, 26].

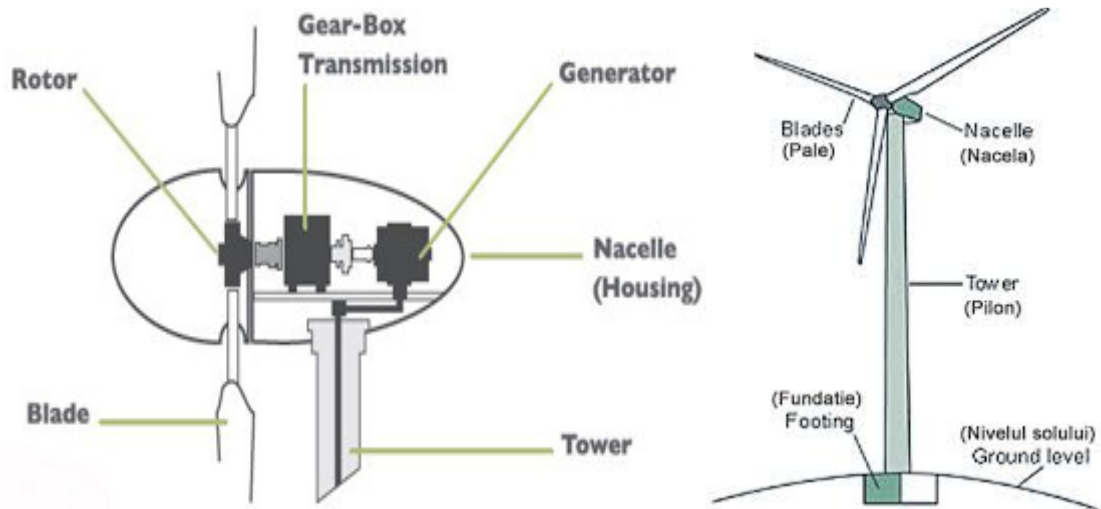


Figure 1.11. Wind turbine configuration [56].

b) Tower

Generation equipment is kept in the tower. The tower raises the blades and generation equipment high above the ground into the smoother, stronger wind currents. Access to the nacelle and rotor is through the tower [23, 24, 25, 26].

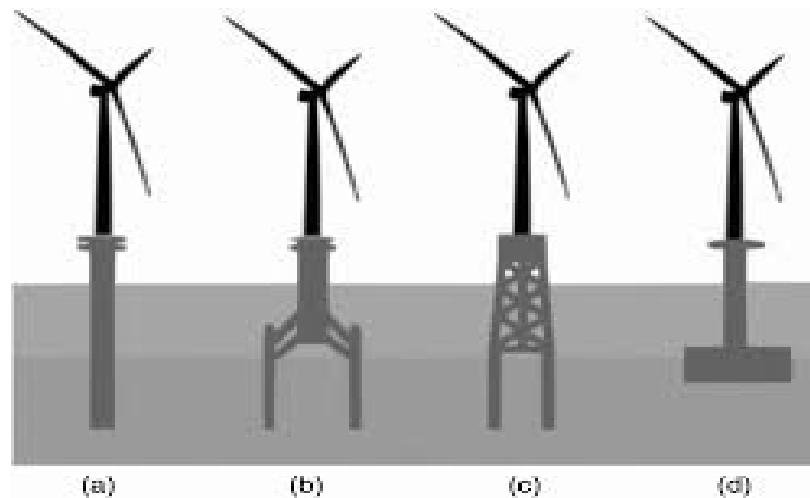


Figure 1.12. Wind turbine foundation types [56].

c) Nacelle

The nacelle is the heart of the turbine, where the generator, gearbox and rotor are held. The generator inside the nacelle is used to convert the wind energy into electrical energy [23, 24, 25, 26].

d) Gearbox

The rotational speed of a wind turbine is fairly low and must therefore be adjusted to the electrical frequency. This can be done in two ways: with a gearbox or with the number of pole pairs of the generator. The number of pole pairs sets the mechanical speed of the generator with respect to the electrical frequency

and the gearbox adjusts the rotor speed of the turbine to the mechanical speed of the generator [23, 24, 25, 26].

e) *Blades*

Most wind turbines have three blades that are attached to the rotor [23, 24, 25, 26].

1.3.4. *Wind Power and wind power Density (WPD)*

Wind energy systems convert the kinetic energy of the wind into the electrical energy. The kinetic energy produced by a moving object is expressed as [27]:

$$E = \frac{1}{2}mV^2 \quad (1.1)$$

Wind power density is measure of capacity of wind resources in specified site. It is well known that the power of wind that flows at (v) through a blade swept area (S= 1m²) increases as the cube of its velocity by (W/m²) and is given by [27]:

$$WPD = \frac{1}{2}\rho V^3 \quad (1.2)$$

This method permits the evaluation for the wind speed density of any places before the installation of turbines. Table shows the wind turbine density with speed variation in the coast at temperature equal to 15° [27].

Table 1.1. Wind Power Density [27]

Wind speed [m/s]	Wind power density [W/m ²]
<100	<5.5
100-200	5.5-6.9
200-400	6.9-8.7
400-600	8.7-9.9
600-800	9.9-10.9
800-1000	10.9-11.8
1000-2000	11.8-14.8

1.3.5. *Betz limit*

The coefficient of power of a wind turbine (C_p) is a measurement of how efficiently the wind turbine converts the energy in the wind into electricity as follow [27, 29, 30]:

$$C_p = \frac{\text{Electricity produced by wind turbine}}{\text{Total Energy available in the wind}} \quad (1.3)$$

Wind turbines extract energy by slowing down the wind. For a wind turbine to be 100% efficient it would need to stop 100% of the wind - but then the rotor would have to be a solid disk and it would not turn and no kinetic energy would be converted. On the other extreme, if you had a wind turbine with just one rotor blade, most of the wind passing through the area swept by the turbine blade would miss the blade completely and so the kinetic energy would be kept by the wind.

The theoretical maximum efficiency of an ideal wind turbo-machine was derived by Lanchester in 1915 and Betz in 1920 [31]. It was revealed that no wind turbine could convert more than 59.3% (16/27) of the kinetic energy of the wind into mechanical energy turning a rotor. This is known as Lanchester–Betz limit (or Lanchester–Betz law). However; in the reality and with the exciting of losses in the wind energy system parts; the turbine cannot convert totally the wind energy into electricity. On account of this the good wind turbines generally fall in the 35-45% range [27, 29, 30].

1.4. Variable-Speed Wind Turbine based on Doubly-Fed Induction Generator system modeling

Figure 1.13, consists of a wind turbine with doubly-fed induction generator. This means that the stator is directly connected to the grid while the rotor winding is connected via slip rings to a converter. This system has recently become very popular as generators for variable-speed wind turbines [28]. This is mainly due to the fact that the power electronic converter only has to handle a fraction (20–30%) of the total power. Therefore, the losses in the power electronic converters can be reduced, compared to a system where the converter has to handle the total power. In addition, the cost of the converter becomes lower [31].

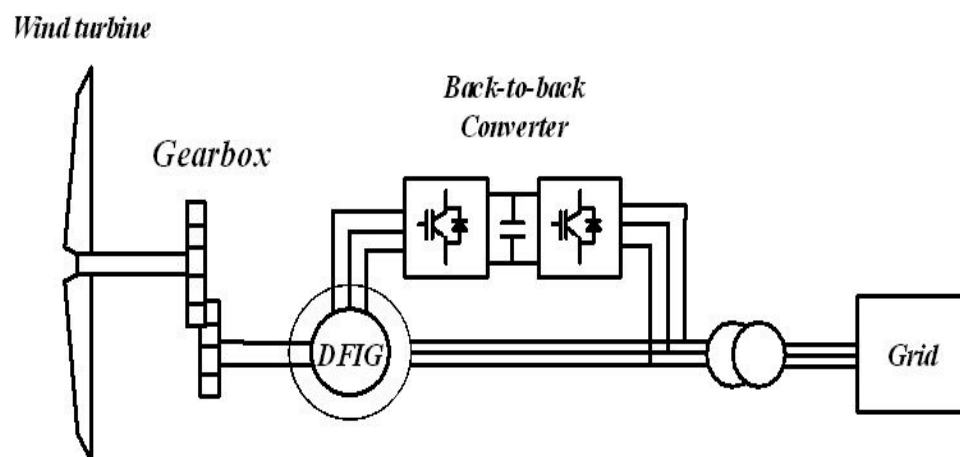


Figure 1.13. Variable-speed wind turbine with a doubly-fed induction generator.

1.4.1. Wind turbine modeling

1.4.1.1. Power content of free flowing wind stream

The power content in cylindrical column of free unobstructed air moving at a constant speed V is the rate of change in its kinetic energy [33, 34]:

$$P = \frac{dE}{dt} \quad (1.4)$$

Expressing the kinetic energy as:

$$E = \frac{1}{2}mV^2 \quad (1.5)$$

Substituting from Equations 1.4 and 1.5, we get:

$$P = \frac{dE}{dt} = \frac{d}{dt} \left(\frac{1}{2}mV^2 \right) \quad (1.6)$$

By the simplification; the power can be expressed in terms of its speed V and its mass flow rate for a constant wind speed as:

$$P = \frac{1}{2} \left(\frac{d}{dt} (mV^2) \right) = \frac{1}{2} \dot{m} V^2 \quad (1.7)$$

If the cross sectional area of column of air is S , and its density is ρ , the mass flow rate is:

$$\dot{m} = \rho SV \quad (1.8)$$

Substituting from Equations 1.7 and 1.8, we get:

$$P = \frac{1}{2} \rho SV^3 \quad (1.9)$$

Where: $S = \frac{\pi D^2}{4}$

As we see in Equation 1.9; the power content of the cylindrical of air is proportional to the square of its diameter D , and more significantly to the cube of its speed V .

1.4.2. Doubly Fed Induction Machine modeling

Large doubly fed electric machines in the industry are three-phase wound-rotor type. Although their principles of operation have been known for decades, the massive application has only recently entered and is almost exclusively due to the advent of wind power technologies.

The main advantage of doubly fed induction generator when used in wind turbines is that it has the ability to maintain the amplitude and the frequency of the output voltage essentially constant at grid values, no matter the speed of the wind turbine rotor. Because of this, doubly-fed induction generator can be directly connected to the AC power network and remain synchronized at all times. Other advantages include the ability to control reactive power from the rotor circuits to the grid, which enables the DFIG to support the voltage stability and power factor correction at the point of common coupling (PCC) [35, 36, 37].

1.4.2.1 Principle Operation of DFIG

Doubly fed electric machines are electric motors or electric generators that have windings on both stationary and rotating parts, where both windings transfer significant active power between shaft and electrical system. Usually the stator winding is directly connected to the three-phase grid and the three-phase rotor winding is fed from the grid through a rotating or static frequency converter [35, 36, 37].

Both stator and rotor have three sinusoidally distributed windings, corresponding to three phases, displaced by 120° . The three phases are called a, b and c. The stator has p pairs of poles. The rotor is connected to the grid through converters. Three-winding transformer gives different voltage levels for stator and rotor side. A schematic of such a system is presented in Figure 1.14. When the machine produces energy, only a small part of the generated power flows from the rotor to the grid. The converters can then be chosen in accordance with this small rotor power [35, 36, 37].

The stator windings are connected to the grid which imposes the stator current frequency f_s . The stator currents create a rotating magnetic field in the air gap. The rotational speed of this field, ω_s , is proportional to the stator frequency as follow:

$$\omega_s = 2\pi f_s \quad (1.10)$$

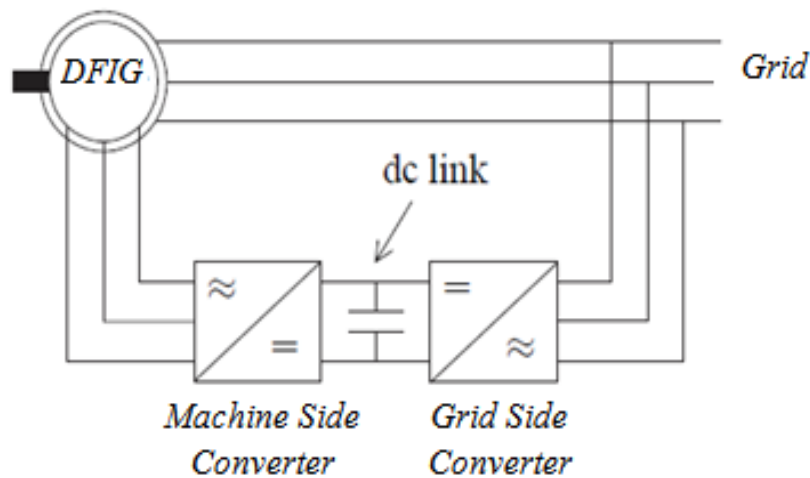


Figure 1.14. DFIG with its converters.

If the rotor spins at a speed different from that of the rotational field, it sees a variation of magnetic flux. Therefore, by Faraday's law of induction, currents are induced in the rotor windings. The rotor mechanical speed ω_m and the rotor electrical speed ω_r are defined by:

$$\omega_m = \omega_s \pm \omega_r \quad (1.11)$$

$$\omega_m = p\Omega \quad (1.12)$$

The flux linked by the rotor windings change with time if $\omega_r \neq \omega_s$. The machine operates usually as a generator if $\omega_r > \omega_s$ and as a motor otherwise.

The slip, s , defines the relative speed of the rotor compared with that of the stator:

$$s = \frac{f_r}{f_s} = \frac{(\omega_s - \omega_m)}{\omega_s} \quad (1.13)$$

In Equation 1.11; the positive (+) sign means that the stator and rotor magnetic fields rotate in the same direction ($\omega_m < \omega_s$) which named Sub-synchronous; however, the negative (-) sign means that the stator and rotor magnetic fields rotate in the opposite direction ($\omega_m > \omega_s$) which named super-synchronous [35, 36, 37].

The slip is usually negative for a generator and positive for a motor. The currents induced in the rotor windings pulse at an angular speed defined by the difference between the synchronous speed and the rotor speed. Indeed, the stator currents at ω_r see the rotating magnetic field created by the stator pulsating at $\omega_s - \omega_r$. It means the frequency of the rotor currents, f_r is:

$$f_r = s \cdot f_s \quad (1.14)$$

If the rotor were to rotate at the synchronous speed, it would not see any change in magnetic fluxes. No currents would then be induced in its windings. Therefore, the machine operates always at speeds different from synchronous speed.

The rotor-side inverter controls the rotor currents, from Equation 1.13, it can be noted that for controlling the rotor currents it must be control the slip and so the speed of the machine.

Doubly fed machines are typically used in applications that require varying speed of the machine's shaft in a limited range around the synchronous speed, for example $\pm 30\%$, because the power rating of the frequency converter is reduced similarly.

1.4.2.1.1. Sub-synchronous and super-synchronous

The machine is operated in the sub-synchronous mode, at, $\omega_m < \omega_s$, if and only if its speed is exactly $\omega_m = \omega_s - \omega_r > 0$ and both the phase sequences of the rotor and stator mmf's are the same and in the positive direction, as referred to as positive phase sequence ($\omega_r > 0$) and it is positive for negative slip (speed greater than synchronous speed). The machine is operated in the super-synchronous mode, i.e., $\omega_m > \omega_s$, if and only if its speed is exactly $\omega_m = \omega_s - (-\omega_r) = \omega_s + \omega_r > 0$, and the phase sequence in the rotor rotates in opposite direction to that of the stator, negative phase sequence ($\omega_r < 0$).

Therefore, the DFIG is able to work as a generator in both sub-synchronous (positive slip $s > 0$) and over-synchronous (negative slip $s < 0$) operating area. Depending on the operating condition of the drive, the power is fed in or out of the rotor. If ($P_{rotor} < 0$): it is flowing from the grid via the converter to the rotor in sub-synchronous mode or vice versa ($P_{rotor} > 0$) in over-synchronous mode. In both cases (sub-synchronous and over-synchronous) the stator is feeding energy to the grid ($P_{stator} > 0$) [37, 38].

1.4.2.2. Mathematical Models of the DFIG System

In order to study and analyses the DFIG working, it was necessary to obtain its general mathematical model which enables us to know the equations that describe its work in the both transient and steady states.

Therefore, we start by studying the equivalent circuit and static model of the machine in a, b, c frame then moving to d, q frame, showing the differences and conversion mechanisms between the two frames [35, 36, 37, 38].

We note here that the DFIG must be subject to certain hypotheses which permit to simplify the mathematical model as follow [38, 50]:

- The three phase windings placed on the stator and in the rotor are identical with a similar difference of phase.
- The machine Air-gap is also supposed to be constantly thick (close slots in an ideal approach).
- The magneto-motive forces created by different stator and rotor phases are spread in a sinusoidal way along the air gap, which permit to produce with turn a sinusoidal magnetic flux in the air-gap.
- The magnetic fields are not saturated, are not submitted to the hysteresis phenomenon and are not the center of Foucault's currents.
- The temperature in the motor stays constant whatever the operating point is, which leads to constant parameters in mathematical models.
- Balanced stator and rotor windings, with sinusoidally distributed winding.

1.4.2.2. 1. Equivalent representation and vectors formulation in a, b, c frame

Figure 1.15 shows stator and rotor windings of DFIG in a, b, c frame reference. Where, the stator and the rotor consist of three windings (each one) displaced between them by 120°. The rotor windings rotate with ω_m speed and create a mechanical angle with the stator windings which named θ_r . This angle is changing by time as follow [39]:

$$\theta_r = \theta_0 + \int_0^t \omega_r \cdot dt \quad (1.15)$$

Where θ_0 is the initial position of the rotor from the stator at time $t=0$, and ω_r is the magnetic flux speed produced by the rotor which calculate as follow:

$$\omega_r = \frac{d\theta_r}{dt} \quad (1.16)$$

a) Electrical equations

The equivalent circuit of the doubly fed induction machine in a, b, c frame is given as shown Figure 1.16. The subscripts r and s denote rotor and stator quantities, respectively. The subscripts a, b and c are used for phases a, b and c quantities, respectively. The symbols V and I are for voltages and currents and φ represents flux linkages.

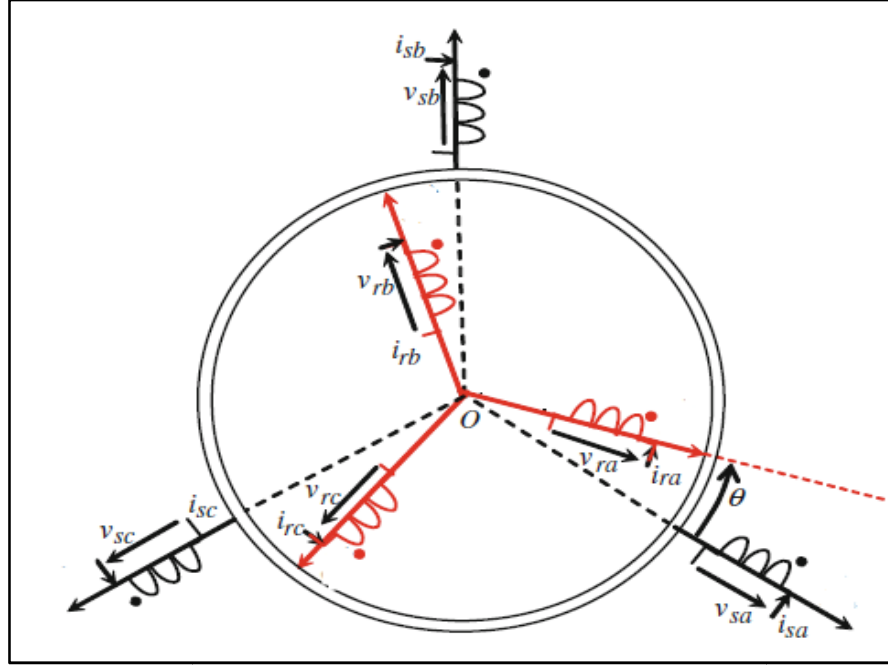


Figure 1.15. Stator and rotor windings of DFIG in a, b, c frame reference

Based on the a, b, c equivalent circuit model of the induction machine shown in Figure 1.16, the voltage equations on rotor and stator are obtained by Kirchhoff's and Faraday's law in a matrix form are as follow:

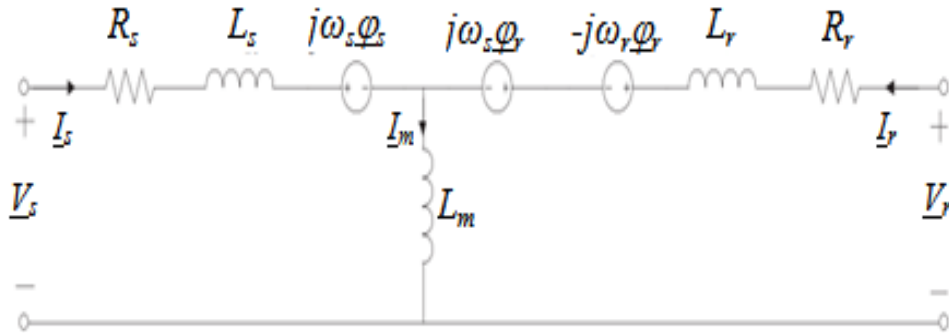


Figure 1.16. DFIG equivalent circuit

$$\begin{bmatrix} v_{sa} \\ v_{sb} \\ v_{sc} \end{bmatrix} = R_s \begin{bmatrix} i_{sa} \\ i_{sb} \\ i_{sc} \end{bmatrix} + \frac{d}{dt} \begin{bmatrix} \phi_{sa} \\ \phi_{sb} \\ \phi_{sc} \end{bmatrix} + j\omega_s \begin{bmatrix} \phi_{sa} \\ \phi_{sb} \\ \phi_{sc} \end{bmatrix} \quad (1.17)$$

$$\begin{bmatrix} v_{ra} \\ v_{rb} \\ v_{rc} \end{bmatrix} = R_r \begin{bmatrix} i_{ra} \\ i_{rb} \\ i_{rc} \end{bmatrix} + \frac{d}{dt} \begin{bmatrix} \phi_{ra} \\ \phi_{rb} \\ \phi_{rc} \end{bmatrix} + j(\omega_s - \omega_r) \begin{bmatrix} \phi_{ra} \\ \phi_{rb} \\ \phi_{rc} \end{bmatrix} \quad (1.18)$$

The stator and rotor windings resistances are R_s and R_r . They are assumed to be equal for all phase windings and they are done in a matrix form as follow:

$$R_s = \begin{bmatrix} R_s & 0 & 0 \\ 0 & R_s & 0 \\ 0 & 0 & R_s \end{bmatrix} \quad R_r = \begin{bmatrix} R_r & 0 & 0 \\ 0 & R_r & 0 \\ 0 & 0 & R_r \end{bmatrix}$$

We can write the flux terms as functions of the currents, via an equation for each flux of the form

$$\phi = \sum L_k I_k \quad (1.19)$$

Where the summation is over all six winding currents which symbolized with k . However, we must take note that there are four kinds of terms in each summation.

- Stator-stator terms: These are terms which relate a stator winding flux to a stator winding current. Because the positional relationship between any pair of stator windings does not change with rotor position, these inductances are not a function of rotor position; they are constants.
- Rotor-rotor terms: These are terms which relate a rotor winding flux to a rotor winding current. As in stator-stator-terms, these are constants.
- Rotor-stator terms: These are terms which relate a rotor winding flux to a stator winding current. As the rotor turns, the positional relationship between the rotor winding and the stator winding will change, and so the inductance will change. Therefore the inductance will be a function of rotor position, characterized by rotor angle θ .
- Stator-rotor terms: These are terms which relate a stator winding flux to a rotor winding current. As described for the rotor-stator terms, the inductance will be a function of rotor position, characterized by rotor angle θ .

The flux linkages related to the stator and rotor current windings are given as follow:

$$\begin{bmatrix} \phi_{sa} \\ \phi_{sb} \\ \phi_{sc} \end{bmatrix} = [L_s] \cdot \begin{bmatrix} i_{sa} \\ i_{sb} \\ i_{sc} \end{bmatrix} + [M_{sr}] \cdot \begin{bmatrix} i_{ra} \\ i_{rb} \\ i_{rc} \end{bmatrix} \quad (1.20)$$

$$\begin{bmatrix} \phi_{ra} \\ \phi_{rb} \\ \phi_{rc} \end{bmatrix} = [L_r] \cdot \begin{bmatrix} i_{ra} \\ i_{rb} \\ i_{rc} \end{bmatrix} + [M_{rs}] \cdot \begin{bmatrix} i_{sa} \\ i_{sb} \\ i_{sc} \end{bmatrix} \quad (1.21)$$

Note that L_s and L_r are respectively, the stator inductance matrix and rotor inductance matrix as shows below.

$$L_s = \begin{bmatrix} L_s & M_s & M_s \\ M_s & L_s & M_s \\ M_s & M_s & L_s \end{bmatrix} \quad L_r = \begin{bmatrix} L_r & M_r & M_r \\ M_r & L_r & M_r \\ M_r & M_r & L_r \end{bmatrix}$$

Where l_s and l_r are respectively the stator self-inductance and rotor self-inductance and they are similar for the three windings. M_s is the mutual induction exchanging between two distinct stator phases and M_r is the mutual induction exchanging between two distinct rotor phases.

The mutual induction between two distinct stator phases is written as follows:

$$M_{sa,b,c} = L_s \cos\left(\frac{2\pi}{3}\right) \quad (1.22)$$

M_{sr} and M_{rs} represent the mutual inductances exchanging between the stator phase and rotor phase which depend the angular position θ_r . Equation 1.23 shows the mutual inductances exchanging between stator phase and the three rotor phases.

$$\begin{cases} M_{sa,ra} = M \cos(\theta) \\ M_{sa,rb} = M \cos\left(\theta + \frac{2\pi}{3}\right) \\ M_{sa,rc} = M \cos\left(\theta - \frac{2\pi}{3}\right) \end{cases} \quad (1.23)$$

b) Mechanical equations

The dynamics of the generator shaft relate the rotor speed and the electromagnetic torque:

$$J \frac{d\omega_m}{dt} = T_m - T_{em} \quad (1.24)$$

Where J is the inertia of the machine, T_m is the mechanical torque and T_{em} is the electromagnetic torque.

1.4.2.2.2. Moving from three phase frame to bi-phase frame

a) Park and Clarke transformations

The behavior of three-phase machines is usually described by their voltage and current equations. The coefficients of the differential equations that describe their behavior are time varying. The mathematical modeling of such a system tends to be complex since the flux linkages, induced voltages, and currents change continuously as the electric circuit is in relative motion. For such a complex electrical machine analysis, mathematical transformations are often used to decouple variables and to solve equations involving time varying quantities by referring all variables to a common frame of reference.

From Equation 1.23; it can be seen that the inductance matrix in this model is rotor position dependent and hence time dependent, which means that the inductance matrix needs to be calculated at each time step, and thus this increases the computation time. Therefore, the induction machine model expressed in various dq reference frames will be chosen because of the advantages of simplicity of formulation, fast simulation time and ease of implementation [37].

Among the various transformation methods available, the well known are:

- **Clarke Transformation:** This transformation converts balanced three-phase quantities into balanced two-phase perpendicular stationary quantities [50, 51].
- **Park Transformation:** This transformation converts balanced three-phase quantities or vectors in balanced two-phase orthogonal stationary system into orthogonal rotating reference frame [50, 51].

The three reference frames considered in this implementation are presented in Figure 1.17 where we considerate the current as a vector:

Where:

- Three-phase reference frame, in which I_a , I_b , and I_c are co-planar three-phase quantities at an angle of 120° degrees to each other.
- Orthogonal stationary reference frame, in which I_α (along α axis) and I_β (along β axis) are perpendicular to each other, but in the same plane as the three-phase reference frame.
- Orthogonal rotating reference frame, in which I_d is at an angle θ (rotation angle) to α axis and I_q is perpendicular to I_d along the q axis.

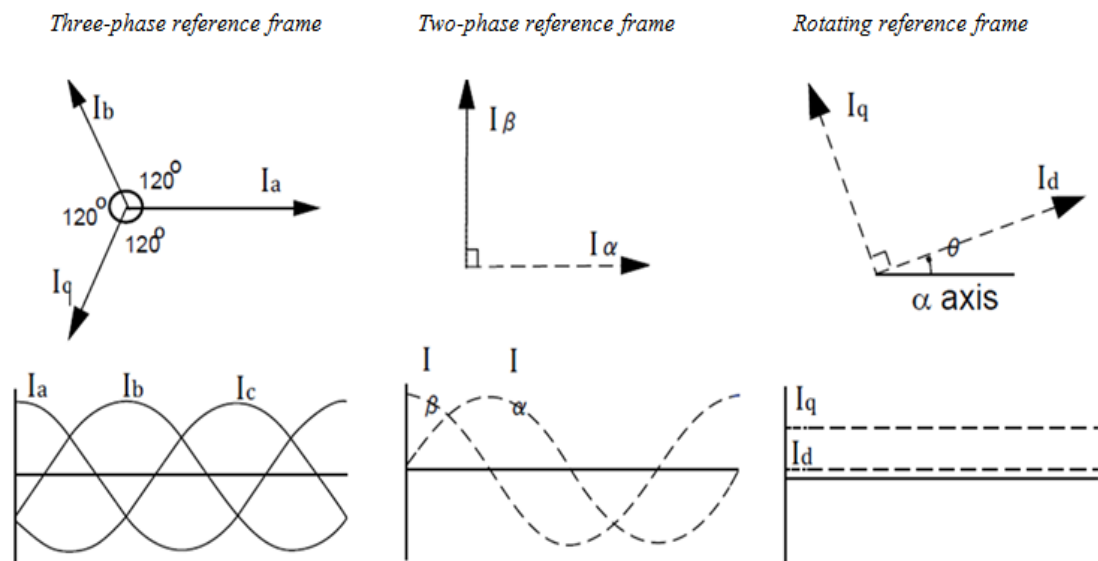


Figure 1.17. reference frames

a) Park transformation

In the case of balanced three phase circuits, application of dq rotating transformation reduces the three AC quantities to 2 quantities which rotate with random angular speed named ω_k . Simplified calculations can then be carried out on these imaginary quantities before performing the inverse transformation to recover the actual three phase ac results [51, 52].

The dq transformations (direct transformation and inverse transformation) applied to three phase unknown vector (named X which describe the electrical components) are shown below in Equations 1.24 and 1.25.

$$[X_{dq0}] = [T_{dq0}(\theta_k)] \cdot [X_{abc}] \quad (1.24)$$

The constants K and k_0 are chosen differently by different authors in order to obtain magnitudes preserve or power reserve [39, 52].

$$\begin{bmatrix} X_d \\ X_q \\ X_0 \end{bmatrix} = K \begin{bmatrix} \cos(\theta_k) & \cos(\theta_k - \frac{2\pi}{3}) & \cos(\theta_k + \frac{2\pi}{3}) \\ -\sin(\theta_k) & -\sin(\theta_k - \frac{2\pi}{3}) & -\sin(\theta_k + \frac{2\pi}{3}) \\ k_0 & k_0 & k_0 \end{bmatrix} \begin{bmatrix} X_a \\ X_b \\ X_c \end{bmatrix} \quad (1.25)$$

One popular choice is $K=2/3$ and $k_0=1/2$, which causes the magnitude of the d-q quantities to be equal to that of the three-phase quantities. However, these constants equal to $k_0=1/\sqrt{2}$, $K=\sqrt{(2/3)}$ to get a power invariant expression.

Under balanced conditions, X_0 is zero.

$$X_0 = k_0(X_a + X_b + X_c) = 0 \quad (1.26)$$

The inverse Park transformation becomes:

$$[X_{dq0}] = [T_{dq0}(\theta_k)]^{-1} \cdot [X_{abc}] \quad (1.27)$$

Where:

$$[T_{dq0}(\theta_k)]^{-1} = \begin{bmatrix} \cos(\theta_k) & -\sin(\theta_k) & 1 \\ \cos(\theta_k - \frac{2\pi}{3}) & -\sin(\theta_k - \frac{2\pi}{3}) & 1 \\ \cos(\theta_k + \frac{2\pi}{3}) & -\sin(\theta_k + \frac{2\pi}{3}) & 1 \end{bmatrix}$$

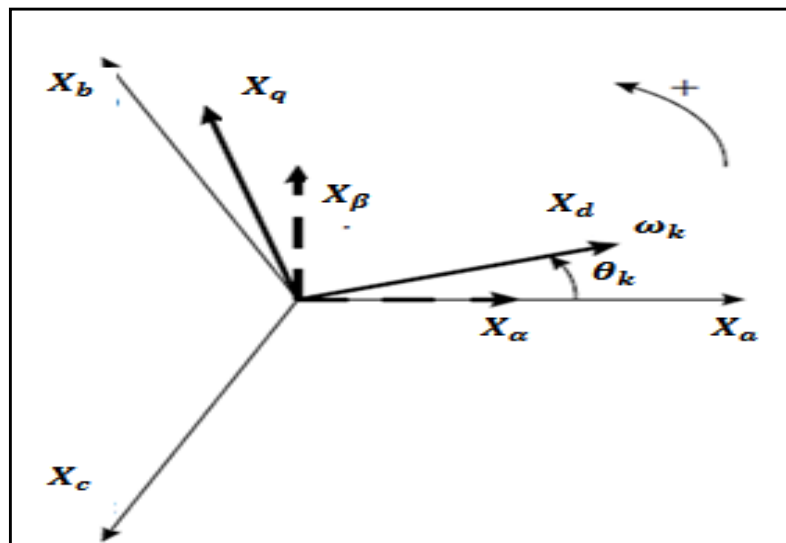


Figure 1.18. Combined vector representation

b) Clarke Transformation

The three-phase quantities are translated from the three-phase reference frame to the two-axis orthogonal stationary reference frame using Clarke transformation as shown in Figure 1.18. The Clarke transformation is expressed by the following equations:

$$[X_{\alpha\beta 0}] = [T_{\alpha\beta 0}(\theta_k)] \cdot [X_{abc}] \quad (1.28)$$

$$[T_{\alpha\beta 0}] = K \begin{bmatrix} 1 & -\frac{1}{2} & -\frac{1}{2} \\ 0 & \frac{\sqrt{3}}{2} & -\frac{\sqrt{3}}{2} \\ k_0 & k_0 & k_0 \end{bmatrix} \quad (1.29)$$

Where the constants K and k_0 is chosen as we have already mentioned. The inverse Clarke transformation becomes:

$$[T_{\alpha\beta 0}] = \begin{bmatrix} 1 & 0 & 1 \\ -\frac{1}{2} & \frac{\sqrt{3}}{2} & 1 \\ -\frac{1}{2} & -\frac{\sqrt{3}}{2} & 1 \end{bmatrix} \quad (1.30)$$

1.4.2.2.3. Modeling of DFIG in dq reference frame

In the dq frame, the inductance parameters become constant, independent of position. Figure 1.19 shows stator and rotor windings of DFIG in dq frame reference rotates with ω_k . Where, the perpendicular dq axis is equivalent to the abc axis in the stator and in the rotor. The angular position between the a -stator axis and d_s axis is named θ_k , and between a -rotor axis and d_r axis equal to $(\theta_k - \theta)$; where θ is the angular position between the stator and the rotor [37, 39].

Among possible choices of dq frames are the following [37, 39]:

- Stator frame where $\omega_k = 0$;
- Rotor frame where $\omega_k = \omega_m$;
- Synchronous frame associated with the frequency $\omega_k = \omega_s$;
- Rotor flux frame in which the d-axis lines up with the direction of the rotor flux vector.

a) Electrical relations

The equivalent circuit of the doubly fed induction machine in dq frame is given as shown Figure 1.20.

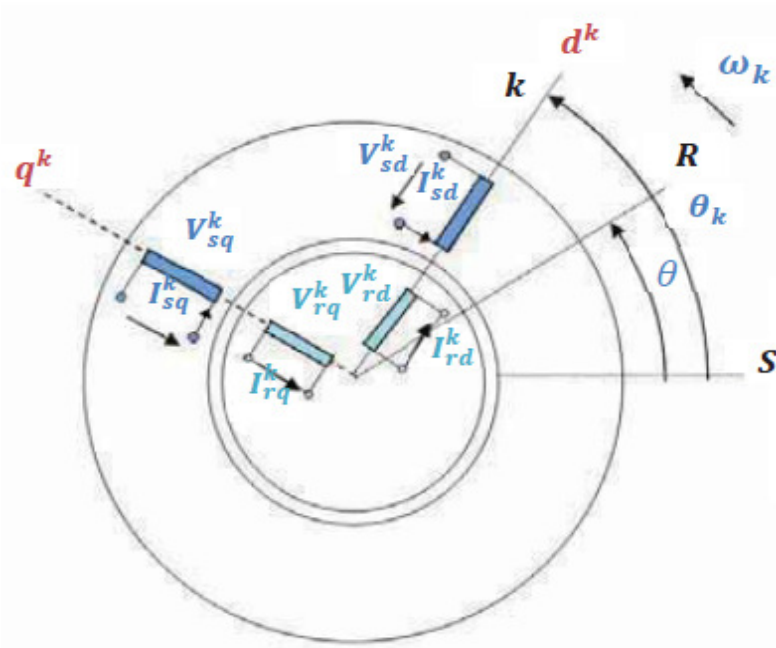


Figure 1.19. stator and rotor windings of DFIG in dq frame reference rotates with ω_k .

The differential equations of the induction machine stator and rotor voltage windings described in vector mode and in dq reference frame are shown in Equation 1.33. Here, d_s and q_s , are the stator direct and quadrature axes components, while d_r and q_r , are the rotor direct and quadrature axes components.

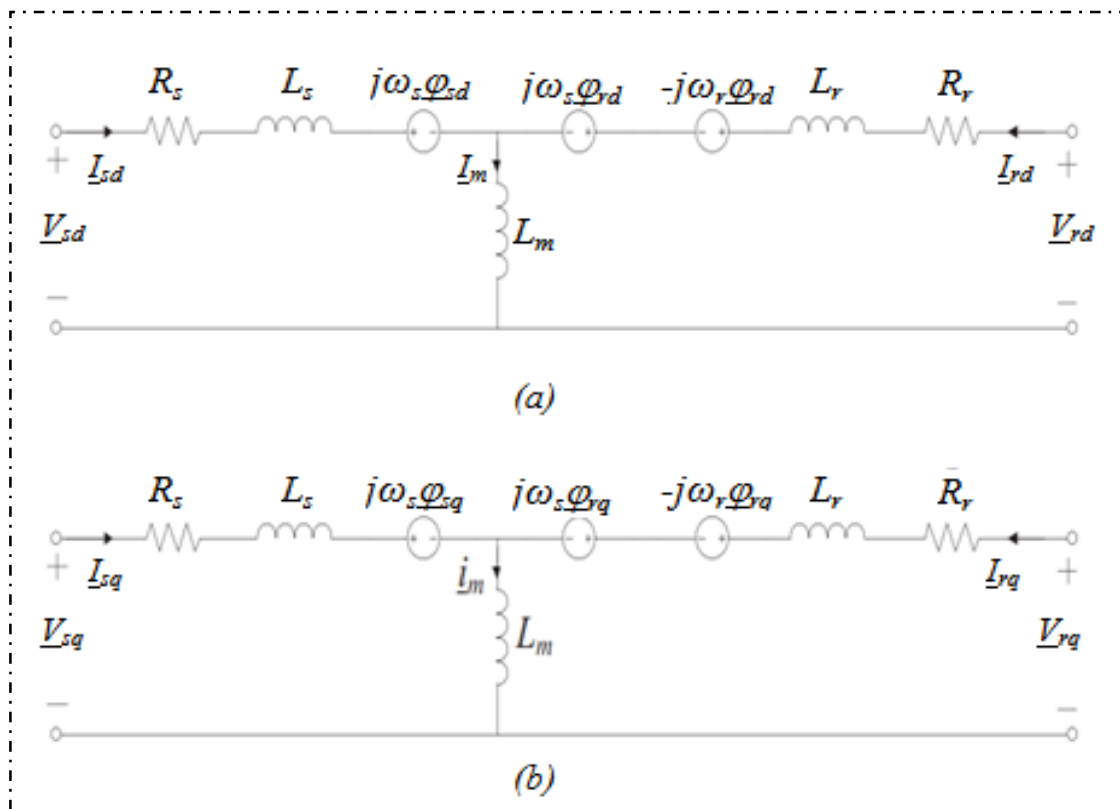


Figure 1.20. DFIG equivalent circuit in dq frame

$$\left\{ \begin{array}{l} V_{sd} = R_s I_{sd} + \frac{d\varphi_{sd}}{dt} - \frac{d\theta_k}{dt} \varphi_{sd} \\ V_{sq} = R_s I_{sq} + \frac{d\varphi_{sq}}{dt} + \frac{d\theta_k}{dt} \varphi_{sq} \\ V_{so} = R_s I_{so} + \frac{d\varphi_{so}}{dt} \end{array} \right. \quad (1.33)$$

$$\left\{ \begin{array}{l} V_{rd} = R_r I_{rd} + \frac{d\varphi_{rd}}{dt} - \frac{d(\theta_k - \theta_r)}{dt} \varphi_{rd} \\ V_{rq} = R_r I_{rq} + \frac{d\varphi_{rq}}{dt} + \frac{d(\theta_k - \theta_r)}{dt} \varphi_{rq} \\ V_{ro} = R_r I_{ro} + \frac{d\varphi_{ro}}{dt} \end{array} \right. \quad (1.34)$$

Where, $(\theta_k - \theta_r) = \theta$.

Under balanced conditions, X_0 is zero, and therefore it produces no flux at all.

Relationships between vectors of magnetic fluxes and vectors of stator and rotor currents are:

$$\left\{ \begin{array}{l} \varphi_{sd} = L_s I_{sd} + M_{sr} I_{rd} \\ \varphi_{sq} = L_s I_{sq} + M_{sr} I_{rq} \\ \varphi_{rd} = L_r I_{rd} + M_{rs} I_{sd} \\ \varphi_{rq} = L_r I_{rq} + M_{rs} I_{sq} \end{array} \right. \quad (1.35)$$

The rotor to stator turns ratio was assumed to be one. The active and reactive powers are define as:

$$\left\{ \begin{array}{l} P_s = V_{sd} I_{sd} + V_{sq} I_{sq} \\ Q_s = V_{sq} I_{sd} - V_{sd} I_{sq} \\ P_r = V_{rd} I_{rd} + V_{rq} I_{rq} \\ Q_r = V_{rq} I_{rd} - V_{rd} I_{rq} \end{array} \right. \quad (1.36)$$

b) Mechanical relations

Equation of electromagnetic generator expressed in base quantities is:

$$J \frac{d\omega_m}{dt} = T_m - T_{em} \quad (1.37)$$

The electromagnetic torque may be derived from the expressions above, as follows:

$$T_{em} = \frac{3}{2} p (\varphi_{sd} i_{sq} - \varphi_{sq} i_{sd}) \quad (1.38)$$

$$T_{em} = \frac{3}{2} p M_{rs} (i_{rq} i_{rd} - i_{rd} i_{rq}) \quad (1.39)$$

1.4.3. Grid side converter and machine side converter modeling

As shown Figure 1.21; the generator connects to the grid directly from the stator and through back-to-back converter (AC/DC/AC) via the rotor.

This connection gives different advantages: voltage and frequency (if needed) control of the local grid, improvement of the power quality and better integration of wind energy to the electrical grid and permits to insure the exchange power between the grid and the rotor [28, 37].

The only difference between rectifier and inverter is the definition of power flow direction. Where, when the power flows from the machine to the grid, it is considerate as rectifier/inverter and inverter/rectifier in the opposite power flow direction [28, 37].

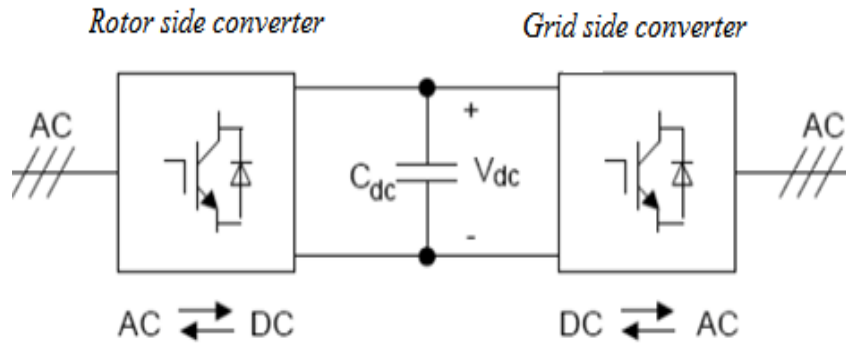


Figure 1.21. Back-to-back converter.

In our studies we propose that the power flows from grid to generator rotor, which permits to take the rotor side converter as a rectifier (AC/DC converter) and the grid side converter as an inverter (DC/AC converter). Figure 1.21 shows a power circuit of Two-level three-phase voltage-source back-to-back converters including twelve power semiconductor of IGBT type with free-wheeling diode, Where the two converters are linked through a DC capacitor which work as a DC filter capacitor to smooth the ripples across the load, and there are two other RL passive filters in the AC side of each one which permits to filter the power exchanging between the grid and the rotor.

1.4.3.1. Back-to-Back converter modeling

The RSC uses six bi-directional switches (IGBT switches with free-wheeling diode) that are capable of

conducting currents in both directions. The switches operate in the continuous conduction mode and are turned on and off, such that the output DC voltage is never shorted.

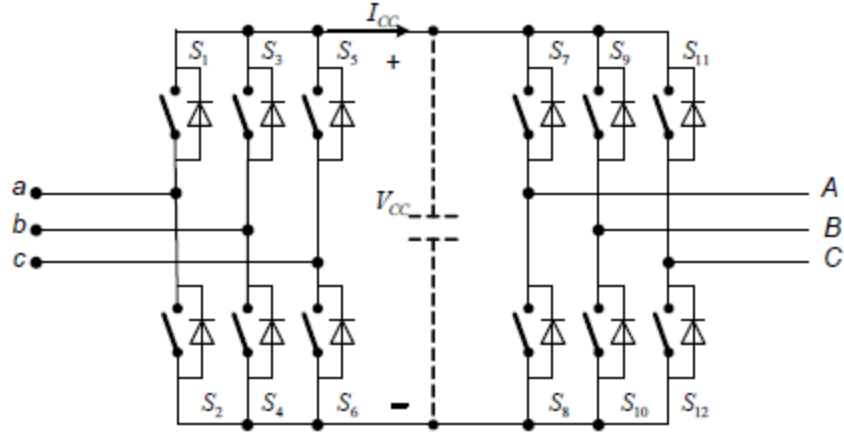


Figure 1.22. Circuit configuration of two-level back-to-back converter.

The simplified equivalent circuit of this converter is represented in Figure 1.23.

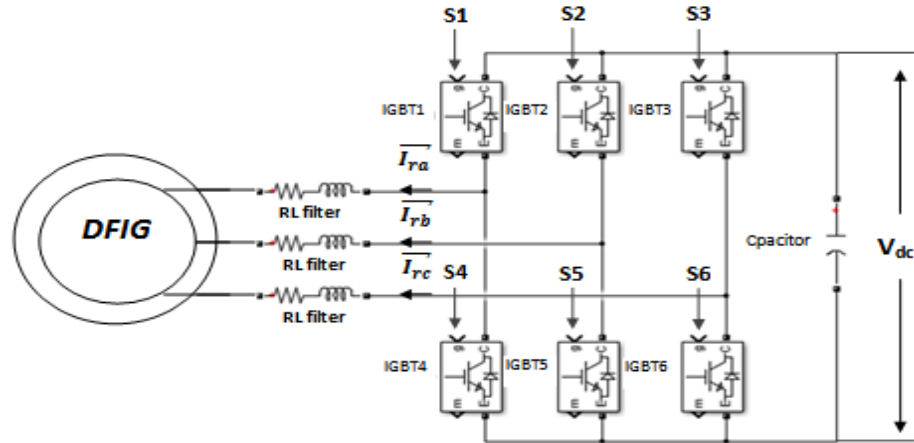


Figure 1.23. Rotor side converter circuit diagram

Assuming that the three phase system is balanced and the IGBTs are ideals. Where V_{ra} , V_{rb} and V_{rc} present the rotor three phase voltages and I_{ra} , I_{rb} and I_{rc} are the rotor three phase currents, R and L are the resistance and the inductance of the line passive filter respectively, I_{dc} and C are the DC output current and the dc-link capacitor respectively [41, 42].

The mathematical model of three-phase RSC in three-phase stationary coordinates (abc) is presented in Equations 1.40 and 1.41.

$$\begin{cases} v_{ab} = (s_a - s_b) \cdot V_{dc} \\ v_{bc} = (s_b - s_c) \cdot V_{dc} \\ v_{ca} = (s_c - s_a) \cdot V_{dc} \end{cases} \quad (1.40)$$

With S_i the switching function defined by: $S_i = \begin{cases} 1 \cdot \text{upper} \cdot \text{switch} \cdot \text{ON} \\ 0 \cdot \text{bottom} \cdot \text{switch} \cdot \text{OFF} \end{cases}$ with $i=a, b, c$

$$\begin{cases} v_a = f_a \cdot V_{dc} \\ v_b = f_b \cdot V_{dc} \\ v_c = f_c \cdot V_{dc} \end{cases} \quad (1.41)$$

Where;

$$\begin{cases} f_a = s_a - \frac{1}{3}(s_a + s_b + s_c) = \frac{2s_a - s_b - s_c}{3} \\ f_b = \frac{2s_b - s_a - s_c}{3} \\ f_c = \frac{2s_c - s_a - s_b}{3} \end{cases}$$

With f_{abc} are 0 or $\pm 1/3$ or $\pm 2/3$.

The table bellow (Table 1.2) shows the eight states of the converter switches with phase voltages and line voltages values.

Table 1.2. Possible interruption states for RSC

K	S_a	S_b	S_c	V_{ab}	V_{bc}	V_{ca}
0	1	0	0	U_{dc}	0	$-U_{dc}$
1	1	1	0	0	U_{dc}	$-U_{dc}$
2	0	1	0	$-U_{dc}$	U_{dc}	0
3	0	1	1	$-U_{dc}$	0	U_{dc}
4	0	0	1	0	$-U_{dc}$	U_{dc}
5	1	0	1	U_{dc}	$-U_{dc}$	0
6	0	0	0	0	0	0
7	1	1	1	0	0	0

The AC/DC converter is defined by four equations, three for the voltage phases and one for the currents (DC-link) as shown Equation 1.42 and Equation 1.43 respectively.

$$\begin{cases} u_a = Ri_a + L \frac{di_a}{dt} + v_a \\ u_b = Ri_b + L \frac{di_b}{dt} + v_b \\ u_c = Ri_c + L \frac{di_c}{dt} + v_c \end{cases} \quad (1.42)$$

$$C \frac{dV_{dc}}{dt} = i_C \quad (1.43)$$

Where: $i_C = i_{dc-RSC} - i_{dc-GSC}$ and $i_{dc-RSC} = s_a I_a + s_b I_b + s_c I_c$

$$C \frac{dV_{dc}}{dt} = s_a i_a + s_b i_b + s_c i_c - i_{dc-RSC} \quad (1.44)$$

The combination of the previous equations (Equations 1.41, 1.42, 1.43 and 1.44) can be represented as a block diagram in Figure 1.24.

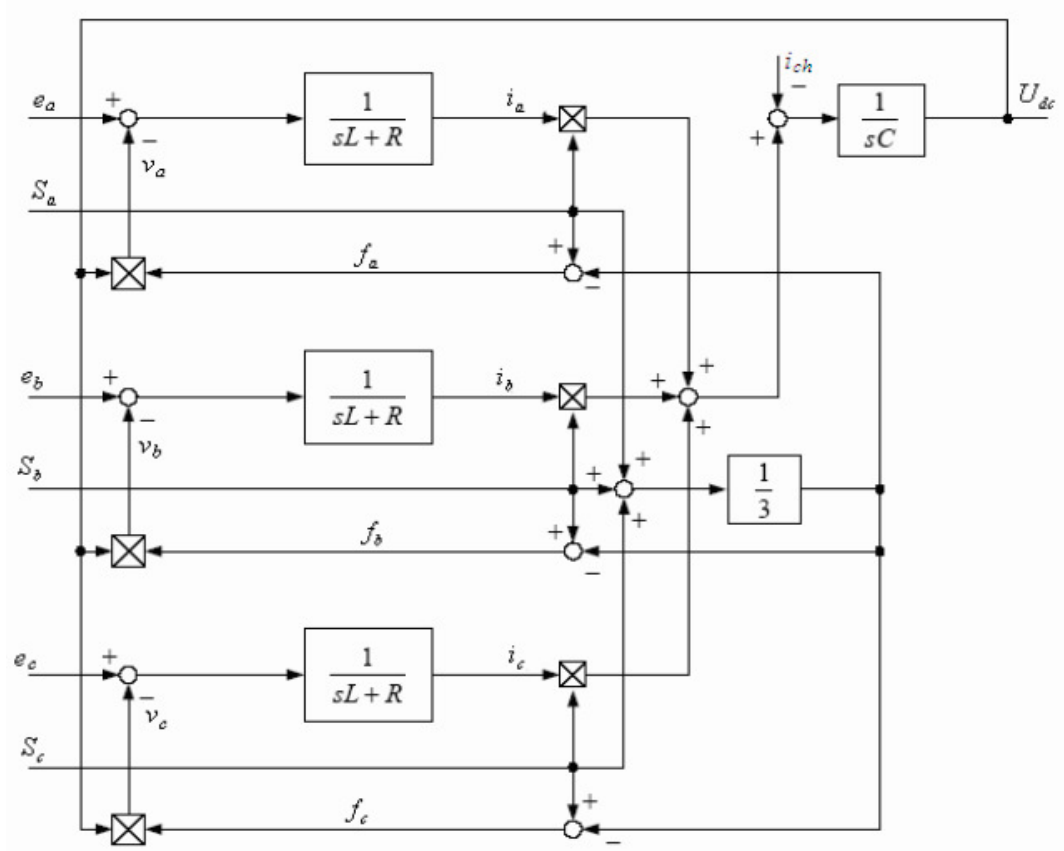


Figure 1.24. Rotor side converter model

To simplify the control of the RSC [40], it is necessary to convert this model into a linear model using the d-q representation. Therefore, after the application of dq transformation (see reference [40]) the RSC model is become as follow:

$$\begin{cases} u_d = Ri_d + L \frac{di_d}{dt} - \omega Li_q + v_d \\ u_q = Ri_q + L \frac{di_q}{dt} + \omega Li_d + v_q \\ C \frac{dV_{dc}}{dt} = \frac{3}{2} (s_d i_d + s_q i_q) - i_{dc} \end{cases} \quad (1.45)$$

Where

$$\begin{cases} s_d = \frac{1}{\sqrt{6}}(2s_a - s_b - s_c)\cos\omega t + \frac{1}{\sqrt{2}}(s_b - s_c)\sin\omega t \\ s_q = \frac{1}{\sqrt{2}}(s_b - s_c)\cos\omega t - \frac{1}{\sqrt{6}}(2s_a - s_b - s_c)\sin\omega t \end{cases} \quad (1.46)$$

The RSC block diagram in the dq reference is shown in Figure 1.25.

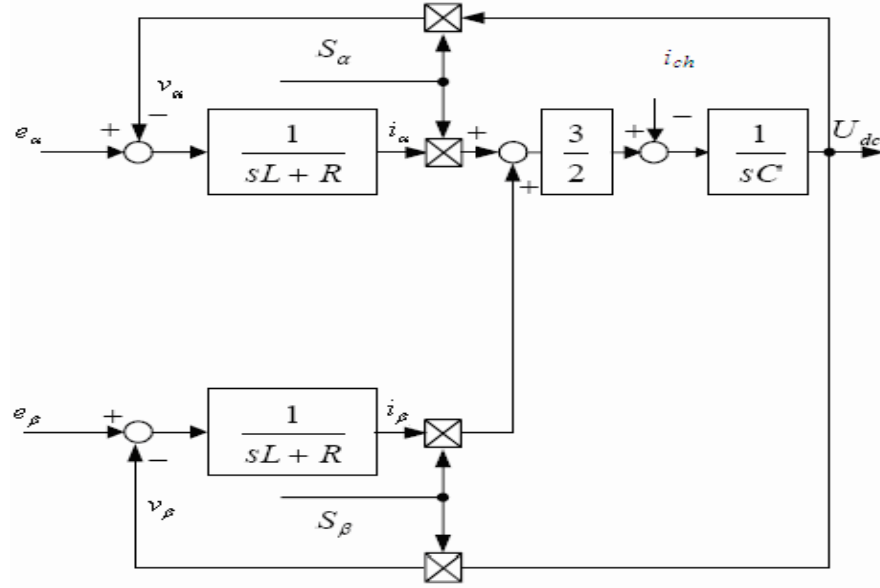


Figure 1.25. Rotor side converter diagram block in dq reference frame

1.4.3.2. Grid side converter modeling

Figure 1.26 illustrates the Grid Side Converter modulation, consisting the DC-link bus and input RL filter for the three phases [46].

Where:

I_{RSC} and I_{GSC} : are the RSC and GSC modulated currents respectively.

I_C : is the capacitor flowing current.

V_{dc} : DC-link voltage.

R_f and L_f : are the resistance and inductance of the RL filter.

$V_{s(a,b,c)}$: the grid side simple voltages.

$V_{s(a,b,c)-f}$: are the simple GSC voltages modulated.

$I_{s(a,b,c)-f}$: RL filter circulating current.

The DC-link bus voltage is obtained from the integration of the capacitor flowing as shown Equation 1.43 in the section above (it's the same for both of converters).

From Figure 1.26, we can write the three-phase converter model, according to the laws of Kirchhoff as follow:

$$\begin{cases} V_{sa} = R_f I_{sa-f} + L \frac{dI_{sa-f}}{dt} - V_{sa-f} \\ V_{sb} = R_f I_{sb-f} + L \frac{dI_{sb-f}}{dt} - V_{sb-f} \\ V_{sc} = R_f I_{sc-f} + L \frac{dI_{sc-f}}{dt} - V_{sc-f} \end{cases} \quad (1.47)$$

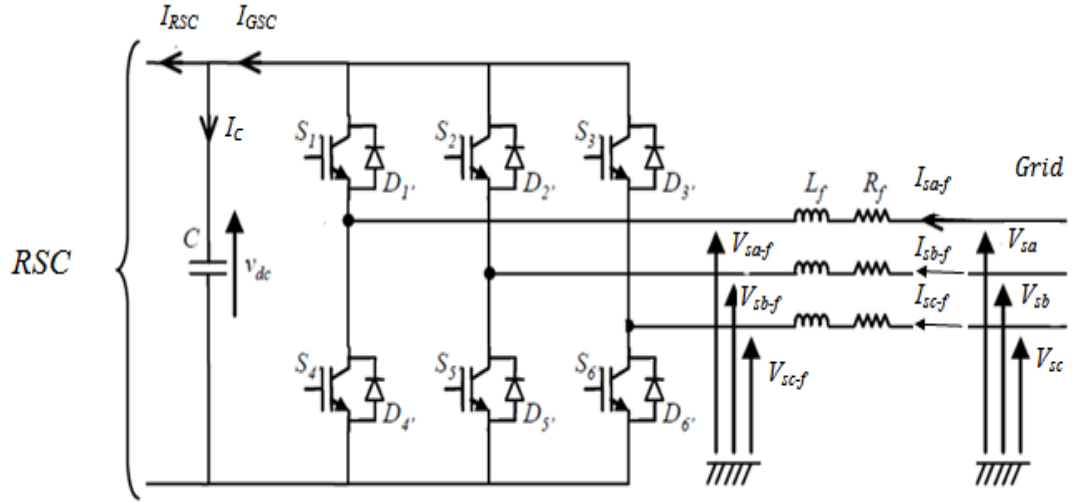


Figure 1.26. Grid Side Converter modeling.

1.5. Control of variable speed wind turbine Based on Doubly-Fed Induction Generator System

From Equation 1.23; it can be seen that the inductance matrix in this model is rotor position dependent and hence time dependent, which means that the inductance matrix needs to be calculated at each time step, and thus this increases the computation time. Therefore, the induction machine model must be expressed in dq reference frame because of the advantages of simplicity of formulation, fast simulation time and ease of implementation [39].

There are three types of dq reference frame used to model the DFIG system which mentioned as follow [39]:

- **DFIG Model Expressed in a dq Reference Frame Fixed on the Rotor**

A dynamic model is set up in the form of the dq reference frame rotating at rotor speed type of representation. Thereby; the complexity of the inductance matrix in the abc model, where the inductances vary with the rotor position or time, is avoided.

- **DFIG Model Expressed in a dq Stationary Stator Reference Frame**

Instead of fixing the d-axis on the rotor, the induction machine model expressed in a stationary stator reference frame with the d-axis fixed on the stator.

▪ DFIG Model Expressed in a dq Synchronously Rotating Reference Frame

The DFIG model expressed in a synchronously rotating reference frame has the advantage that the time varying variables of the three-phase system, such as stator currents and voltages become constants. This feature will be very useful in formulating and implementing any digital control systems.

In this thesis, the DFIG model expressed in a synchronously rotating reference frame will be chosen, and the deduction of the develop torque, active power and reactive power expressed in a synchronously rotating reference frame will be given later in this section.

1.5.1. Modeling in dq reference frame with stator-flux orientation

Instead of fixing the d-axis on the rotor or on the stator, the d-axis in the induction machine model expressed in a synchronous rotating reference frame will rotate at synchronous speed. Consider the schematic diagram of the abc to dq synchronous rotating reference frame transformation, which is shown in Figure 1.27. Where; $\theta_k = \theta_s$ and $\omega_k = \omega_s$.

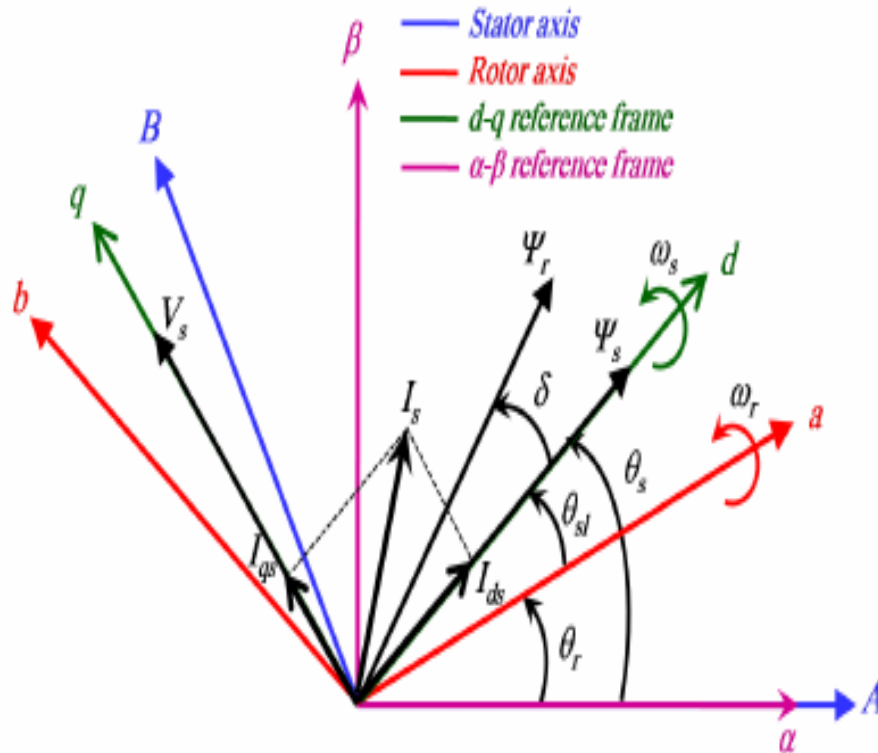


Figure 1.27. Voltages currents and flux vectors in dq Synchronously Rotating Reference Frame.

In this frame, the d-axis reference frame is chosen to align with the stator flux of the DFIG. To this end, the q-component of this flux vector is defined equal to zero.

$$\begin{cases} \Phi_{sd} = \Phi_s = cst \\ \Phi_{sq} = 0 \end{cases} \quad (1.48)$$

From the Equation 1.48, the Equation 1.35 becomes as follow:

$$\left\{ \begin{array}{l} \varphi_{sd} = L_s I_{sd} + M_{sr} I_{rd} = \varphi_s \\ \varphi_{sq} = L_s I_{sq} + M_{sr} I_{rq} = 0 \\ \varphi_{rd} = L_r I_{rd} + M_{rs} I_{sd} \\ \varphi_{rq} = L_r I_{rq} + M_{rs} I_{sq} \end{array} \right. \quad (1.49)$$

From Equation 1.49, we can define the rotor and the stator currents as follow:

$$\left\{ \begin{array}{l} I_{sd} = \frac{\varphi_{sd}}{L_s} - \frac{M_{sr}}{L_s} I_{rd} \\ I_{sq} = -\frac{M_{sr}}{L_s} I_{rq} \end{array} \right. \quad (1.50)$$

The stator and rotor voltages defined in Equations 1.33 and 1.34 are become as follow:

$$\left\{ \begin{array}{l} V_{sd} = 0 \\ V_{sq} = V_s = \omega_s \varphi_{sq} \end{array} \right. \quad (1.51)$$

$$\left\{ \begin{array}{l} V_{rd} = R_r I_{rd} + \frac{d\varphi_{rd}}{dt} - \frac{d\theta_r}{dt} \varphi_{rd} \\ V_{rq} = R_r I_{rq} + \frac{d\varphi_{rq}}{dt} + \frac{d\theta_r}{dt} \varphi_{rq} \end{array} \right. \quad (1.52)$$

The active and reactive stator and rotor powers are expressed as:

$$\left\{ \begin{array}{l} P_s = V_{sq} I_{sq} \\ Q_s = V_{sq} I_{sd} \\ P_r = V_{rd} I_{rd} + V_{rq} I_{rq} \\ Q_r = V_{rq} I_{rd} - V_{rd} I_{rq} \end{array} \right. \quad (1.53)$$

The relationship between the rotor voltages and rotor currents is expressed from the above equations (see the reference [40]) as follow:

$$\left\{ \begin{array}{l} V_{rd} = R_r I_{rd} + \left(L_r - \frac{M_{sr}^2}{L_s} \right) \frac{dI_{rd}}{dt} - \omega_r \left(L_r - \frac{M_{sr}^2}{L_s} \right) I_{rq} \\ V_{rq} = R_r I_{rq} + \left(L_r - \frac{M_{sr}^2}{L_s} \right) \frac{dI_{rq}}{dt} + \omega_r \left(L_r - \frac{M_{sr}^2}{L_s} \right) I_{rd} + \omega_r \frac{M_{sr}}{\omega_s L_s} V_s \end{array} \right. \quad (1.54)$$

After the reduction of this equation, we obtain the new equation bellow:

$$\begin{cases} V_{rd} = R_r I_{rd} - g \omega_s \left(L_r - \frac{M_{sr}^2}{L_s} \right) I_{rq} \\ V_{rq} = R_r I_{rq} + g \omega_s \left(L_r - \frac{M_{sr}^2}{L_s} \right) I_{rd} + g \omega_s \frac{M_{sr} V_s}{\omega_s L_s} \end{cases} \quad (1.55)$$

The Equations 1.50, 1.53 and 1.55 permit to established the controlling system schematic block as shown Figure 1.28.

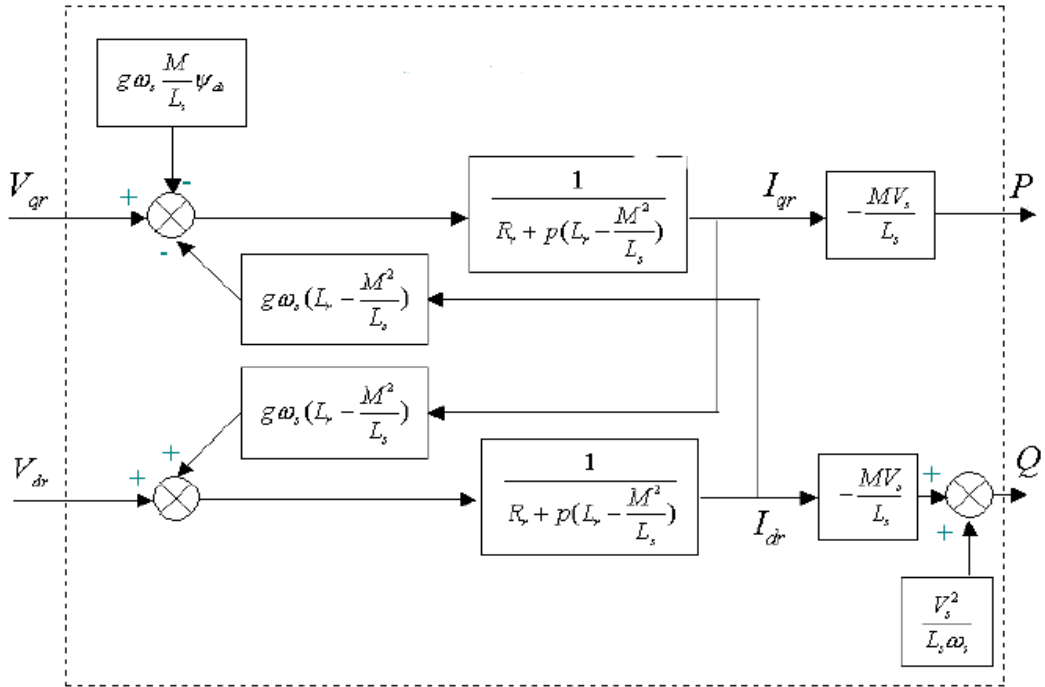


Figure 1.28. Schematic block diagram of the inner system.

b) Mechanical relations

Equation of mechanical generator stays the same expression as follow:

$$J \frac{d\omega_m}{dt} = T_m - T_{em} \quad (1.56)$$

The electromagnetic torque expressions become as follows:

$$T_{em} = \frac{3}{2} p \varphi_{ds} i_{qs} \quad (1.57)$$

$$T_{em} = \frac{3}{2} p M_{rs} (i_{qs} i_{dr} - i_{ds} i_{qr}) \quad (1.58)$$

$$T_{em} = \frac{3}{2} p (\varphi_{qr} i_{dr} - \varphi_{dr} i_{qr}) \quad (1.59)$$

1.5.2. DFIG-Based Wind Power System control goal

The system control consists of three control blocks named as follow (as shown Figure 1.29):

- MPPT control block.
- Rotor side converter control block.
- Grid side converter control block.

The MPPT block allows variable-speed wind turbine to operate at an optimal rotation speed as a function of wind speed which permits to capture the maximum power from the available wind energy [44, 46].

The RSC control block ensures a decoupled active and reactive stator power control, P and Q according to the reference torque delivered by the maximum power point tracking control (MPPT) [37, 46].

The GSC block controls the power flow exchange with the grid via the rotor, by maintaining the DC bus at a constant voltage level [37, 46].

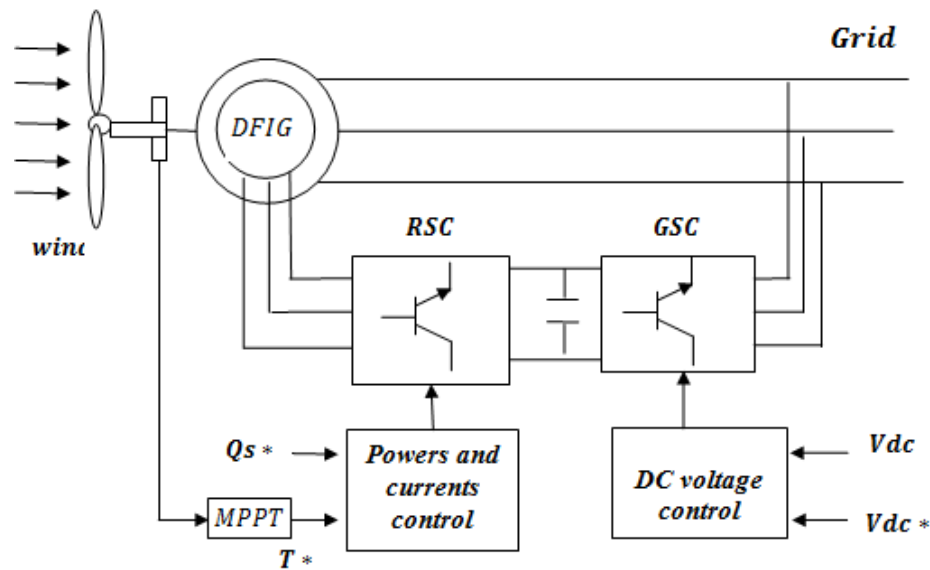


Figure 1.29. DFIG-Based Wind Power System Model control.

1.5.3. Maximum Power Point Tracking (MPPT) control

Due to the intermittent and variable nature of wind power, it is desirable to determine the optimal generator speed which extracts the maximum power from the turbine. MPPT allows variable-speed wind turbine to operate at an optimal rotation speed as a function of wind speed and capture the maximum power from the available wind energy [47, 48].

Many different MPPT control strategies for DFIG wind turbine system have been proposed in the literature [47].

1.5.3.1. Tip Speed Rotor (TSR) control

The MPPT method used in this paper is termed Tip Speed Rotor (TSR) control. This method regulates the rotational speed of the generator in order to maintain the TSR to an optimal value at which the power extracted is maximum. It requires both the wind speed and the turbine speed to be measured or estimated in addition to the knowledge of the optimal TSR of the turbine in order to be able extract maximum possible power. Figure 1.30 shows the block diagram of a MPPT control with TSR control [46, 47, 48].

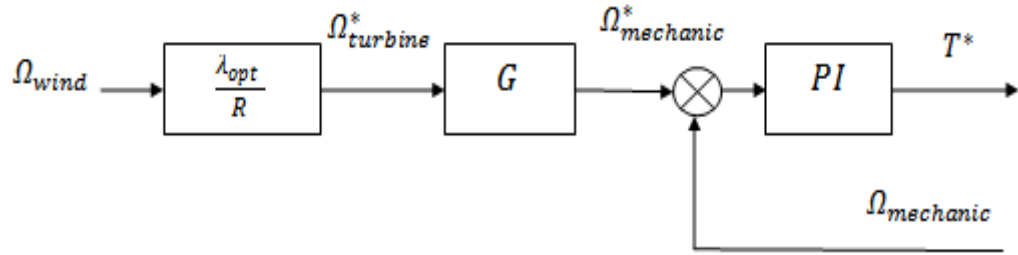


Figure 1.30. MPPT control.

Where R is the radius of wind turbine, λ_{opt} is the optimal TSR of the turbine and G is the inverted gain of the reducer.

1.5.3.2. MPPT-PI regulator

The transfer function relating the mechanical speed and the electromagnetic torque is:

$$G_{MPPT}(s) = \frac{1}{Js + F} \quad (1.60)$$

Where J and F represent the inertia and friction coefficient of the overall respectively.

The transfer function of the speed control loop can be calculated as:

$$G_{MPPT}(s)_{fb} = \frac{K_{p\Omega} \left(s + \frac{K_{i\Omega}}{K_{p\Omega}} \right) / J}{s^2 + \left(\frac{F + K_{p\Omega}}{J} \right) s + \frac{K_{i\Omega}}{J}} \quad (1.61)$$

From the performance desirable, can we calculate the controller's gains of PI regulator using comparison method as shown:

$$\begin{cases} d_{power}(S) = S^2 + 2\xi_{\Omega} \cdot \omega_{n\Omega} \cdot S + \omega_{n\Omega}^2 \\ K_{p_ \Omega} = 2\xi_{\Omega} \cdot \omega_n \cdot J - F \\ K_{i_ \Omega} = J\omega_{n\Omega}^2 \end{cases} \quad (1.62)$$

The performance desiring control parameters are defined as bellow:

$$\left\{ \begin{array}{l} \xi_{\Omega} = 0.707 \\ \tau_{\Omega_open_loop} = \frac{J}{F} \\ \tau_{\Omega_close_loop} = \frac{\tau_{\Omega_open_loop}}{3} = \frac{1}{3 \cdot \xi_{\Omega} \cdot \omega_{n\Omega}} \\ \omega_{n\Omega} = 3 \cdot \xi_{\Omega} \cdot \tau_{\Omega_open_loop} \end{array} \right. \quad (1.63)$$

1.5.4. Rotor-Side Converter Control (RSC)

The DFIG connected directly to the network through the stator, and controlled by its rotor through an ac/dc/ac converter. To control the power exchanged between the stator and the network, one uses the vector control with synchronous frame reference.

The control objective of RSC is to regulate the stator-side active power (P_s) and reactive power (Q_s) independently via the rotor components [43, 46]. Therefore, we need to define the relationships between the stator and the rotor components as seen in the bottom.

By the offsetting the Equation 1.40 in the Equation 1.53; the active and reactive stator powers are written a function of the rotor currents as follows:

$$\left\{ \begin{array}{l} Q_s = V_s I_{sd} = \frac{\varphi_s}{L_s} V_s - \frac{M_{sr}}{L_s} I_{rd} V_s \\ P_s = V_s I_{sq} = -\frac{M_{sr}}{L_s} I_{rq} V_s \end{array} \right. \quad (1.64)$$

The direct and quadrature rotor voltages can be written with another form as follow:

$$\left\{ \begin{array}{l} V_{rd} = R_r I_{rd} + \sigma \cdot L_r \frac{dI_{rd}}{dt} - \sigma \cdot L_r \omega_r I_{rq} \\ V_{rq} = R_r I_{rq} + \sigma \cdot L_r \frac{dI_{rq}}{dt} + \sigma \cdot L_r \omega_r I_{rd} + \omega_r \frac{M_{sr}}{\omega_s L_s} V_s \end{array} \right. \quad (1.65)$$

$$\text{Where: } \sigma = 1 - \frac{M_{sr}^2}{L_s L_r}$$

Figure 1.31 illustrates the vector control scheme of the RSC, in which the independent control of the stator active power (P_s) and reactive power (Q_s) is achieved by means of rotor current regulation in synchronous reference frame. The overall RSC control scheme consists of two cascaded control loops. The outer control loop regulates the stator active and reactive power independently, generating the reference signals I_{rq}^* and I_{rd}^* respectively. The inner control loop regulates the q-axis and d-axis rotor currents. The output of the two current controllers are compensated by the corresponding cross-coupling terms to form the total voltage signals and V_{rq}^* and V_{rd}^* . These voltage control signals are then used by the PWM module to

produce gate control signals to drive the RSC. To reduce the size and complexity of the model, commanded signals were assumed to be equal to actual signals and so commanded signals were directly fed to the DFIM rotor circuitry.

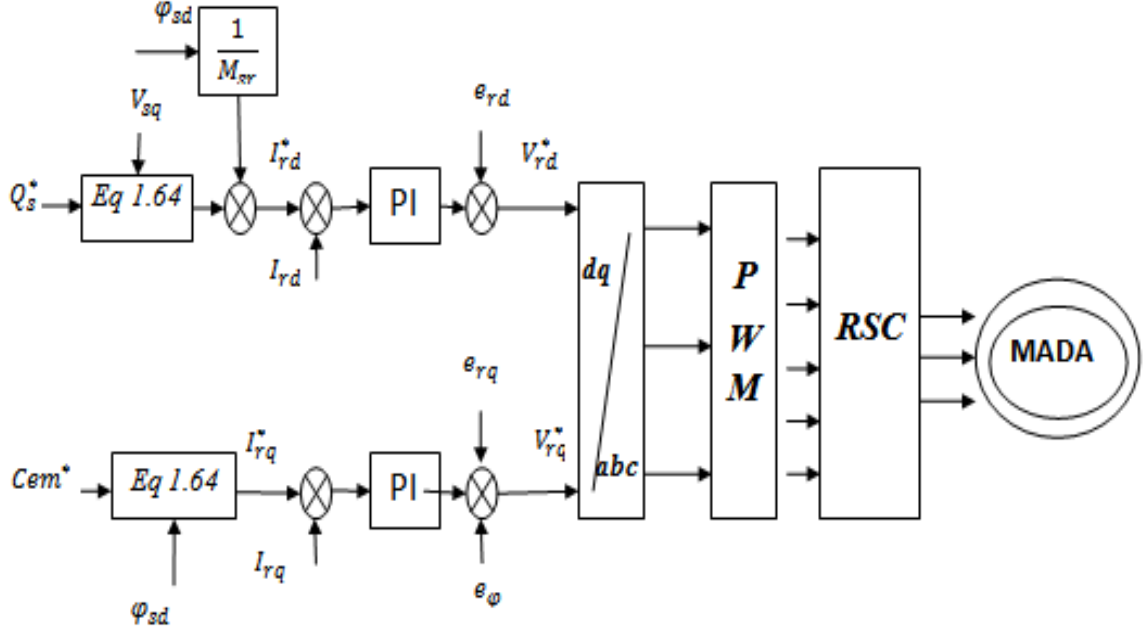


Figure 1.31. Block diagram for the RSC control

1.5.4.1. Stator powers control loop

The reference value of the active stator power is defined by the Equation 1.64 as below, where the reactive one takes a null value in order to obtain a unit factor.

$$\begin{cases} Q_s^* = 0 \\ P_s^* = \frac{1}{p\omega_s} T_{em}^* \end{cases} \quad (1.66)$$

The transfer function of the stator powers a function of the rotor voltages can be written as follow:

$$G_{power-open.loop} = \frac{P_s}{I_{rq}} = \frac{Q_s}{I_{rd}} = \frac{M_{sr}V_s}{L_s R_r + S \cdot L_s L_r \sigma} \quad (1.67)$$

The close loop for the stator powers control is defined as follow:

$$G_{power-close.loop} = \frac{P_s}{I_{rq}} = \frac{Q_s}{I_{rd}} = \frac{(K_{p-p} \cdot S + K_{i-p}) M_{sr} V_s}{L_s L_r \sigma} \quad (1.68)$$

$$= \frac{L_s L_r \sigma}{S^2 + \frac{(L_s R_r + K_{p-p} M_{sr} V_s)}{L_s L_r \sigma} S + \frac{K_{i-p} M_{sr} V_s}{L_s L_r \sigma}}$$

By the comparison method with the performance desirable; we can calculate the PI gains as follow:

$$\begin{cases} d_{power}(s) = s^2 + 2\xi_p \omega_{np} s + \omega_{np}^2 \\ K_{p-p} = \frac{2\xi_p \omega_{np} L_s L_r \sigma - L_s R_r}{M_{sr} V_s} \\ K_{i-p} = \frac{L_s L_r \sigma \omega_{np}^2}{M_{sr} V_s} \end{cases} \quad (1.69)$$

The performance desiring control parameters are defined as bellow:

$$\begin{cases} \xi_p = 0.707 \\ \tau_{p_open_loop} = \frac{L_r \sigma}{R_r} \\ \tau_{p_close_loop} = \frac{\tau_{p_open_loop}}{3} = \frac{1}{3 \cdot \xi_p \omega_{np}} \\ \omega_{np} = 3 \cdot \xi_p \cdot \tau_{p_open_loop} \end{cases} \quad (1.70)$$

1.5.4.2. Rotor currents control loop

The rotor currents a function of the rotor voltages can be defined from the Equation 1.65 as follow:

$$\begin{cases} I_{rd}(R_r + \sigma L_r s) = V_{rd} - e_{rd} \\ I_{rq}(R_r + \sigma L_r s) = V_{rq} - e_{rq} - e_\varphi \end{cases} \quad (1.71)$$

Where:

$$\begin{cases} e_{rd} = -\sigma \cdot L_r \omega_r I_{rq} \\ e_{rq} = \sigma \cdot L_r \omega_r I_{rd} \\ e_\varphi = \omega_r \frac{M_{sr}}{L_s \omega_s} V_s \end{cases} \quad (1.72)$$

There transfer function is defined as follow:

$$G_{current-open.loop} = \frac{I_{rq}}{V_{rq}} = \frac{I_{rd}}{V_{rd}} = \frac{1}{R_r + S \cdot L_r \sigma} \quad (1.73)$$

The PI rotor currents control loop block is shown in Figure 1.32 and Figure 1.33.

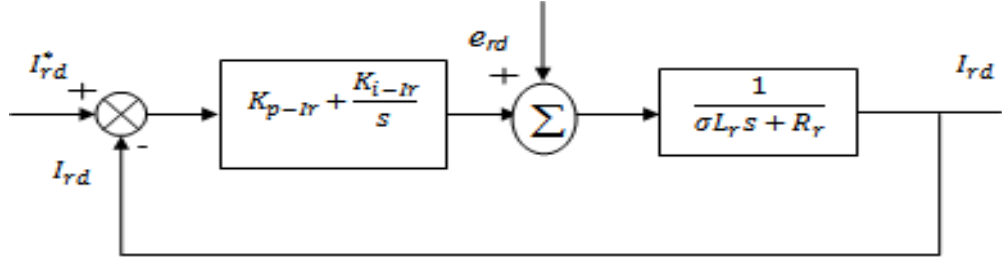


Figure 1.32. Block diagram of the rotor current control of the d-axis reference frame.

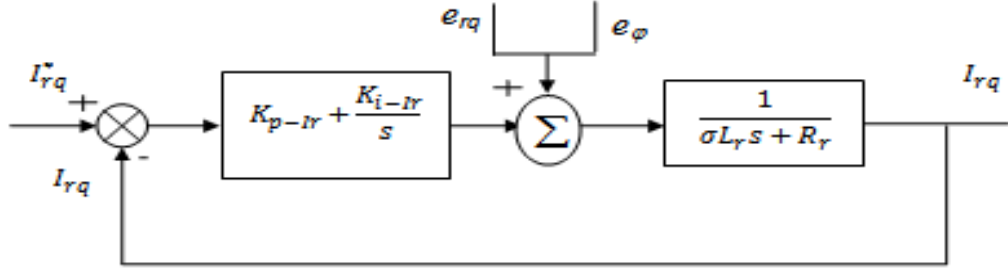


Figure 1.33. Block diagram of the rotor current control of the q-axis reference frame.

In order to gain a high performance, we can decouple the I_{rd} and I_{rq} by adding the e_{rq} term to output signal of the d-axis current controller, and e_{rd} and e_{ϕ} to the output signal of the q-axis current controller [43, 46].

The close loop transfer function for the rotor currents control is calculated as follow:

$$G_{\text{current-close.loop}} = \frac{(K_{p_Ir} \cdot S + K_{i_Ir})}{S^2 + \frac{(R_r + K_{p_Ir})}{L_r \sigma} S + \frac{K_{i_Ir}}{L_r \sigma}} \quad (1.74)$$

By the comparison method with the performance desirable, we can calculate the PI gains as follow:

$$\begin{cases} d_{\text{current}}(S) = S^2 + 2\xi_i \omega_{ni} S + \omega_{ni}^2 \\ K_{p_Ir} = 2\xi_i \omega_{ni} L_r \sigma - R_r \\ K_{i_Ir} = L_r \sigma \omega_{ni}^2 \end{cases} \quad (1.75)$$

The desired control parameters are defined as bellow:

$$\begin{cases} \xi_i = 0.707 \\ \tau_{i_open_loop} = \frac{L_r \sigma}{R_r} \\ \tau_{i_open_loop} = \frac{\tau_{i_open_loop}}{3} = \frac{1}{\xi_i \omega_{ni}} \\ \omega_{ni} = \xi_i \cdot \tau_{i_open_loop} \end{cases} \quad (1.76)$$

1.5.5. Grid-Side Converter (GSC) control

The GSC is connected between the grid via RL filter and the DC-link. The role of this converter is to maintain the DC-link voltage as the constant value [43, 46, 40]. The control of this voltage is achieved by the control of the rectifier currents as shown in the Figure 1.35.

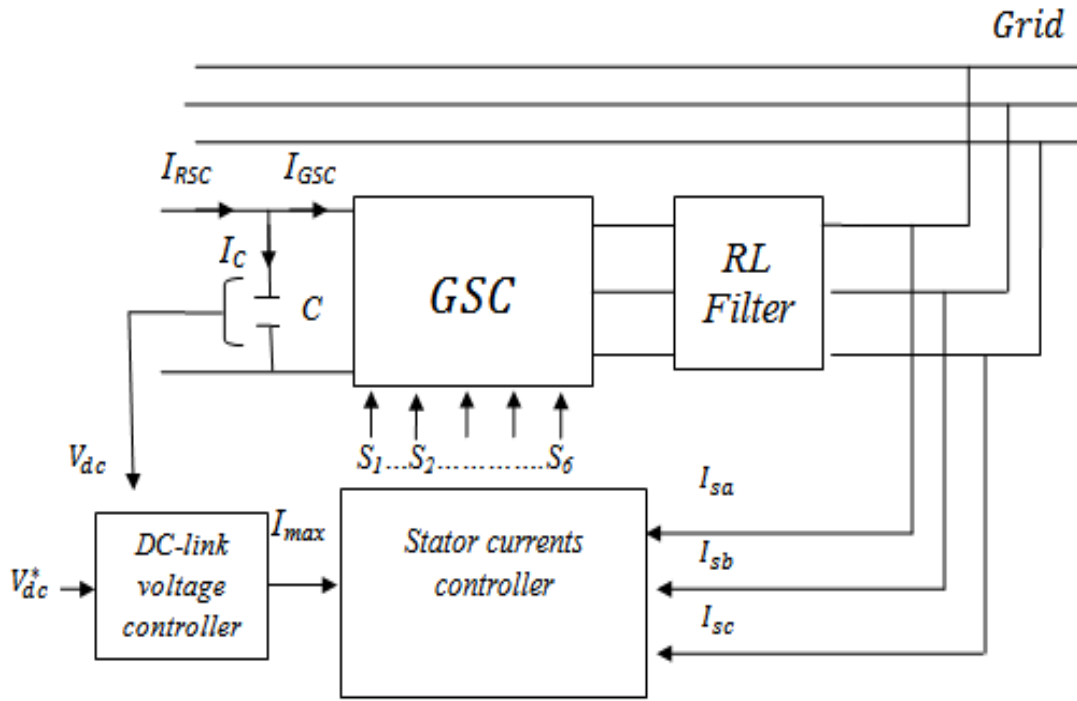


Figure 1.34. Principal block diagram of Grid-Side Converter (GSC) control.

The overall vector control scheme consists of two cascaded control loops. The outer control loop regulates the dc-link voltage; where the measured DC-link voltage V_{dc} is compared to its reference signal V_{dc}^* and the error signal from inputs to the proportional-integral (PI) regulator which generates the reference amplitude current I_{max} as shown Figure 1.35. This amplitude multiplies with a three phases sinusoidal functions which have a same input voltage frequency and compared with measurements grid currents (inner control loop) to generate the switching pulse for the converter through the PWM block.

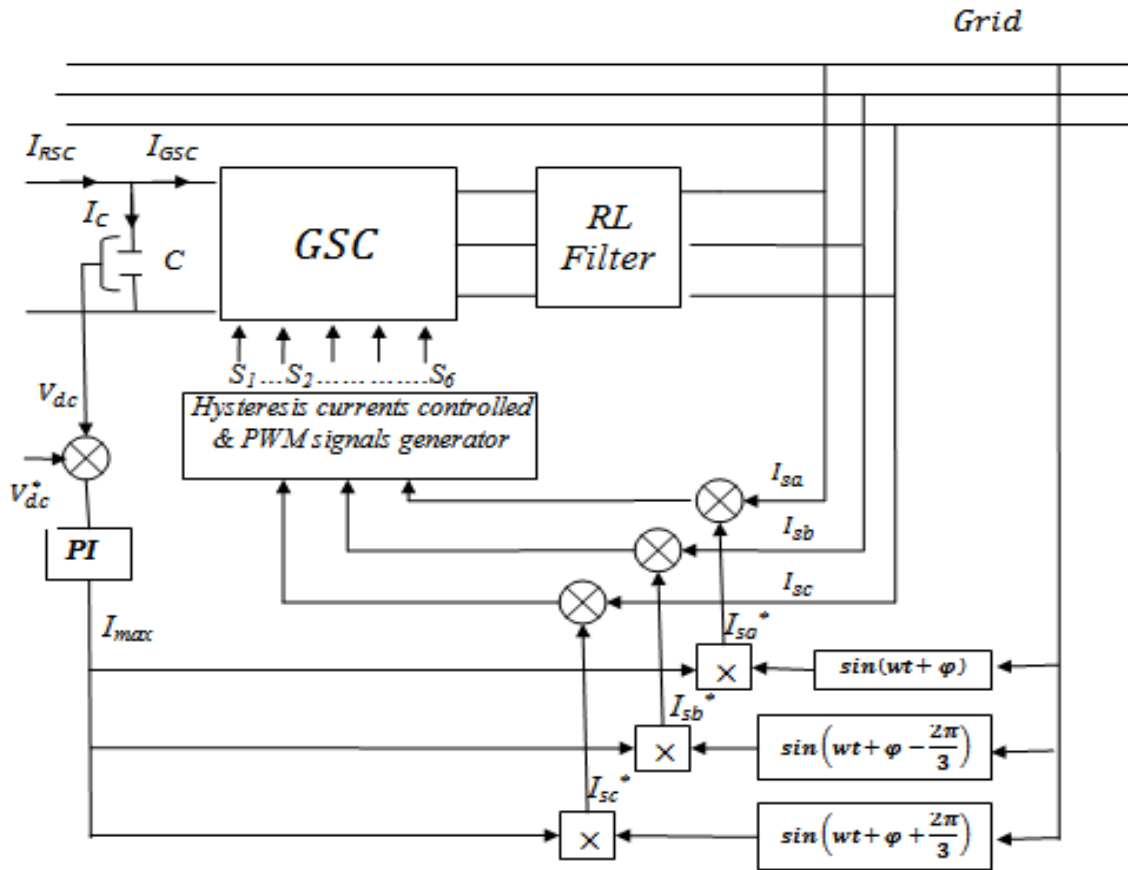


Figure 1.35. Block diagram of stator currents and direct voltage GSC control.

1.5.5.1. Control of the DC-link voltage

The control of the DC-link voltage requires a feedback control loop as shown Figure 1.36. The DC voltage V_{dc} is compared with a reference V_{dc}^* and the error signal obtained from this comparison is regulated with a PI-controller. The output value of this regulator is used to generate a template waveform of the three phase currents.

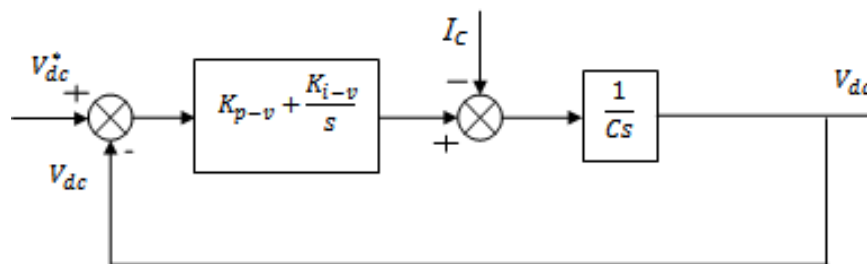


Figure 1.36. DC-link voltage feedback control loop.

The transfer function of outer loop is written as follow:

$$G_{voltage_open_loop}(s) = \frac{1}{Cs} \tag{1.77}$$

Where C is the capacitor value of the DC side.

The transfer function of the feedback control loop is written as follow:

$$G_{\text{voltage_close_loop}}(S) = \frac{(K_{p-v}S + K_{i-v})}{S^2 + \frac{K_{p-v}}{C}S + \frac{K_{i-v}}{C}} \quad (1.78)$$

By the comparison method with the performance desirable, we can calculate the *PI* gains as follow:

$$\begin{cases} d_{\text{voltage}}(S) = S^2 + 2\xi_v \omega_{nv} S + \omega_{nv}^2 \\ K_{i-v} = \omega_{nv}^2 C \\ K_{p-v} = 2\xi_v \omega_{nv} C \end{cases} \quad (1.79)$$

The output value of voltage outer loop of *PI* regulator is used to produce the PWM pattern, and allows controlling the GSC in two different ways:

- 1) As a voltage source current controlled PWM GSC.
- 2) As a voltage source voltage controlled PWM GSC.

The first method controls the input current, and the second controls the magnitude and phase of the voltage. The current controlled method is simpler and more stable than the voltage-controlled method [40,], and for these reasons it will be used in this work.

1.5.5.2. Hysteresis voltage source currents controlled PWM for GSC

This method of control is shown in Figure 1.37. The control is achieved by measuring the instantaneous phase currents and forcing them to follow a sinusoidal current reference template (I_{ref}) using current hysteresis controller. The amplitude of the current reference template I_{max} is evaluated using the following equation:

$$I_{\max} = G_c \cdot (V_{dc}^* - V_{dc}) \quad (1.80)$$

Where G_c represents a DC-link voltage *PI* controller.

The sinusoidal waveform of the template is obtained by multiplying I_{max} with a sine functions (for each phase), with the same frequency of the mains supply, and with the desired phase-shift angle.

Once the stability problems have been solved, and the sinusoidal current desired has been generated, a modulation method will be required to produce the PWM pattern for the power valves. The PWM pattern

will switch the power valves to force the input currents (I_{sa} , I_{sb} , I_{sc}) to follow the desired currents (I_{sa}^* , I_{sb}^* , I_{sc}^*) using Hysteresis Band (HB) PWM modulation method with a band value between ± 0.01 .

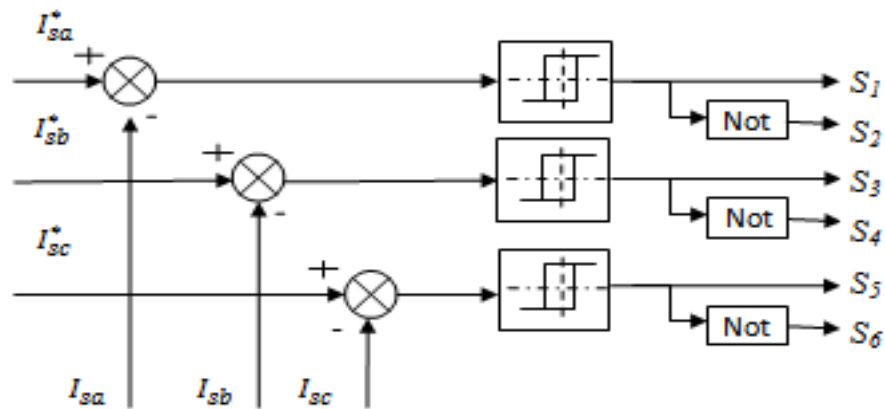


Figure 1.37. Block diagram of current hysteresis control

1.6. Simulation resultants

Simulation results were performed using software Matlab/Simulink. For these simulations, we consider that the wind system is steady and working in the zone of optimal functioning. The DFIG is rated at 2 Mw and its parameters are given in the table below (Table 1.3).

The simulations results are presented in the Figure 1.38. Where, Figure 1.38-(g) shows the wind speed profile applied to the wind turbine blades with an average value of 8 m/s, which corresponds to the speed of DFIG under MPPT control as shown Figure 1.38-(h).

Figure 1.38-(a) and Figure 1.38-(b) show quadrature and direct rotor currents responses; where the measurements currents flow exactly the references one.

Figure 1.38-(c) and Figure 1.38-(d) show the active and reactive stator powers responses; where the wind power system operates as a unity power factor and the reactive power equals zero. The active stator power flows the reference value corresponding of the torque value which generated by the MPPT control block.

The DC link voltage is perfectly regulated to 800V as shown Figure 1.38-(f) where the response value time is around 0.15s without.

Figure 1.38-(e) show the response torque value of the DFIG machine injected by the MPPT control.

Figure 1.39 and Figure 1.40 represent respectively the three-phase stator currents generated by the global system.

Table 1.3. System parameters

<i>Rated power</i>	<i>7.5 Mw</i>
<i>Stator voltage</i>	<i>220 V</i>
<i>Stator/rotor turns Ratio</i>	<i>1</i>
R_s	<i>0.455 ohm</i>
R_r	<i>0.62 ohm</i>
L_s	<i>0.084 H</i>
L_r	<i>0.081 H</i>
M_{sr}	<i>0.078 H</i>
<i>Lumped inertia constant</i>	<i>0.3125</i>
<i>Number of pole pairs</i>	<i>2</i>
<i>Turbine power</i>	<i>10 Mw</i>
<i>Radius pale</i>	<i>3 m</i>
<i>Reducer gain G</i>	<i>5.4</i>
L_f filter	<i>0.014 H</i>
R_f filter	<i>0.3 ohm</i>
C filter	<i>2 mF</i>
<i>DC Link Voltage</i>	<i>800</i>
<i>Switching Frequency F_s</i>	<i>10 KHz</i>
R_l load charge	<i>4 ohm</i>
L_l load charge	<i>0.04 mH</i>

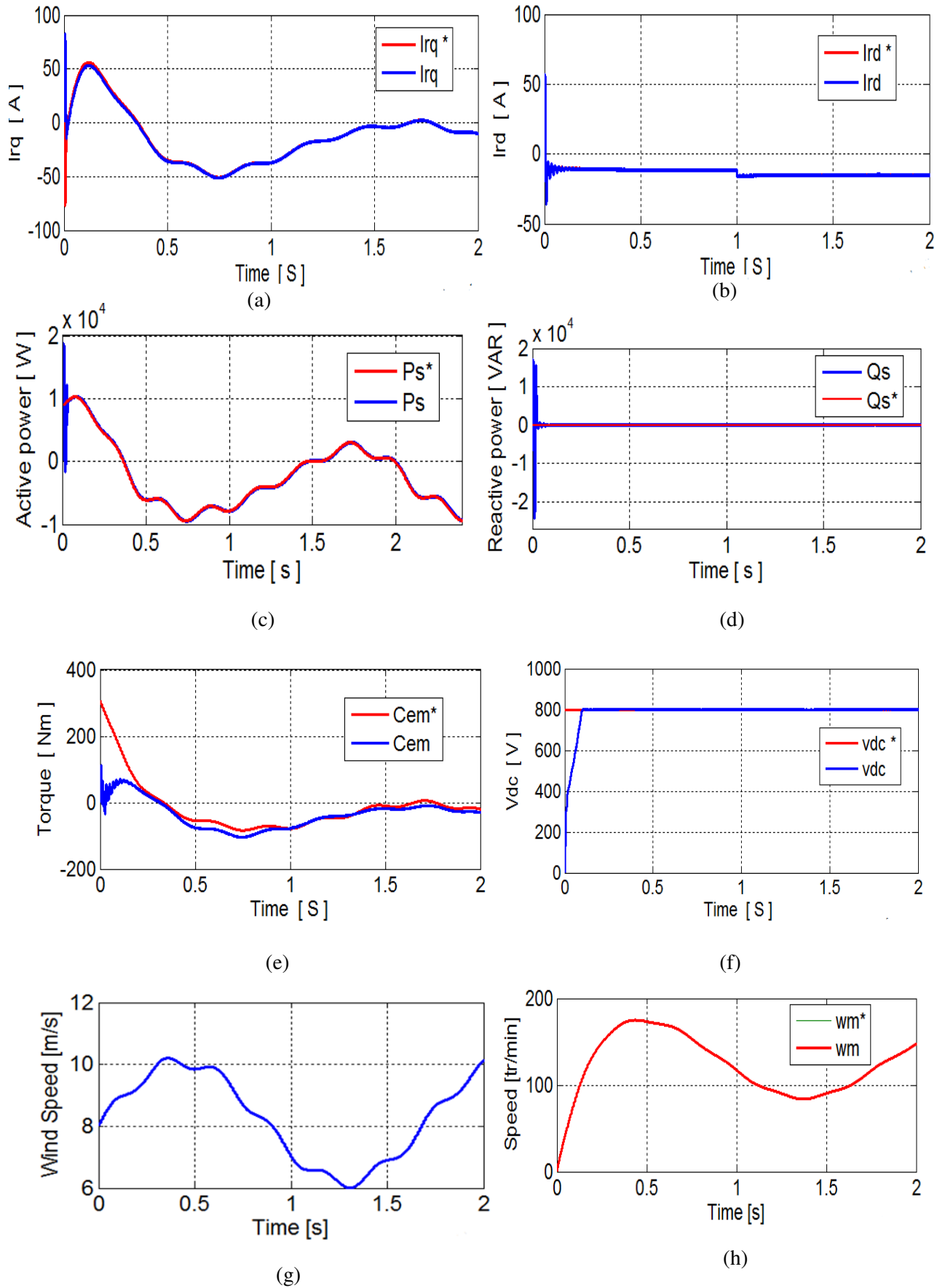


Figure. 1.38. (a) I_{rq} current, (b) I_{rd} Current ; (c) active stator power P_s (d) reactive stator power Q_s ; (e) Torque C_{em} (f) DC-voltage V_{dc} ; (g) Wind speed (h) Speed of DFIG with MPPT.

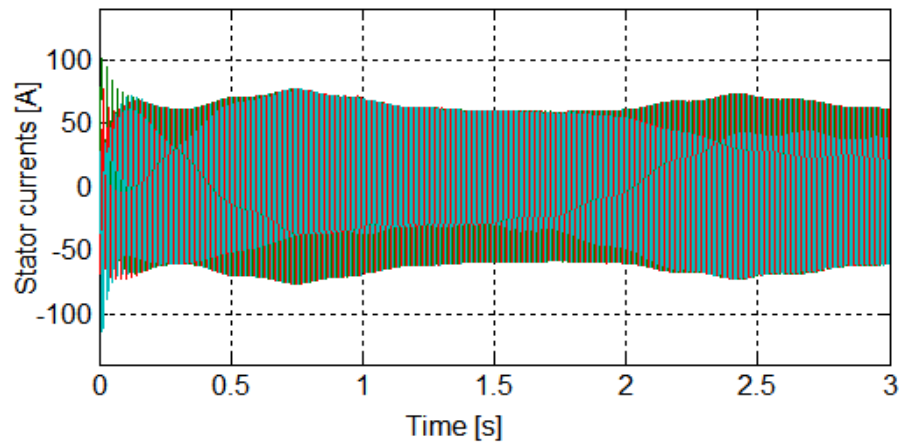


Figure 1.39. Three-phase stator currents

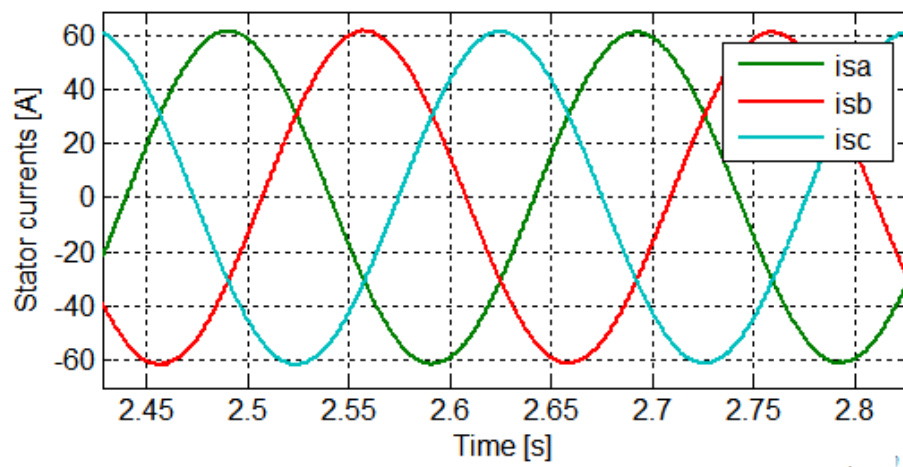


Figure 1.40. Three-phase stator currents zoom

1.7. Conclusion

The doubly-fed induction generator wind turbine is a variable speed wind turbine widely used in the modern wind power industry. At present, commercial DFIG wind turbines primarily make use of the technology that was developed a decade ago especially in wind turbine systems.

In this chapter, a brief overview of renewable and non-renewable energies was presented in second section. In addition, fossil fuels description proprieties, problems and statistics were been discussed. Then, renewable type's definitions were presented and compared especially wind turbine.

In the third section, a wind turbine system history, construction, types and its principal work has been discussed with its main expressions which mainly using in this domain.

In the fourth section, equivalent circuits and mathematical models for the doubly fed induction generator DFI, turbine and back-to-back converter were presented. In order to provide the needed feedback about the tuning of the controller the electrical equivalent of the DFIG is illustrated and analyzed. Moreover, all equations of the equivalent system are presented in *abc* reference and transformed into *dq* with stator flux oriented reference frame. Further the decoupled active and the reactive power equations are exposed in d and q axis for both the stator and the rotor.

The controlling of wind turbine is very important especially for variable speed operation to make the wind energy conversion system efficient, reliable and feasible. The major control goals of a variable speed wind turbine, thus a DFIG based wind turbine are: maximum power extraction and active and reactive stator powers control at the Point of Common Coupling (PCC). Therefore, a general control strategy of a variable speed wind turbine can be divided into three different control levels: MPPT control, RSC control and GSC control were presented in section five.

The simulation results developed in Matalab/Simulink environment. The results show that the control strategy can effectively produce a maximum power extracted from the wind energy with unity power factor to the grid.

1.8. References

- [1] Hepbasli A, Ozgener O. “A review on the development of wind energy in Turkey. *Renewable and Sustainable Energy Reviews*”, 2004, pp: 257–76.
- [2] Deal WF. “*Wind power: an emerging energy resource*”. *Technology and Engineering Teacher* 2010;9:9–15.
- [3] Ackermann T, Der LS. “*An overview of wind energy status 2002*”. *Renewable and Sustainable Energy Reviews* 2002, pp: 67–127.
- [4] Wenping Cao, Ying Xie and Zheng Tan “*Wind Turbine Generator Technologies*”, *Advances in Wind Power*, chapter 7, 2012.
- [5] Rechesteiner, R. (2008). “*Wind power in context- A clean revolution in the energy sector*”. online, http://www.energywatchgroup.org/fileadmin/global/pdf/2009-01_Wind_Power_Report.pdf, 2018.
- [6] Christina N. Papadimitriou and Nicholas A. Vovos, “*Fuzzy Control of WT with DFIG for Integration into Micro-grids*”, www.intechopen.com.
- [7] <http://tecalive.mtu.edu/mecc/module19/Page2.htm>; March 2018.
- [8] <http://energy.matters.euanmearns.com/?s=energy+consumed+in+2014>.
- [9] <http://cr.middlebury.edu/es/altenergylife/70%27s.htm>, March 2018.
- [10] <https://news.alibaba.com/article/detail/report/101011429-1-mapping-china-global-production-consumption.html>; March 2018.
- [11] Nada Kh. M. A. Alrikabi, “*Renewable Energy Types*”, *Journal of Clean Energy Technologies*, Vol. 2, No. 1, January 2014.
- [12] Rinkesh, “*RENEWABLE ENERGY AND OTHER ALTERNATIVE ENERGY SOURCES*”, *Advanced Biomass Gasification. Power Generation System*, 1986.
- [13] Mr Eleftherios Giakoumelos and al, “*HANDBOOK ON RENEWABLE ENERGY SOURCES*”, *Handbook on Renewable Energy Sources*.
- [14] Y. Demirel, “*Energy and Energy Types*”, *Energy, Green Energy and Technology*, Springer-Verlag London Limited 2012.
- [15] http://geoinfo.amu.edu.pl/wpk/geos/GEO_8/GEO_CHAPTER_8.HTML, January 2018.
- [16] <http://www.speglobal.net/home/page/?pid=002006001>, January 2018.
- [17] <http://www.mediwatt.com/business-fermes-eoliennes-gisement-eolien.php>, January 2018.
- [18] <http://gwec.net/global-figures/graphs/>, January 2018.
- [19] <https://fr.slideshare.net/YassineBouhara/the-mediterranean-leadership-summit-tell-group-april-2016-v2>, January 2018.
- [20] Société CEEG. Spa , « *Production d’électricité d’origine renouvelable* », Octobre 2014.
- [21] John K. Kaldellis*, D. Zafirakis, “*The wind energy (r)evolution: A short review of a long history*”, *Renewable Energy*, 2011, pp: 1887-1901.
- [22] M. Malaty, M. Morel, “*Wind energy history*”, GRETA.
- [23] A. P. Schaffarczyk, “*Introduction to Wind Turbine Aerodynamics*”, *Green Energy and Technology*, Springer-Verlag Berlin Heidelberg, 2014.

- [24] L. Stano, V. Chudoba, M. Morvova, “*The design, construction and analysis of horizontal wind turbine for small scale electric energy production*”, Acta Physica Universitatis Comenianae, Volume, p.57-69, 2016.
- [25] Sanjeev Malhotra, PE, GE, “*Selection, Design and Construction of Offshore Wind Turbine Foundations*”, Parsons Brinckerhoff, Inc, United States of America.
- [26] M. Burger, S. Colella, S. Quinlivan, J. Rousseau, « *Construction of a wind turbine project in the town of florida. MA* », March, 2007.
- [27] Schonhauser Allee, “ReGrid: Wind Power”, renac, renewable academy, sept.2013.
- [28] Gary L. Johnson, “*WIND ENERGY SYSTEMS* “,Electronic Edition, October 10, 2006.
- [29] M. Ragheb, “*Wind energy conversion theory, Betz equation*”, October 2017.
- [30] Zervos, A., “*Wind power as a mainstream energy source*”; Proc. of the 2009, European Wind Energy Conf. , Marseille, March 2009.
- [31] Wei Tong, “*Fundamentals of wind energy*”, WIT Transactions on State of the Art in Science and Engineering, Vol 44, 2010.
- [32] Abhijeet Awasthi and al, “*Study for Performance Comparison of SFIG and DFIG Based Wind Turbines*”, International Journal of Latest Trends in Engineering and Technology (IJLTET); Vol. 2 , Issue 4, July 2013.
- [33] Juleff, G., “*An ancient wind-power iron smelting technology in Sri Lanka. Nature*”, 379(6560) , pp. 60–63, 1996.
- [34] Wei Tong, “*Fundamentals of wind energy*”, WIT Transactions on State of the Art in Science and Engineering, Vol 44, 2010.
- [35] A. kumar agrawal and al, “*Study of wind turbine driven DFIG using AC/DC/AC converter*”, Electrical Engineering.
- [36] R. Pena, J.C.Clare, G. M. As her, “*Doubly fed induction generator uising back-to-back PWM converters and its application to variablespeed wind-energy generation*”, IEE Puoc.-Electr. Power Appl., Vol. 143, No 3, May 1996.
- [37] A. Petersson, “*Analysis, Modeling and Control of Doubly-Fed Induction Generators for Wind Turbines*”, thesis, CHALMERS UNIVERSITY OF TECHNOLOGY G”oteborg, Sweden 2005.
- [38] Courseware Sample by the staff of Lab-Volt Ltd. “*PRINCIPLES OF DOUBLY-FED INDUCTION GENERATORS (DFIG)*”2011.
- [39] M. Hassan Alothman, “*Three-phase induction machine studying and its using in the control*”, university of electronic and engineering of Halab, Thesis, 2010-2011.
- [40] Abdelmalek BOULAHIA; “ *Etude des Convertisseurs Statiques destinés à la Qualité de l'Energie Electrique*”, Thesis, 2008/2009.
- [41] Kada HARTANI, Yahia MILOUD, « *Control Strategy for Three Phase Voltage Source PWM Rectifier Based on the Space Vector Modulation*”, Advances in Electrical and Computer Engineering Volume 10, Number 3, 2010.
- [42] M. Devadarshanam, B. M. Manjunatha, K. Damodaram, “*Modeling and Simulation of PWM Line Converter feeding to Vector Controlled Induction Motor Drive*”, International Journal of Advanced Research in Computer Science and Software Engineering; Volume 2, Issue 8, August 2012.

- [43] Frédéric POITIERS, “*ETUDE ET COMMANDE DE GENERATRICES ASYNCHRONES POUR L'UTILISATION DE L'ENERGIE EOLIENNE* », Thesis, l'Ecole polytechnique de l'Université de Nantes, décembre 2003.
- [44] Q. Wang and L. Chang, “An intelligent maximum power extraction algorithm for inverter-based variable speed wind turbine systems,” *IEEE Trans.*
- [45] B.Chitti Babu , K.B.Mohanty “Doubly-Fed Induction Generator for Variable Speed Wind Energy Conversion Systems- Modeling & Simulation “*International Journal of Computer and Electrical Engineering*, February, 2010.
- [46] Arnaud GAILLARD, “*Système éolien basé sur une MADA : contribution à l'étude de la qualité de l'énergie électrique et de la continuité de service* », FACULTE DES SCIENCES & TECHNIQUES, de Nancy, avril 2010.
- [47] Jogendra Singh Thongam1 and Mohand Ouhrouche, “*MPPT Control Methods in Wind Energy Conversion Systems*”, University of Quebec at Chicoutimi Quebec, Canada.
- [48] K. Maheswari1, T.Porselvi, “*Comparison of TSR and PSO based MPPT Algorithm for Wind Energy Conversion System*”, *International Journal of Advanced Research in Electrical, Electronics and Instrumentation Engineering*, Vol. 3, Special Issue 1, February 2014.
- [49] <http://www.uncoverenergy.com/hail-to-the-shale/>, January 2018.
- [50] Mr. Punit L. Ratnani1, Dr. A. G. Thosar, “*Mathematical Modelling of an 3 Phase Induction Motor Using MATLAB/Simulink*”, *International Of Modern Engineering Research (IJMER)*, Vol. 4, Iss. 6, June 2014.
- [51] “*Park, Inverse Park and Clarke, Inverse Clarke Transformations MSS Software Implementation*”, Microsemi Corporation, 2013.
- [52] B. Robyns et al, “*Dynamic Modeling of Induction Machines*”, chapter 2; *Vector Control of Induction Machines*, Power Systems, Springer-Verlag London 2012.
- [53] R. D. Shukla, R. K. Tripathi, “*Maximum Power Extraction Schemes and Power Control in Wind Energy Conversion System*”, *International Journal of Scientific and Engineering Research*, Vol.3. Issue 6, June 2012.
- [54].http://mstudioblackboard.tudelft.nl/duwind/Wind%20energy%20online%20reader/Static_pages/upwind_downwind.htm, March 2018.
- [55]https://www.google.com/url?sa=i&rct=j&q=&esrc=s&source=imgres&cd=&ved=2ahUKEwj688KV6cjaAhWIXBQKHbQDWcQjhx6BAgAEAM&url=https%3A%2F%2Fwww.ecosources.info%2Fdossiers%2FEolienne_verticale_Darrieus&psig=AOvVaw2ruZ11Ww_98Hmizm4hYyxf&ust=1524312619549307, March 2018.
- [56] <https://www.theengineer.co.uk/issues/30-april-2012/wind-energy-gets-serial/>, January 2018.

Chapter II: Artificial Intelligence

Abstract: AI is one of the newest fields in science and engineering which work started in earnest soon after World War II. This science divided in many research areas such as: Expert System, Fuzzy Logic, Algorithm Genetic, Neural Network, Robotic and Natural language processing. This chapter has reviewed the meaning of artificial intelligence; its basic concepts and terminology including its applications, goals and various research areas. After that, we has focused our studying about three research areas which we will use them in the next chapters like as: Expert System, Fuzzy Logic and Algorithm Genetic. Where, we have talked about their basic concepts, terminology and their several applications areas.

2.1. Introduction

2.1.1. Overview

Humankind has given itself the scientific name homo sapiens—man the wise—because our mental capacities are so important to our everyday lives and our sense of self [1]. The field of artificial intelligence, or AI, attempts to understand intelligent entities. Thus, one reason to study it is to learn more about ourselves. But unlike philosophy and psychology, which are also concerned with intelligence, AI strives to build intelligent entities as well as understand them [1, 2]. Another reason to study AI is that these constructed intelligent entities are interesting and useful in their own right. AI has produced many significant and impressive products even at this early stage in its development. Although no one can predict the future in detail, it is clear that computers with human-level intelligence would have a huge impact on our everyday lives and on the future course of civilization [3].

2.1.2. Chapter goal and organization

The goal of artificial intelligence is to create computers whose intelligence equals or surpasses humans. Therefore, this chapter defines AI theory and establishes the cultural background against which it has developed. It can be divided into various parts such as: Expert System, Fuzzy Logic, Algorithm Genetic, Neural network, Robotics and Natural language processing, in this chapter; we will focus being on three first types only.

In section two, we will present the basic concepts and terminology involved in Artificial Intelligence. Therefore, we will discuss about definition of the intelligence in the philosophy and psychology domains, types of intelligence, its goals, its applications and their research areas.

In third section, we will be able to understand also the basic concepts and terminology involved in Expert System. Where, we will discuss about the components of Expert Systems, rules creation, inference engines types and ES several applications areas.

In section four; broadly reviewed FL principals and their application will be presented. The analogy and the differences between FL and Boolean logic and fuzzy inference system will be explained, particularly relating to operations on fuzzy sets.

In section five, we will present the basic concepts and terminology involved in Genetic Algorithms. We will also discuss about the various crossover and mutation operators, survivor selection, and other components as well.

2.2. Artificial Intelligence

While studying artificial intelligence, we need to know first of all what intelligence is.

2.2.1. Intelligence definition

Intelligence has been defined in many different ways but when they do it by the machine or animals; we consider it to be as intelligent behavior [4]. These ways are including as one's capacity for: Creativity, Solving problems, pattern recognition, Classification, Induction, Learning, deduction, building analogies, language processing, Optimization, knowledge and many more [4].

While the Intelligent behavior appears in different ways including [4]:

- perceiving one's environment;
- learning and understanding from experience;
- knowledge applying successfully in new situations;
- communicating with others, and more like;
- acting in complex environments;
- reasoning to solve problems and discover hidden knowledge;
- thinking abstractly, using analogies.

2.2.2. Types of Intelligence

This categorization of intelligence was first theorized by developmental psychologist Howard Gardner in his 1983 book, the Intelligence comes in multifold as shown Table 2.1[1, 5, 6]:

You can say a machine or a system is artificially intelligent when it is equipped with at least one and at most all intelligences in it. For example: the ability of a system to calculate, reason, perceive relationships and analogies, learn from experience, store and retrieve information from memory, solve problems, comprehend complex ideas, use natural language fluently, classify, generalize, and adapt new situations [1, 2, 4].

2.2.3. Philosophy of AI

While exploiting the power of the computer systems, the curiosity of human, lead him to wonder, "Can a machine think and behave like humans do?".

Thus, the development of AI started with the intention of creating similar intelligence in machines that we find and regard high in humans [1].

2.2.4. Artificial Intelligence definition

AI is accomplished by studying how human brain thinks and how humans learn, decide, and work while trying to solve a problem, and then using the outcomes of this study as a basis of developing intelligent software and systems [1].

The definitions on the left measure success in terms of a human performance, whereas the others on the right measure against an ideal concept of intelligence, which we will call rationality. A system is rational if it does the right thing. This gives us four possible goals to pursue in artificial intelligence which are:

- Systems that think like humans.
- Systems that think rationally.
- System that act like humans.
- System that act rationally.

Table 2.1. Psychologiste Howard Gardner Intelligence type [1, 6]

<i>Intelligence</i>	<i>Description</i>	<i>Example</i>
Linguistic intelligence	It is the ability to speak, recognized and use mechanisms of phonology (speech sounds), syntax (grammar), and semantics (meaning).	Narrators, orators.
Musical intelligence	It is the ability to create, communicate with, and understand meaning made of sound, understanding of pitch, rhythm.	Musicians, singers and composers.
Logical-mathematical intelligence	It is the ability of use and understands relationships in the absence of action or objects. Understanding complex and abstract ideas	Mathematicians; Scientists
Spatial intelligence	It is the ability to perceive visual or spatial information, changes it, and re-creates visual images without reference to the objects, construct 3D images and to move and rotate them.	Map readers, astronauts, physicists
Bodily-Kinesthetic intelligence	It is the ability to use complete or part of the body to solve problems or fashion products, control over fine and coarse motor skills and manipulate the objects.	Players, dancers
Intra-personal intelligence	It is the ability to distinguish among one's own feelings, intentions and motivations.	Religion
Interpersonal intelligence	It is the ability to recognize and make distinctions among other people's feelings, beliefs and intentions.	Mass communications; interviewers.

Historically, all four approaches have been followed. As one might expect, a tension exists between approaches centered around humans and approaches centered around rationality.² A human-centered approach must be an empirical science, involving hypothesis and experimental confirmation. A rationalist approach involves a combination of mathematics and engineering. People in each group sometimes cast aspersions on work done in the other groups, but the truth is that each direction has yielded valuable insights. Let us look at each in more detail.

Table 2.2. Some definitions of AI [1]

<p>“The exciting new effort to make computers think ... machines with minds. In the full and literal sense” (Haugeland, 1985).</p> <p>“The automation of activities that we associate with human thinking, activities such as decision-making, problem solving, learning...” (Bellman, 1978)</p>	<p>“The study of mental faculties through the use of computational models” (Charniak and McDermott, 1985).</p> <p>“The study of the computations that makes it possible to perceive, reason and act” (Winston, 1992).</p>
<p>“The art of creating machines that performs functions that require intelligence when performed by people” (Kurzweil, 1990).</p> <p>“The study of how to make computers do things at which, at the moment people are better” (Rich and Knight, 1991).</p>	<p>A field of study that seeks to explain and emulate intelligent behavior in terms of computational processes” (Schalkoff, 1990).</p> <p>“The branch of computer science that is concerned with the automation of intelligent behavior” (Luger and Stubblefield, 1993).</p>

2.2.5. Goals of AI

- To Create Expert Systems: The systems which exhibit intelligent behavior, learn, demonstrate, explain, and advice its users [1, 4].
- To Implement Human Intelligence in Machines: Creating systems that understand, think, learn, and behave like humans.

2.2.6. Applications of AI

AI has been dominant in various fields such as [4]:

- a) **Gaming:** AI plays crucial role in strategic games such as chess, poker, tic-tac-toe...etc, where machine can think of large number of possible positions based on heuristic knowledge.
- b) **Natural Language Processing:** It is possible to interact with the computer that understands natural language spoken by humans.
- c) **Expert Systems:** There are some applications which integrate machine, software, and special information to impart reasoning and advising. They provide explanation and advice to the users.
- d) **Vision Systems:** These systems understand, interpret, and comprehend visual input on the computer. For example,
 - A spying aero plane takes photographs which are used to figure out spatial information or map of the areas.
 - Doctors use clinical expert system to diagnose the patient.
 - Police use computer software that can recognize the face of criminal with the stored portrait made by forensic artist.

- e) **Speech Recognition:** Some intelligent systems are capable of hearing and comprehending the language in terms of sentences and their meanings while a human talks to it. It can handle different accents, slang words, noise in the background, change in human's noise due to cold, etc.
- f) **Handwriting Recognition:** The handwriting recognition software reads the text written on paper by a pen or on screen by a stylus. It can recognize the shapes of the letters and convert it into editable text.
- g) **Intelligent Robots:** Robots are able to perform the tasks given by a human. They have sensors to detect physical data from the real world such as light, heat, temperature, movement, sound, bump, and pressure. They have efficient processors, multiple sensors and huge memory, to exhibit intelligence. In addition, they are capable of learning from their mistakes and they can adapt to the new environment.

2.2.7. Research areas of AI

The domain of artificial intelligence is huge in breadth and width. While proceeding, we consider the broadly common and prospering research areas in the domain of AI [1, 2, 3, 4]:

- fuzzy logic;
- neural network;
- genetic algorithm;
- expert systems;
- robotics;
- natural language processing.

2.3. Expert system

Expert systems (ES) are one of the prominent research domains of AI. The first expert system is introduced in the early 70's by the researchers at Stanford University, Computer Science Department [13]. According to Efrain Turban (2001), the ES is a system that uses human knowledge stored inside a computer to solve problems that requires human expertise to solve. A good ES is a system that can copy the process of reasoning in a human.

What is meant by expert? An expert is a person that has the expertise and knowledge of his specialized field. Examples of experts are a heart specialist and mathematics expert. Through experience, an expert expands his skills to enable him to solve problems heuristically, efficiently and effectively [13, 14].

2.3.1. Definition

Professor Edward Feigenbuan (1983) from Stanford University, a famous researcher on ES defines ES as [13]:

“It is an intelligent computer program that uses knowledge and reasoning procedures to solve difficult

problems that need certain expertise to solve the problems.”

2.3.2. Expert system & Expert human

Why an expert system needed ? Table 2.3 will answer our query by comparing the expert system to that of human.

Table 2.3. Comparisons between an expert system and that of a human expert [13]

<i>Factor</i>	<i>Human expert</i>	<i>Expert system</i>
Time (can be obtained)	Working days only	Anytime
Geography	Local	Anywhere
Safety	Cannot be replaced	Can be replaced
Damages	Yes	No
Speed and efficiency	Changes	Consistent
Cost	High	intermediate

2.3.3. Components of Expert Systems

The components of ES include (as shown Figure 2.1) [14]:

- domain expert (Human expert),
- knowledge engineer;
- knowledge Base;
- inference Engine;
- user Interface;
- end user.

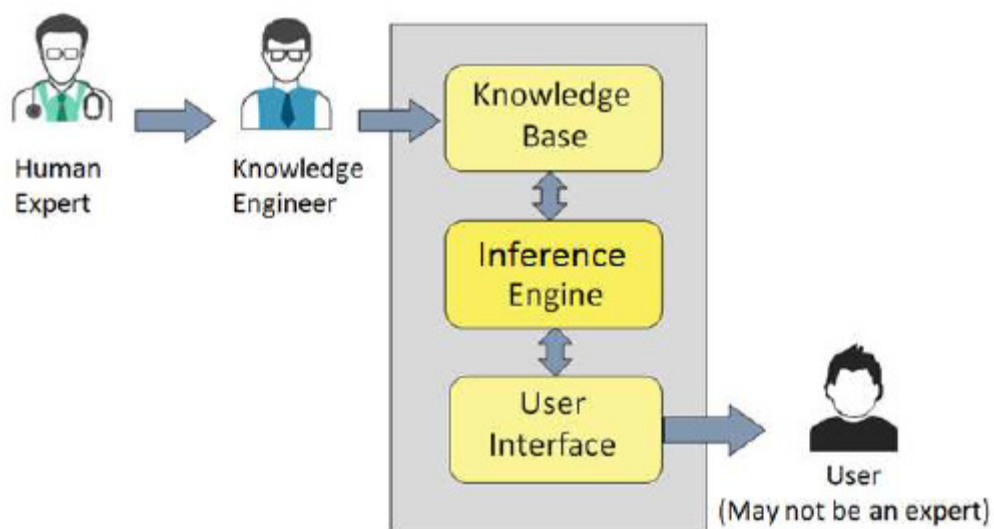


Figure 2.1. Expert System components [14].

a) Domain expert:

It's the individual who is currently expert to solve the problems.

b) Knowledge engineer

It's the individual who encodes the expert's knowledge in a declarative form that can be used by the expert system.

c) Knowledge base

It's a declarative representation of the expertise the most popular expert system type based on rules which often in IF.....THEN rules.

d) Inference engine

The inference engine is the most important component and is considered the "brain" of an ES. It is the knowledge process that is modeled on the methods of human expert reasoning. It is a process in the Expert System that pairs the facts stored in the working memory with the knowledge domain that is stored in the knowledge database, to get the method from the problem. It is also known as the control structure or the rule interpreter for an ES base rule [15].

e) User interface

It's the code that controls the dialog between the end-user and the system.

f) End-user

It's the individual who will be consulting with the system to get advice which would have been provided by the expert.

2.3.4. Rules Creation

Rules are divided into two operators [16]:

- IF, called before (a premise or condition); and
- THEN, it is called effect (conclusions or actions).

In general, rules can have a few conditions by relating each condition to the keywords "AND, OR" or a combination (AND and OR). On the contrary, it is better to avoid combining both in one rule. The example below shows how a few conditions are related to AND.

1) Rule with "AND" and "OR": The next example shows how a few conditions are related to "AND, OR".

$$\left. \begin{array}{l} IF \langle condition .1 \rangle \\ AND \langle condition .2 \rangle \\ OR \langle condition .3 \rangle \end{array} \right\} \\ TTHEN \langle Action \rangle$$

- 2) **Rule with “AND” or “OR”**: The example below shows how a few conditions are related to AND.

$$\left\{ \begin{array}{l} IF \langle condition.1 \rangle \\ AND..IF \langle condition.2 \rangle \\ \cdot \\ \cdot \\ \cdot \\ AND..IF \langle condition.n \rangle \end{array} \right\}$$

TTHEN $\langle Action \rangle$

According to Durkin, rules can represent a relationship, suggestion, instruction, strategy and heuristic.

Examples:

- **Relationship**

$$\left\{ \begin{array}{l} IF \langle tank.is.empty \rangle \\ THEN \langle car.is.cannot.start \rangle \end{array} \right\}$$

- **Suggestions**

$$\left\{ \begin{array}{l} IF \langle monsoon.season \rangle \\ AND \langle cloudy.sky \rangle \\ AND \langle weather.station.predicted.rain \rangle \\ THEN \langle you\ are\ advised\ to\ bring\ an\ umbrella \rangle \end{array} \right\}$$

- **Strategy**

$$\left\{ \begin{array}{l} IF \langle car\ cannot\ start \rangle \\ AND \langle tank\ is\ empty \rangle \\ THEN \langle put\ petrol\ in\ the\ tank \rangle \\ Step\ 1\ is\ done \\ IF \langle Step\ 1\ is\ done \rangle \\ AND \langle tank\ is\ full \rangle \\ THEN \langle check\ the\ car\ battery \rangle \\ Step\ 2\ is\ done \end{array} \right\}$$

- **Instructions**

$$\left\{ \begin{array}{l} IF \langle car\ cannot\ start \rangle \\ AND \langle tank\ is\ empty \rangle \\ THEN \langle put\ petrol\ in\ the\ tank \rangle \end{array} \right\}$$

- **Heuristic**

$$\left\{ \begin{array}{l} \text{IF } \langle \text{fluid spills} \rangle \\ \text{AND } \langle \text{pH of the spill} < 6 \rangle \\ \text{AND } \langle \text{smells acidic or sour} \rangle \\ \text{THEN } \langle \text{the spills is an acetic acid} \rangle \end{array} \right.$$

2.3.5. Types of inference engine

There are two strategies used by the inference engine when making decisions or conclusions. These strategies are forward and backward chaining. The strategy of forward chaining can obtain a decision and produce more information with fewer questions compared to backward chaining. Thus, it is always used for large scale and complex ES. However, the weakness in this approach is the long duration taken for processing. Certain ES developed employs a combination of both the strategies of chaining, which is called the mixed chaining [15, 16].

a) Forward chaining strategy:

The inference engine starts reasoning from the facts provided and moves on until it achieves its decision or conclusion. This strategy is guided by the provided facts in the memory space and the premises which it can obtain them from. The inference engine will try to match the required premise (IF) for all rules in the knowledge database with the facts given, which are in its memory. If there are several rules that match, the solving procedures will be used. The inference engine will repeatedly match the rules of the basic knowledge to the data stored in its memory [15, 16].

b) Backward chaining strategy:

This strategy is the opposite of the forward chaining strategy. It starts from the decision and moves backward to obtain supporting facts for the decision made. If there are no matching facts that support the chosen decision, the decision will be rejected and another decision will be selected. The process continues until a suitable decision and the facts that support it are obtained [15, 16].

2.5.6. Expert system applications

Expert system is widely in all types of fields and sectors like: medicine, engineering, education, marketing, tax planning and more as shown Table 2.4.

2.4. Fuzzy Logic

FL is another class of AI; but its history and applications are more recent than those of the expert system (ES). Based on the nature of fuzzy human thinking; Lofti Zadeh, a computer scientist at the University of California, Berkely, originated the “Fuzzy Logic” or fuzzy set theory in 1965 [17]. In the beginning, he was highly criticized by the professional community, but gradually, FL captured the imagination of the professional community and eventually emerged as an entirely new discipline of AI [17, 18].

Table 2.4. Expert system applications domain [15]

<i>Fields</i>	<i>Example of ES applications</i>
control	Controlling the behavior of the system according to specification
Design	Aligning objects following limits
Diagnosis	Providing reasons for system malfunction based on observation
Instruction	Diagnosing and improving behavior of students
Translation	Providing reasons for situations based on data given
Planning	Designing a plan of action
Prediction	Providing the best selection from all alternatives and probabilities
Prescription	Suggesting solution to improve a malfunction system

2.4.1. Definition

According to Georg Boole, human thinking and decisions are based on “yes/no” reasoning, or “1/0” logic but after the development of Boolean logic, it has been argued that human thinking does not always follow crisp “yes/no” logic but is often vague, qualitative, uncertain, imprecise or fuzzy in nature [16].

Therefore, the approach of FL is a form of many-valued logic in which the truth values of variables may be any real number between 0 and 1. It is employed to handle the concept of partial truth, where the truth value may range between completely true and completely false [17]. Furthermore, when linguistic variables are used, these degrees may be managed by specific (membership) functions [17].

2.4.2. Fuzzy sets

In mathematics, fuzzy sets are sets whose elements have degrees of membership. In classical set theory, the membership of elements in a set is assessed in binary terms according to a bivalent condition an element either belongs or does not belong to the set. By contrast, fuzzy set theory permits the gradual assessment of the membership of elements in a set; this is described with the aid of a membership function valued in the real unit interval $[0, 1]$. Fuzzy sets generalize classical sets, since the indicator functions of classical sets are special cases of the membership functions of fuzzy sets, if the latter only take values 0 or 1 [15]. In fuzzy set theory, classical bivalent sets are usually called crisp sets. The fuzzy set theory can be used in a wide range of domains in which information is incomplete or imprecise, such as bioinformatics.

2.4.2.1. Membership functions

The membership function (MF) is a curve that defines how each point in the input space is mapped to a membership value (or degree of membership) between 0 and 1. The input space is sometimes referred to as

the universe of discourse [16, 17].

For any set X , a membership function on X is any function from X to the real unit interval $[0, 1]$. Membership functions on X represent fuzzy subsets of X . The membership function which represents a fuzzy set A is usually denoted by U_A as shown Equation 2.1 and Equation 2.2.

$$\begin{cases} U_A(x) : X \mapsto [0;1] \\ A = \{(x, U_A(x)); x \in X, U_A(x) \in [0;1]\} \end{cases} \quad (2.1)$$

$$A = U_A(x_1)/x_1 + U_A(x_2)/x_2 + \dots + U_A(x_i)/x_i + \dots = \sum_{x_i \in X} U_A(x_i)/x_i \quad (2.2)$$

For an element x of X , the value $U_A(x)$ is called the membership degree of x in the fuzzy set A . The membership degree $U_A(x)$ quantifies the grade of membership of the element x to the fuzzy set A . The value 0 means that x is not a member of the fuzzy set; the value 1 means that x is fully a member of the fuzzy set as shown Equation 2.3. The values between 0 and 1 characterize fuzzy members, which belong to the fuzzy set only partially.

$$U_A(x) = \begin{cases} 1; \text{if } (x \in A) \\ 0; \text{if } (x \notin A) \end{cases} \quad (2.3)$$

2.4.2.2. Membership functions types

As shown Figure 2.2, a MF can have different shapes such as [16, 17]:

- triangular;
- trapezoidal;
- Gaussian;
- sigmoid right;
- sigmoid left;
- sigmoid difference;
- Ssingleton.

The simplest and the most commonly used MF is the triangular type, which can be symmetrical or asymmetrical in shape. In addition to these types, any arbitrary MF can be generated by the user. In practice, one or two types of MFs (such as triangular and Gaussian) are more than enough to solve most problems.

A singleton is special type of MF that has a value of 1 at one point on the universe of discourse and zero elsewhere as shown Figure 2.2 (g).

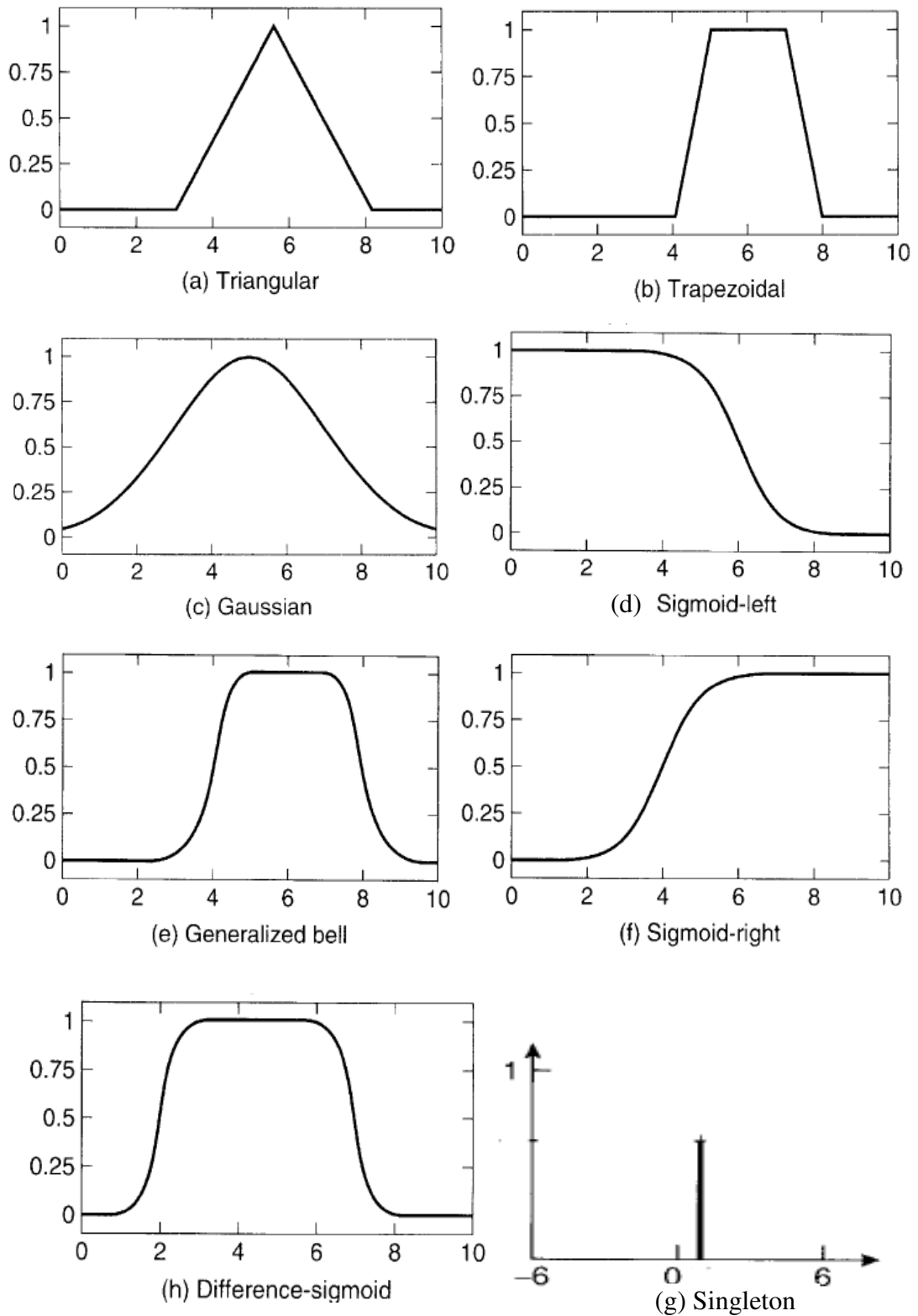


Figure 2.2. Different types of membership functions [9].

2.4.3. Operators on Fuzzy sets

The basic properties of Boolean logic are also valid for FL. Figure 2.3 shows sets A and B using triangular MFs (Figure 2.3 (a-1)) and compared them with the corresponding Boolean operations on the right [16, 17] (Figure 2.3 (b-1)).

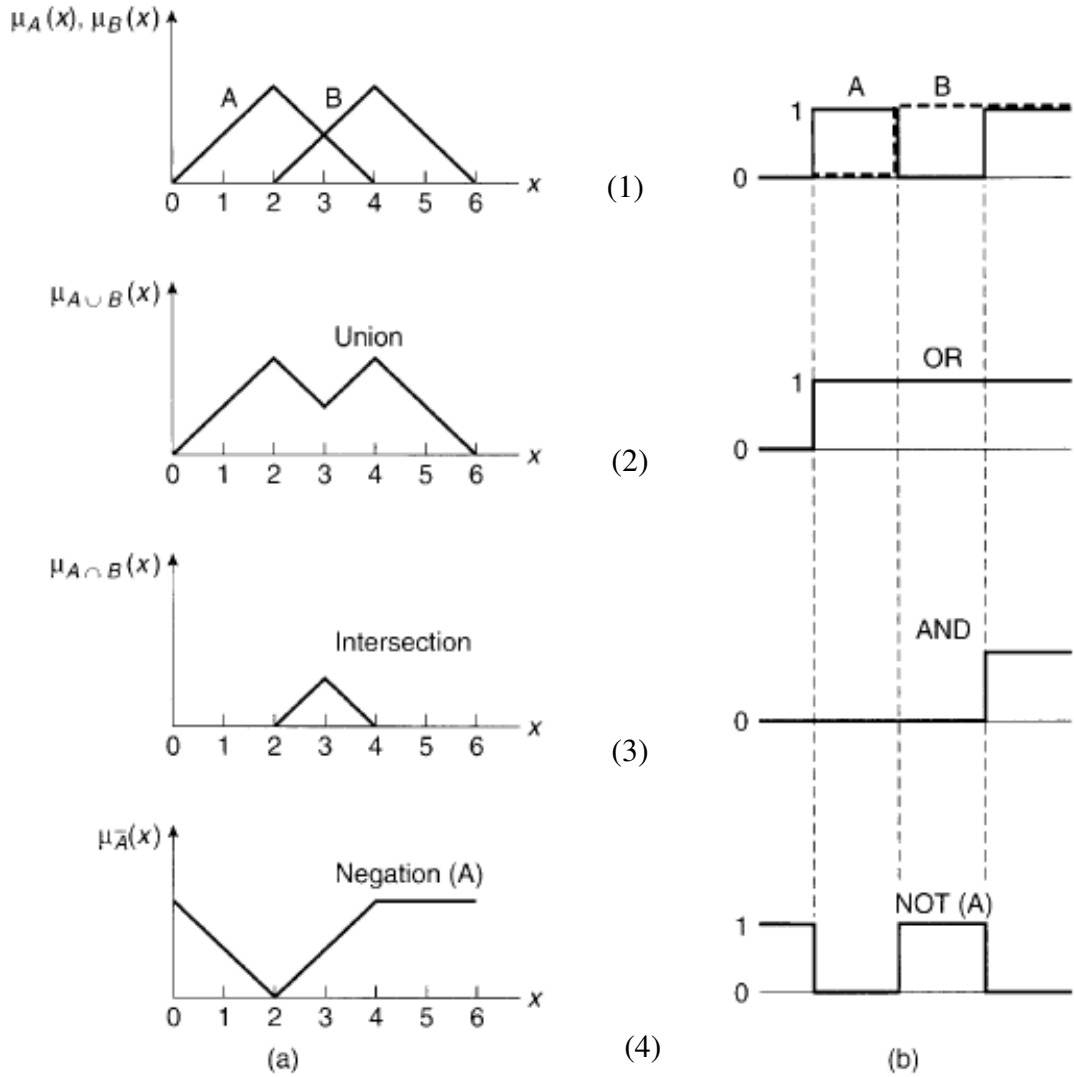


Figure 2.3. Logical operations (a) Fuzzy sets, (b) Crisp sets [9].

a) Complement or negation

The complement of given set A in the universe of discourse X is denoted by \bar{A} and has the membership function (Figure 2.3 (3)).

$$U_{\bar{A}}(x) = 1 - U_A(x) \text{ for all } x \in X \tag{2.4}$$

b) Union

Given two fuzzy sets A and B , defined in the universe of discourse X ; the union $(A \cup B)$ is also a fuzzy set of X , with the membership function given as (Figure 2.3 (2)):

$$U_{A \cup B}(x) = \max[U_A(x); U_B(x)], \forall x \in X \tag{2.5}$$

c) Intersection

The intersection of two fuzzy sets A and B in the universe of discourse X denoted by $(A \cap B)$ has the membership function given by (Figure 2.3 (3)):

$$U_{A \cap B}(x) = \min[U_A(x); U_B(x)], \forall x \in X \quad (2.6)$$

d) **Others lows operations:** of fuzzy sets are mentioned in Table 2.5 as follow:

Table 2.5. Others lows operations of fuzzy sets [12, 9]

Operation	Truth value equivalence
Product	$U_{A \cdot B}(x) = U_A(x) \cdot U_B(x)$
Multiplying by crisp number	$U_{kA}(x) = kU_A(x)$
Power	$U_{A^m}(x) = [U_A(x)]^m$ where m positive real number
Double negation	$\overline{(\overline{A})} = A$
Idempotency	$A \cup A = A$ and $A \cap A = A$
Commutatively	$A \cap B = B \cap A$ and $A \cup B = B \cup A$
Associative property	$(A \cap B) \cap C = A \cap (B \cap C)$ and $(A \cup B) \cup C = A \cup (B \cup C)$
Distributive property	$A \cap (B \cup C) = (A \cap B) \cup (A \cap C)$ and $A \cup (B \cap C) = (A \cup B) \cap (A \cup C)$
Absorption	$A \cap (A \cup B) = A$ and $A \cup (A \cap B) = A$
De Morgan's Theorems	$\overline{A \cup B} = \overline{A} \cap \overline{B}$ and $\overline{A \cap B} = \overline{A} \cup \overline{B}$

2.4.4. Fuzzy logic system

FLS is basically consists of a formulation of mapping from a given input set to an output set using FL. This mapping process provides the basis from which the inference or conclusion can be made. A FLS consists of main parts [16, 17]:

- 1) **Fuzzification:** It transforms the system inputs, which are crisp numbers, into fuzzy sets.
- 2) **Rules:** It stores IF-THEN rules provided by experts.
- 3) **Inference engine:** It simulates the human reasoning process by making fuzzy inference on the inputs and IF-THEN rules.
- 4) **Defuzzification:** It simulates the human reasoning process by making fuzzy inference on the inputs and IF-THEN rules.

These complements and the general architecture of FLS are shown in Figure 2.4.

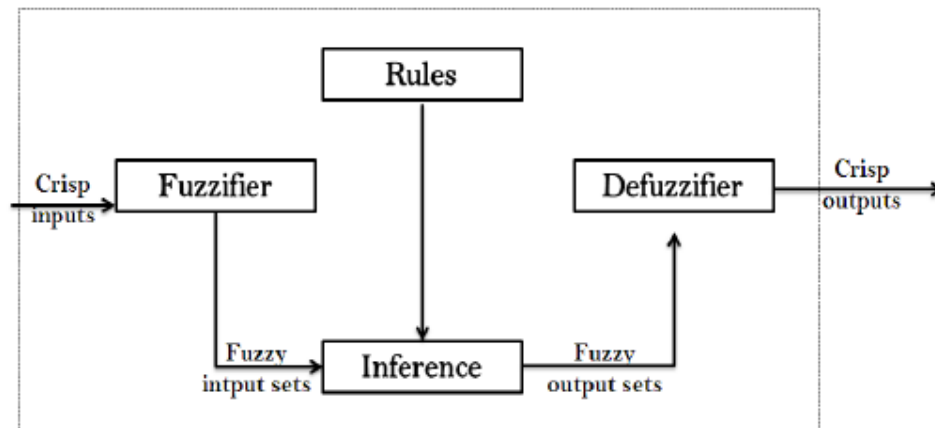


Figure 2.4. Fuzzy Logic System (FLS).

2.4.5. Fuzzy logic applications

The fuzzy logic is applied in many domain; some key application areas of fuzzy logic are as shown Table 2.6 follow [11]:

Table 2.6. Fuzzy logic applications

<i>Fields</i>	<i>Example of FL applications</i>
Electronics	<ul style="list-style-type: none"> ▪ Control of automatic exposure in video cameras ▪ Humidity in a clean room ▪ Air conditioning systems ▪ Washing machine timing
Industrial Sector	<ul style="list-style-type: none"> ▪ Cement kiln controls heat exchanger control ▪ Activated sludge wastewater treatment process control ▪ Water purification plant control ▪ Quantitative pattern analysis for industrial quality assurance ▪ Control of constraint satisfaction problems in structural design ▪ Control of water purification plants
Marine	<ul style="list-style-type: none"> ▪ Autopilot for ships ▪ Optimal route selection ▪ Control of autonomous underwater vehicles ▪ Ship steering
Medical	<ul style="list-style-type: none"> ▪ Medical diagnostic support system ▪ Radiology diagnoses ▪ Fuzzy inference diagnosis of diabetes and prostate cancer
Aerospace	<ul style="list-style-type: none"> ▪ Altitude control of spacecraft ▪ Satellite altitude control

	<ul style="list-style-type: none"> ▪ Flow and mixture regulation in aircraft deicing vehicles
Automotive	<ul style="list-style-type: none"> ▪ Trainable fuzzy systems for idle speed control ▪ Intelligent highway systems ▪ Traffic control ▪ Improving efficiency of automatic transmissions
Business	<ul style="list-style-type: none"> ▪ Decision-making support systems ▪ Personnel evaluation in a large company
Defense	<ul style="list-style-type: none"> ▪ Underwater target recognition ▪ Naval decision support aids ▪ Control of a hypervelocity interceptor

2.5. Algorithm Genetic

Genetic Algorithm is one of the search areas of artificial intelligence science. It was developed by John Holland and his students and colleagues at the University of Michigan, most notably David E. Goldberg and has since been tried on various optimization problems with a high degree of success [18]. It is a subset of a much larger branch of computation known as Evolutionary Computation.

2.5.1. Definition

It is a search used optimization technique based on the principles of Genetics and Natural Selection. It is frequently used to find optimal or near optimal solutions to difficult problems which otherwise would take a lifetime to solve [18, 19].

In GAs, we have a pool or a population of possible solutions to the given problem. These solutions then undergo recombination and mutation (like in natural genetics), producing new children, and the process is repeated over various generations. Each individual (or candidate solution) is assigned a fitness value (based on its objective function value) and the fitter individuals are given a higher chance to mate and yield more “fitter” individuals. This is in line with the Darwinian Theory of “Survival of the Fittest” but this theory is not truth in our life as we can see the human and others animals don’t evaluate within the time for millions years.

2.5.2. Basic Terminology

Before beginning a discussion on Genetic Algorithms, it is essential to be familiar with some basic terminology which will be used throughout this tutorial [18, 19].

- **Population:** It is a subset of all the possible (encoded) solutions to the given problem. The population for a GA is analogous to the population for human beings except that instead of human beings, we have Candidate Solutions representing human beings.

- **Chromosomes:** A chromosome is one such solution to the given problem.
- **Gene:** A gene is one element position of a chromosome.
- **Fitness Function:** A fitness function simply defined is a function which takes the solution as input and produces the suitability of the solution as the output. In some cases, the fitness function and the objective function may be the same, while in others it might be different based on the problem.
- **Genetic Operators:** These alter the genetic composition of the offspring. These include crossover, mutation, selection, etc.

2.5.3. Basic Structure

The basic structure of a GA is as Figure 2.5. We start with an initial population (which may be generated at random or seeded by other heuristics), select parents from this population for mating. Apply crossover and mutation operators on the parents to generate new off springs. And finally these off springs replace the existing individuals in the population and the process repeats. In this way genetic algorithms actually try to mimic the human evolution to some extent [18, 19, 20].

2.5.4. Population initialization

Population is a subset of solutions in the current generation. It can also be defined as a set of chromosomes. There are two primary methods to initialize a population in a GA [18, 19]. They are:

- **Random Initialization:** Populate the initial population with completely random solutions.
- **Heuristic initialization:** Populate the initial population using a known heuristic for the problem.

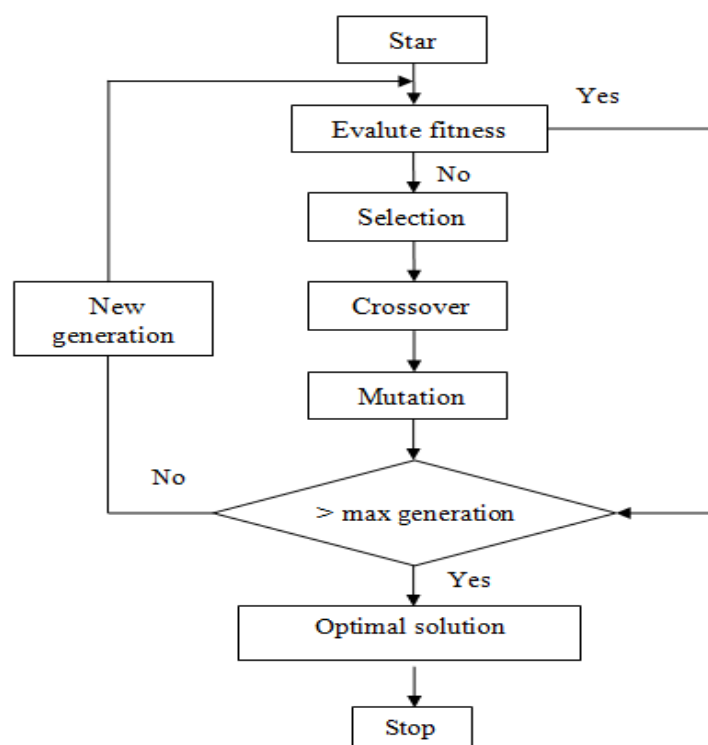


Figure 2.5. Flowchart of the GA optimization technique.

2.5.5. GA encoding

Before a genetic algorithm can be put to work on any problem, a method is needed to encode potential solutions to that problem in a form so that a computer can process. Therefore; we must to think about the most appropriate representation of these solutions which permit to accelerate the algorithm to reach the optimal solution, and of course the process of selecting the most appropriate representation process of the issue that we seek to solve; but there are a number of methods of encoding which are:

a) *Binary encoding*

Binary encoding is the most common to represent information contained. In genetic algorithms, it was first used because of its relative simplicity [19].

In binary encoding; every chromosome is a string of bits “0” and “1”; like follow:

Chromosome 1: 1 0 1 1 0 0 1 0 1 1 0 0 1 0 1 1 1 0 0 1 0 1

Chromosome 2: 1 1 1 1 1 1 0 0 0 0 0 1 1 0 1 0 0 1 1 1 1 1

Binary encoding gives many possible chromosomes even with a small number of alleles which means possible setting for a trait.

This encoding is often not natural for many problems and sometimes corrections must be made after crossover and/or mutation.

b) *Permutation Encoding*

In this encoding type, each chromosome presents a string of numbers or codes without recurring as follow [19]:

Using numbers: *Chromosome A:* 1 5 3 2 6 4 7 9 8

Chromosome B: 8 5 6 7 2 3 1 4 9

Using alphabets: *Chromosome A:* L I G H T

Chromosome B: I G T H L

c) *Real Valued encoding*

For problems where we want to define the genes using continuous rather than discrete variables, the real valued representation is the most natural. The precision of these real valued or floating point numbers is however limited to the computer as follow [19]:

Chromosome A : 1.2324 5.3243 0.4556 2.3293 2.4545

d) *Tree encoding*

This type of coding is used primarily for programs or expressions and programming genetic. Such as appendices or commands in languages, where each chromosome in the tree's encoding serves as a tree of some purpose programming as shown Figure 2.6 [19].

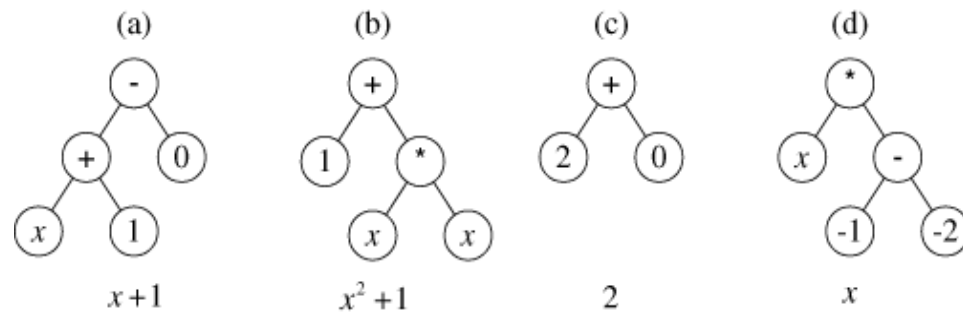


Figure 2.6. Chromosomes using tree encoding [18].

2.5.6. Fitness Function

The fitness function simply defined is a function which takes a candidate solution to the problem as input and produces as output how “fit” or how “good” the solution is with respect to the problem in consideration [18].

Calculation of fitness value is done repeatedly in a GA and therefore it should be sufficiently fast. A slow computation of the fitness value can adversely affect a GA and make it exceptionally slow.

In most cases the fitness function and the objective function are the same as the objective is to either maximize or minimize the given objective function. However, for more complex problems with multiple objectives and constraints, an Algorithm Designer might choose to have a different fitness function.

A fitness function should possess the following characteristics:

- The fitness function should be sufficiently fast to compute.
- It must quantitatively measure how fit a given solution is or how fit individuals can be produced from the given solution.

2.5.7. Genetic Operators

The importance of genetic operators stems from finding solutions that were not previously present in the space of solutions. Among the most important genetic operators [18, 19, 20]:

2.5.7.1. Crossover or recombination

It is to be noted that these crossover operators are very generic and the GA Designer might choose to implement a problem-specific crossover operator as well. There are many crossover methods which are [18, 19, 20]:

- **Single point crossover:** In this one-point crossover, a random crossover point is selected and the tails of its two parents are swapped to get new off-springs.
- **Multi point crossover:** Multi point crossover is a generalization of the one-point crossover wherein alternating segments are swapped to get new off-springs.

- **Uniform crossover:** In a uniform crossover, we don't divide the chromosome into segments; rather we treat each gene separately. In this, we essentially flip a coin for each chromosome to decide whether or not it'll be included in the off-spring. We can also bias the coin to one parent, to have more genetic material in the child from that parent.
- **Arithmetic crossover:** This is commonly used for integer representations and works by taking the weighted average.

2.5.7.2. Mutation

Mutation is the part of the GA which is related to the "exploration" of the search space. It has been observed that mutation is essential to the convergence of the GA while crossover is not [18, 19, 20].

2.5.7.3. Selection

The Survivor Selection Policy determines which individuals are to be kicked out and which are to be kept in the next generation. It is crucial as it should ensure that the fitter individuals are not kicked out of the population, while at the same time diversity should be maintained in the population [18, 19, 20].

There are several ways to determine how chromosomes are selected which are as follow:

- Roulette wheel Selection
- Boltzman selection
- Tournament selection
- Steady state selection

2.5.8. Genetic Algorithms application area

Genetic Algorithms are primarily used in optimization problems of various kinds, but they are frequently used in other application areas as well. In Table 2.7, we list some of the areas in which Genetic Algorithms are frequently used [18].

2.6. Conclusion

AI is one of the newest fields in science and engineering which work started in earnest soon after World War II. This science divided in many research areas such as: Expert System, Fuzzy Logic, Algorithm Genetic, Neural Network, Robotic and Natural language processing. This chapter reviews the meaning of artificial intelligence and its basic concepts and terminology including its applications, goals and various research areas.

In section two, we were presented the basic concepts and terminology involved in Artificial Intelligence. Therefore, we were discussed about definition of the intelligence in the philosophy and psychology domains, types of intelligence, goals, applications and their research areas.

Table 2.7. Genetic Algorithms application area [18]

<i>Fields</i>	<i>Example of GA applications</i>
Optimization	Genetic Algorithms are most commonly used in optimization problems wherein we have to maximize or minimize a given objective function value under a given set of constraints.
Economics	characterize various economic models like the cobweb model, game theory equilibrium resolution, asset pricing, etc.
Neural Networks	Used to train neural networks, particularly recurrent neural networks.
Image Processing	Used for various digital image processing (DIP) tasks as well like dense pixel matching.
Machine Learning	Genetics based machine learning (GBML) is a niche area in machine learning.
Robot Trajectory Generation	GAs have been used to plan the path which a robot arm takes by moving from one point to another.
Traveling salesman problem and its applications	GAs have been used to solve the TSP, which is a well-known combinatorial problem using novel crossover and packing strategies.

In section two, we were understood also the basic concepts and terminology involved in Expert System. Where, we were discussed about the components of Expert Systems, rules creation, inference engines, its types and ES several applications areas.

In section three broadly reviewed FL principals and their application will were presented. The analogy and the differences between FL and Boolean logic and fuzzy inference system were being explained, particularly relating to operations on fuzzy sets.

In section five, we were understood the basic concepts and terminology involved in Genetic Algorithms. We were also discussed the various steps of AG such as: crossover and mutation operators, survivor selection, and other components as well.

2.7. References

- [1] Kit Po Wong, “*Artificial intelligence and neural network applications in power systems*”, Advances in Power System Control, Operation and Management, APSCOM-93., 2nd International Conference on, 1993.
- [2] Stuart J. Russell and Peter Norvig, “*Artificial Intelligence A Modern Approach*”, 1995 by Prentice-Hall, Inc.
- [3] John Haugeland; “*Artificial intelligence: The very idea*”; book, the Massachusetts Institute of Technology, 1985.
- [4] Jatin Borana, “*Applications of Artificial Intelligence & Associated Technologies*”, Proceeding of International Conference on Emerging Technologies in Engineering, Biomedical, Management and Science [ETEBMS-2016], 5-6 March 2016.
- [5] Tony Buzan; “*Both Sides of Your Brain*”; book; 2011.
- [6] Walim Karamiz, “*The seven chapters of the Intelligence*”; Arabic version, dar-elkholoud. 2011.
- [7] Ford, K. And Hayes, P. (1998), “*On Computational Wing: Rethinking the Goals of Artificial Intelligence*”, Scientific American Presents 9 (4): 78-83.
- [8] Luger, G. F. And Stubblefield, W.A. (1998), “*Artificial Intelligence: Structures And Strategies For Complex Problem Solving*”, Third Edition, Harlow, England: Addison Wesley Longman, Inc.
- [9] Bimal K. Bose, “*Bose-Modern power electronics and AC drives*”, book, Prentice Hall PTR (2002).
- [10] Takagi, T., and Sugeno, M., Fuzzy identification of systems and its application to modeling and control, IEEE Trans. Systems Man Cybernet. SMC-15, 116-132, 1985.
- [11] www.tutorialpoint.com/fuzzy, March 2018.
- [12] Zadeh, L.A. (1965), “*Fuzzy Sets, Information and Control*”, 8: pp: 338-353.
- [13] gnizio, J.P. (1991), “*Introduction to Expert Systems: The Development And Implementation of Rule-Based Expert Systems*”, McGraw-Hill International Editions.
- [14] Bag T, Samanta SK.” *A comparative study of fuzzy norms on a linear space*”. Fuzzy Set Syst 2008, 159:670–684.
- [15] Subramanian,D. (1993). “*Artificial intelligence and conceptual design*”, In Proceedings of the Thirteenth International Joint Conference on Artificial Intelligence (IJCAI-93), pages 800-809, Chambéry, France. Morgan Kaufmann.
- [16] B. K. Bose, “*Expert-system, fuzzy logic and neaural network applications in power electronics and motion control*”, Proc. IEEE. Vol. 82. Pp. 1303- 1323. Aug. 1994.
- [17] M. G. Simeos and B. K. Bose. “*Application of fuzzy logic in the estimation of power electronic waveforms*”, IEEE, IAS Annu. Meet. Conf. Rec, pp. 342-346. 1991.

- [18] Eiben, A. E. et al (1994). "Genetic algorithms with multi-parent recombination". PPSN III: Proceedings of the International Conference on Evolutionary Computation. The Third Conference on Parallel Problem Solving from Nature: 78–87. ISBN 3-540-58484-6.
- [19] D.E. Goldberg, "*Genetic Algorithms in Search, Optimization, and Machine Learning*", Addison-Wesley, New York, USA, 1989.
- [20] F. Herrera, J.L. Verdegay (Eds.), "*Genetic Algorithms & Soft Computing*", Springer, New York, USA, 1996.
- [21] Booker, L, "*Improving search in genetic algorithms*". in [Dav87], pp. 61-73, 1987.

Chapter III :Power Quality Enhancement of DFIG Based Wind Energy System

Abstract: *Power quality is a set of limits or conditions of electrical properties that allows electrical devices to function in their planned manner without loss of performance. Without the proper power, an electrical utility may malfunction, fail permanently, or not operate well. Therefore, main problems of the power quality especially the harmonics power distortion are discussed and presented in this chapter. These distortions should be within limits according to national and international guidelines framed for power quality. Therefore, a mitigation technique with a shunt active power filter has been used to reduce harmonics distortion into the permitted limits. The proposed solution uses the wind turbine system's converter in goal to reduce the cost of the global control system including a new strategy named priority method technique. This priority control method permits to manage the priority among three different controls which are: the active stator power control; reactive stator power control and suppression harmonics currents control by using the shunt active filter with Synchronous Reference Frame (SRF) harmonic extraction current method and in order to have a high performance and robustness of the control strategy; PI-adaptive fuzzy controller are including for rotor currents control and compared with other classical regulators. The simulation model was developed in Matlab/Simulink environment and the simulation results show that the proposed control schema can effectively reduce the Total Harmonic Distortion (THD) in the grid currents within the international guidelines framed.*

3.1. Introduction

3.1.1. Overview

The electricity generated by the wind turbine system or any other types of energy moves through a complex system (called a grid), of electrical substations, transformers and power lines that connect electricity producers and consumers. A good power quality can be defined as pure sinusoidal voltage/current waveform with 1 p.u magnitude and 1 p.u frequency and the phase shift of 120 degree between the adjacent phases in the three phase system of voltage/current, these are the important characteristics which is aimed by the system to produce and delivered to the consumers [1, 2]. Therefore, any changing in this power waveform (voltage/current) is generally defined as a power quality disturbance or problem which can results a failure or mal-operation of equipments user's or a complete shutdown [3, 4].

Power quality problems are classified in eight categories which are: transients, interruptions, long-duration voltage variations, short-duration voltage variations, waveform distortions; voltage imbalance; voltage fluctuations and frequency variations; each type of these problems has different categories that define by their proper consequences from the less to the most dangerous [3, 5]. One of the most severe problems of power quality is harmonic distortion and its consequences [6]. Particularly, the increasing penetration of power electronics-based loads (non-linear loads) is creating a growing concern for harmonic distortion in the grid. The negative impact of harmonics may not be immediately evident, but over time can result in increased power demand, system loss, and shorter equipment lifetimes [6]. In order to suppress or at least reduce the influence of harmonics, several possible ways have been previously proposed among of those are the passive and active filters [7].

The performance of passive filters is strongly dependent on the system impedance at the harmonic frequencies. The system impedance depends on the distribution network configuration and the loads. Therefore, design of passive filters involves thorough system analysis in order to obtain adequate filtering performance of the filter. Whereas; the active filters measure the harmonic currents present in the system and generate opposite harmonics to cancel those produced by the harmonic sources [8].

3.1.2. Chapter objectives and organization

In this chapter, we present a system model with a shunt active filter in order to reduce the currents harmonics in the grid. Therefore, we remind firstly the different power quality problems existing in the grid then we will detail especially in the currents harmonics, their basics including Fourier theory, their caused, their consequences and their solutions are explained briefly in second and third sections.

In section four, a brief review about the active power filters existing in the domain and their principal working, using and drawbacks will be discussed.

In order to reduce the harmonics existing in the grid (in section five); a Shunt Active Power Filter (SAPF) based on a priority method which permit to filtering the harmonics in the grid via the system's converter (RSC), the aim of this method is to manage the priority among three different controls: active stator power control; reactive stator power control and harmonic rotor current control by using the active shunt filter with

Synchronous Reference Frame (SRF) harmonic method compensation. In other side, and in order to have a high performance and control robustness; a PI-adaptive fuzzy logic controller are including for rotor currents control compared with hysteresis and PI controllers. Where, the simulation results will be presented in MATLAB environment.

Finally, the chapter will summarized by a conclusion in section six.

3.2. Power Quality (PQ) problems

3.2.1. Power quality definition

One of the properties of electricity is that some of its characteristics depend not only on the electricity producer/distributor but also on the equipment manufacturers and the consumer. The large number of players combined with the use of terminology and definitions which may sometimes be imprecise partly explain why this subject area is so complex. Institute of Electrical and Electrical Engineers (IEEE) standard IEEE 1100 defines power quality “as the concept of powering and grounding sensitive electronic equipment in a manner suitable for the equipment”. So; the PQ is simply the interaction of electric power with electrical equipments [1, 2, 3].

Generally, it's linked by the electric wave form. This last is determined by the following factors [1]:

- Amplitude
- Frequency
- Harmonics
- Symmetry of 3-phase system

Therefore; any changing performs in any of the previous factors loads an impact and changing in the electric power sinusoidal waveform; while principal goodness of the power quality is achieved if all values are within the permissible standard limits [1].

3.2.2. Types of power disturbances

Power quality is a science that searches in the sources of the disturbances and their mitigation. So; there are many methods to classify the kinds of disturbances, we mention them as follow [1]:

- In terms of frequency.
- In terms of time.
- In terms of utility responsibility and consumer responsibility.

The IEEE defined power quality disturbances and has been organized into eight categories based on wave shape as follow [1, 3, 9, 10, 11]:

- Transients
- Interruptions
- Short-duration voltage variations

- Long- duration voltage variations
- Waveform distortions
- Voltage fluctuations
- Voltage imbalance
- Frequency variations

3.2.2.1. Transients

Transients are sub-cycle disturbances in the AC waveform and can be categorized as either impulsive or oscillatory. Transients are possibly the most damaging type voltage disturbance [1, 3].

a) Impulsive

It is defined by IEEE 1159 as a sudden, high peak events and non-power frequency change in the steady-state condition of voltage, current, or both that is unidirectional in polarity – either primarily positive or negative. Many different terms, such as bump, glitch, power surge, and spike have been used to describe impulsive transients [10]. These types of events can be categorized further by the speed at which they occur (fast, medium, and slow). One example of positive impulsive transient is illustrated in Figure 3.1.

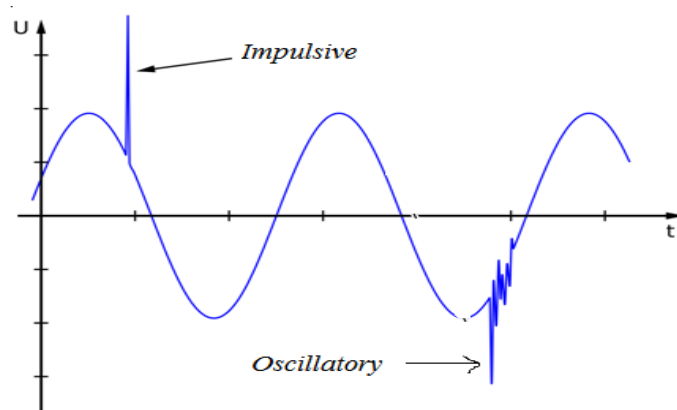


Figure 3.1. Impulsive and oscillatory transients [40].

b) Oscillatory

It is a sudden, non-power frequency change in the steady-state condition of voltage, current, or both, that includes both positive and negative polarity values at the natural system frequency as shown Figure 3.1 [1, 10].

3.2.2.2. Interruptions

An interruption occurs when the supply voltage or load current decreases to less than 0.1 pu for a period of time not exceeding 1 min as shown Figure 3.2 (b).

When the supply voltage has been zero for a period of time in excess of 1 min, the long-duration voltage interruption is considered a sustained interruption as shown Figure 3.2 (a). This problem is often permanent and requires human intervention to repair the system for restoration [3, 11].

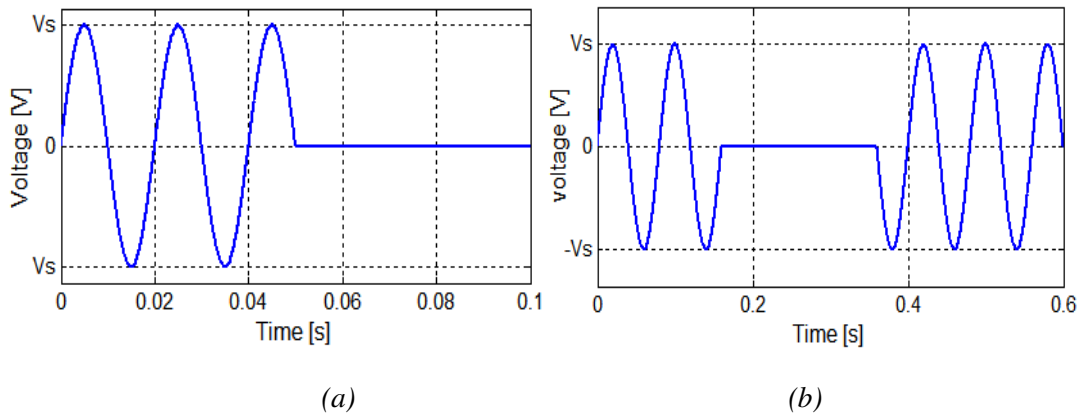


Figure 3.2. Supply voltage short and long interruption.

3.2.2.3. Voltage variations

It is defined as a decrease or increase of supply voltage than 1 p.u. Depending on its duration; it is categorized as short-duration and long-duration voltage variations [3, 9].

a) **Short-duration voltage variations:** it consists of two types: sag and swell.

- **Sag:** It is a decrease to between 0.1 and 0.9 pu in rms voltage or current at the power frequency for durations less than 2 min (Instantaneous 0.5 to 30 cycles; Momentary 30 cycles to 2 seconds; Temporary 2 seconds to 2 minutes) as shown Figure .3.3.

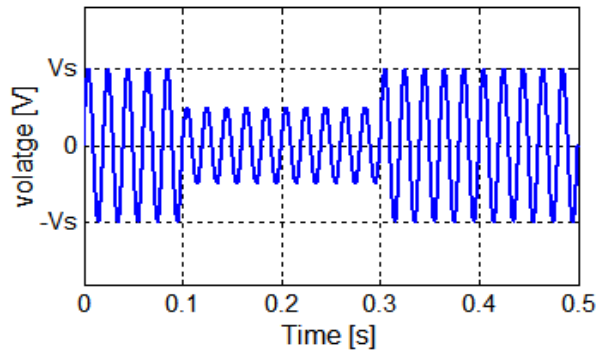


Figure 3.3. Short-duration voltage variations: sag.

- **Swell:** It is defined as an increase to between 1.1 and 1.8 pu in rms voltage or current at the power frequency for durations less than 2 min. it's considerate as a Instantaneous swell; when it's 0.5 to 30 cycles; Momentary 30 cycles to 2 seconds; Temporary 2 seconds to 2 minutes) as shown Figure 3.4.

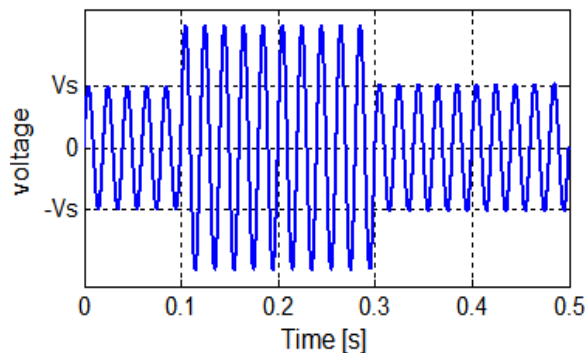


Figure 3.4. Short-duration voltage variations: swell.

b) **Long-duration voltage variations** : It consists of two types: under-voltage and over-voltage voltage variations [3, 11].

- **Under-voltage:** It is a decrease in the rms ac voltage to less than 90 per-cents at the power frequency for duration longer than 2 min as shown Figure 3.5 (a).

- **Over-voltage:** It is an increase in the rms ac voltage greater than 110 percent at the power frequency for duration longer than 2 min Figure 3.5 (b).

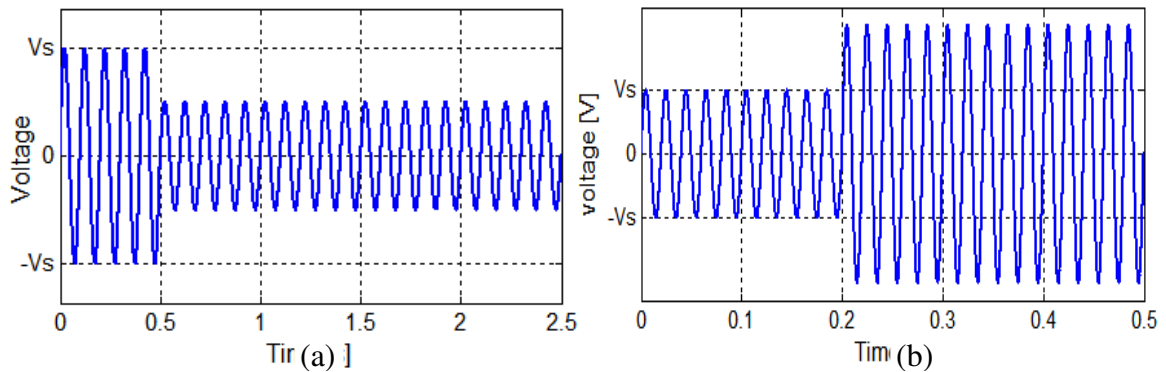


Figure 3.5. Long duration voltage variations.

3.2.2.4. Voltage fluctuations

It is systematic variations of the voltage envelope or a series of random voltage changes, the magnitude of which does not normally exceed the voltage ranges (namely 95% to 105% of nominal at a low frequency, generally below 25Hz) as shown Figure 3.6 [1, 3, 9].

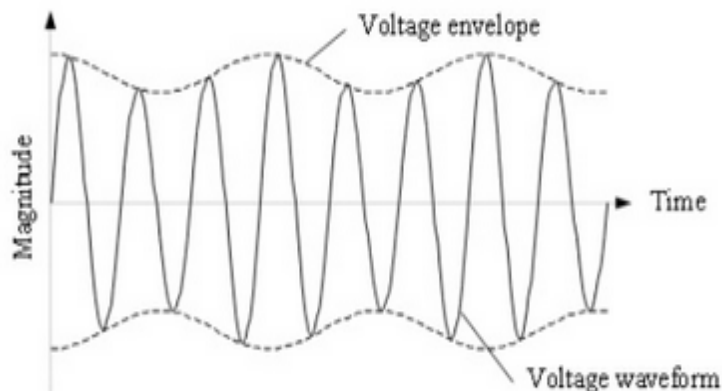


Figure 3.6. Voltage fluctuation.

3.2.2.5. Voltage unbalance

A situation, in which either the voltages of a three phase voltage source are not identical in magnitude, frequency or the phase differences between them are not 120 electrical degrees as shown Figure 3.7.

3.2.2.6. Power frequency variations

Power frequency variations are defined as the deviation of the power system fundamental frequency from

it specified nominal value (e.g., 50 or 60 Hz) as shown Figure 3.8.

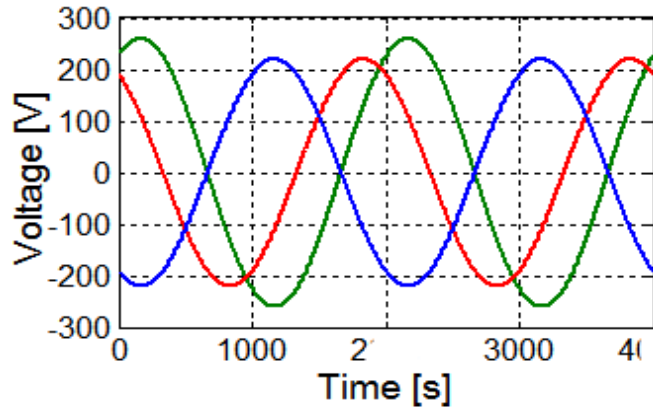


Figure 3.7. Voltage unbalance.

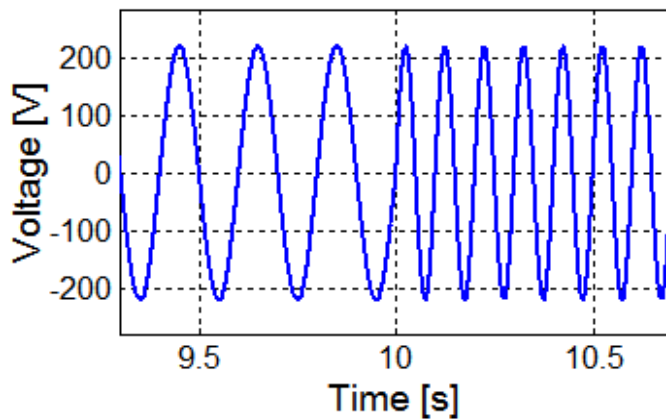


Figure 3.8. Power frequency variations.

3.2.2.7. Waveform distortions

It is a steady-state deviation from an ideal sine wave of power frequency principally characterized by the spectral content of the deviation. There are five primary types of waveform distortion [1, 9, 10]:

- DC offset
- Harmonics
- Inter-harmonics
- Notching
- Noise

a) DC offset

Direct current (DC) can be induced into an AC distribution system, often due to failure of rectifiers within the many AC to DC conversion technologies that have proliferated modern equipment. DC can traverse the ac power system and add unwanted current to devices already operating at their rated level. Overheating and saturation of transformers can be the result of circulating DC currents. When a transformer saturates, it not only gets hot, but also is unable to deliver full power to the load, and the subsequent waveform distortion can create further instability in electronic load equipment. A DC offset is illustrated in Figure 3.9.

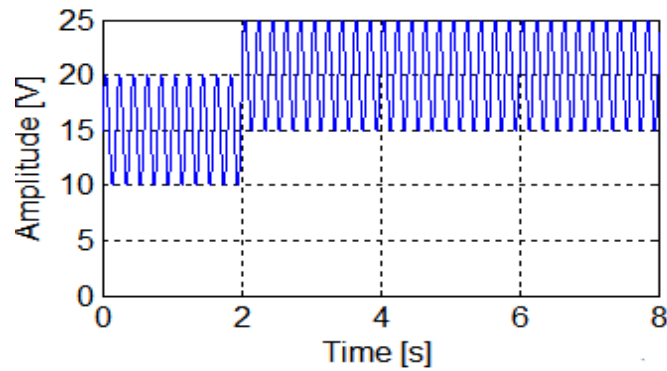


Figure 3.9. Direct current offset.

b) Harmonics

Harmonic distortion is the corruption of the fundamental sine wave at frequencies that are multiples of fundamental as shown figure 3.10. It is the results of non-linear loads such as: rectifiers, inverters, electrical welders, arc furnaces, voltage controllers, electronic devices, variable frequency drives...etc [6, 8].

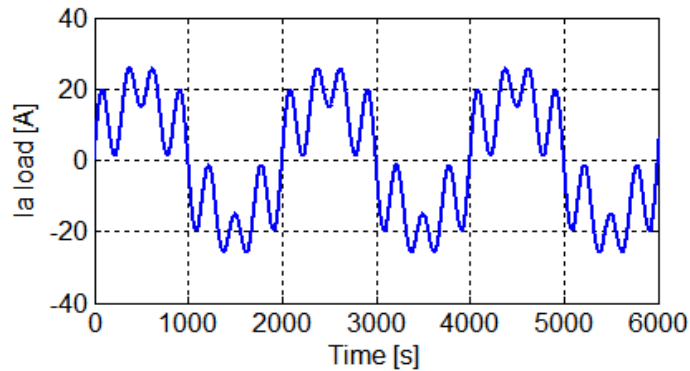


Figure 3.10. Harmonic current distortion.

c) Notching

Notching (Figure 3.11) is a periodic voltage disturbance caused by electronic devices, such as variable speed drives, light dimmers and arc welders under normal operation. This problem could be described as a transient impulse problem, but because the notches are periodic over each $\frac{1}{2}$ cycle, notching is considered a waveform distortion problem. The usual consequences of notching are system halts, data loss, and data transmission problems [10, 12].

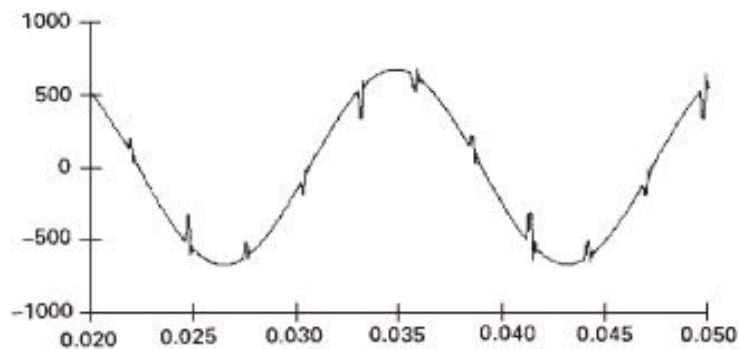


Figure 3.11. Notching voltage variation.

d) Noise

Noise (Figure 3.12) is unwanted voltage or current superimposed on the power system voltage or current waveform. Noise can be generated by power electronic devices, control circuits, arc welders, switching power supplies, radio transmitters and so on. Poorly grounded sites make the system more susceptible to noise. Noise can cause technical equipment problems such as data errors, equipment malfunction, long-term component failure, hard disk failure, and distorted video displays [6, 8].

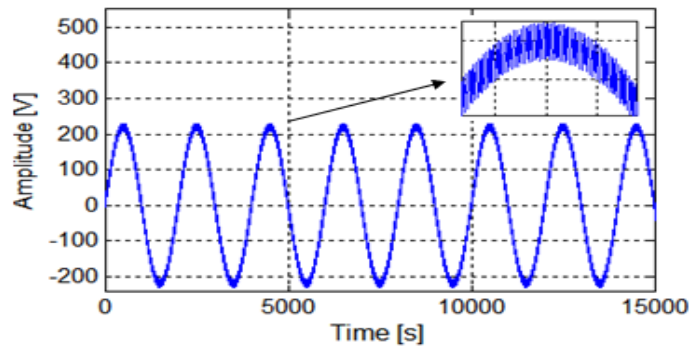


Figure 3.12. Noise voltage variation.

3.2.3. Sources of disturbances

The power quality and therefore the sensitive electronic devices are very affected by the disturbances which event in the power system. These disturbances are divided into [1, 6]:

- Disturbances resulting from the electric utility.
- Disturbances resulting from grid and consumer's equipments.

3.2.3.1. Disturbances resulting from the electric utility

One of the main responsibilities of utility system is to supply electric power in the form of sinusoidal voltages and currents with appropriate magnitudes and frequency for the customers at the point of common coupling (PCC). Some undesired and/or unpredictable magnitudes condition such as short-circuit faults or damage devices in the grid cause unstable state or transient voltage and current disturbances. All components of the electrical grid shall be equipped with different protection substrates to isolate all kinds of faults that may occur on the grid [1]. These faults result from one of the following cases:

- Weather swings like wind, snow and storms.
- Wrong connections.
- Vandalism of the public property like electric equipments and stations.
- Equipments mal-function or failure in the power system network.

3.2.3.2. Disturbances resulting from grid and consumer's equipments

The consumer's equipments may cause the disturbances in the power in following cases [1, 6]:

- Incorrect devices coupling.
- Storms and objects (tree, cars) striking lines or poles.
- Human error and bad coordination.

- Connection/disconnection of heavy loads.
- Badly dimensioned power sources.
- Non-linear loads connection (we explain their after).
- Unbalanced 3-phase power system.

3.2.4. Compatibility levels of power quality disturbances

In theory, the currents and voltages in a three-phase electricity distribution system have a perfect sinusoidal waveform, have unity power factor, they are balanced (i.e. the voltages and currents in each phase have identical magnitudes) and the phases are displaced by exactly 120 degrees [1, 6].

In practice, the nature of the consumers' loads (primarily) causes distortion of current and voltages and poor balance between the phases [1]. Over the last two decades the situation has become worse and today's networks have distorted voltages and currents, even in their steady state, cannot be considered as a 'balanced, sinusoidal regime.

The compatibility level is defined as the disturbance level that must not be exceeded for 95% of the measurements in the entire network [13]. Note that compatibility level is a statistical value that characterizes the state of the whole network, it cannot be used to describe the situation on a particular bus.

The international specification IEC 555-2 mentioned the harmonics currents and voltages limits for single-phase equipments with voltage characteristics of 220V and 50Hz as shown Table 3.1. Where, class 1 is special for protected supplies, class 2 is special for Point Common Coupling (PCC), class 3 is special for Internal Point Coupling (IPC) [1].

Table 3.1. Compatibility levels of power quality disturbances [1]

<i>Disturbance</i>	<i>Class 1</i>	<i>Class 2</i>	<i>Class 3</i>
Voltage changes, deviation with respect to nominal voltage V_n	$\pm 8\%$	$\pm 10\%$	$\pm 10\%$ to $\pm 15\%$
Voltage Unbalance	$\pm 2\%$	$\pm 2\%$	$\pm 2\%$
Power frequency deviation	$\pm 1\%$	$\pm 1\%$	$\pm 2\%$
Total Harmonic Distortion THD	$\pm 5\%$	$\pm 8\%$	$\pm 10\%$

3.2.5. Mitigation of power quality disturbances

The power quality disturbances can be effect the performance of the electrical equipments. Therefore; the concept of good or bad power based on the possibility to reduce or to mitigate the disturbances in the grid.

There are two general approaches to mitigate the PQ problems. One, named as load conditioning, it is to

ensure that the process equipment is less sensitive to disturbances, allowing it to ride through the disturbances. The other is to install a line conditioning device that suppresses or counteracts the disturbances [1, 14]. Among of them, we mentioned as follow:

- Filters
- Voltage regulators
- Motor/Generator set
- Uninterruptible power supplies
- Isolation transformers
- Surge suppressions

These solutions will be chosen after the determination of the power quality disturbance in the grid. One of the most problems which are detected usually in the grid is the harmonics, where; we will talk about their sources, consequences and mitigation in the next part.

3.3. Harmonic

Generally, the electrical energy distributes as a three-phase voltages sinusoidal form. In a normal alternating current power system, the current varies sinusoidally at a specific frequency, usually 50 hertz. When a linear electrical load is connected to the system, it draws a sinusoidal current at the same frequency as the voltage. However, when a non-linear load is connected to the system, it draws a current that is not necessarily sinusoidal. This deformation of current or voltage grandeurs is caused by the harmonics producing in the power system by these non linear loads (non-linear devices) [6, 8].

3.3.1. Linear and non-linear loads

When a sinusoidal voltage is applied to a certain type of load, the current drawn by the load is determined by the voltage and impedance and follows the voltage waveform. These loads are referred to as linear loads. Examples of linear loads are: resistive heaters, incandescent lamps, and constant speed induction and synchronous motors at the steady state. The current and voltage waveforms associated with linear loads are shown in Figure .3.13 [6, 8].

In contrast, some loads cause the current to vary disproportionately with the voltage during each cyclic period. These are classified as nonlinear loads, On account of its impedance changing; non-linear loads change the shape of the current waveform from a sine wave to some other forms (Figure 3.14). The nature of non-linear loads is to generate harmonics in the current waveform. This distortion of the current waveform eventually leads the distortion of voltage waveform at the point of common coupling, especially if the feeding grid is weak (large impedance) and proportion of non-sinusoidal currents is high enough. These loads are divided as traditional or established and new harmonic sources. The established harmonic sources define as: rectifiers; inverters; electrical welders, arc furnaces, voltage controllers, the frequency converters, power transformers and the rotating machines at the case of non steady state (the ripples presence in the voltage waveform, pole pitch reactance changing, and magnetic field form distortion). The second type (new

harmonic sources) presents in the all of the power electronics devices such as: household appliances, motor control devices, static var compensators, ac/dc converters (storage battery), cycloconverters...etc [6].

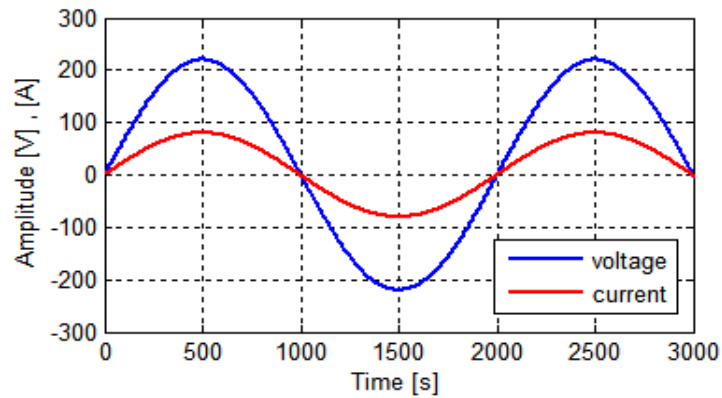


Figure 3.13. Voltage and current waveforms for linear loads.

Harmonics voltages and currents are integer multiple of the fundamental frequency. On 50Hz supplies, for instance, the 3rd harmonic is 150Hz, the 5th harmonic is 250Hz, and the 7th harmonic is 350Hz and so on. When all harmonic voltages and currents are added to the fundamental; a waveform known as a “complex wave” is formed. An example of complex waveform fundamental (1st harmonic) with 3rd to 15th harmonics is illustrated in Figure 3.14 [6, 14].

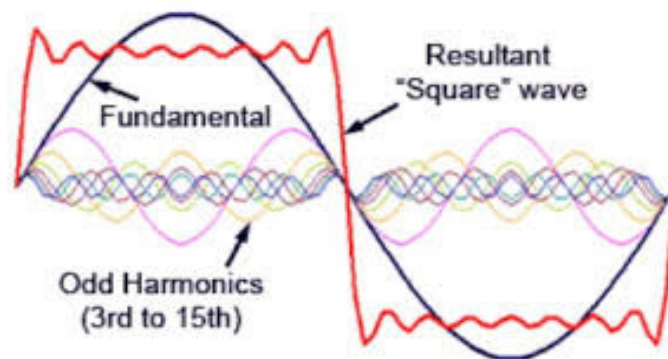


Figure 3.14. Effect of Harmonics in the waveform of the power of non-linear loads.

3.3.2. Harmonics mathematical analysis

A. The Fourier Transformation

Fourier theory (French mathematician Joseph Fourier (1768–1830)) [15] tells us that any periodic electrical power wave-shapes, whether current or voltage, can be defined in terms of summing sinusoidal waveforms. One of the terms has a period equal to that of the function, and is called the fundamental. Other terms have shortened periods that are integral submultiples of the fundamental; these are called harmonics [6], which can be expressed as follows:

Where:

$$y(t) = Y_0 + \sum_{n=1}^{n=\infty} Y_n \sqrt{2} \sin(n\omega t - \phi_n) \quad (3.1)$$

$Y(t)$ is the time domain function.

Y_0 : value of the DC component, generally zero and considered as such hereinafter.

Y_n : r.m.s (efficient value of the nth harmonic component).

ω : angular frequency of the fundamental frequency.

ϕ_n : displacement of the harmonic component at $t = 0$.

B. Total Harmonic Distortion (THD)

Total harmonic distortion or THD is a common measurement of the level of harmonic distortion present in power systems, which is calculated as follow:

$$THD(\%) = 100 \frac{\sqrt{\sum_{n=2}^{n=\infty} Y_n^2}}{Y_1} \quad (3.2)$$

Where, THD is the ratio of the r.m.s. value of all the harmonic components of the signal y , to the fundamental Y_1 . THD can exceed 1 and is generally expressed as a percentage.

Some measuring devices use another definition that replace the fundamental (Y_1) with the total root mean square (Y_{eff}).

IEEE 519-1992, Recommended Practices and Requirements for Harmonic Control in Electric Power Systems, established limits on harmonic currents and voltages at the point of common coupling (PCC), or point of metering [1, 6,15]. The limits of IEEE 519 are intended to:

- 1) Assure that the electric utility can deliver relatively clean power to all of its customers;
- 2) Assure that the electric utility can protect its electrical equipment from overheating, loss of life from excessive harmonic currents, and excessive voltage stress due to excessive harmonic voltage.

Each point from IEEE 519 lists the limits for harmonic distortion at the point of common coupling (PCC) or metering point with the utility. The voltage distortion limits are three percent (3%) for an individual frequency component and five percent (5%) for Total Harmonic Distortion (THD) [9, 6, 16].

C. Individual harmonic component

The individual harmonic component is defined as the percentage of harmonics for order h with respect to the fundamental [15]. Particularly:

$$H_n(\%) = 100 \frac{Y_n}{Y_1} \quad (3.3)$$

D. Root Mean Square (RMS) value

The root mean square value also known as the effective value. It is the true measure of electrical parameters. Equation (3.4) shows how to find the RMS value of a current waveform where the amplitude of each of the harmonic is known [15].

$$(\text{rmsvalue}) = \sqrt{\frac{1}{T} \int_0^T v^2(t) dt} \quad (3.4)$$

Thus, the presence of harmonics in a waveform always increases its rms value. In particular, in the case where the voltage $v(t)$ contains only fundamental while the current $i(t)$ contains harmonics, then the harmonics increase the rms value of the current while leaving the average power unchanged. This is undesirable, because the harmonics do not lead to net delivery of energy to the load, yet they increase the I_{rms} $2R$ losses in the system [15].

E. Power factor and displacement Power Factor ($\cos\phi$)

The power factor λ is the ratio of the active power P (kW) to the apparent power S (kVA) as shown Equation (3.5).

$$\lambda = \frac{P(\text{kW})}{S(\text{kVA})} \quad (3.5)$$

The Power Factor must not be mixed-up with the Displacement Power Factor ($\cos\phi$), relative to fundamental signals only as shown Equation (3.6).

$$\text{Cos}\phi_1 = \frac{P_1}{S_1} \quad (3.6)$$

When the signal is sinusoidal waveform: $\text{Cos}\phi_1 = \text{Cos}\phi = \lambda$.

F. Crest Factor (CF) and Form Factor (FF)

Two others measures of distortion are the crest factor and the form factor. The crest factor is the ratio of the peak of a waveform to its RMS value as shown Equation (3.7) [15]. For a linear sinusoidal waveform, the crest factor would be the square root of 2, or 1.414.

$$\text{Crest}_{\text{Factor}} = \frac{I_{\text{peak}}}{I_{\text{RMS}}} \quad (3.7)$$

- For a sinusoidal signal, the crest factor is therefore equal to $\sqrt{2}$.
- For a non-sinusoidal signal, the crest factor can be either greater than or less than $\sqrt{2}$.

The form factor or distortion factor is the ratio of the RMS value of a waveform to the RMS of the waveform's fundamental component value as shown Equation (3.8) [15]. For a linear sinusoidal waveform, the form factor would be equal to 1.

$$\text{Form}_{\text{Factor}} = \frac{I_{\text{RMS}}}{I_1} \quad (3.8)$$

G. Harmonic spectrum

The harmonic spectrum is the representation of the amplitude of each harmonic order with respect to its frequency as shown Figure 3.15 [15]. Each type of device causing harmonics draws a particular form of

current, with a particular harmonic content. This characteristic can be displayed by using the harmonic spectrum.

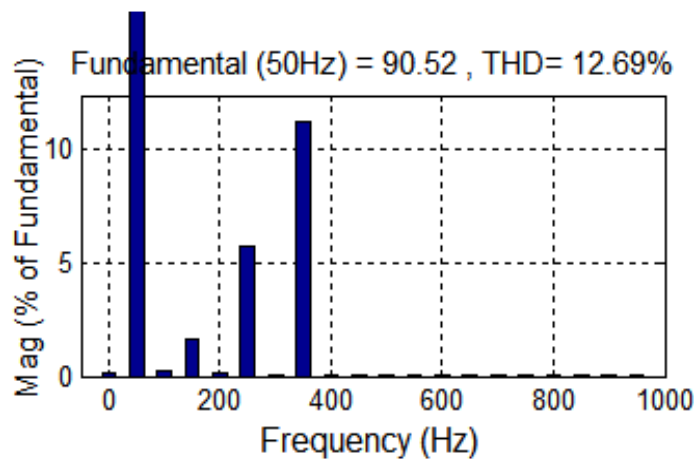


Figure 3.15. Harmonic spectrum.

3.3.3. Harmonics consequences

There are many consequences of the harmonics in the grid, among of them are [6, 1, 14, 19]:

- Increased utility current requirement.
- Components overheating.
- Reduced utility power factor.
- Equipments malfunction.
- Excitation of power system resonance's creating overheating.

3.3.4. Harmonics mitigation

There are various harmonics mitigation techniques available to solve harmonics problems in electric power systems; each method has their advantages and disadvantages, we mentioned them as follow [6, 1, 14, 17, 18]:

- Reactors or chokes.
- Drive isolation transformer.
- Harmonics filters.
- High pulse count rectification.
- Drive Active Front End (DAFE).

From the harmonics mitigation methods mentioned above; it concludes from many search that there is no single product that is best solution for reducing the harmonics in power. The best economical and technical solution for this problem is based on objective of user severity of harmonics, cost and benefits associated with various technologies used at that place.

Hence, in our studying we will use an active power filter including with the principal system regulation in order to reduce the cost of the harmonics mitigation techniques.

3.4. Active Power Filters

Active Power Filters (APF) was developed to provide better dynamic control of current harmonics and voltage distortion control. This is achievable thanks to the developments in solid-state switching devices and control technology in recent years.

Several APF design topologies as illustrated in the block diagram shown in Figure 3.16 have been proposed [20, 21]. They can be classified as follow:

- 1) Shunt active power filters (Shunt APF).
- 2) Series active power filters (Series APF).
- 3) Hybrid APF.
- 4) Unified Power Quality Conditioner (UPQC).

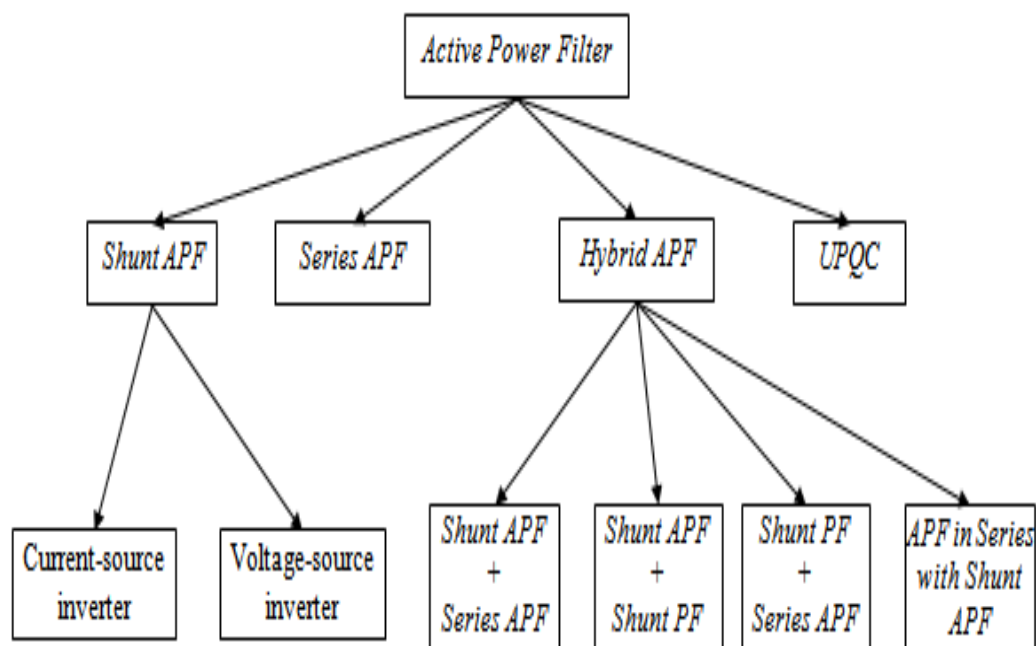


Figure 3.16. Subdivision of active power filter.

3.4.1. Shunt Active Power Filters (Shunt APF)

This principle is applicable to any type of load considered a harmonic source. Moreover, with an appropriate control scheme, the active power filter can also compensate the load power factor. In this way, the power distribution system sees the non linear load and the active power filter as an ideal resistor. The current compensation characteristic of the shunt active power filter is shown in Figure 3.17. It operates by injecting harmonic current into the utility system with the same magnitudes as the harmonic currents generated by a given non-linear load; but with opposite phases to maintain a sinusoidal current at the PCC [22].

3.4.2. Series Active Power Filters (Series APF)

As shown Figure 3.18, it is well known that series active power filters compensate current system distortion caused by non-linear loads by imposing a high impedance path to the current harmonics which

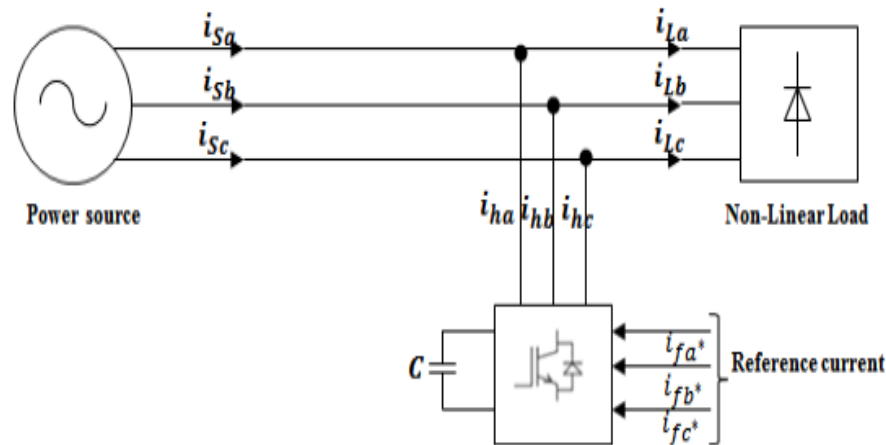


Figure 3.17. Shunt active power filter.

forces the high frequency currents to flow through the LC passive filter connected in parallel to the load [23]. The high impedance imposed by the series active power filter is created by generating a voltage of the same frequency that the current harmonic component needs to be eliminated.

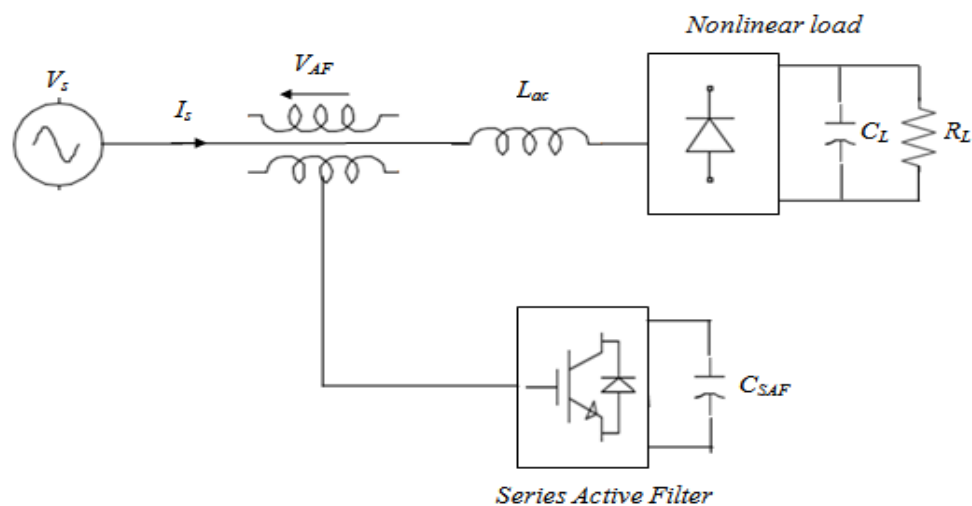


Figure 3.18. Series active power filters.

3.4.3. Hybrid active power filters

Hybrid power filters combine active power filter with traditional passive filters. This connection allows to take advantages from both solutions, usually by improving the properties of the filter in relation to the passive filters and by reducing the required power rate of the active part [23]. Depending on the connection method and applied systems, hybrid filters are used in order to reduce currents and voltages harmonics and to compensate reactive power. One of the possible configurations of hybrid system is a series connection of parallel passive filter with a series active power filter as shown Figure 3.19.

3.4.4. Unified Power Quality Conditioner (UPQC)

Unified power quality conditioners (UPQCs) consist of combined series and shunt active power filters (APFs) for simultaneous compensation of voltage and current disturbances and reactive power as shown

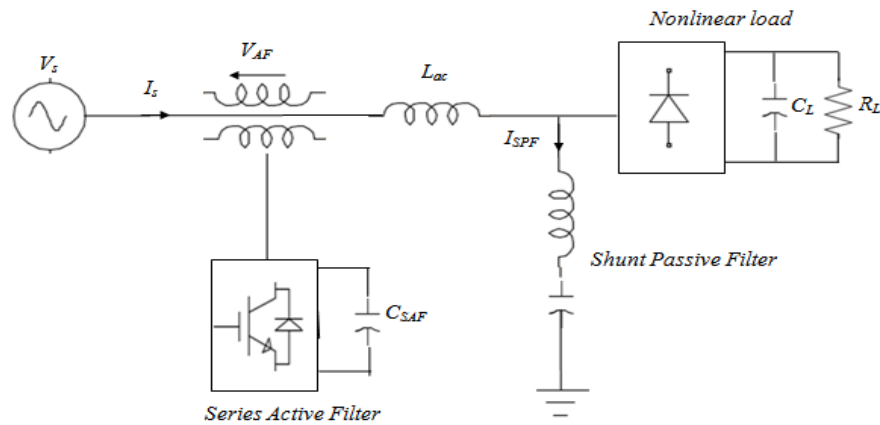


Figure 3.19. Hybrid filter.

Figure 3.20. They are applicable to power distribution systems, being connected at the point of common coupling (PCC) of loads that generate harmonic currents [24].

The main purpose of a UPQC is to compensate for supply voltage flicker/imbalance, reactive power, negative sequence current, and harmonics. In other words, the UPQC has the capability of improving power quality at the point of installation on power distribution systems or industrial power systems. The UPQC, therefore, is expected as one of the most powerful solutions to large capacity sensitive loads to voltage flicker/imbalance [25].

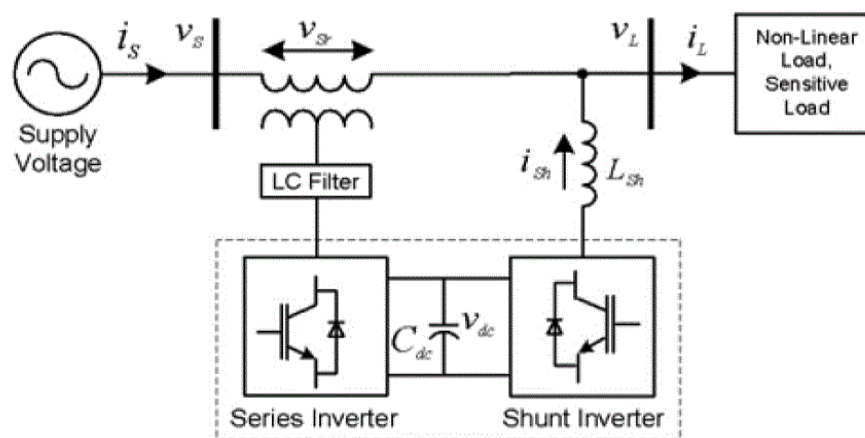


Figure 3.20. Unified Power Quality Conditioner (UPQC) structure.

In our studying, we choose a shunt APF technique to reduce the harmonics injected by the equipments consumer's in the grid, with an appropriate control schema named priority method control. Where, it can be possible to reduce the cost of filtering and take the back-to-back converter system instead of using an additional converter.

3.5. Shunt active power filter in wind turbine system

3.5.1. THD global system calculation without filter

THD is a measurement that shows us the distortion of current signals incoming from the harmonics.

Therefore, we added some harmonics signals to the grid current signal at point common coupling (PCC) as a non-linear load. Then; we have used a FFT analysis in *Power Gui Tool* block in MATLAB/Simulink environment to calculate the THD of three current signal which are: stator current machine $I_{sa-machine}$ (current generated by the wind turbine system), non-linear load current signal I_{a-load} (harmonics signals added to the PCC) and the grid current signal $I_{sa-grid}$ (the sum of the two previous currents signals at PCC). This block provides a visual comparison in time and frequency domain of the three currents as shown Figure 3.21. Where, we take like parameters: the fundamental frequency at 50 Hz, Max frequency=1000Hz and Number of cycle=1.

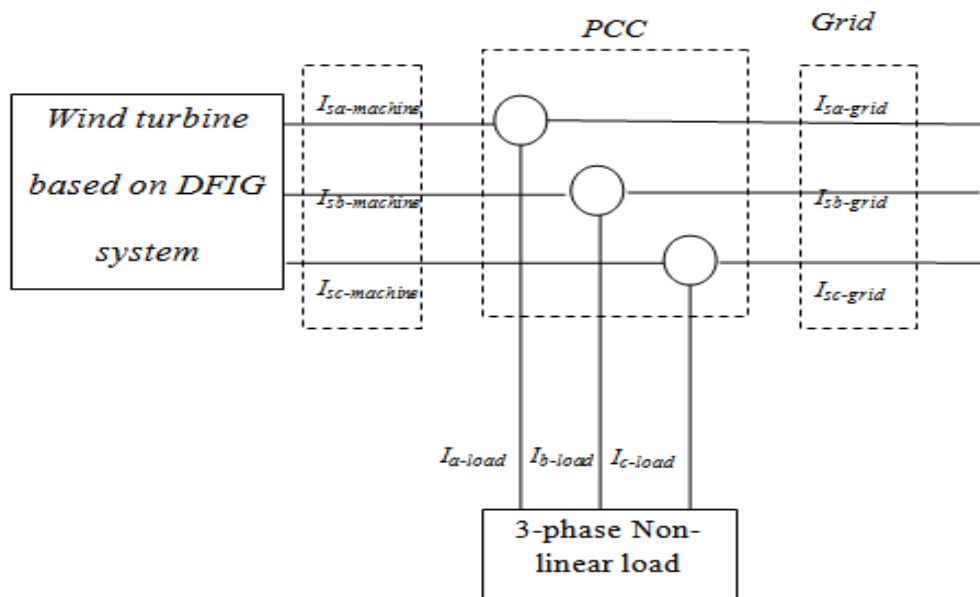


Figure 3.21. Point power common coupling wind turbine system connection.

It's easy to see the harmonic distortion when examining the time domain and frequency domain representation of the grid current and load current signals. But, it's also important to quantify the harmonics distortion for each current as shown Figure 3.22.

- THD of current machine $I_{sa-machine}$ equal to 0.46% with amplitude equal to 78.37%. The less THD value of this signal means that the signal is very smooth as shown Figure 3.22 (a).
- THD of load current I_{a-load} equal to 55.90% with amplitude equal to 20%. A high THD value of this signal means that is much distorted as shown Figure 3.22 (b).
- THD of grid current $I_{sa-grid}$ equal to 16.09% with amplitude equal to 73.75%. The summation of the two signals above generates another distorted current in the grid as shown Figure 3.22 (c).

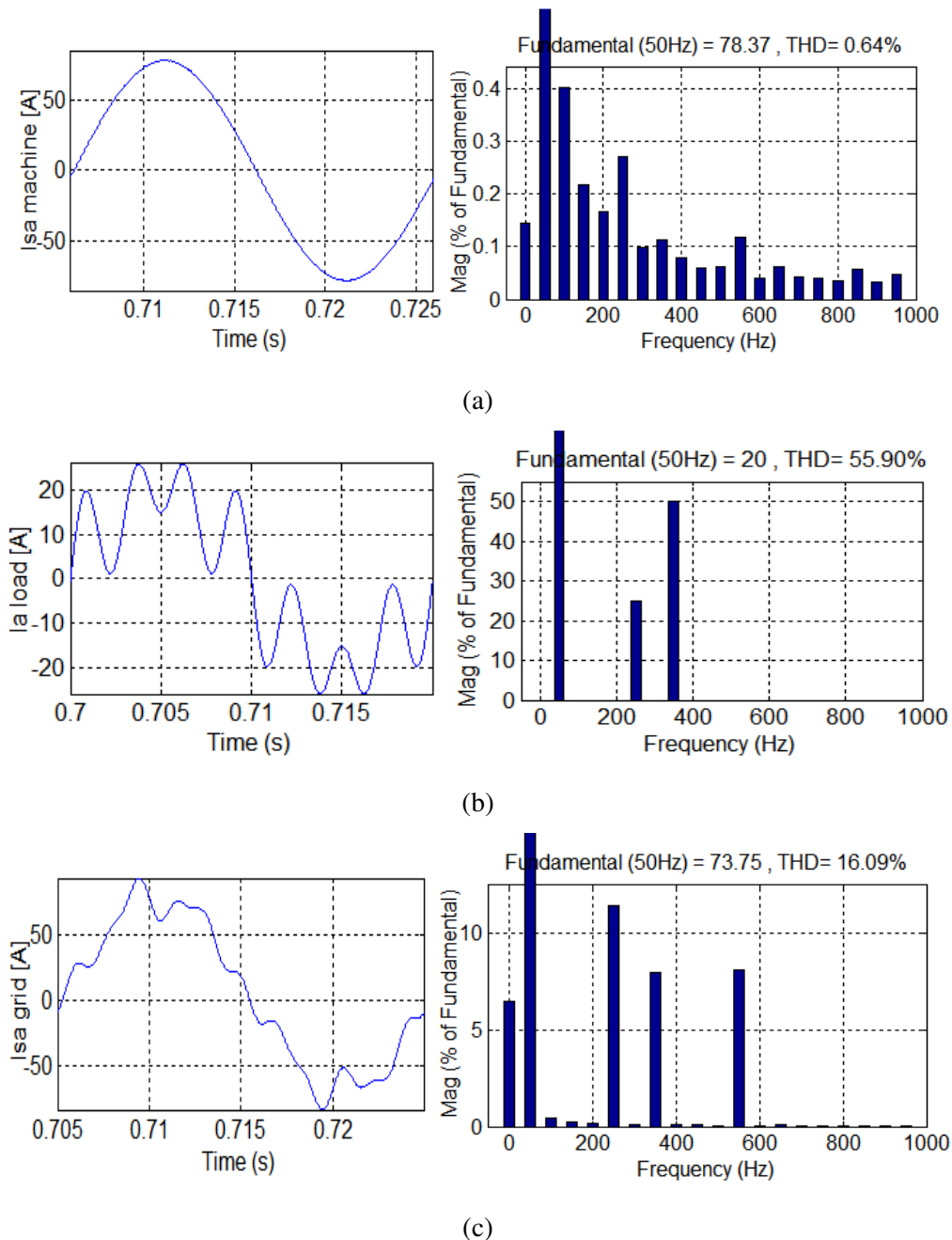


Figure 3.22. Current waveforms and their FFT (a) generator, (b) non-linear load, (c) grid.

3.5.2. Global schematic with shunt active power filter

In order to improve the power quality at the point of common coupling (PCC) and reduce the harmonic currents in the grid, a new control strategy termed priority control method is proposed in the rotor-side converter control as shown Figure 3.23. Therefore, the precedent control block of RSC (in the first chapter) is modified to include the priority control algorithm. This control method permits to manage the priority between the stator powers control and the harmonics suppression as follow:

- Electromagnetic torque control which allows in turn controlling the active stator power (first priority).
- Reactive power control to ensure the unity power factor (second priority).
- Harmonics rotor currents suppression for the active filter.

3.5.4.1. Active and reactive powers method (PQ)

The first version of the PQ theory for active filtering application was published in 1984 in a prestigious international journal by professor Akagi, his coauthors Knazawa and Nabae [29]. It is also known as the instantaneous reactive power theory for three-phase circuit; its block diagram is shown in Figure 3.24. It is based on the $(\alpha\beta)$ transformation which consists in a real matrix to transform three-phase voltages and currents into the $(\alpha\beta)$ stationary reference frame given by [29, 30]:

$$\begin{bmatrix} V_o \\ V_\alpha \\ V_\beta \end{bmatrix} = \sqrt{\frac{2}{3}} \begin{bmatrix} \frac{1}{\sqrt{2}} & \frac{1}{\sqrt{2}} & \frac{1}{\sqrt{2}} \\ 1 & -1 & -1 \\ 0 & \sqrt{\frac{2}{3}} & -\sqrt{\frac{2}{3}} \end{bmatrix} \begin{bmatrix} V_{sa} \\ V_{sb} \\ V_{sc} \end{bmatrix} \quad (3.9)$$

Similarly generic instantaneous three-phase line currents (a,b,c) can be transformed into $(\alpha\beta)$ axis.

$$\begin{bmatrix} I_o \\ I_\alpha \\ I_\beta \end{bmatrix} = \sqrt{\frac{2}{3}} \begin{bmatrix} \frac{1}{\sqrt{2}} & \frac{1}{\sqrt{2}} & \frac{1}{\sqrt{2}} \\ 1 & -1 & -1 \\ 0 & \sqrt{\frac{2}{3}} & -\sqrt{\frac{2}{3}} \end{bmatrix} \begin{bmatrix} I_{sa} \\ I_{sb} \\ I_{sc} \end{bmatrix} \quad (3.10)$$

The power component P and Q are related to the same $(\alpha\beta)$ voltages and currents by:

$$\begin{bmatrix} P \\ Q \end{bmatrix} = \begin{bmatrix} V_\alpha & V_\beta \\ -V_\beta & V_\alpha \end{bmatrix} \begin{bmatrix} I_\alpha \\ I_\beta \end{bmatrix} \quad (3.11)$$

From the Equation 3.11 results the currents expression as follow:

$$\begin{bmatrix} I_\alpha \\ I_\beta \end{bmatrix} = \frac{1}{\Delta} \begin{bmatrix} V_\alpha & -V_\beta \\ V_\beta & V_\alpha \end{bmatrix} \begin{bmatrix} P \\ Q \end{bmatrix} \quad (3.12)$$

Where: $\Delta = V_\alpha^2 + V_\beta^2$

According to the Akagi's p – q theory based approach [30], the shunt active filter could compensate the instantaneous active and reactive powers to the continuous and sinusoidal components \bar{p} and \tilde{p} for active power, \bar{q} and \tilde{q} for reactive power).

$$\begin{cases} p = \bar{p} + \tilde{p} \\ q = \bar{q} + \tilde{q} \end{cases} \quad (3.13)$$

Where:

\bar{p} : is the DC component of the instantaneous power p , and is related to the fundamental active current,

\tilde{p} : is the AC component of the instantaneous power p , it does not have average value, and is related to harmonic current caused by the AC component of the instantaneous real power

\bar{q} : is the DC component of the instantaneous imaginary power q , and is related to the reactive power generated by the fundamental components of the voltages and current.

\tilde{q} : is the AC component of the instantaneous imaginary power q , and is related to the harmonic current generated by the AC components of instantaneous reactive power.

In general, each one of the active and reactive currents contains a direct component and an alternating component. The direct component represents the fundamentals of current and the alternating term represents the harmonics of currents. In order to separate the harmonics from the fundamentals of the load currents, it is enough to separate the direct term of the current from the alternating one [31]. A Low Pass Filter (LPF) with feed-forward effect can be used to accomplish this task as shown in Figure 3.24.

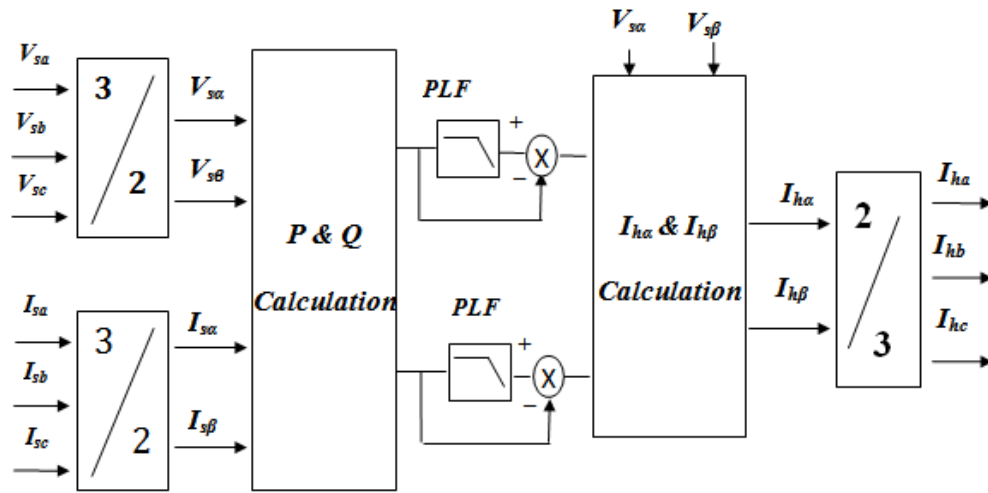


Figure 3.24. Active and reactive powers method (PQ) block.

3.5.4.2. Synchronous Reference Frame (SRF) method

In this method, the load current is transformed into the conventional rotating frame d-q. The block diagram of a current reference generator that uses the synchronous reference frame algorithm is shown in Figure 3.25. The distorted currents are first transformed into two-phase stationary coordinates using α - β and d-q transformations and then a low pass filter (LPF) is applied to separate the harmonics from the fundamentals of the load currents [32].

$$\begin{bmatrix} I_{ld} \\ I_{lq} \\ I_{l0} \end{bmatrix} = \sqrt{\frac{2}{3}} \begin{bmatrix} \cos \theta & \cos\left(\theta - \frac{2\pi}{3}\right) & \cos\left(\theta + \frac{2\pi}{3}\right) \\ -\sin \theta & -\sin\left(\theta - \frac{2\pi}{3}\right) & -\sin\left(\theta + \frac{2\pi}{3}\right) \\ \frac{1}{\sqrt{2}} & \frac{1}{\sqrt{2}} & \frac{1}{\sqrt{2}} \end{bmatrix} \begin{bmatrix} I_{sa} \\ I_{sb} \\ I_{sc} \end{bmatrix} \quad (3.14)$$

Where, θ is the angular position of the synchronous reference frame. This is a linear function of the fundamental frequency. The harmonic reference current can extract from the load currents using a simple Low Pass Filter (LPF). The currents in the synchronous reference can be decomposed into two terms as follow:

$$\begin{cases} I_{ld} = \bar{I}_{ld} + \tilde{I}_{ld} \\ I_{lq} = \bar{I}_{lq} + \tilde{I}_{lq} \end{cases} \quad (3.15)$$

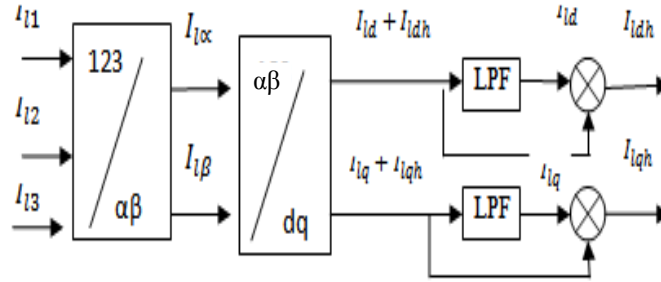


Figure 3.25. Block diagram of SRF method.

Only the alternating terms which are related to the harmonic contents will be seen at the output of the extraction system.

One of the most important characteristics of this algorithm is that the reference currents are obtained directly from the loads currents without considering the source voltages. This is an important advantage since the generation of the reference signals is not affected by voltage unbalance or voltage distortion, therefore increasing the compensation robustness and performance [33].

3.5.5. Modified rotor side converter control

In order to improve the power quality at the point of common coupling (PCC) and reduce the harmonic currents in the grid, a new control strategy termed priority control method is proposed in the rotor-side converter control [34]. For that the precedent control block of RSC studied in the first chapter will be modified to include the priority control algorithm as shown Figure 3.26.

3.5.5.1. Priority method

3.5.5.1.1. The priority control method

The block diagram of the priority control method algorithm is presented in Figure 3.27. Where, $I_{rd-reactif}^*$, $I_{rq-actif}^*$ are the references rotor currents and I_{rdh}^* , I_{rqh}^* are the injected harmonics rotor currents.

The MPPT control imposes the reference electromagnetic torque (T^*) which generates the reference quadrature rotor current $I_{rq-actif}^*$ which should remain in the range of $\pm I_{rmax}$ to ensure the first priority as shown Equation 3.16.

$$\sqrt{I_{rd}^2 + I_{rq}^2} = \sqrt{3}I_r = I_{rmax} \quad (3.16)$$

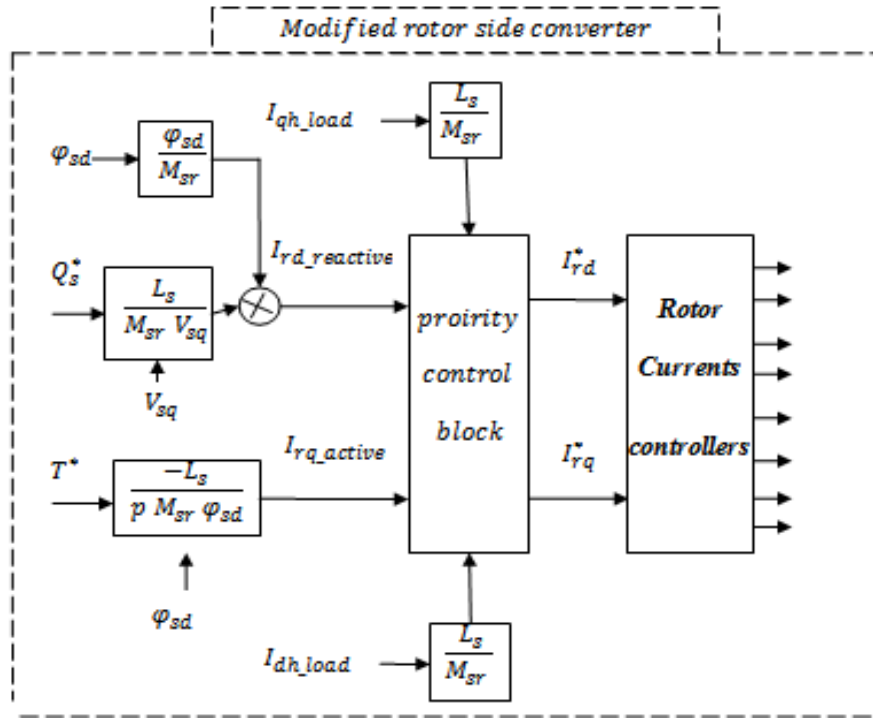


Figure 3.26. Modified Rotor-Side Converter Control (MRSC).

The direct rotor current reference $I_{rd_reactif}^*$ is generated by the control of the reactive power and should remain between $\pm I_{rdmax}$ to ensure the second priority as shown Equation.3.17 and Figure 3.27.

$$I_{rdmax} = \sqrt{I_{rmax}^2 - I_{rq_actif}^2} \tag{3.17}$$

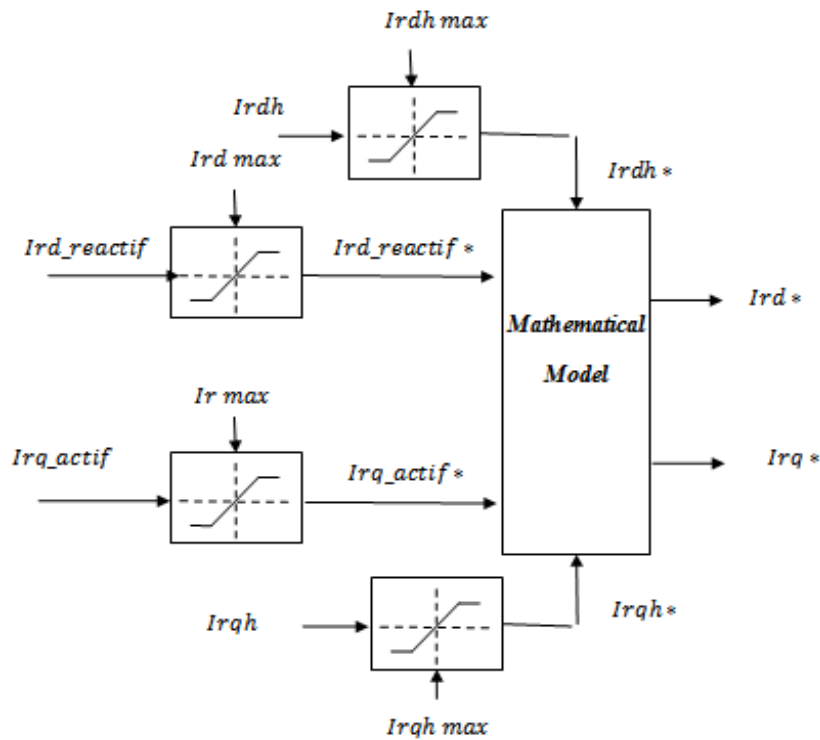


Figure 3.27. Priority control method.

The third priority which is the harmonics currents control has achieved by the generation of the injected harmonics rotor currents I_{rdh}^*, I_{rqh}^* which must remain between $\pm I_{rdh_max}, \pm I_{rqh_max}$ respectively. This priority constraint is implemented using the following rules:

$$\left\{ \begin{array}{l} \text{if } \left(I_{rd_reactive}^* = \pm I_{rdmax} \right) \\ \cdot \\ \text{then } \left(\begin{array}{l} I_{rdh_max} = 0 \\ I_{rqh_max} = 0 \end{array} \right) \end{array} \right\} \quad (3.18)$$

$$\left\{ \begin{array}{l} \text{if } \left(-I_{rdmax} < I_{rd_reactive}^* < I_{rdmax} \right) \\ \cdot \\ \text{then } \left(\begin{array}{l} I_{rdh_max} = I_{rdmax} - I_{rd_reactive}^* \\ I_{rqh_max} = I_{max} - I_{rq_active}^* \end{array} \right) \end{array} \right\} \quad (3.19)$$

The references for the d and q rotor currents are defined as follows:

$$\left\{ \begin{array}{l} \left[\sqrt{\left(I_{rd_reactive}^* + I_{rdh}^* \right)^2 + \left(I_{rq_active}^* + I_{rqh}^* \right)^2} \leq I_{rmax} \right. \\ \cdot \\ \text{then } \left(\begin{array}{l} I_{rd}^* = I_{rd_reactive}^* - I_{rdh}^* \\ I_{rq}^* = I_{rq_active}^* - I_{rqh}^* \end{array} \right) \\ \cdot \\ \text{else } \left(\begin{array}{l} I_{rd}^* = I_{rd_reactive}^* \\ I_{rq}^* = I_{rq_active}^* \end{array} \right) \end{array} \right\} \quad (3.20)$$

3.5.5. 2. Rotor currents control methods

There are many methods are used to control the rotor currents, among of them: Hysteresis rotor currents control, conventional PI currents control and PI-adaptive fuzzy logic rotor currents control.

3.5.5.2.1. Hysteresis rotor currents control

The principle of hysteresis current control method can be seen in figure 3.28. Where, the difference between the reference value and the actual value will be directed to one comparator with a tolerance band. The controller generates the sinusoidal reference current of desired magnitude and frequency that is compared with the measured current. Hence, the actual current is forced to track the reference current within the hysteresis band as shown in Figure 3.29.

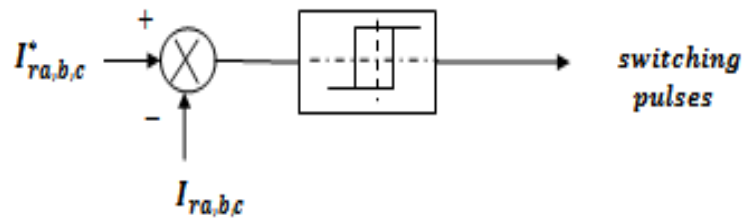


Figure 3.28. Hysteresis rotor currents control.

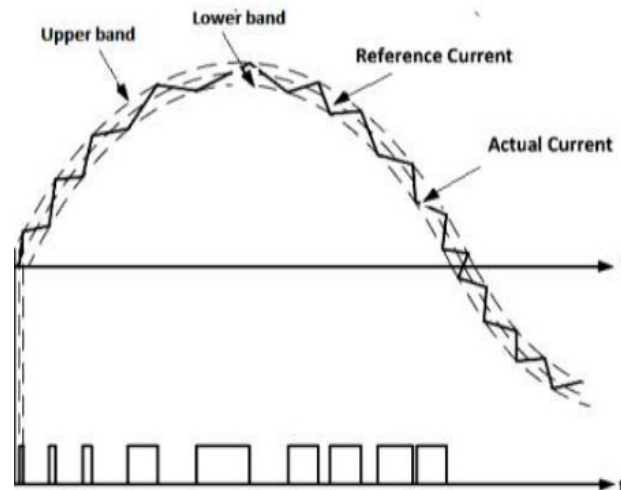


Figure 3.29. Hysteresis band [39].

▪ Simulation result

The simulation results of the hysteresis current method control of the modified rotor side converter are shown in Figure 3.30, where, the simulation results are obtained by using MATLAB/Simulink.

The SRF theory is used for harmonic currents identification and calculation where we had taken a cutter frequency value equal to 100Hz which permit to give a 0.01s value of a time response for the LPF.

The system parameters are mentioned above in the first chapter and we take a hysteresis band value between ± 0.01 .

The grid current without active filter is given in Figure 3.22. The simulation results for shunt active power filter using hysteresis current method control is given in Figure 3.30. Where, Figure 3.30-(a) shows the quadrature rotor current measurement where, it flows seriously its reference, Figure 3.30-(b) shows direct rotor current measurement with its reference and Figure 3.30-(c) shows control rotor current in three-phase frame.

Figure 3.31 shows the direct and quadrature rotor currents injected in the grid through the hysteresis rotor currents control.

Figure 3.32 shows the quadrature and direct stator powers, DC-link voltage and Torque machine, and a phase grid and machine (DFIG) stator current responses. As we can see; the responses follows the reference

currents with their injected currents generated from the filter and controlled with the priority method algorithm.

Figure 3.33 shows the wind speed and MPPT control responses, where there is no changing in these two responses from the first chapter responses.

Figure 3.34 shows the current waveforms and their FFT for (a) generator, (b) non-linear load, (c) grid. When, we compared with Figure 3.22, we have seen that the THD in this figure was decreased from 16,90% to 2,49% in the system filtering. However; the THD of the current produced by the generator has increased from 0,64% to 12,75% contains the opposite harmonics to injected in the grid.

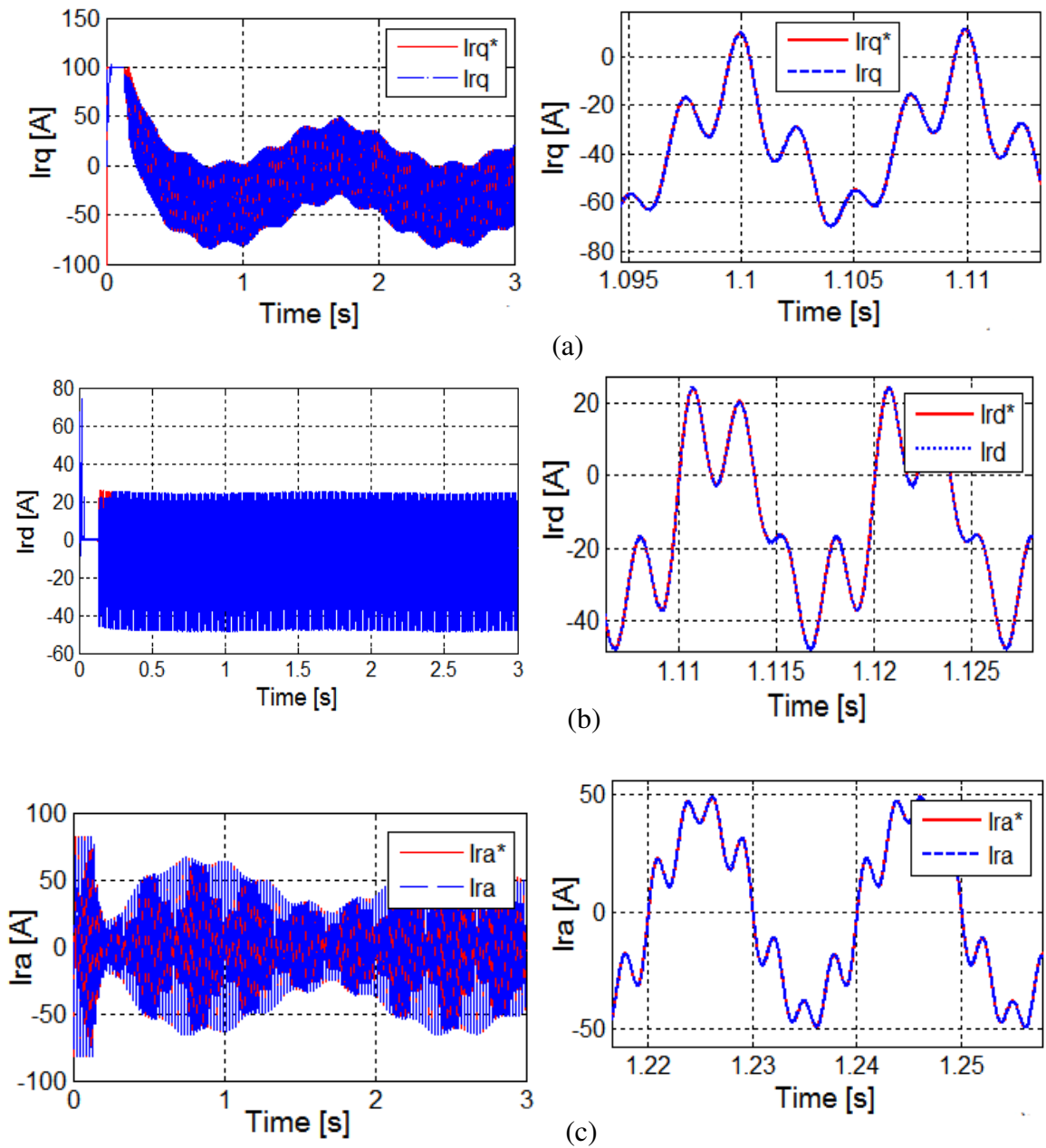


Figure 3.30. Hysteresis currents control: (a) quadrature rotor current and its Zoom I_{rd} ; (b) direct rotor current and its Zoom I_{rd} , (c) a phase rotor current and its Zoom I_{ra} .

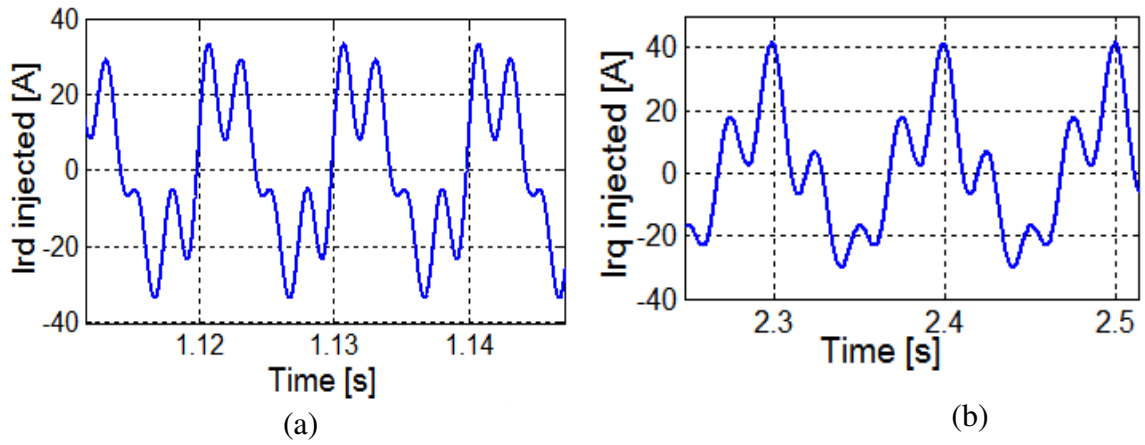


Figure 3.31. Direct and quadrature rotor currents injected in hysteresis rotor currents control.

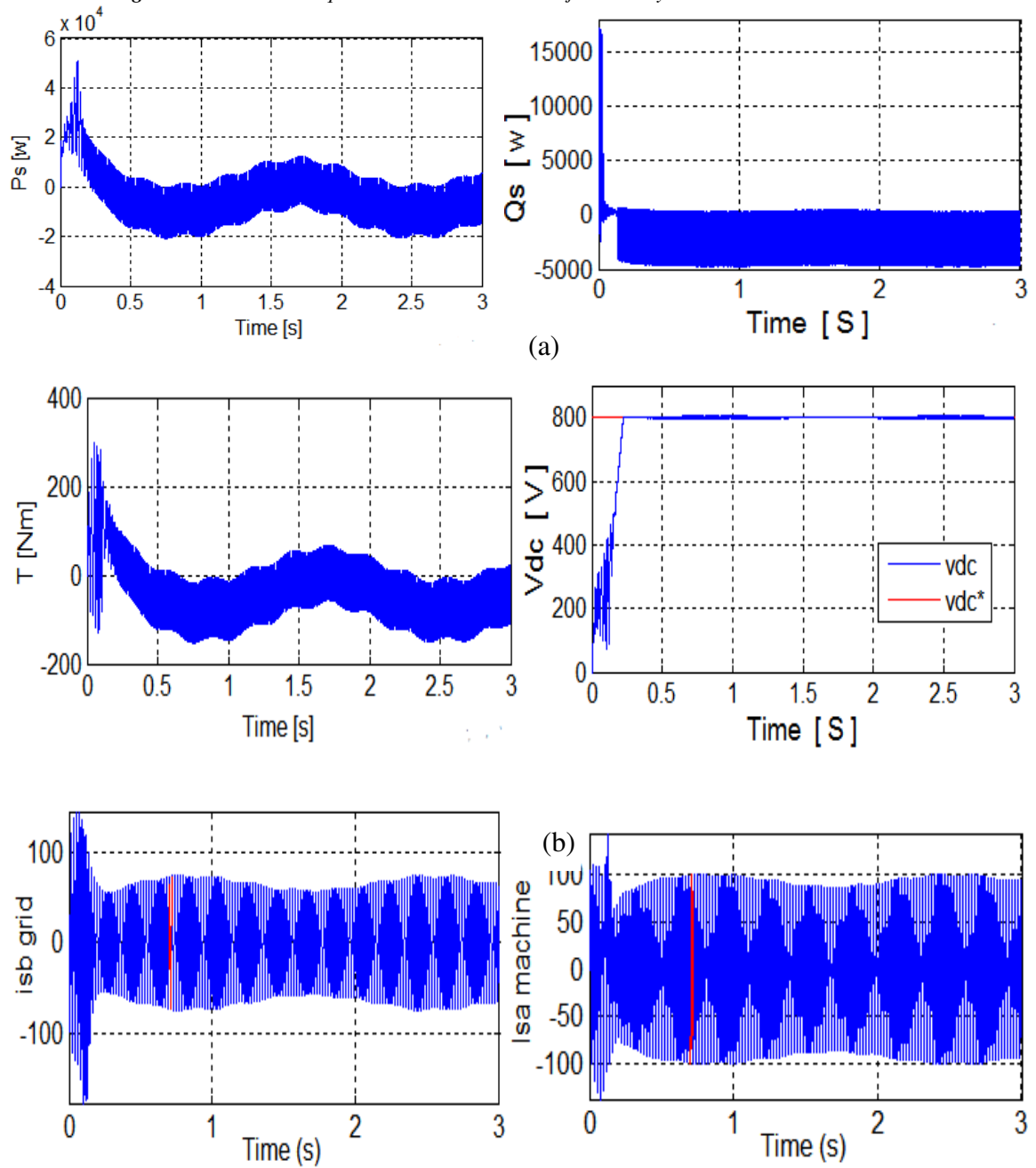


Figure 3.32. (a) quadrature and direct stator powers; (b) DC-link voltage and Torque machine, (c) a phase stator current for grid and machine (DFIG).

(c)

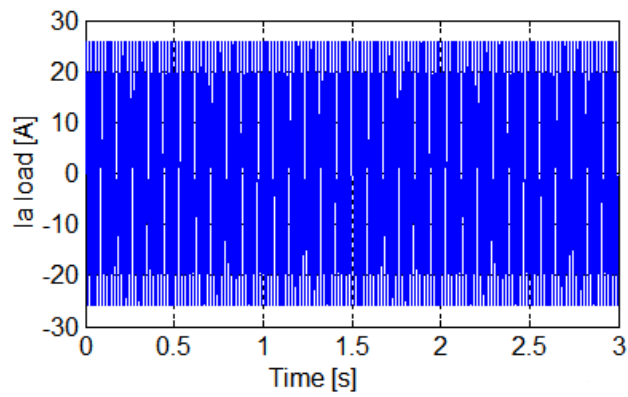


Figure 3.33. Non-linear load current.

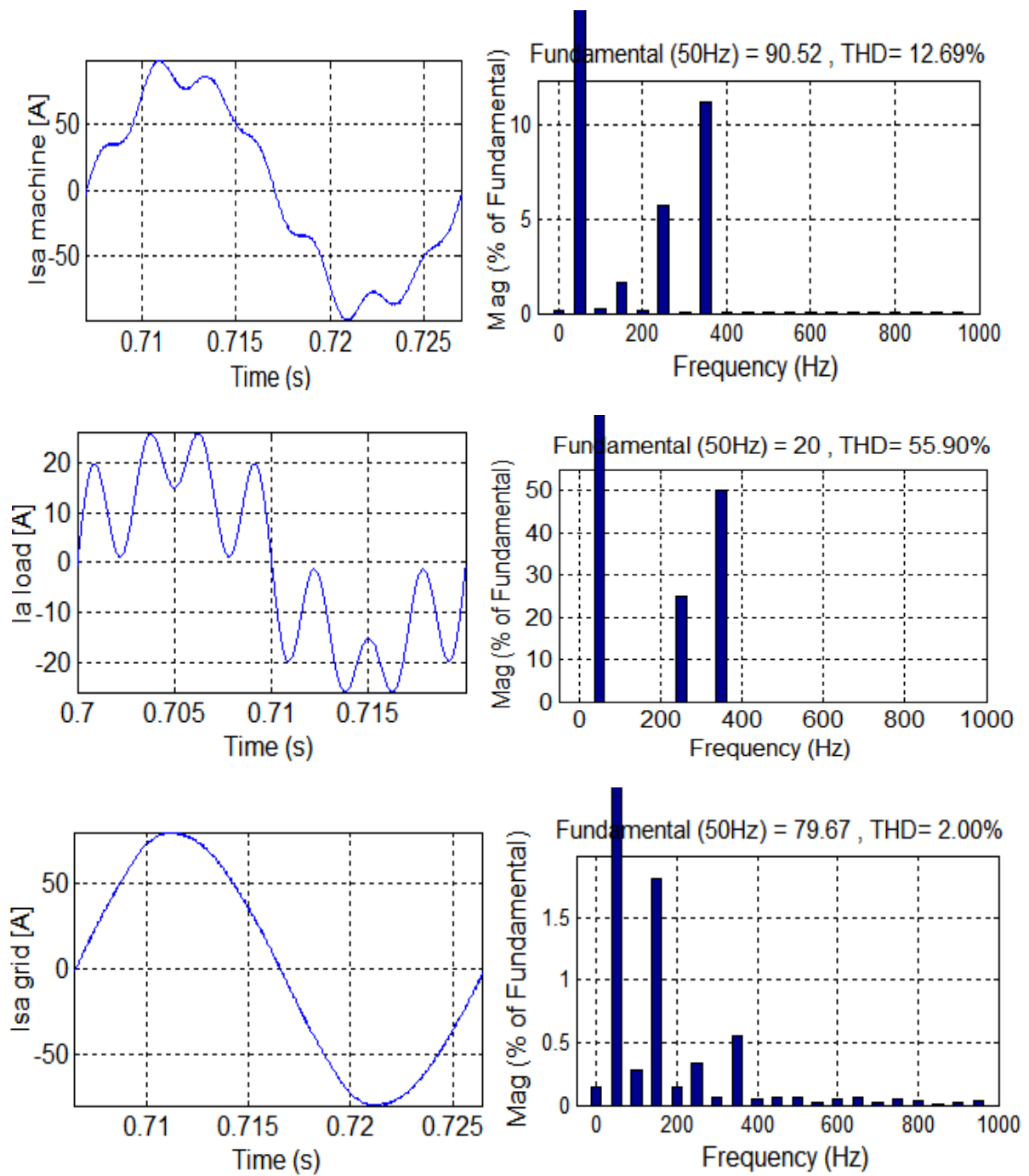


Figure 3.34. Current waveforms and their FFT for (a) generator, (b) non-linear load, (c) grid.

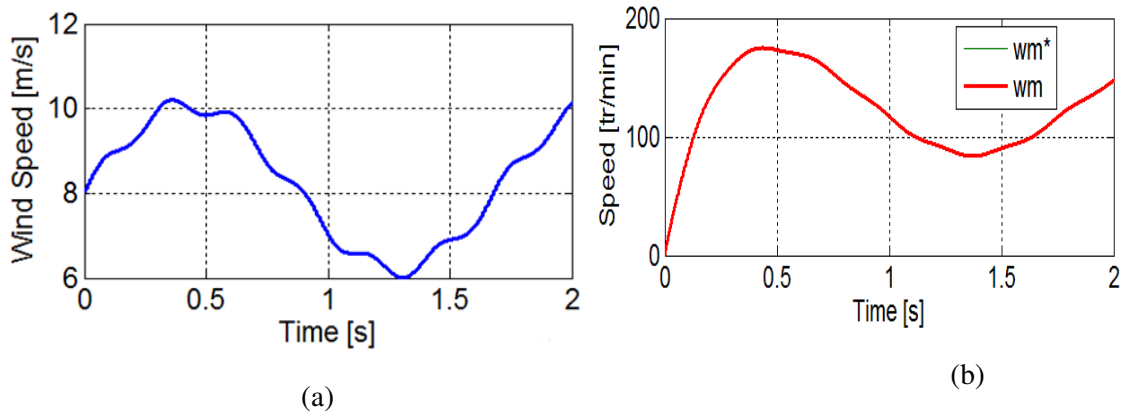


Figure 3.35. (a) Wind speed (b) Speed of DFIG with MPPT.

5.5.5.2.2. Conventional PI rotor currents control

In this control method, we use a conventional PI-regulator as which used in the first chapter (with same transfer function and PI gains calculation). Where, the close loop rotor currents control is presented in Figure 3.36.

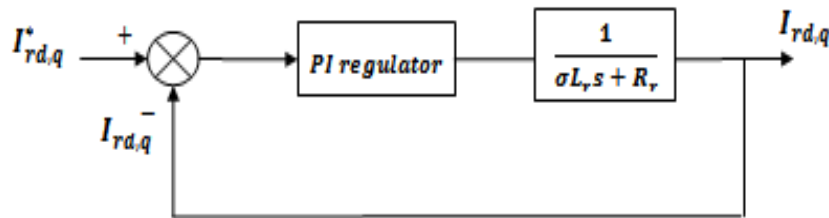


Figure 3.36. Close loop conventional PI rotor currents control.

▪ Simulation result

The grid current without active filter is given in Figure 3.22. The grid current for shunt active filter using Conventional PI rotor currents control is given in Figure 3.37. As we can see, there are considerable errors in the rotor currents responses which reduce the performance of the system control, especially in the harmonics suppression as shown Figure 3.41.

This last figure shows the current waveforms and their FFT for (a) generator, (b) non-linear load, (c) grid. By the comparison between this figure and Figure 3.22, we have seen that the THD was decreased from 16,90% to 8,54% in the system filtering. However; the THD of the current produced by the generator has increased from 0,64% to 11,15% contains the opposite harmonic to injected in the grid.

In other side, when we compared it by the hysteresis rotor control active filter results; we find that there is a THD= 6% of difference between the hysteresis and conventional PI control method and this results from the error existing in the rotor currents controller.

Figure 3.38 shows the direct and quadrature rotor currents injected in the grid through the Conventional PI rotor currents control.

Figure 3.39 shows the non-linear load current.

Figure 3.40 shows the quadrature and direct stator powers, DC-link voltage and Torque machine, and a phase grid and machine (DFIG) stator current responses. As we can see; the responses follows the reference currents with their injected currents generated from the filter and the priority method algorithm.

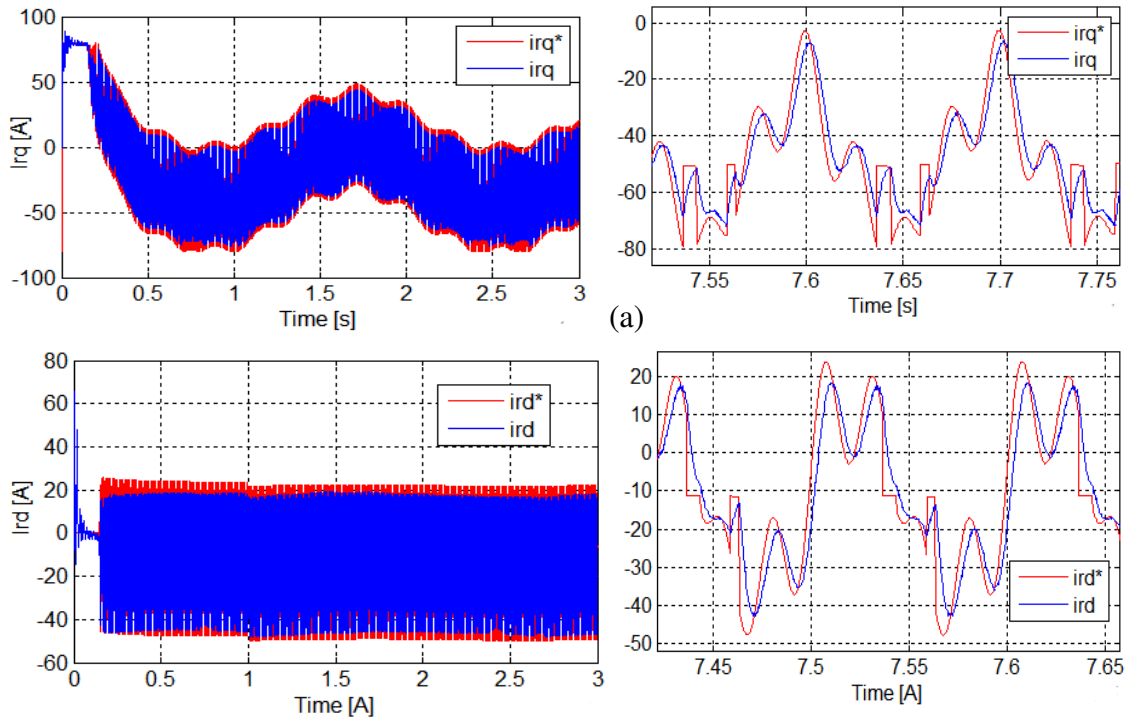


Figure 3.37. Conventional PI rotor currents control: (a) quadrature rotor current with its Zoom i_{rd} ; (b) direct rotor current with its Zoom i_{rq} .

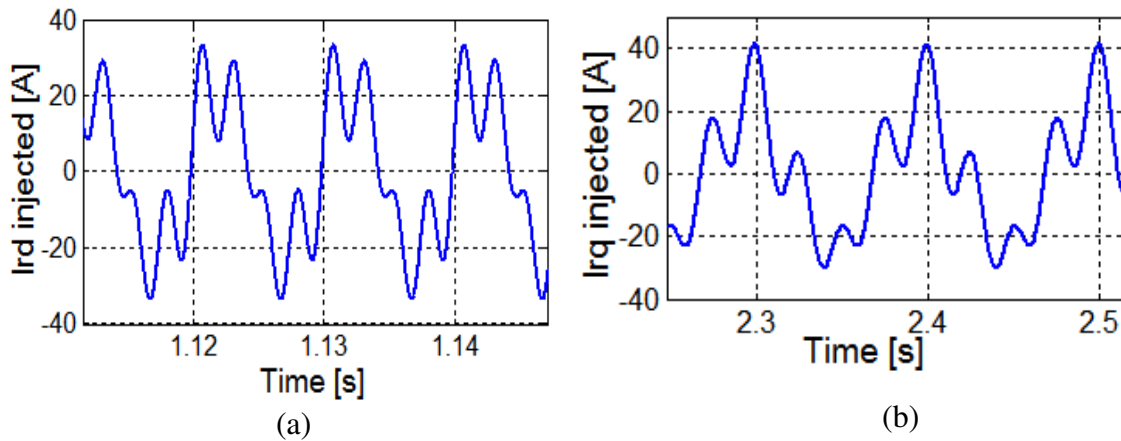


Figure 3.38. Direct and quadrature rotor currents injected in Conventional PI rotor currents control.

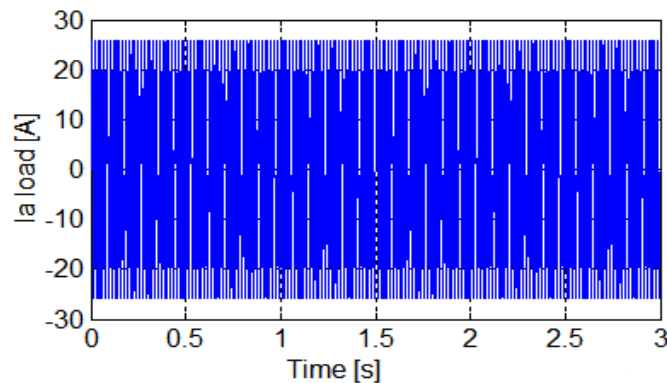


Figure 3.39. Non-linear load current.

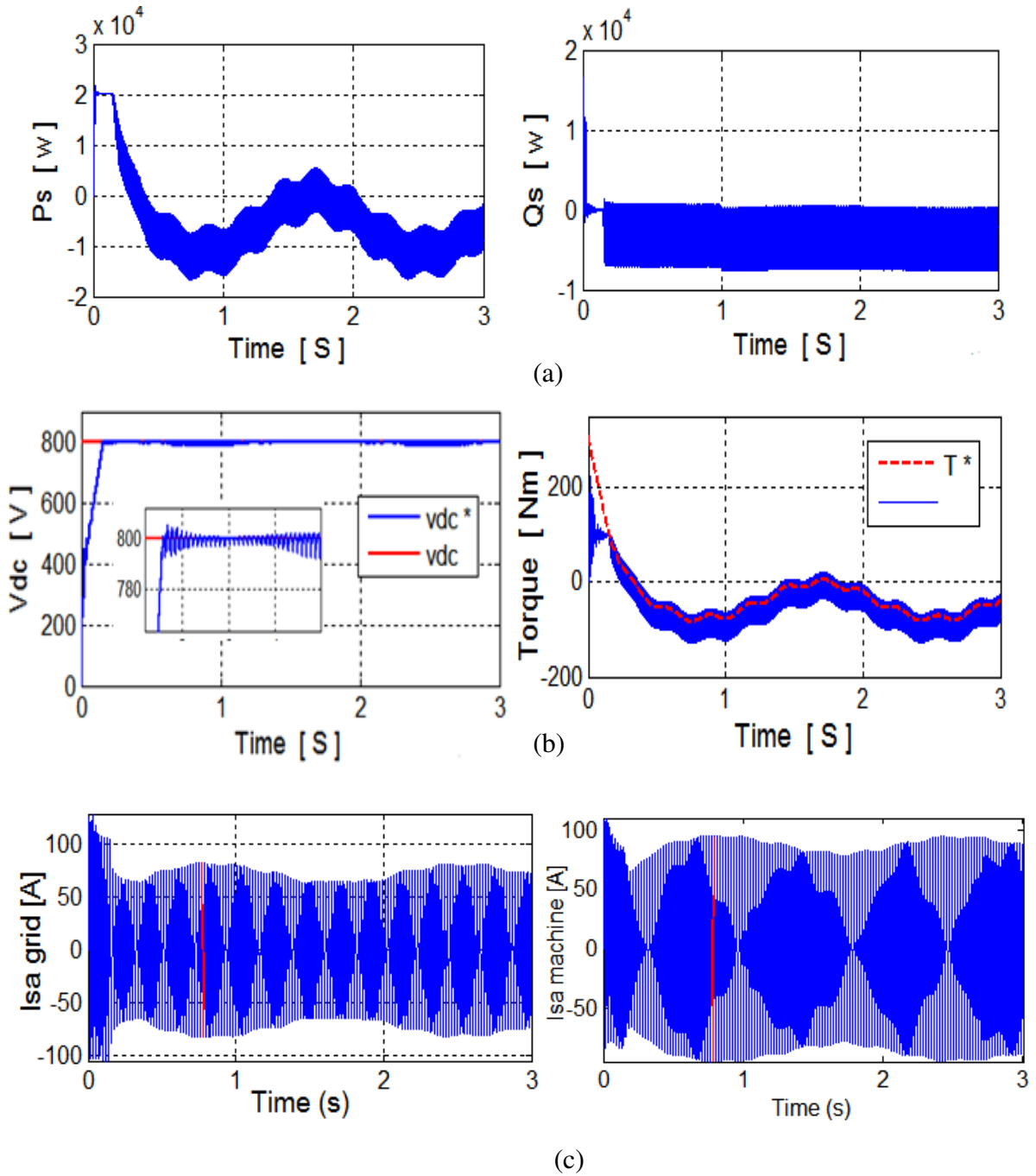


Figure 3.40. (a) quadrature and direct stator powers; (b) DC-link voltage and Torque machine, (c) a phase stator current for grid and machine (DFIG) for Conventional PI rotor currents control.

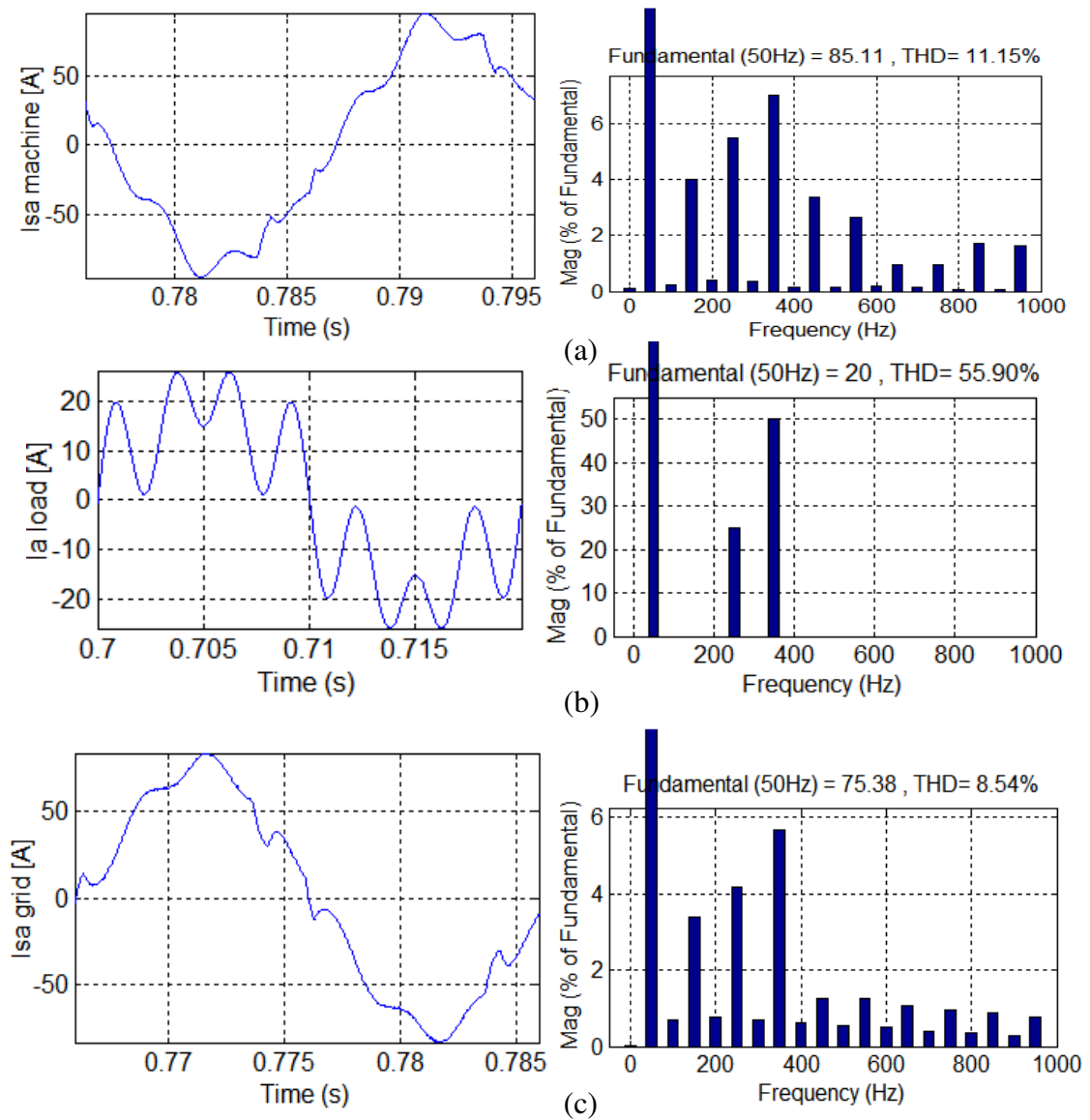


Figure 3.41. Current waveforms and their FFT for (a) generator, (b) non-linear load, (c) grid for Conventional PI rotor currents control.

3.5.5.2.3. PI-adaptive fuzzy logic rotor currents control

Conventional PI controller is the most used controller in industrial applications but does not give acceptable performance for systems with uncertain dynamics, time delays and non-linearity [35]. Hence it is necessary to automatically tune the PI parameters for obtaining satisfactory responses. Therefore, an adaptive control is basically a method which can tune and operate a system in a real time environment. So, this can be improved using a fuzzy logic control [36].

The rotor currents controller based on fuzzy-adaptive *PI* (proportional-integral) controllers is implemented as shown in Figure 3.42. Where, there are two input signals to the fuzzy self-tuning controllers; the error ($err = I_{rdq}^* - I_{rdq}$) and the change in error (Δerr) which is related to the derivative (dE/dt) of the error. The controller's outputs are the changing in the *PI* regulator gains ΔK_{p-i} and ΔK_{i-i} as shown Figure 3.43. These two values permit to adaptive the *PI* controller gains by the following equations:

$$\begin{cases} K_{p-new} = K_{p-old} + \Delta K_p \\ K_{i-new} = K_{i-old} + \Delta K_i \end{cases} \quad (3.21)$$

In Figure 3.43; the two inputs variables must be defined in terms of linguistics. There are five linguistic terms of the error in rotor current: negative big (NB), negative (N), zero (Z), positive (P), and positive big (PB). The error (err) in rotor current is expressed by a number in the interval from -7 to 7A (Figure 3.45 (a)).

Similarly, the fuzzy set of the error change of the rotor current (Δerr) is presented as {NB, N, Z, P, PB} over the interval from -3 to 3 A (Figure 3.45 (b)).

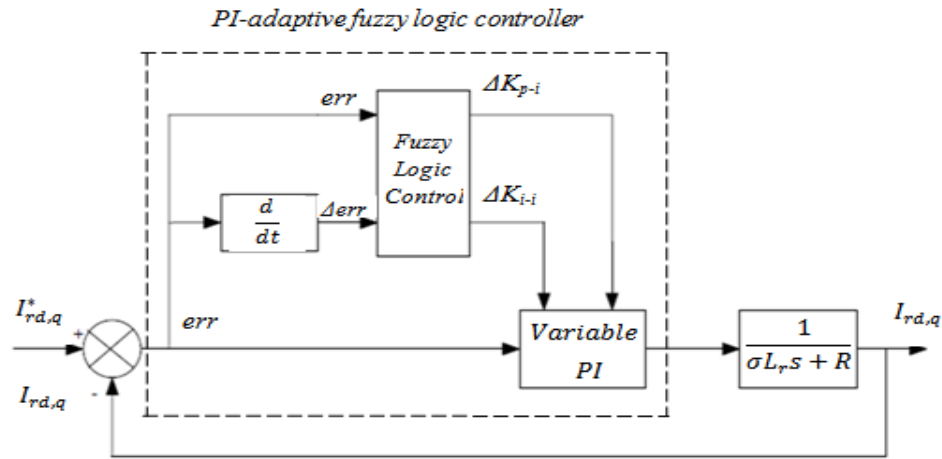


Figure 3.42. PI-adaptive fuzzy logic rotor currents control Bloc diagram.

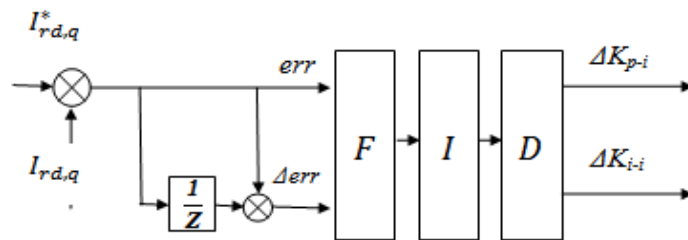


Figure 3.43. Fuzzy logic bloc diagram controller.

Finally, the fuzzy set of the outputs signals are presented as {NB, N, Z, P, PB} over the interval from 0 to 50 and from 0 to 5 for ΔK_{p-i} and ΔK_{i-i} respectively (Figure 3.45 (c) and (d)). The membership function used by fuzzy controller is triangular membership function as shown Figure 3.45.

The rules base consist of a set of linguistic *IF-THEN* rules containing two antecedences and two consequences, as expressed in the following form:

- *IF* (current *err* is Negative Big (NB)) *AND* (change error is Positive Small (PS)) *THEN* the output gains; ΔK_{p-i} is Positive Small (PS) and ΔK_{i-i} is Positive Big (PB).

The total number of IF-THEN rules is 25 for each output gains as shown in Table 3.2 and Table 3.3.

This control rules are framed using the fuzzy logic toolbox available in MATLAB with Mamdani-type fuzzy inference system and with defuzzification based on the centre of gravity method. Figure 3.44 shows

Fuzzy Inference System (FIS) plot diagram in Matlab environment and Figure 3.46 shows the Output variables surface of ΔK_{p-i} and ΔK_{i-i} .

Table 3.2. Fuzzy rules for ΔK_{p-i} gain

$\begin{matrix} err \\ \Delta err \end{matrix}$	NB	NS	Z	PS	PB
NB	PB	PS	PS	PS	Z
NS	PB	PB	PS	Z	Z
Z	PS	PS	Z	NS	NS
PS	Z	Z	NS	NS	NB
PB	Z	NS	NB	NB	NB

Table 3.3. Fuzzy rules for ΔK_{i-i} gain

$\begin{matrix} err \\ \Delta err \end{matrix}$	NB	NS	Zp	PS	PB
NB	PS	PS	Z	PB	PB
NS	NS	NS	NS	NS	PS
Z	NB	NS	NS	PS	PS
PS	NS	NS	NS	PS	PS
PB	PS	Z	Z	PB	PB

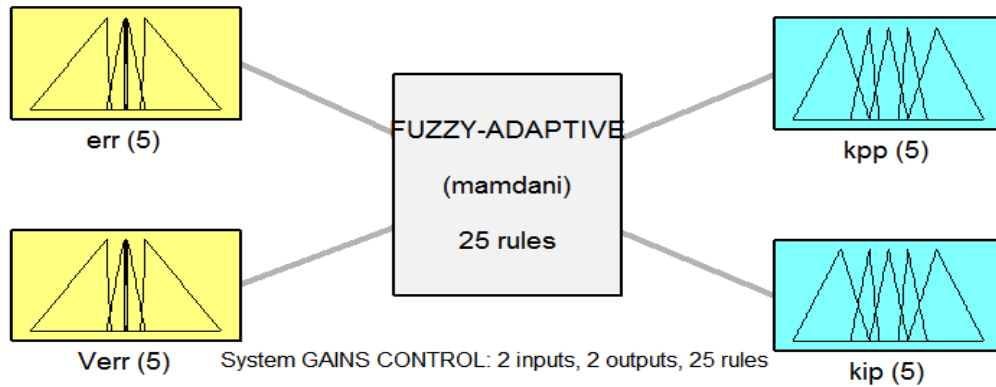


Figure 3.44. Fuzzy Inference System (FIS) plot diagram.

▪ **Simulation results**

The grid current without active filter is given in Figure 3.22. The grid current for shunt active filter using PI-adaptive fuzzy logic rotor currents control is given in Figure 3.47. As we can see, in Figure 3.47-(a) shows the quadrature rotor current measurement flows seriously its reference however, there is a little error in the direct rotor current measurement where we considerate as a delay time.

Figure 3.48 shows the direct and quadrature rotor currents injected in the grid through the PI-adaptive fuzzy logic rotor currents control. Figure 3.49 shows the non-linear load current response.

Figure 3.50 and 3.51 show the changing gains of the PI-adaptive fuzzy logic controller for the direct and quadrature rotor currents respectively. Where, we add a zoom of each gain near to them for better review.

Figure 3.52 shows the quadrature and direct stator powers, DC-link voltage and Torque machine, and a

phase grid and machine (DFIG) stator current responses. As we can see; the responses follows the reference currents with their injected currents generated from the filter and controlled with the priority method algorithm.

Figure 3.53 shows the current waveforms and their FFT for (a) generator, (b) non-linear load, (c) grid. When, we compared with Figure 3.22, we have seen that the THD in this figure was decreased from 16,90% to 1, 98% in the system filtering. However; the THD of the current produced by the generator has increased from 0,64% to 12,24% contains the opposite harmonics to injected in the grid.

In other side, when we compared it with the hysteresis and conventional PI rotor control results; we find that the PI-adaptive fuzzy logic controller is the best method used here to reduce the harmonics currents in the grid.

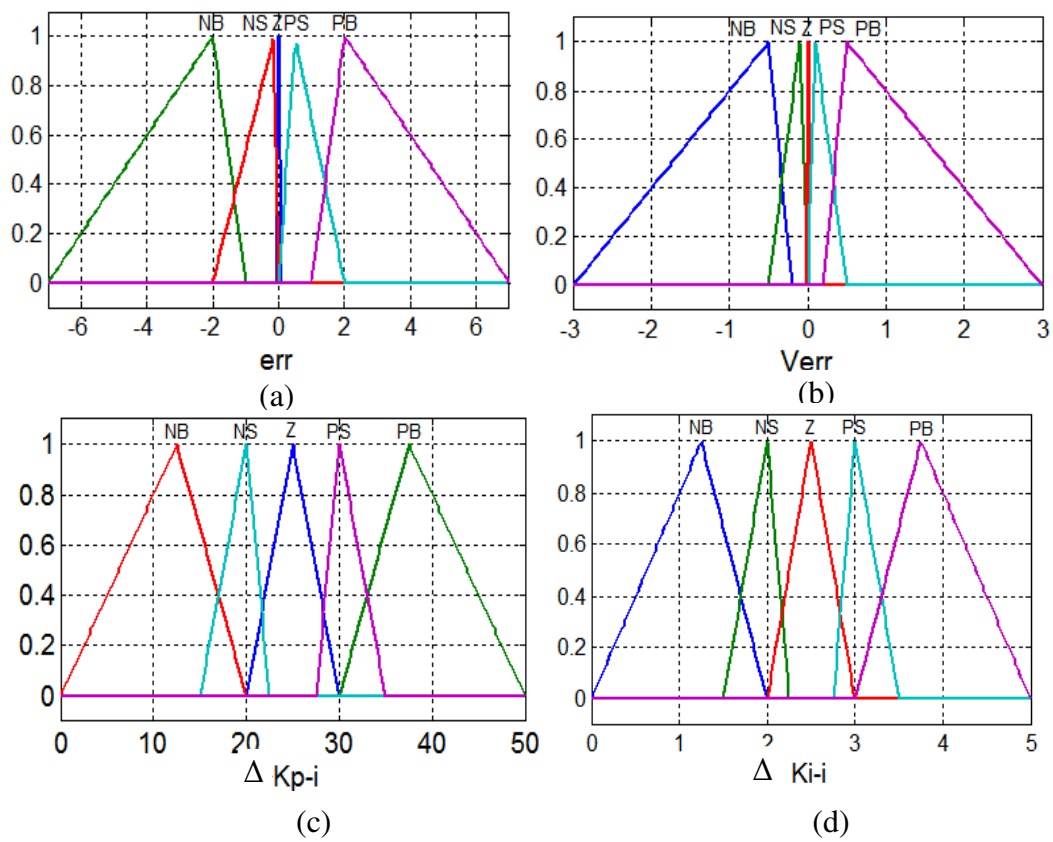


Figure 3.45. Membership functions for (a) inputs variables err , Δerr (b) and outputs $\Delta Kp-i$ and $\Delta Ki-i$.

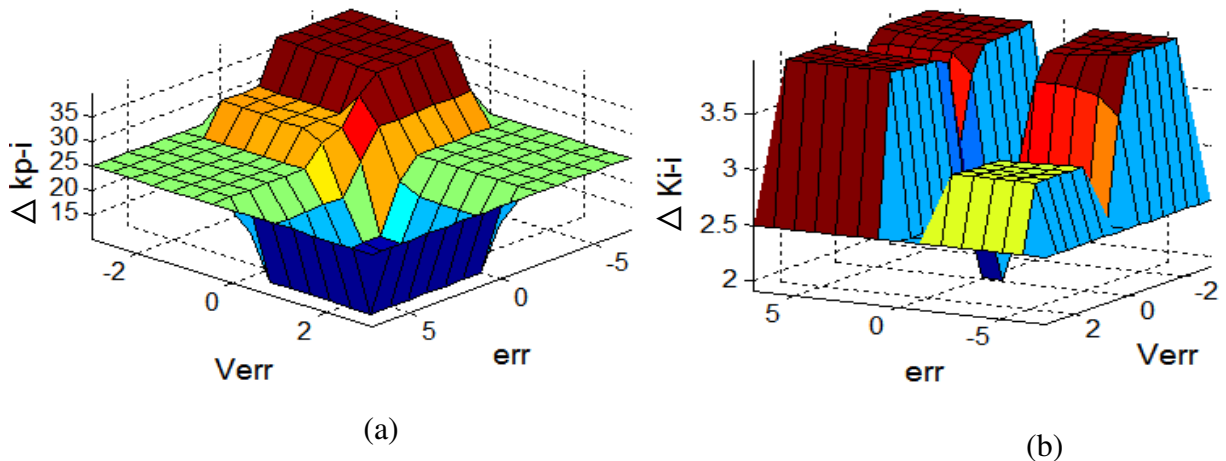


Figure 3.46. Output variables surface of $\Delta Kp-i$ and $\Delta Ki-i$.

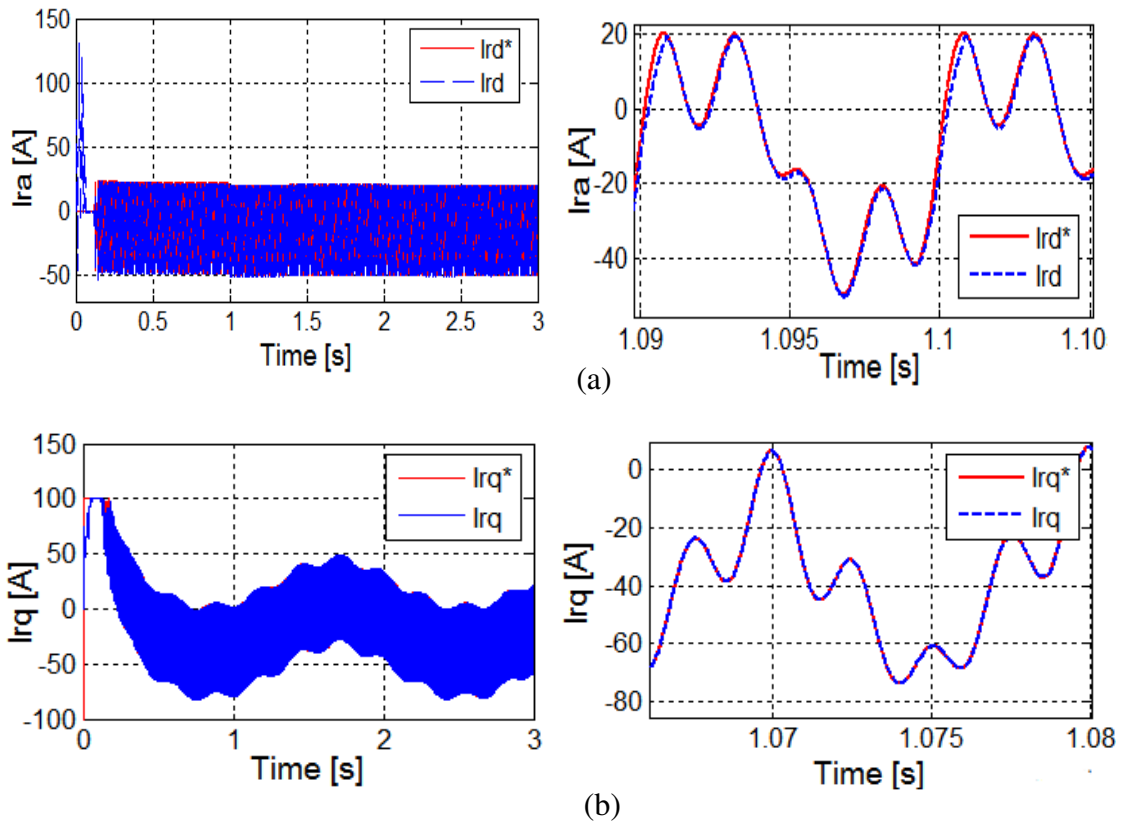


Figure 3.47. PI-adaptive fuzzy logic rotor currents control: (a) quadrature rotor current with its Zoom I_{rd} ; (b) direct rotor current with its Zoom I_{rq} .

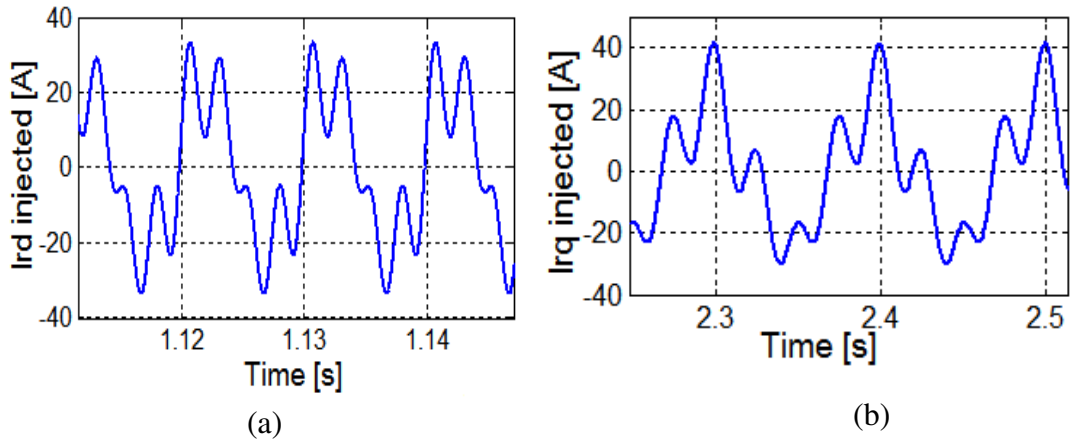


Figure 3.48. Direct and quadrature rotor currents injected in Conventional PI rotor currents control.

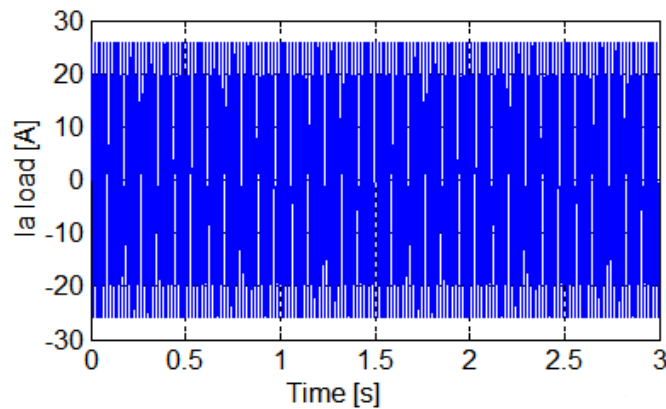


Figure 3.49. Non-linear load current.

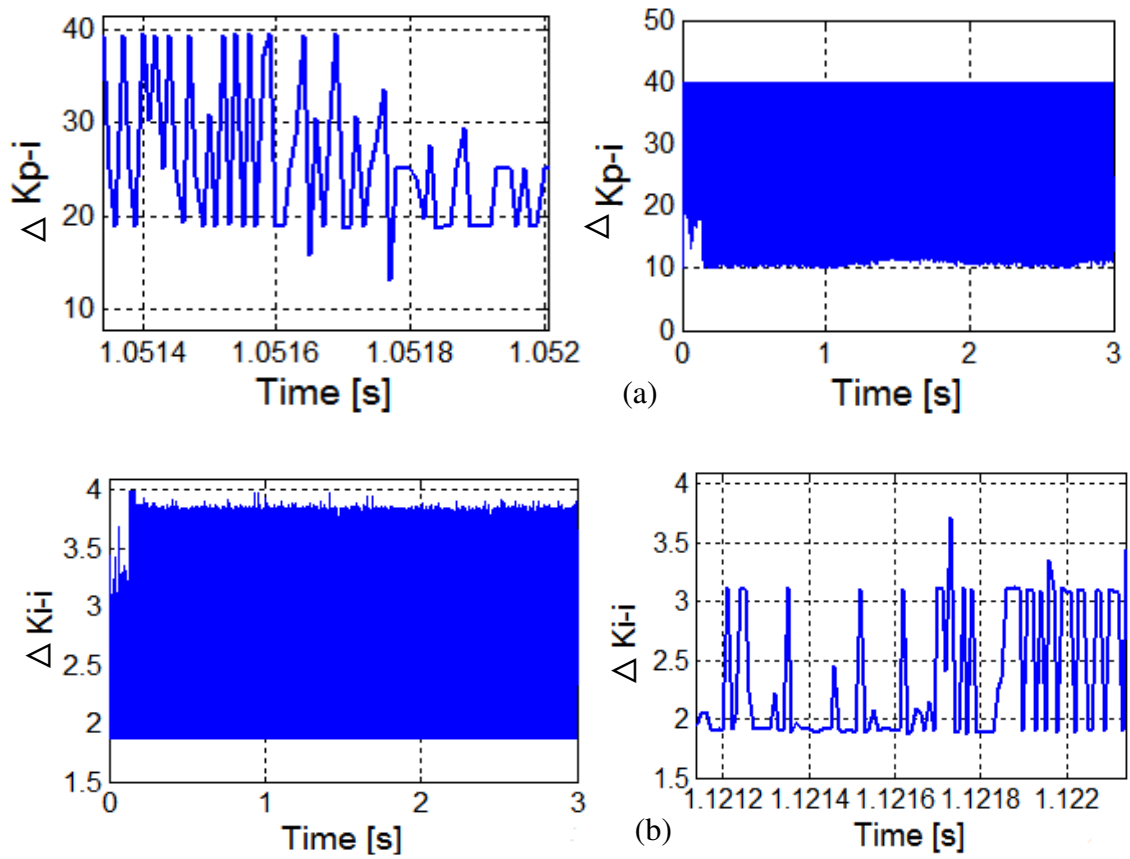


Figure 3.50. ΔK_{p-i} and ΔK_{i-i} Variation gains for direct rotor current PI-adaptive fuzzy logic controller.

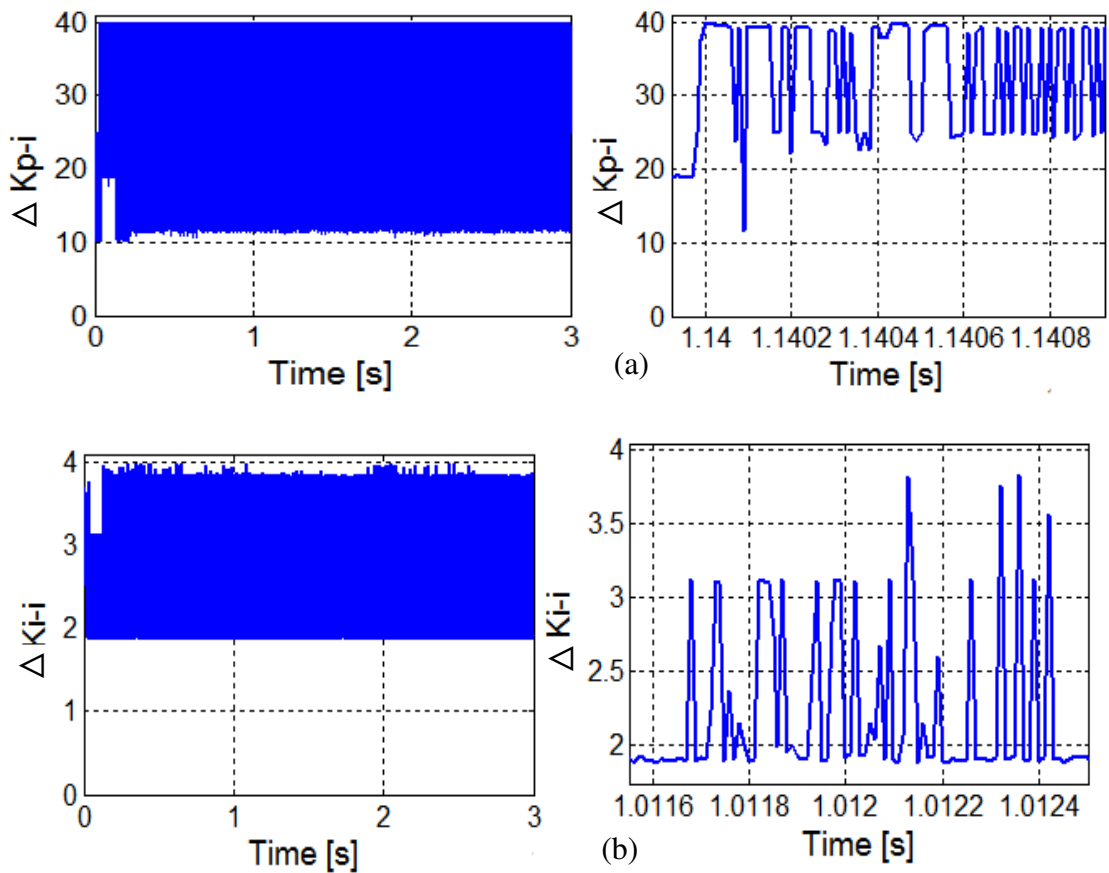


Figure 3.51. ΔK_{p-i} and ΔK_{i-i} Variation gains for quadrature rotor current PI-adaptive fuzzy logic controller.

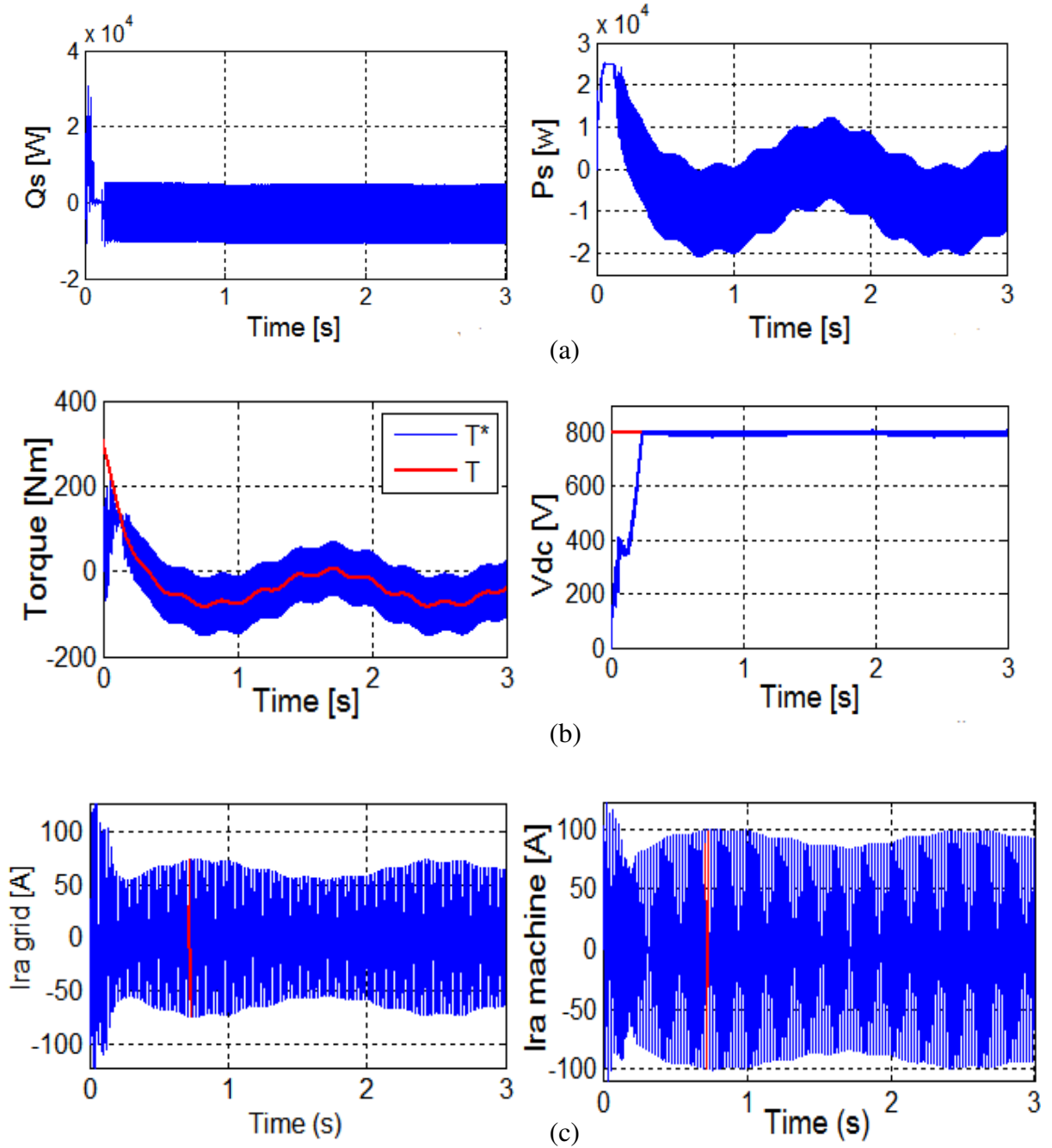


Figure 3.52. (a) quadrature and direct stator powers; (b)DC-link voltage and Torque machine, (c) a phase stator current for grid and machine (DFIG) for PI-adaptive fuzzy logic rotor currents control.

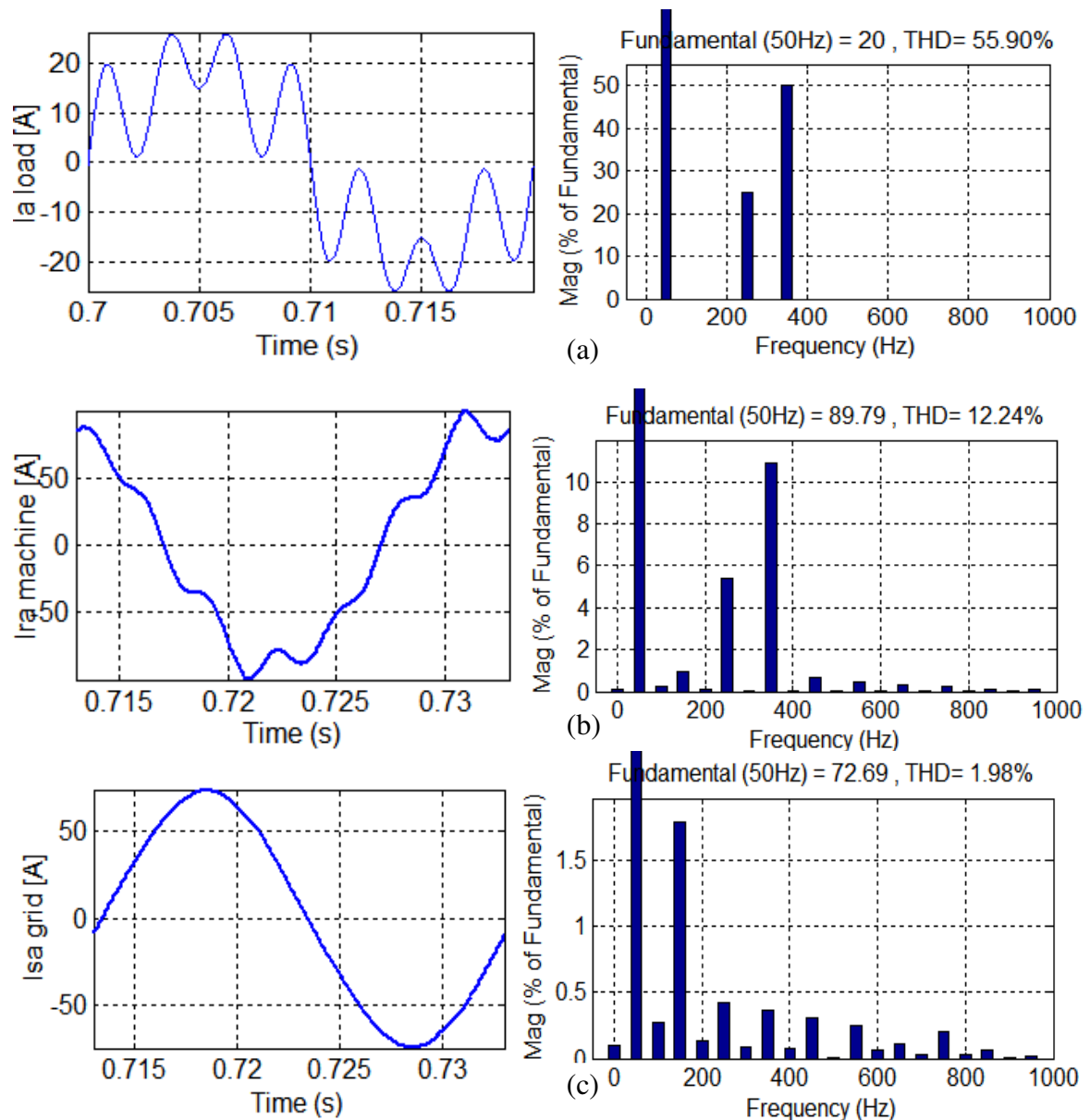


Figure 3.53. Current waveforms and their FFT for (a) generator, (b) non-linear load, (c) grid for PI-adaptive fuzzy logic rotor currents control.

3.5.5.2.4. Comparison rotor currents controllers' methods

The comparison direct and quadrature rotor currents control responses for the three controllers are illustrated in Figure 3.54 and Figure 3.55. As we can see in these figures, the best rotor currents responses are those of the hysteresis and PI-adaptive fuzzy logic controllers in both direct and quadrature currents. However, there is a considerable error in PI-conventional responses.

❖ Comparison consequences

a) Hysteresis rotor currents control

The simple implementation procedure is the main advantage of this control method. However, the variable switching frequency is the major draw-back of this method. This variable frequency affects mainly the function of power electronic elements which can't support high switching frequency in high power applications.

b) Conventional PI rotor currents control VS PI-adaptive fuzzy logic rotor currents control

Adaptive control has many advantages over conventional control such as:

- In conventional control disturbance in system measurements are done using control variables whereas in adaptive control measurements are done using index of Performance.
- Adaptive control uses index of Performance to control the system whereas in conventional control we take reference input for the purpose of control.
- Conventional control only uses controller whereas in adaptive control controller and adaptation mechanism is used in parallel to achieve the desired output.

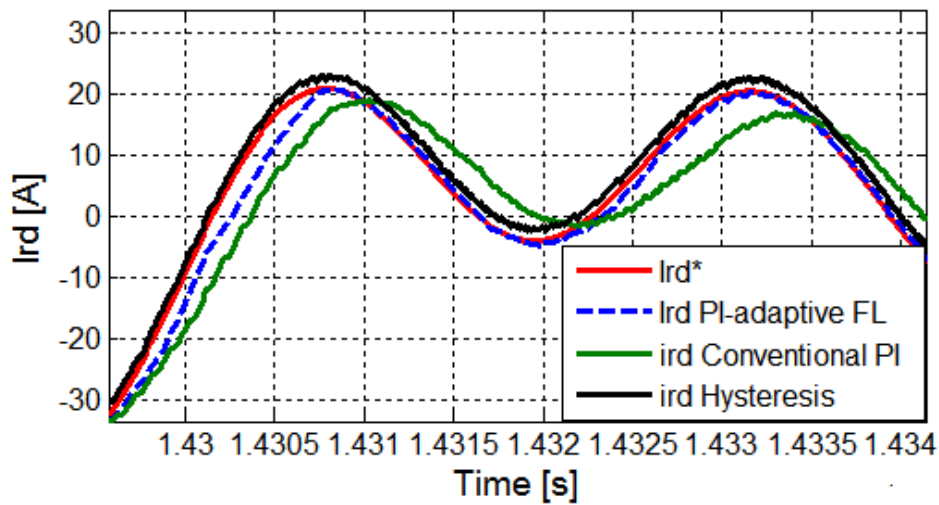


Figure 3.54. Comparison direct rotor currents controller's methods.

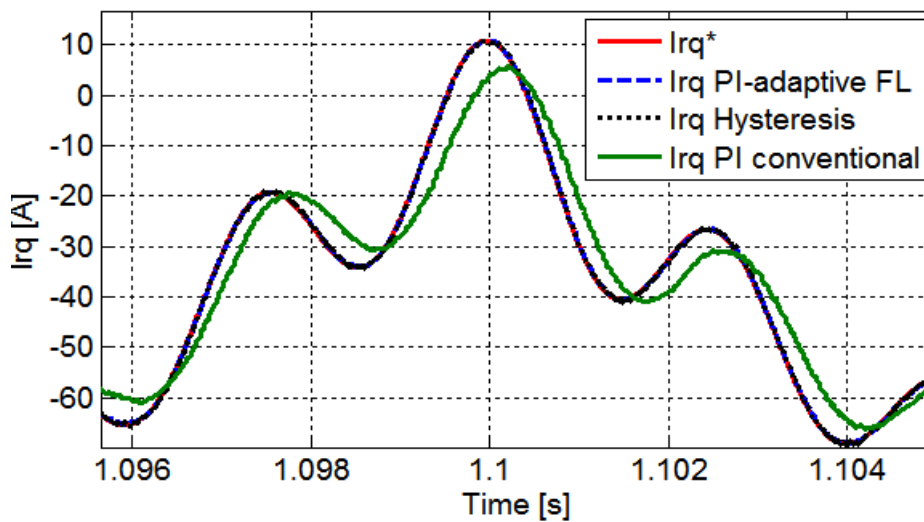


Figure 3.55. Comparison quadrature rotor current controller's methods.

3.6. Conclusion

The availability of electric power with high quality is crucial for the running of the modern society. Even the most advanced transmission and distribution systems are not able to provide electrical energy with the desired level of reliability for the proper functioning of the loads in this modern society. This chapter aims to design shunt active power filter (SAPF) for harmonic cancelation of grid-connected wind turbine (WT) based on DFIG.

First of all, main Power Quality (PQ) problems are presented in this chapter, which are voltage sag/swell, voltage interruption, voltage fluctuation, voltage unbalance, current harmonic, voltage unbalance and current unbalance. Among them, current harmonics are the most common power quality problems which are presented with their associated causes and consequences.

Secondly, some solutions to mitigate the harmonics current problems are presented among of them; a Shunt Active Power Filter (SAPF) is used to minimize these harmonics existing in the grid using Synchronous Reference Frame (SRF) harmonics currents extraction. In addition, in order to reduce the cost of the system filtering; a new method called priority method control is including to reduce these harmonics currents through the wind turbine system's converter saving the principal system controls priorities (stator powers control and MPPT control).

Finally, in goal to improve the control performance; a three different controller are used to regulate the rotor currents for better filter results which are: hysteresis currents controller, conventional PI controller and PI-adaptive fuzzy logic controller regarding the harmonics currents suppression.

The THD of the grid currents was decreased from 16,90% to 1, 98% using PI-adaptive fuzzy logic controller where it was decreased just into 8.54% using conventional PI controllers. Furthermore, the designed PI with Adaptive Fuzzy Controller has much faster response than using the conventional one, where this last is good for giving us the starting point of the PI gains values.

The Hysteresis current controller in turn was produced good results in the suppression of the currents harmonics where, the THD was decreased from 16,90% to 2% in the grid. However, the variable switching frequency is the major draw-back of this method which affects mainly the function of power electronic elements which cannot support high switching frequency in high power applications.

3.7. References

- [1] Camelia Youcef .M, “ *Power Quality*”, Dar eldjamiain lltibaa, 1995.
- [2] R. C. Sermon, “*An overview of power quality standards and guidelines from the end-user's point-of-view*”, Rural Electric Power Conference, 2005.
- [3] Joseph Seymour, “*The Seven Types of Power Problems*”, Electric Power Research Institute, The Cost of Power Disturbances to Industrial & Digital Economy Companies, 2001.
- [4] Ph. Ferracci, “*Power Quality*”, Cahier Technique Schneider Electric no. 199, October 2001.
- [5] Basarab Dan GUZUN, Mahfoud FERAS, Porumb RADU, “*POWER QUALITY*”, Universitatea Politehnica București, 2015.
- [6] Camelia Youcef .M, “ *The Harmonics in Electrical Networks*”, Dar Eldjamiain Litibaa, 2005.
- [7] Nikita Lovinskiy, “*Effects of Imbalances and Non-linear Loads in Electricity Distribution System*”, Master’s thesis, Lappeenranta University of Technology, Faculty of Technology, Electrical Engineering, 2010.
- [8] E. Forehand E. Mc. William, “*An Evaluation of Harmonic Mitigation Techniques A Major Qualifying Project*”, Bachelor of Science in Electrical and Computer Engineering.
- [9] Aníbal T. de Almeida, “*Power Quality Problems and New Solutions*”, International Conference on Renewable Power and Power Quality '03 Vigo, April 9 – 11, 2003.
- [10] Kevin Olikara, “*Power Quality Issues, Impacts, and Mitigation for Industrial Customers*”, Power and Energy Management Products – Rockwell Automation, Inc, September 2015.
- [11] Appleton Group, “*Power Quality Guide Book*”, W. Higgins Road Rosemont, IL 60018, solahd.com, 2016.
- [12] Yiting Zhao, “*Electrical Power Systems Quality*”, University at Buffalo, The state University of New York.
- [13] Rafael Asensi, “*Power Quality Application Guide, Harmonics Understanding Compatibility Levels*”, Universidad Politécnica de Madrid, March 2005.
- [14] Camelia Youcef .M, “ *Power Quality Distrubances*”, Dar eldjamiain lltibaa, 2002.
- [15] Salomon Bochner, “*Harmonic Analysis and the Theory of Probability (Dover Books on Mathematics)*
- [16] Robert G. Ellis, P.; “*POWER SYSTEM HARMONICS: A Reference Guide to Causes, Effects and Corrective Measures*”, AN ALLEN-BRADLEY SERIES OF ISSUES AND ANSWERS”, book, August 27, 2005.
- [17] G. Sandoval J. Houdek, “*A Review of Harmonic Mitigation Techniques*”, article, 2005.
- [18] Jyotsana Kaiwart, Uma P. Bala Raju , “*Harmonic Mitigation Techniques: A Review*”, International Journal of Advanced Research in Electrical, Electronics and Instrumentation Engineering, Vol. 5, Issue 11, November 2016.
- [19] https://www.schneiderelectric.com.tw/documents/Event/2016_electrical_engineering_seminar/IEEE_STD_519_1992vs2014.pdf, March 2018.
- [20] LJ Giacoletto and GL Park. “*Harmonic filtering in power applications*”, In Industrial and Commercial Power Systems Technical Conference, 1989, Conference Record., pages 123–128. IEEE, 1989.
- [21] Akagi H., “*Active harmonic filters*”, Proc. IEEE, Vol. 93 (2005), No. 12, pp. 2128-2141.

- [22] K.N.M. Hasan and M.F. Romlie. “Comparative study on combined series active and shunt passive power filter using two different control methods”. In Intelligent and Advanced Systems, 2007. ICIAS 2007. International Conference on, pages 928–933. IEEE, 2007.
- [23] S. Rajesh Rajan, “POWER QUALITY IMPROVEMENT IN GRID CONNECTED WIND ENERGY SYSTEM USING UPQC”, International Journal of Research in Engineering & Technology (IJRET) Vol. 1, Issue 1, June 2013, 13-20.
- [24] A.M. Al-Zamil and D.A. Torrey. “A passive series, active shunt filters for high power applications”, Power Electronics, IEEE Transactions on, 101–109, 2001.
- [25] Ms. Sushma Parihar, Laith O. Maheemed, Prof. D.S. Bankar, “THE UNIFIED POWER QUALITY CONDITIONER TECHNIQUE IN WIND ENERGY CONVERSION SYSTEM”, International Journal of Advanced Engineering Technology, April-June.
- [26] H. Benalla, H. Djeghloud, “Shunt Active Filter Controlled by Fuzzy Logic”, J. King Saud Univ., Vol. 18, Eng. Sci. (2), pp. 231-247, 2005.
- [27] B. Singh, K. Al-Haddad, A. Chandra, “A Review of Active Filters for Power Quality Improvement”, IEEE Trans. Ind. Electron., vol. 46, no.5, pp. 960-971, 1999.
- [28] A.M. Massoud ; S.J. Finney ; B.W. Williams, “Review of harmonic current extraction techniques for an active power filter”, Harmonics and Quality of Power, 11th International Conference on 2004.
- [29] H. Akagi, E.H. Watanabe, and M. Aredes, “Instantaneous Power Theory and Applications to Power Conditioning”. Hoboken, NJ: Wiley, 2007.
- [30] Akagi H., Watanabe E.H., Aredes M., “Instantaneous Power Theory and Applications to Power Conditioning”, New Jersey: IEEE Press/Wiley-Interscience, 2007.
- [31] Hanju Cha and Trung-Kien Vu, “Comparative Analysis of Low-pass Output Filter for Single-phase Grid-connected Photovoltaic Inverter”, IEEE, 2010.
- [32] I. Colak, R. Bayindir, E. Irmak, O. Kaplan, “A comparative study of harmonic extraction methods for single phase shunt active power filter”, International Conference on Power Engineering, Energy and Electrical Drives Torremolinos (Málaga), Spain. May 2011.
- [33] Buso S., Malesani L., Mattavelli P., “Comparison of Current Control Techniques for Active Filter Applications”, IEEE Trans. on Industrial Electronics, Vol. 45 (1998), No. 5, pp. 722-729.
- [34] Arnaud GAILLARD, “Système éolien basé sur une MADA : contribution à l'étude de la qualité de l'énergie électrique et de la continuité de service », Thèse, Faculté des Sciences & Techniques – 54506 Vandoeuvre-lès-Nancy.
- [35] D.P. Atherton ; S. Majhi, “Limitations of PID controllers”, IEEE American Control Conference, 1999.
- [36] A. Bouzekri T. Allaoui, M. Denia, « Power Quality Enhancement of DFIG Based Wind Energy System Using Priority Control Strategies », Journal of Electrical Engineering , vol 15 , no. 4 , 15.4.19 , pp. 145-155, 2015.
- [37] S. Bin Mohamed Ibrahim, “THE PID CONTROLLER DESIGN USING GENETIC ALGORITHM”, Thesis, Bachelor of Engineering, University of Southern Queensland, 2005.

[38] K. Sinthipsomboon et al, “A Hybrid of Fuzzy and Fuzzy Self-Tuning PID Controller for Servo Electro-Hydraulic System”, licensee InTech, chap.13, pp. 299-314, 2012.

[39]

[40]

Chapter IV: Hybrid-Intelligent Fault Tolerant Control Strategy of IGBT Open-switch for RSC in Wind Turbine System

Abstract: *This chapter presents hybrid-intelligent Fault Tolerant Control (FTC) strategy of IGBT open-circuit for Rotor Side Converter (RSC) connecting doubly-fed induction (DFIG) generator wind turbine systems to the grid. The FTC strategy based on Expert System method and combines a simple method detection based on fuzzy logic inference and uses rotor current average values to detect the faulty switch in a very short period of time. In addition, following a power switch failure, the FTC strategy activates the redundant leg and restores the operation of the converter to save a power quality and ensure the service continuity. Furthermore, in order to improve the performance of the closed-loop system during transients and faulty conditions, the currents controllers are based on a PI (proportional-integral) controller optimized using Genetic Algorithms. The simulation model was developed in Matlab/Simulink environment and the simulation results demonstrate the effectiveness of the proposed FTC method and closed-loop current control scheme.*

4.1. Introduction

4.1.1. Overview

Nowadays, power electronics play an important role in motor drives, utility interfaces with renewable energy sources, power transmission (e.g. high-voltage direct current systems, and flexible alternating current transmission systems), electric or hybrid electric vehicles and many other applications. It is interesting to note that the modern technology evolution in power electronics has greatly contributed to the knowledge of power devices materials, processing, fabrication, packaging, modeling, diagnosing and simulation. These power semi-conductors are almost exclusively based on silicon material and can be classified in many categories, one of the most popular devices in power electronic semi-conductor is the IGBT (Insulated Gate Bipolar Transistor) [1]. It is a hybrid bipolar-metal-oxide semiconductor, which has the advantages of low on-state resistance, voltage control of the gate and wide safe operating area [2].

Therefore, the reliability of electronics power becomes more and more vital, and should draw more attention. According to a survey, semiconductor failure and soldering joints failure in power devices take up 34% of power electronic system failures [3]. Another survey shows that around 38% of the faults in variable-speed ac drives are due to failure of power devices [4]. A recent questionnaire on industrial electronic power systems also showed that all the responders consider electronic power reliability as an important issue, and 31% of the responders selected the “semiconductor power device” as the most fragile component [3, 4]. Therefore it is worth investigating IGBT’s failure and exploring the solutions to improve the reliability of IGBT power electronic converters. The failure of IGBTs can be generally classified as catastrophic failure and wear out failure. IGBT wear out failure is mainly induced by accumulated degradation with time, while catastrophic failure is triggered by single-event overstress, such as overvoltage, over-current, overheat and so on [5].

When a fault occurs in a system, the main problem to be addressed is to raise an alarm, ideally diagnose what fault has occurred, and then decide how to deal with it. The problem of detecting a fault, finding the source/location and then taking appropriate action is the basis of fault diagnosis and fault tolerant solution [6].

FTC is divided in two main sections, it contains Passive and Active approaches. The control literature contains a large amount of linear control redesign approaches for AFTC which redesign the nominal controller after Fault Detection and Isolation (FDI). In active FTC, FDI plays a vital role in providing information about faults/failures in the system to enable appropriate reconfiguration to take place. The main function of FDI is to detect a fault or failure and to find its location so that corrective action can be made to eliminate or minimize the effect on the overall system performance [6, 7]. For most FTC systems, the robustness of the FDI has a strong effect on the robustness of the FTC and this is discussed in [6]. There are many classifications of FDI in the literature [6, 25]. One obvious classification is model- and non-model-based FDI.

The use of robust model-based methods usually results in a design which is too conservative and

insensitive to faults, too complicated or limited to certain classes of uncertainty [6]. Since the late 1990s there has been an increase in research on non-model-based FDI methods especially those utilizing artificial intelligence and ‘soft computing’ approaches such as neural networks, and fuzzy logic (see for example [32, 33, 34, 35]).

Expert systems found broad application in fault diagnosis from their early stages because an expert system simulates human reasoning about a problem domain, performs reasoning over representations of human knowledge and solves problems using heuristic knowledge rather than precisely formulated relationships, in forms that reflect more accurately the nature of most human knowledge Feigenbaum (1982) defined an expert system as "an intelligent computer program that uses knowledge and inference procedures to solve problems that are difficult enough to require significant human expertise for their solution" [8]. The first diagnostic expert systems for technical fault diagnosis were developed in the early 1970's at MIT as is reported by Scherer and White (1989). Since then numerous systems have been built. Surveys of the first diagnostic expert systems of technological processes are provided by Pau (1986), Tzafestas (1989), Scherer and White (1989). After 1995 expert system applications started to decline as stand-alone systems and their technology embedded in mainstream of information technology. New expert systems started to combine symbolic with numerical information or with other artificial intelligence techniques to produce more effective systems [8, 9, 10, 11].

4.1.2. Objectives and chapter organization

This chapter is divided in many sections; the second section gives a brief review of the different types of power semiconductor devices that are used in electronic power systems and provides their basic concepts and terminology for understanding, where, we concentrate especially on the IGBT type transistor in section 3.

The fourth section treats the different fault/failure of IGBT switch in power converters which are the open-switch and the short switch faults/failures. An open-switch IGBT fault will be detailed and studied of their mechanism and consequences. Then; different detection methods for an open switch fault will be mentioned and compared in the fifth section.

Section six, starts with a brief review of the fault tolerant control strategies studied in the different pervious searches (for switch fault power converter). Among these strategies, we choose the redundancy leg switch fault tolerant control. Then, in the seventh section; an open-circuit IGBT switch fault affect has been discussed.

In section eight, a fuzzy-logic-expert system FTC strategy has been proposed to detect and isolate the faulty switch in the RSC by changing the faulty leg by the redundancy one in order to realize the safety and reliability of the system production. After that; a Genetic-algorithm adaptive PI-controller will be proposed in order to increase the performance of the rotor currents controllers and the global system control.

Finally, in section nine and the last section; a simulation of results of the proposed intelligent FTC strategy will be presented and discussed using Matlab/Simulink environment and we terminate the chapter by a brief conclusion.

4.2. Electronic devices

4.2.1. Definition

Power electronic is the technology associated with efficient conversion and control of electric power by using efficient semi-conductor devices. (Definition has been given by IEEE power electronic society) [12].

The principal aim of power electronics is the : efficient conversion, conditioning, or processing and controlling electric power using solid-state semiconductor devices in order to supply high quality power to the load like: rectifier, inverter, chopper, matrix converter, cyclo-converter, AC voltage controller...etc. Figure 4.1 shows the power processor that contains electronic devices.

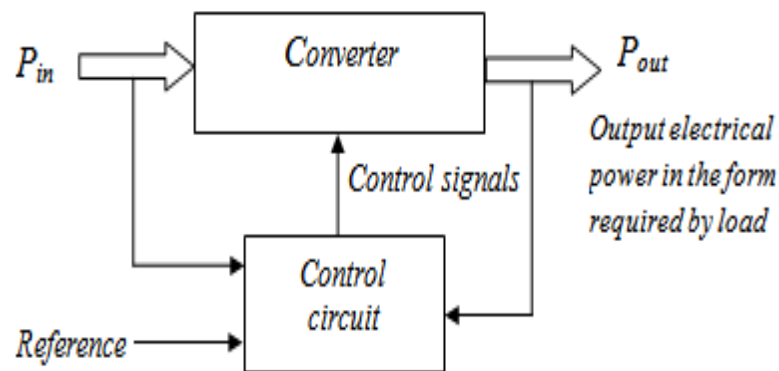


Figure 4.1 Block diagram of a power processor.

4.2.2. Classification of power electronic devices

They are classified into 3 types as follow [13]:

- **Uncontrolled device:**

It has only two terminals and cannot be controlled by control signal. The On and Off states of the device are determined by the power circuit (example of this type is: the diode).

- **Half-controlled device:**

It is turned-on by a control signal and turned-off by the power circuit (example of this type is the Thyristor).

- **Fully-controlled device:**

The On and Off states of the device are controlled by control signals; example of this type are: GTO and transistors like: BJT, MOSFET, IGBT, IGCT...etc.

4.2.3. Transistor

4.2.3.1. Definition

Transistor is a semi-conductor device which is used as a switch or amplificatory application. Generally; transistor is made of solid-state material which contains three or four terminals for connections with other components in the circuit [1, 13].

4.2.3.2 Solid-state material devices

A. Semiconductor materials

General semi-conductor materials used for transistor are Silicon (Si), Germanium (Ge), Indium (In), Phosphor (P), Arsenic (As), Gallium (Ga) Boron (B)...etc [14, 15, 16].

Silicon (Si) and Germanium (Ge) are the two most common single elements that are used to make transistors. They are both group four elements; meaning they have 4 valence electrons as shown Figure 4.2 [14, 15, 16].

In a crystal structure, each Silicon or Germanium atom is surrounded by four nearest neighbors as illustrated in Figure 4.3. A Si/Ge atom is connected to each neighbor with two dots representing the two shared electrons in the covalent band. In the absolute zero temperature, there are no free electrons to conduct electric current. However, at any other temperature; thermal energy will cause a small fraction of the covalent to break loose and can move around in a crystal [14, 15, 16].

Elemental semiconductors C(diamond), Si, Ge		13	IIIA	14	IVA	15	VA
B P-type dopant for C	B	5		C	6	N	7
	Boron	10.81		Carbon	12.011	Nitrogen	14.0067
B, Al, Ga, In P-type dopant for Si	Al	13		Si	14	P	15
	Aluminum	26.9815		Silicon	28.0855	Phosphorus	30.9738
		$3p^1$			$3p^2$		$3p^3$
Al, Ga, In P-type dopant for Ge	Ga	31		Ge	32	As	33
	Gallium	69.723		Germanium	72.61	Arsenic	74.92159
		$4p^1$			$4p^2$		$4p^3$
	In	49				Sb	51
	Indium	114.82				Antimony	121.75
		$5p^1$					$5p^3$

N, P
N-type dopant for C

P, As, Sb
N-type dopant for Si, Ge

Figure .4.2. Semiconductor materials.

The Si/Ge crystal structure takes another reaction when it contains impurity atoms such as P (Phosphor), As or Sb, the group V elements as shown the periodic table in Figure 4.2; which have a five valence electrons in each atom. In this case, the four electrons are shared with the neighboring Si/Ge atoms as shown Figure 4.4 (a). The fifth electron may escape to become a mobile electron; leaving behind a positive Sb ion. These impurities called *donors* for they donate electron. The semi-conductor containing many mobile electrons and few holes are called N-Type semiconductors.

very thin layer has been formed between the P and N layers at the PN junction that is now depleted of charge carriers and so is called the Depletion Layer [14, 15, 16].

When a this PN-junction is connected into a circuit therefore, no current can flow between anode and cathode until the anode is made more positive than the cathode by a forward potential or voltage(VF) at least sufficient to overcome the natural reverse potential of the junction as shown Figure 4.6. This value depends mainly on the materials the P and N layers of the diode are made from and the amount of doping used. Different types of diode have natural reverse potentials ranging from approximately 0.1V to 2 or 3V. Silicon and Germanium PN junction have junction potentials about 0.7V and 0.3V respectively [14, 15, 16].

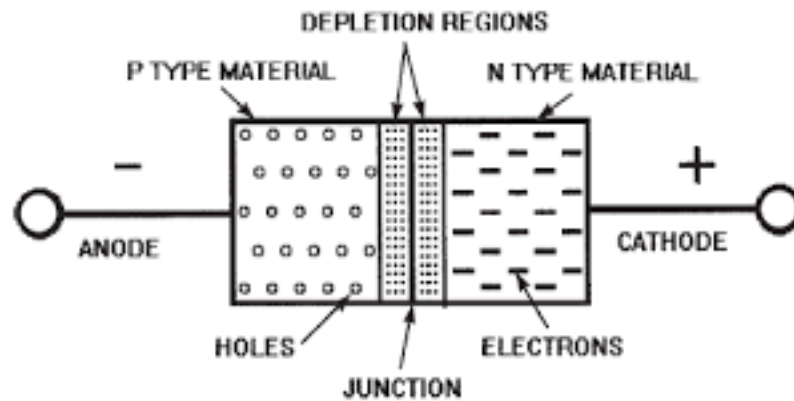


Figure 4.5. P-N junction.

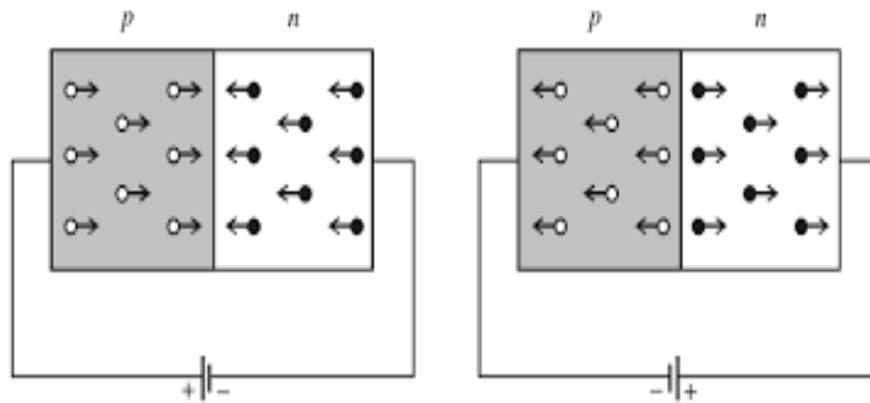


Figure 4.6. PN-junction principal work.

4.2.3.3 Transistor's Types

From the time of first transistor invention to present days; the transistors are classified depending on their structure on two categories as below [14, 15, 16]:

- Bipolar Junction Transistor (BJT).
- Field Effect Transistor (FED).

Each type of transistor has its own characteristics, advantages and disadvantages and they are divided also in other sub-categories which are illustrated in Figure 4.7.

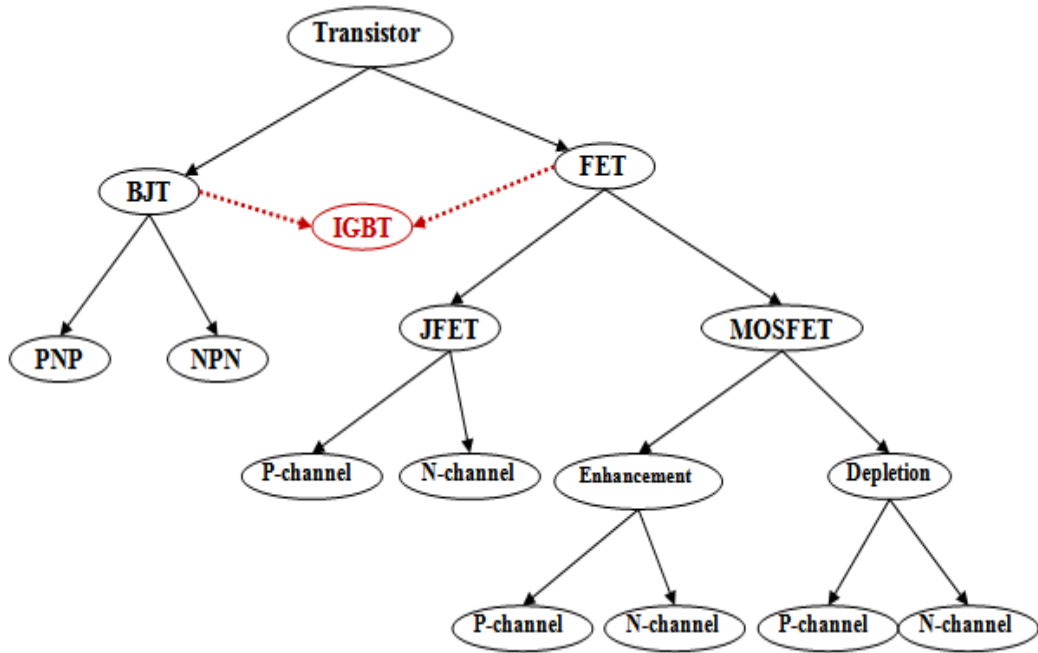


Figure 4.7. Transistor type's classification.

4.2.3.3.1 Bipolar Junction Transistor (BJT)

The BJT transistors have three terminals named Emitter (E); Base (B) and Collector (C). The name itself indicates that it has two junctions between P-type and N-type semi-conductors. The BJT transistors are classified into NPN and PNP transistors depending on its construction as shown in Figure 4.8 [14, 15, 16].

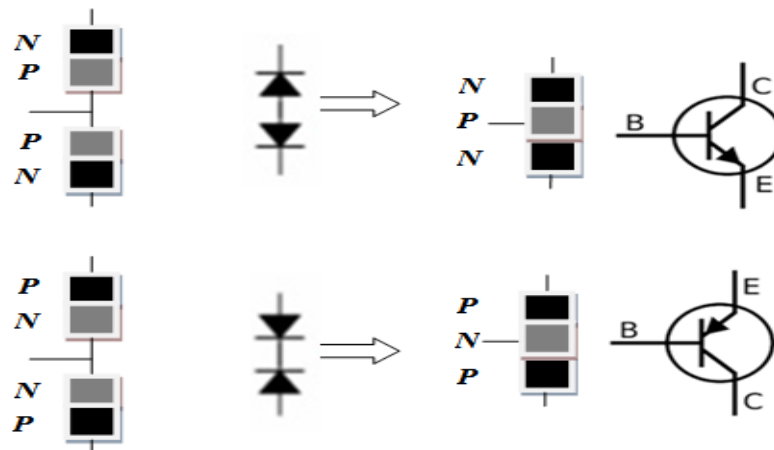


Figure 4.8. PNP and NPN Bipolar Junction Transistor.

4.2.3.3.2 Field Effect Transistor (FET)

The FET transistor is a voltage-controlled device in which current flows from the SOURCE (S) terminal (equivalent to the emitter in a bipolar transistor) to the DRAIN (D) (equivalent to the collector). A voltage applied between the source terminal and a GATE (G) terminal (equivalent to the base) is used to control the source – drain current (I_{SD}). The main difference between a FET and a BJT is that in a FET no gate current flows, the current through the device is controlled by an electric field, hence "Field effect transistor".

Depending on its structure, the FET transistor defined as unipolar transistor because the charges carriers that carry the current through the device are all of the same type i.e. either holes or electrons (electrons in N-Type channel FET and holes in P-Type FET) [14, 15, 16].

4.2.3.4. Field Effect Transistor (FET) types

Basically; the FET transistor is divided in two main types which are:

4.2.3.4. 1. Junction Field Effect Transistor (JFET)

In this type, the potential on the gate can control the channel conductivity via a reverse biased PN-Junction (also called the JUGFET or Junction Unipolar Gate FET). The JFET construction and circuit symbols are shown in Figures 4.9 and 4.10.

Figure 4.9 shows the (theoretically) simplest form of construction for N-channel Junction FET (JFET) type. It uses a small slab of N-type semiconductor into which are infused two P-type areas to form the Gate. Current in the form of electrons flows through the device from source to drain along the N-type channel. As only one type of charge carrier (electrons) carries current in N-channel JFETs type [14, 15, 16].

Figure 4.10 shows the P-channel JFET type and the principle of operation is the same as the N-channel type, but polarities of the voltages are of course reversed, and the charge carriers are holes [14, 15, 16].

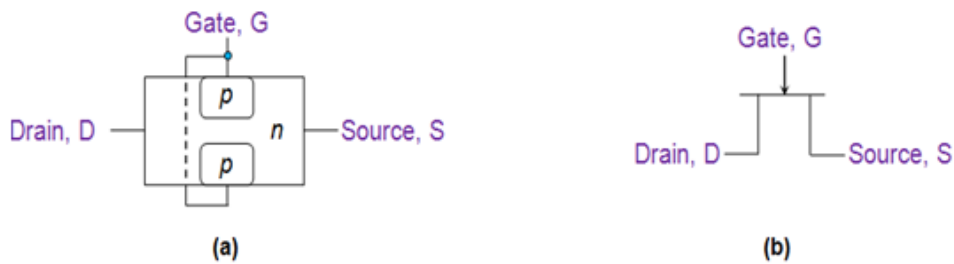


Figure 4.9. PNP Junction Field Effect Transistor



Figure 4.10. NPN Junction Field Effect Transistor.

4.2.3.4. 2. Metal Oxide Semiconductor Field Effect Transistor (MOSFET)

In the MOSFET device the gate is completely insulated from the rest of the transistor by a very thin layer of metal oxide (Silicon dioxide SiO_2). Hence the general name applied to any device of this type, is the Insulated Gate Field Effect Transistor IGFET. It's divided in two categories which are [14, 15, 16]:

- Depletion Mode MOSFET (*DE-MOSFET*).
- Enhancement Mode MOSFET (*E-MOSFET*).

a) Depletion Mode MOSFET (DE-MOSFET)

The depletion mode MOSFET shown as N-channel and P-channel devices in Figure 4.11 is more usually made as a discrete component. In this device a thin layer of N type silicon is deposited just below the gate-insulating layer, and forms a conducting channel between source and drain [14, 15, 16].

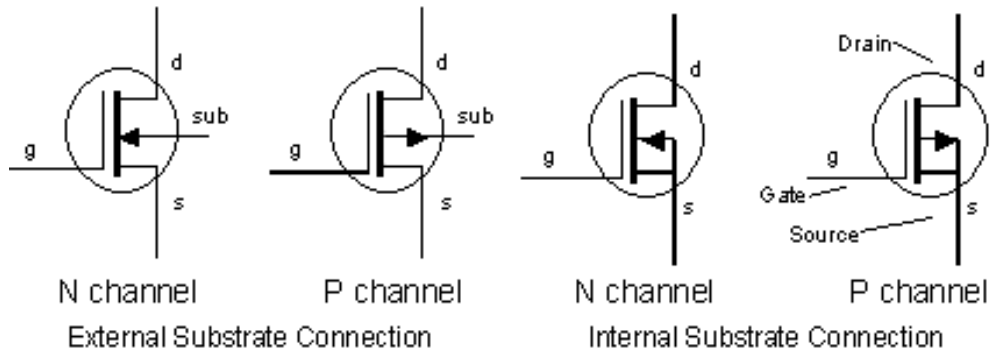


Figure 4.11. Circuit Symbols for Depletion Mode MOSFETs (IGFETs).

b) Enhancement Mode MOSFET (E-MOSFET)

Figure 4.12 depicts construction of enhancement type MOSFET. Here continuous channel does not exist from source to drain. Hence no current flows at zero gate voltage. Symbol depicts broken channel between 'S' to 'D' terminals [14, 15, 16].

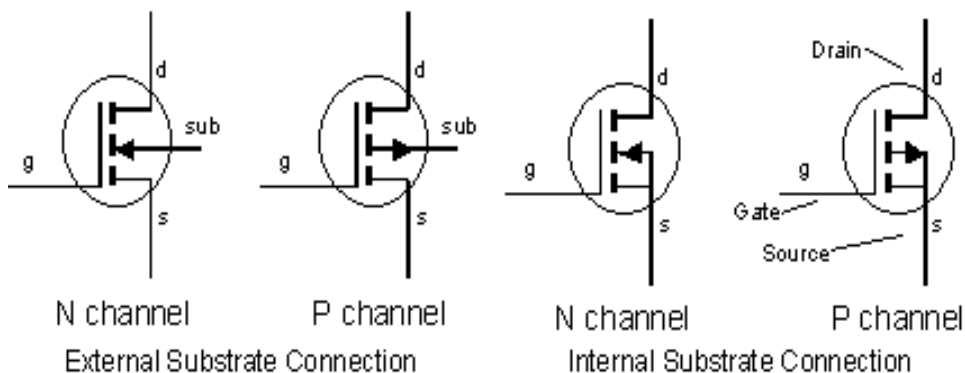


Figure 4.12. Circuit Symbols for Enhancement Mode MOSFETs (IGFETs).

4.3. Insulated-Gate Bipolar Transistor (IGBT)

4.3.1. Definition

The IGBT was first demonstrated by Baliga in 1979 [1] and then in 1980 by Plummer and Scharf [1, 13]. It was commercially introduced in the marketplace in 1983 [13]. Today; IGBT is an established replacement of the power BJT, Darling transistor, MOSFET and GTO thyristor in the medium voltage (600-2500V); medium power (10Kw) and medium frequency range up to 20 KHz.

The combination of BJT and MOSFET transistors creates a new transistor named: Insulated Gate Bipolar Transistor (IGBT) as shown Figure 4.13. Its name comes from the insulated gate (hence the first part of its

name) technology of the MOSFET with the output performance characteristics of a conventional bipolar transistor, (hence the second part of its name) [1, 14, 15].

The IGBT transistor takes the best parts of these two types of transistors, the high input impedance and high switching speeds of a MOSFET with the low saturation voltage of a bipolar transistor, and combines them together to produce another type of transistor switching device. So, it has the output switching and conduction characteristics of a bipolar transistor but is voltage-controlled like a MOSFET [1, 14, 15].

It is constructed from three terminals: Collector (C), Emitter (E) and Gate (G). Two of its terminals (C-E) (from the BJT) are associated with the conductance path which passes current, while its third terminal (G) controls the device (from the MOSFET).

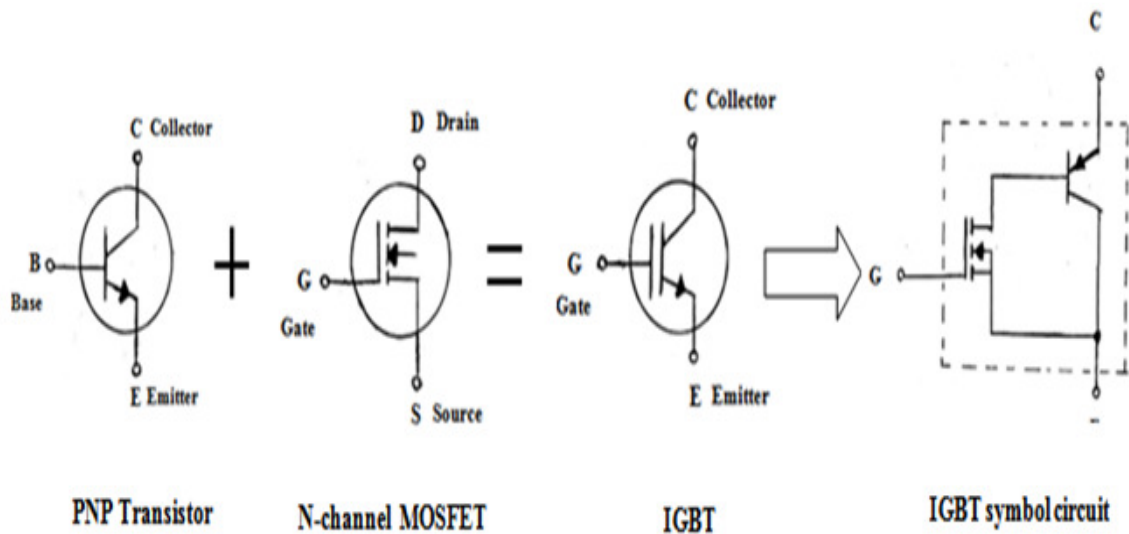


Figure 4.13. Insulated-Gate Bipolar Transistor (IGBT) structure.

4.3.2. Characteristics and applications

IGBTs are mainly used in power electronics applications, such as inverters, converters and power supplies, where the demands of the solid state switching device are not fully met by power bipolar transistors and power MOSFETs. High-current and high-voltage bipolar transistors are available, but their switching speeds are slow, while power MOSFETs may have higher switching speeds, but high-voltage and high-current devices are expensive and hard to achieve [1, 14, 15].

The advantage gained by the insulated gate bipolar transistor device over a BJT or MOSFET is that it offers greater power gain than the standard bipolar type transistor combined with the higher voltage operation and higher switching speeds (which means lower input losses) of the MOSFET as shown Figure 4.14 [1, 14, 15, 17].

These advantages make it a good choice for moderate speed, high voltage applications such as in pulse-width modulated (PWM), variable speed control, switch-mode power supplies or solar powered DC-AC inverter and frequency converter applications operating in hundreds of kilohertz range.

Because the IGBT is a voltage-controlled device, it only requires a small voltage on the Gate to maintain conduction through the device.

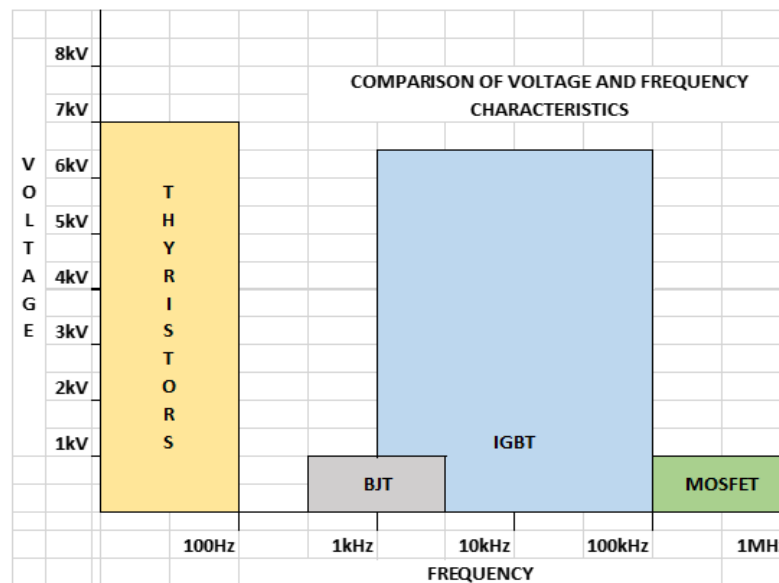


Figure 3.14. Electronic power switches classification [17].

4.3.3. Technical IGBT work

The working principle of gate drive circuits for the IGBT is like N-channel power MOSFET. The main difference is that the resistance offered by the conducting channel when current supplies through the device in its active state is very small in the IGBT. Because of this, the ratings of the current are higher when compared with a corresponding power MOSFET [15, 16].

4.3.4. IGBT switch mode fault

4.3.4.1. Fault description

Fault can be specified as an abnormal condition, defect, or an unexpected change at a component, equipment, or sub-system. It may lead to a failure or an unacceptable system performance. Here, there is a preference for using the word fault rather than failure to denote a malfunction rather than a catastrophe [18, 19].

Malfunction is defined as an unacceptable functionality in the performance of a system that can lead to a catastrophe or a hazardous situation if not recovered. Malfunction is different from catastrophe as this type of functionality can be encircled and recovered, like a failed component which can be isolated, quarantined and its performance can be substituted by those of some other components. The IFAC technical committee, as outlined in [20], makes the following definitions:

- **Fault:** an unpermitted deviation of at least one characteristic property or parameter of the system from the acceptable/usual/standard condition.
- **Failure:** a permanent interruption of a system's ability to perform a required function under specified operating conditions.

The possible most important faults in voltage-fed inverters, either with mains side diode or transistor rectifier, for drives system can be classified as following [21]:

- AC line fault, single line to ground, line to line, missing line;
- DC bus fault, earth fault, capacitor short circuit fault, voltage limiting transistor fault;
- Power semiconductor fault (transistor or diode in inverter or rectifier) short circuit or open circuit;
- DC link capacitor short-circuit fault;
- Sensor faults, ac current sensor, dc bus voltage sensor ...etc.
- Faults in the control equipment.

The percentage of these faults for a switch mode power supply calculated in many reports and mentioned that probably the high percentage for the power converter happened in a capacitor which caused by the circuit design and the high frequency application, but in general this indicates that the capacitor is to be taken into account concerning faults. Another previous report on faults of variable speed ac drives in industry from 1995, with a rougher classification shows 38 % faults in converter power part [2].

Depending on power, current, frequency and voltage, suitable semiconductor type has to be applied. According to the survey; the most used power devices for converter powers and control circuits are IGBTs. Therefore; it is worth investigating IGBTs failure and exploring the solutions to improve the reliability of IGBT power electronic converters.

4.3.4.2. IGBT switch fault classification

The failure of IGBTs can be generally classified as catastrophic failure and wear out failure. IGBT wear out failure is mainly induced by accumulated degradation with time, while catastrophic failure is triggered by single-event overstress, such as overvoltage, over-current, overheat and so on. The wear out failure under field operation could be mitigated by scheduled maintenances based on lifetime prediction and condition monitoring. However, the catastrophic failure is difficult to be predicted and thus may lead to serious consequences of power electronic converters [22, 23, 24].

The most common failures in IGBT semiconductors are short-circuit fault and open-circuit fault, each type has own mechanisms failure as shown Figure 4.15.

- ***Open circuit IGBT switch fault***

IGBT open-circuit failure can happen after external disconnection due to vibration, as well as bond wires lift-off or rupture due to high short-circuit current. It may lead to pulsating current, output current/voltage distortion, and result in secondary failure of other components after some time. Open-circuit can also be due to absence of gate drive signal. The common reasons could be the damage of components in drivers and the disconnection between driver board and IGBTs. The detailed failure mechanisms will be illustrated in the next section [25, 26].

- ***Short-circuit IGBT switch fault***

IGBT short circuit during turn-on can be caused by high gate voltage and external failure. Failure during on-state may be caused by static latch-up or the rapid increase of intrinsic temperature caused by second

breakdown, as well as by energy shocks. Failure during turn-off can be caused by dynamic latch-up and high voltage breakdown. Failure during off-state may be due to thermal runaway phenomenon [25, 26].

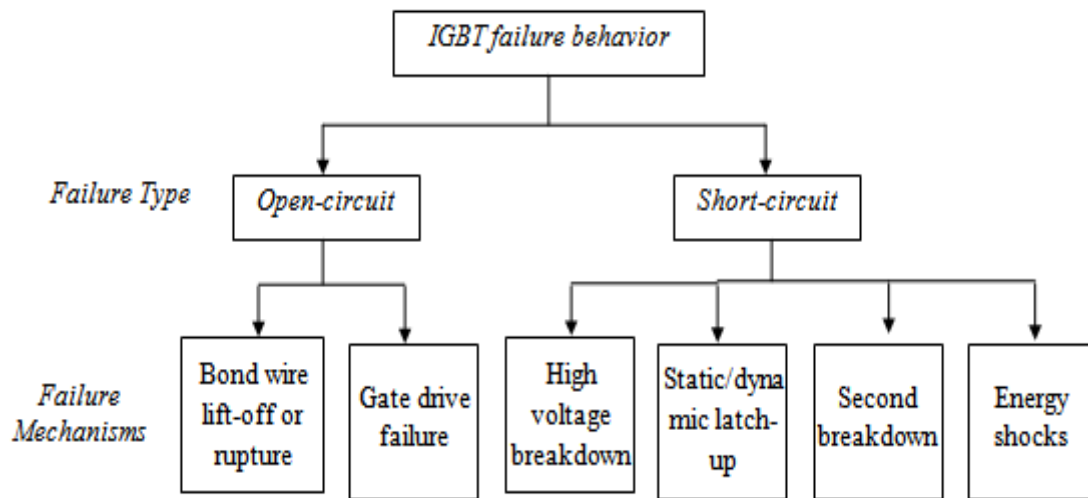


Figure 4.15. IGBT switch faults classification [24].

4.4. Open-circuit IGBT switch fault mechanisms

Power semiconductors have to be protected from non-permissible stress in every operational state. Leaving SOAs (Safe Operating Areas) leads to damage and therefore reduces component's life.

IGBT in switching applications received high electrical and thermal stress under short-circuit or turn-off switching of clamped inductive load; for instance the boost PFC circuit, which include an inductor connected in series to the collector's terminal of the IGBT. If there is a large power loss within the device due to electrical stress, much heat is generated to the limitations in packaging and due to semiconductor's thermal parameters. It would lead to thermal breakdown if this continues [25, 26].

Generally, catastrophic failure mechanisms are more related to semiconductor physics and overstress working conditions. As mentioned in Figure 4.15, there are two failure mechanisms of open-circuit.

4.4.1. Bond wire lift-off or rupture

Bond wire lift-off failure can happen after short-circuit failure. It is generally due to mechanical reasons. The main mechanisms are related to mismatch of coefficients of thermal expansion (CTEs) between Silicon and Aluminum, together with high temperature gradients. Crack initiates at the periphery of the bonding interface, and the bond wire finally lifts-off when crack propagates to the weaker central bond area. Central emitter bond wires normally fail first, and then the survivor bond wires follow. Another failure mechanism is bond wire rupture, which is slower than lift-off and usually observed after long power cycling tests [25, 26, 27].

4.4.2. Gate driver failure

There are various causes of gate driver failure, such as power stage devices (e.g. BJTs or MOSFETs) damaged; wires between drive board and IGBT disconnected. The driver failure may result in IGBT intermittent misfiring, degraded output voltage, and overstress of other IGBTs and capacitors. Abnormal

work conditions in power terminals of IGBT can also lead to driver failure. Continued narrow overvoltage spikes between collector and emitter may open the gate-emitter resistance, while over-current of IGBT's collector may lead to gate-emitter resistance degradation [16]. Gate open-circuit failure can result in thermal runaway or high power dissipation; however detailed research on the physical failure mechanism is still lacking. Moreover, modern IGBTs can work at 175°C junction temperature, which means the case temperature could reach 100°C or more, while most components in the driver cannot work normally at such high temperature. Thus this is a challenge for gate driver working at high temperature [25, 26, 27].

4.5. Open-circuit IGBT switch fault detection methods

In [6], many classifications of Fault Detection and Identification (FDI) have been presented. One obvious classification is model- and non-model-based FDI. Each type can be grouped into two major categories as shown Figure 4.16.

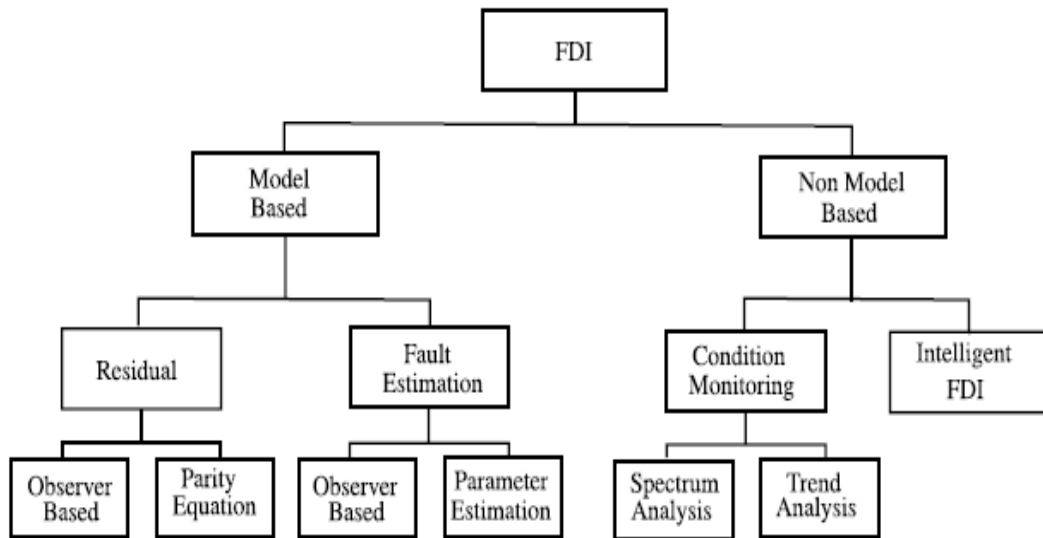


Figure 4.16. FDI classification [6].

Reference [25] has presented a comparative literature review on the existing methods for IGBT diagnostics and protection, including open-circuit, short-circuit, and gate-misfiring faults. More than 20 methods for open-circuit fault and 10 methods for short-circuit fault diagnosis have been evaluated and compared. In [2], a survey on some diagnosis methods for voltage source converters in electrical drives with induction machines is presented with respect to function and properties. Some of open-circuit fault detection methods cited in [25, 2] have been mentioned as follow:

4.5.1 Park's Vector Method

In this method, open-circuit fault detection and defect transistor localization are accomplished by calculating the position of the current trajectory's midpoint, which is the mean value of the ac current space vector over one period as presented in [28].

4.5.2. AC Current Space Vector Instantaneous Frequency

This diagnostic method for open-circuit faults is based on the instantaneous frequency. During open-circuit fault, the frequency of the current space vector is zero on the diameter of the semicircle. To detect the

fault, it is sufficient to test whether f_i is lower than a threshold. This method detects an open-circuit fault but does not isolate the faulty transistor, it is presented in [29].

4.5.3. Diagnosis by Sensing Voltage Across Lower Switch

This method is based on the fact that during open-circuit fault the voltage across the lower switch is around half the bus voltage. Normally, this voltage is either zero or full bus voltage. The detection scheme contains op-amp based voltage conditioning circuit and fault detector using flip-flops. Detection times of around 2.7 ms have been reported achieved in simulation in [30].

4.5.4. Centroid-Based Fault Detection

In this method as mentioned in [31], fault location and type are identified by determination of the centroid. The algorithms use pattern symmetry across the positive and negative α - β axes after the three-phase currents are transformed from abc to $\alpha\beta$ plane using Concordia transform. An open-switch fault is declared if a non-absolute value of the centroid is not at the origin.

4.5.5. Diagnosis by Rule-Based Expert Systems

This is an offline interactive method for diagnosis of ac drives. Basing on the input of the operator; the method advices possible causes and remedies as presented in [32].

4.5.6. Fuzzy logic Algorithm method

This is a real-time condition-monitoring algorithm that uses three-phase currents which presented in [33]. Wavelet analysis is used to identify changes or events in currents. Upon detecting a change, the dc offset of current is calculated. The polarity and value of the dc offset are fed to a fuzzy logic system to determine an open circuit or a misfiring fault. To differentiate between these faults, the duration for which the offset exists is considered.

4.5.7. Neural Network Method

In this method [34], the three-phase currents are used for fault detection and classification. Wavelet transform is applied to obtain information about the fault signatures. The variation in decomposition coefficients contains this information. Normalized approximation coefficients are fed into a back propagation artificial neural network (ANN) model to identify the faulty and healthy mode. Through simulation, a diagnosis error of less than 5% is reported.

4.5.8. ANFI System method

In this method [35], the drive dc-link current is monitored over one cycle for diagnosis. Continuous wavelet transform is applied on the fault characteristic signal and indices are derived to train the adaptive neural-fuzzy inference (ANFI) system. The fuzzy logic renders ability to build knowledge bases and the parameter adaptation enables learning of nonlinear behavior.

In our thesis, we use an Expert system method to detect the faulty open circuit IGBT switch which will be detailed in section 8.

4.6. Fault tolerant control strategy (FTCS)

4.6.1. Definition

The Fault Tolerant Control (FTC) system is a control system that can maintain system performance closely to the desirable one and preserves stability conditions, not only when the system is in fault-free case but also in the presence of faulty component, or at least ensures degraded performances which can be accepted as a trade-off. FTCS were also known as self-repairing, reconfigurable, restructurable, or self designing control systems [6].

4.6.2. Fault tolerant control classification

Broadly speaking, it is worth to note first as a general principle that whatever fault-tolerant circuit or topology adds complexity and cost to the converter, and may fail by itself. For this reason, the final reliability-level is a trade-off between enhancing fault tolerance and increasing weaknesses.

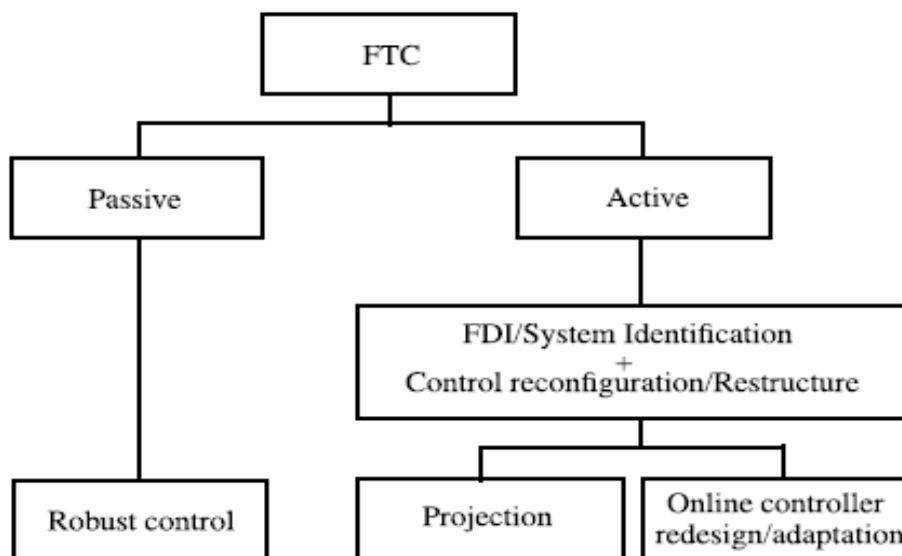


Figure 4.17. FTC classification [6].

Reference [6], classify FTC into two major groups: passive fault tolerant control systems (PFTCS) and active fault tolerant control systems (AFTCS) as shown Figure 4.17.

In reference [24], different fault-tolerant designs for IGBT power electronics at circuit level have been proposed, which are classified as shown in Figure 4.18.

Various studies on FTC are based on hardware or analytical redundancy. The hardware redundancy technique consists of switching from the failed part of the process to another achieving the same task.

In [33], a Fault Tolerant Control strategy dedicated to an active power filter which incorporates reliability analysis into the reconfigurable control structure selection with four-legs has presented.

4.6.3. Phase redundancy (Redundancy leg)

This concept consists of introducing an additional phase leg to replace a faulty phase leg, as shown in Figure 4.19. The fault tolerant control scheme is as follows: firstly, the gate driving signals of the two

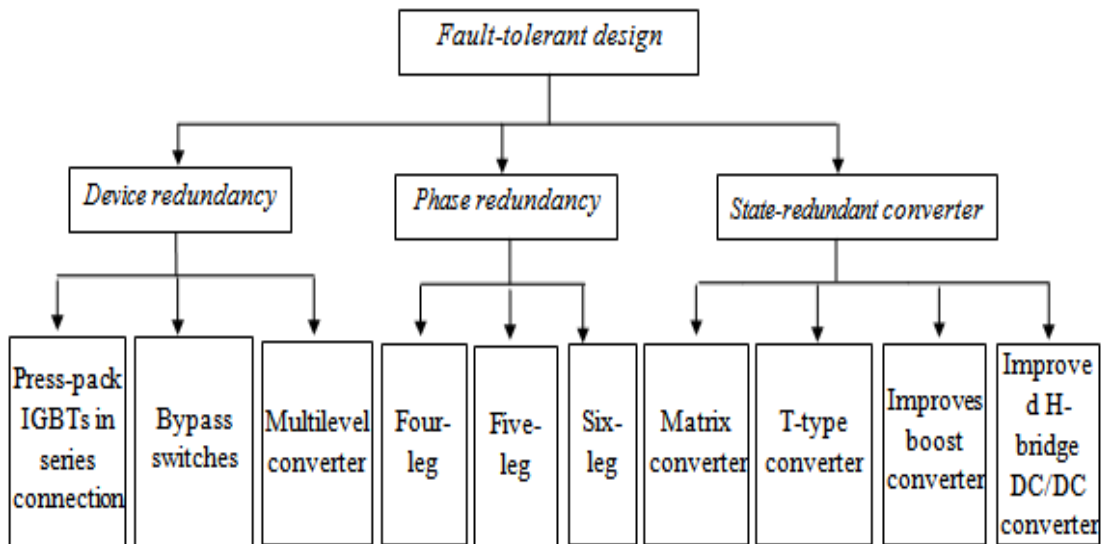


Figure 4.18. Fault-tolerant designs for IGBT power electronics [24].

switches in the faulty leg (e.g. S1 and S2) are set to be zero level; secondly, the suited bidirectional switch is triggered which are Triac (e.g. t1); finally, the two switches in redundant phase (e.g. S7 and S8) are controlled by gate driving signals to resume the role of the two switches in faulty leg. This method has been applied in three-level converters [36, 37]. Five-leg [38, 39] and six-leg converter [40] also have similar fault redundancy.

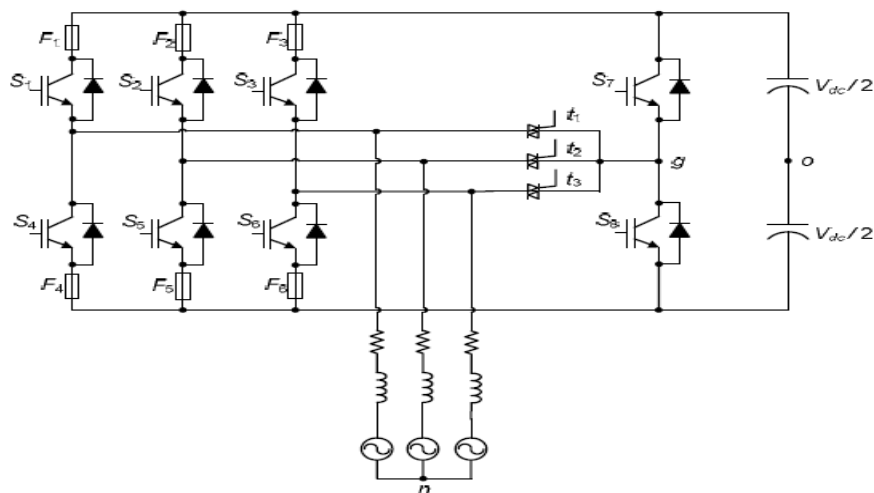


Figure 4.19. Typical phase redundant circuit.

4.6.4. Triac

The triac is similar in operation to two thyristors connected in reverse parallel but using a common gate connection as shown Figure 4.20. This gives the triac the ability to be triggered into conduction while having a voltage of either polarity across it. Either positive or negative gate pulses may be used.

Triacs are mainly used in power control to give full wave control. This enables the voltage to be controlled between zero and full power. With simple "half wave" thyristor circuits the controlled voltage only during half cycle. The triac provides a wider range of control in AC circuits without need for additional components [13].

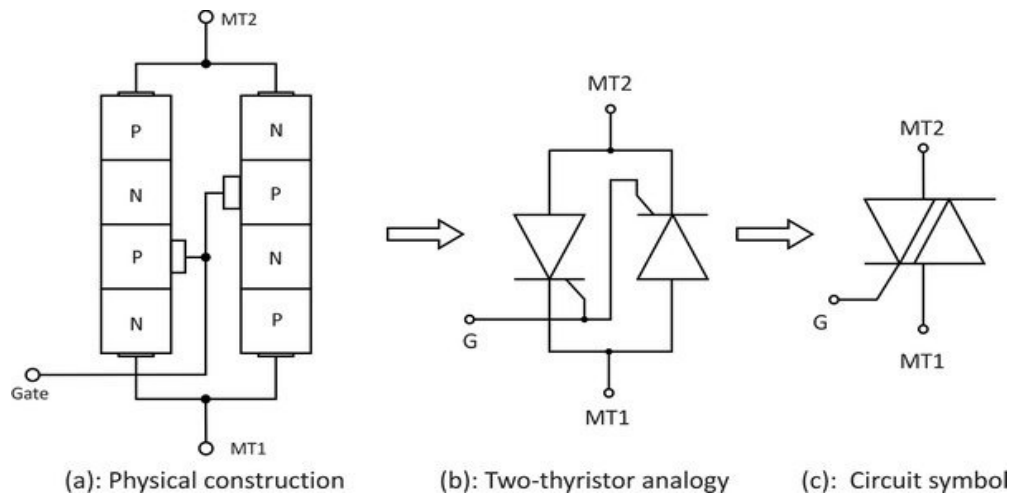


Figure 4.20. Triac Construction and Symbol [41].

4.7. Open-circuit IGBT fault switch affects for RSC in wind turbine system

The considered electric drive system is illustrated in Figure .4.21. It is composed by the parallel connection of three legs VSI, Each leg features two power switches which are controlled by the STPWM modulation. These switches were numbered as follows: assign 1, 2, and 3 for the upper switches starting by the rotor side switch and 4, 5, and 6 for the bottom switches.

Faulty switches produce unbalanced AC input currents including harmonics and distortions, which may result in severe secondary faults in the other devices. An open-circuit fault was created in the first switch $IGBT_1$ among the six RSC switches, and the simulation test is achieved for both normal operating conditions and faulty conditions.

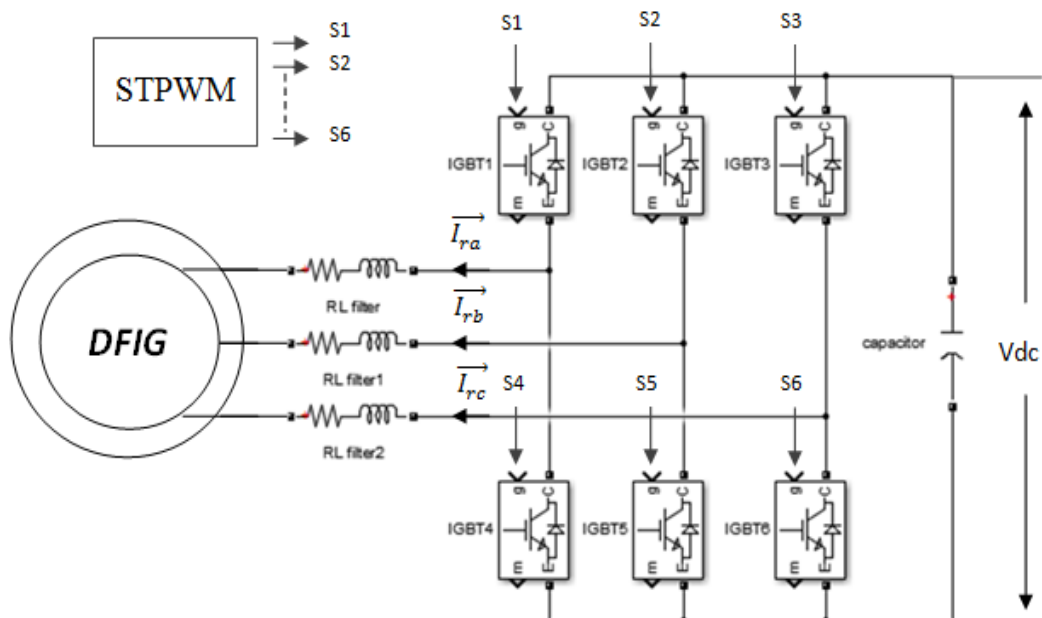


Figure 4.21. RSC topology.

The shape of the currents pattern in a healthy condition is presented in the first chapter as shown in Figure 1.38. When the fault occurred from the first switch ($IGBT_1$), the quadrature and the direct rotor side currents increased considerably and the system control has lost its stability, as shown Figure 4.22 (a). This changing

in the rotor current may be caused an aver-current consequence which increases the heat of the system's components.

Figure 4.22 (b) gives an enlarged view of the variation in the DC-link current with its average value. Off-set Figure 4.22 (c) shows the alternative rotor current and the three-phase stator currents delivered in the grid. These changing in the direct voltage and current create an unbalance voltage in the system.

These effects of the fault on the system may cause short-life equipments and an unscheduled shutdown of the device using or the deterioration of some equipment if they stay for a long time.

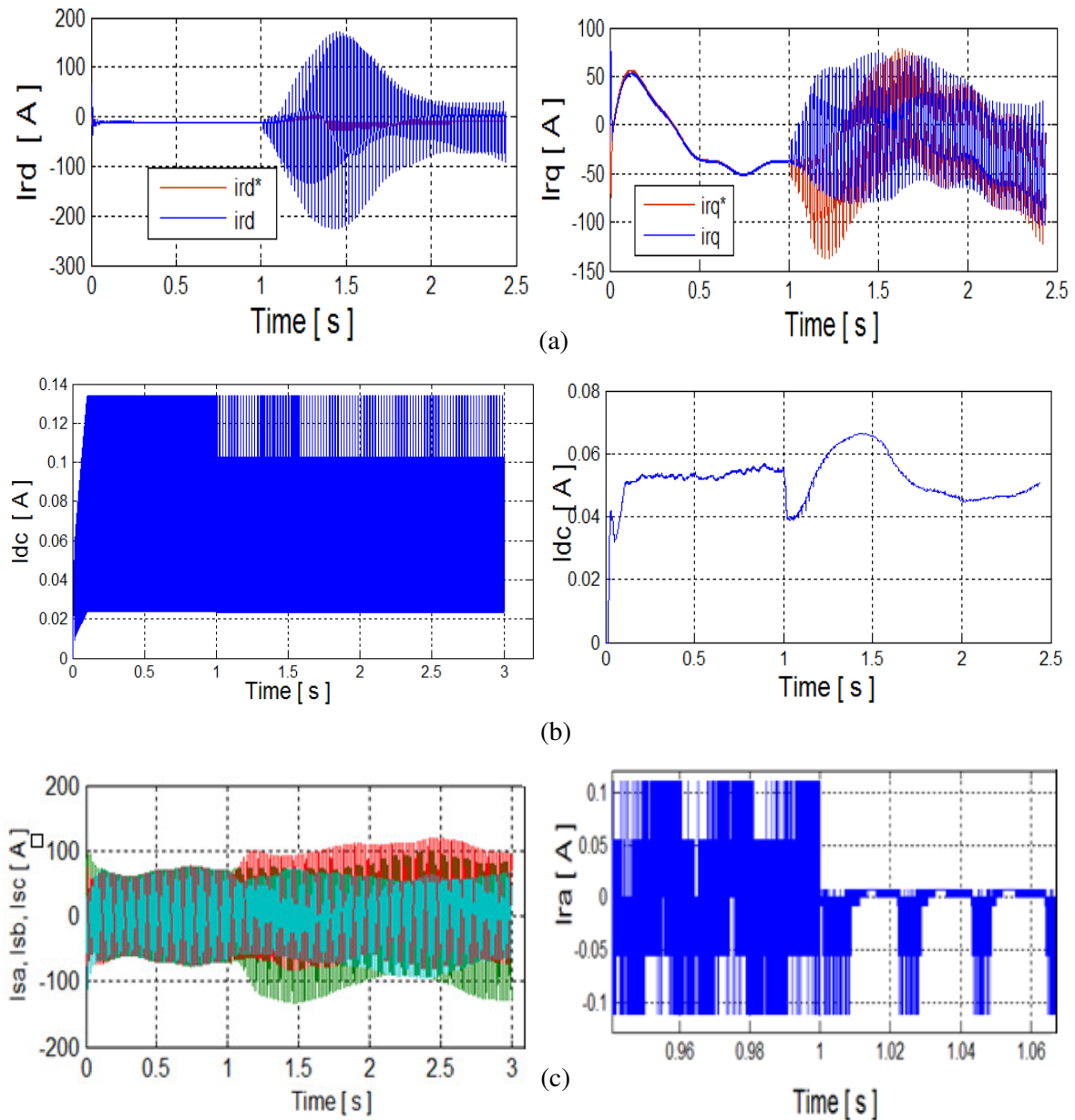


Figure 4.22. IGBT open-switch fault affect: (a) direct and quadrature rotor currents, (b) continuous current, (c) three-phase stator currents and rotor current phase.

4.8. Algorithm Genetic-Fuzzy-Expert FTC strategy of Open-circuit IGBT switch for RSC in wind turbine system

4.8.1. Fuzzy-Expert system Fault tolerant control of IGBT open switch fault in RSC

Fault diagnostics in industrial plants are possibly the most popular and earliest applications of Expert System programs. An experienced engineer can detect and diagnose the circuit faults by checking the voltage/current measurements and operating performance of the drive system.

However, not only are such experts expensive and scarce, they cannot perform continuous on-line monitoring of the system. The knowledge base of the expert system consists of the data base and rules. The data base is facts and information about set values and characteristics of parameters, and component interconnection. Expert systems contain a knowledge base with heuristic skill obtained from a reasoning methodology of a human expert. Account of past experience in fault diagnosing along with normal working conditions obtained from steady state measurements, simulation and statistical data are programmed in the knowledge base. The inference engine with the help of the production rules deduces appropriate steps to be taken from the facts and objects relationships in the knowledge base [9].

Figure 4.23 shows the FTC strategy proposed in this work. It is simple and allows the system to operate without interruption after the occurrence of a switch fault. The proposed strategy uses a redundant-phase as an additional phase leg to replace a faulty phase leg.

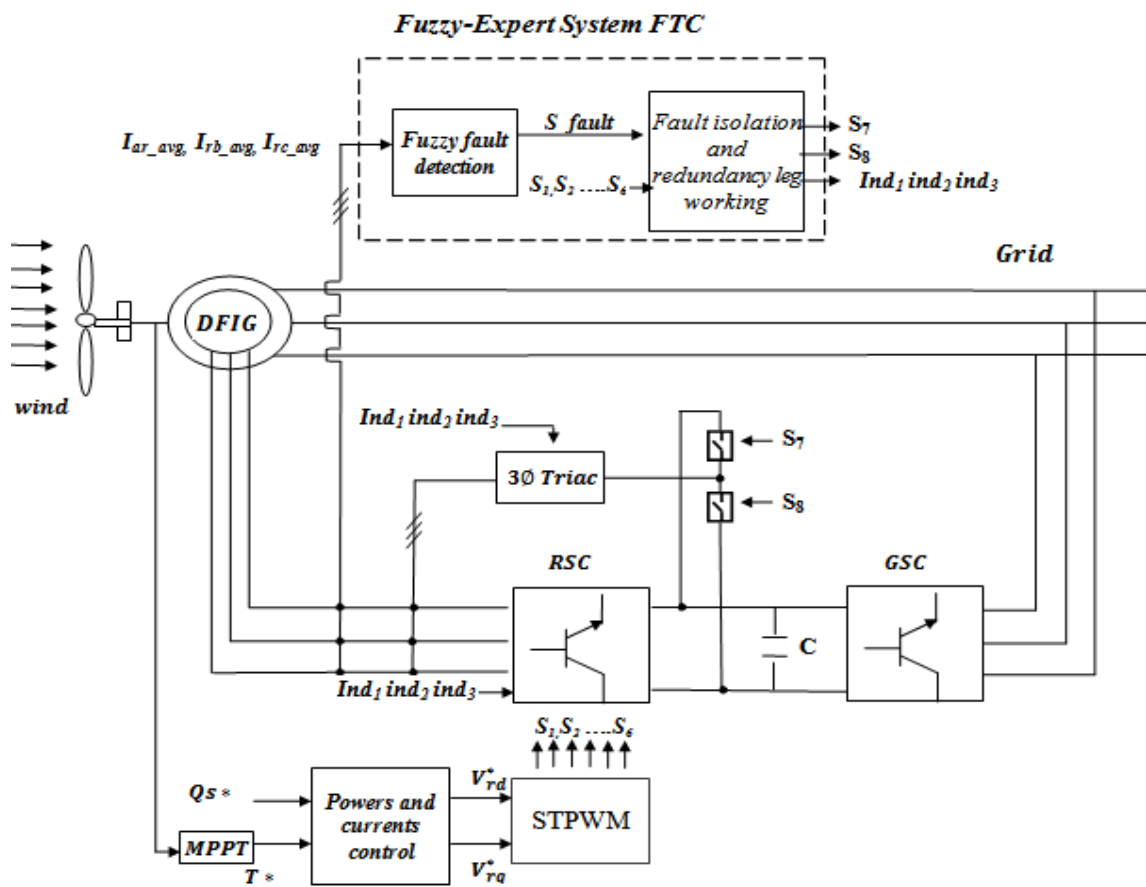


Figure 4.23. Fuzzy-Expert system Fault tolerant control for RSC open switch fault schema.

In order to realize this strategy in a RSC drive we need; the three-phase AC rotor side current values which have been measured by three current sensors, IGBT gate drive logic signals, TRIAC gate drive logic signals, these data can be sensed and fed to a control circuit to embed the diagnostic program.

The first step is the calculation of the three-phase currents average values of the RSC side which provide an indication on the status of the system. Under healthy conditions, these values are ideally equal to zero. However, when a fault occurs in the converter switch, these values are no longer equal to zero.

4.8.2. Fuzzy open switch fault detection method

Figure 4.24 represents the average values of three-phase RSC currents. In the healthy condition, the average values of the currents are almost zero (between $\pm 2 \times 10^{-4}$). However, under fault conditions, they assume other values. Table 4.1 shows the mean values of the three-phase rotor currents codes for the six switches when there are an open-circuit fault has occurred. In the table, When the average rotor current increases above the threshold value of 6×10^{-4} A the output of the detector is 1, when it decreases below the threshold value of -2×10^{-4} A the output of the detector is -1 and when they assume a values between $\pm 2 \times 10^{-4}$ A (healthy condition) the output of the detector is 0.

These reactions of average values of rotor currents are taken as knowledge bases for the proposed expert system.

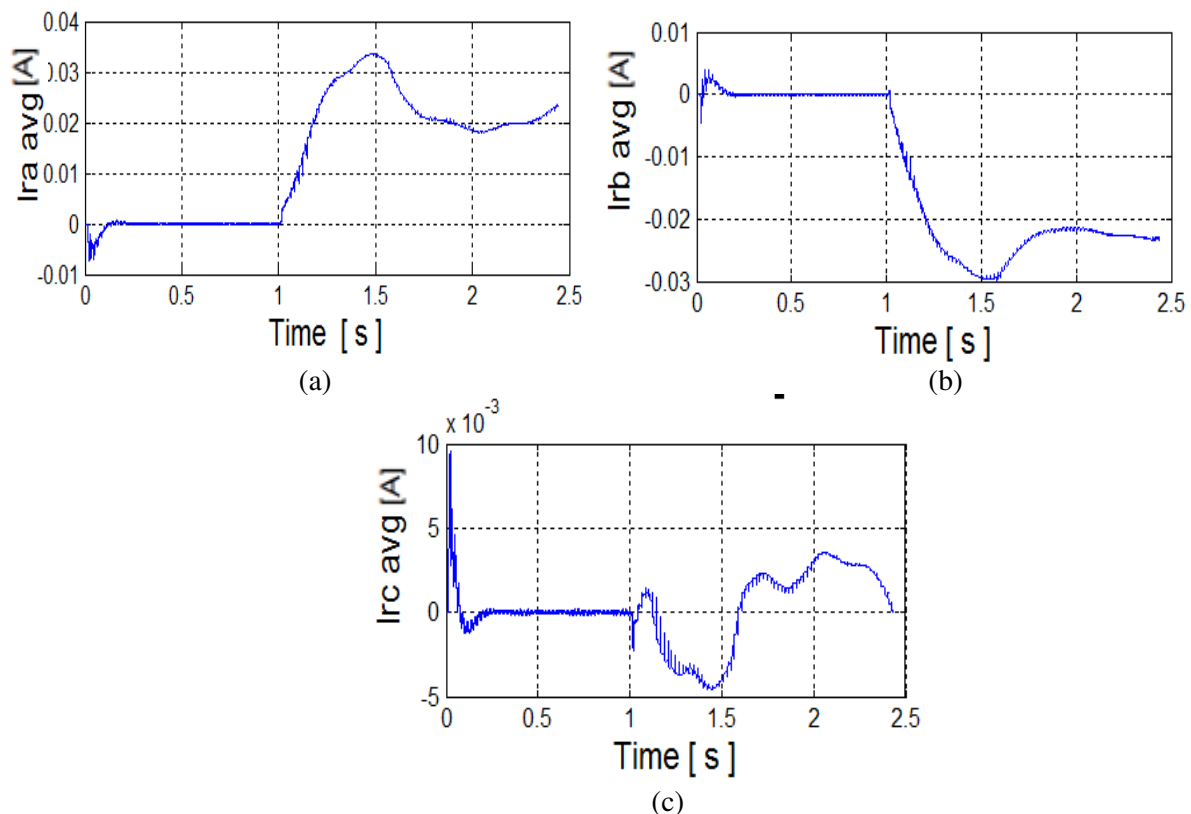


Figure 4.24. Three-phase rotor current average values of rotor side converter.

The waveforms of the 3-phase current average values for all switches fault are studied by experience then represented in Table 4.1.

Table 4.1 Average values of three-phase currents under different open switch fault

I_{ra_avg}	I_{rb_avg}	I_{rc_avg}	Combination	Switch fault
1	-1	-1	1	S1 fault
-1	-1	1	2	S2 fault
-1	1	-1	3	S3 fault
-1	1	1	4	S4 fault
1	1	-1	5	S5 fault
1	-1	1	6	S6 fault
0	0	0	0	No fault

Based on Table 4.1, the flowchart of Figure 4.25 is derived which will simplify the synthesis of the fuzzy logic fault detection method.

The fuzzy sets are designated by the labels:

- S: small when the rotor current mean value takes value equal to -1 (negative),
- Z: zero, when the rotor current mean value takes value equal to 0 (zero),
- P: positive, when the rotor current mean value takes value equal to 1 (positive).

Table 4.2 shows the rules of fault detection. The membership functions for the input variables which present the average values of rotor current I_{ra} , I_{rb} , I_{rc} and the output variable which presents the faulty switch and its surface and rules viewer are shown in Figure 4.26. Sugeno-type fuzzy inference system was used and defuzzification was based on the centre of gravity method.

Table 4.2. Rules of the fuzzy logic-based open switch FDM

I_{ra_avg}	I_{rb_avg}	I_{rc_avg}	Number switch fault	Switch fault
P	S	S	1	S1 fault
S	S	P	2	S2 fault
S	P	S	3	S3 fault
S	P	P	4	S4 fault
P	P	S	5	S5 fault
P	S	P	6	S6 fault
Z	Z	Z	0	No fault

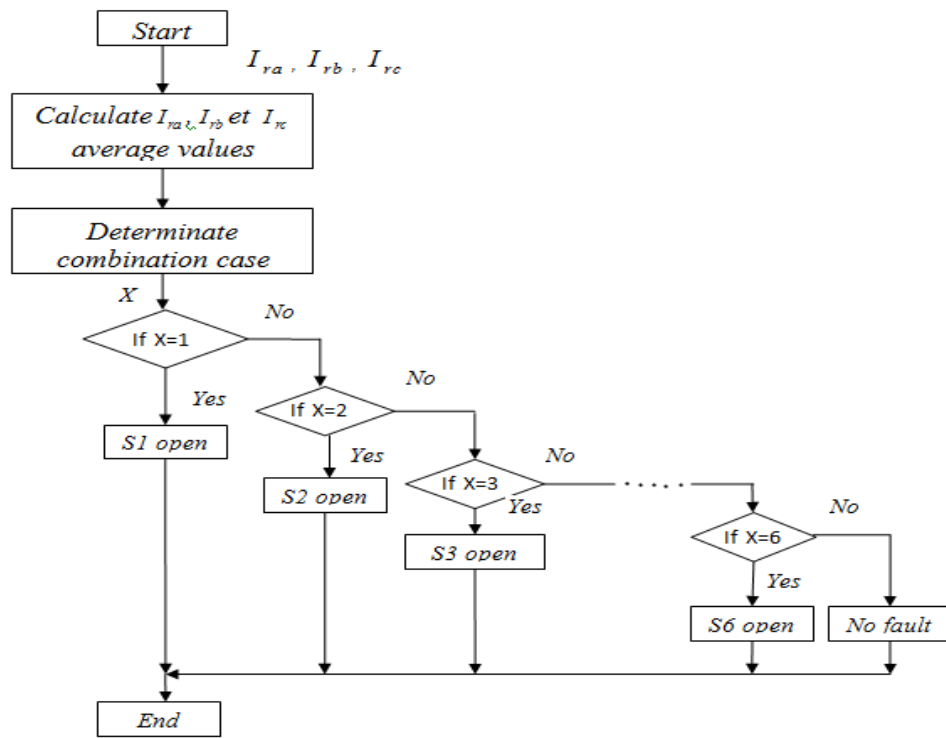


Figure 4.25. Flowchart of the expert system-based open switch FDM.

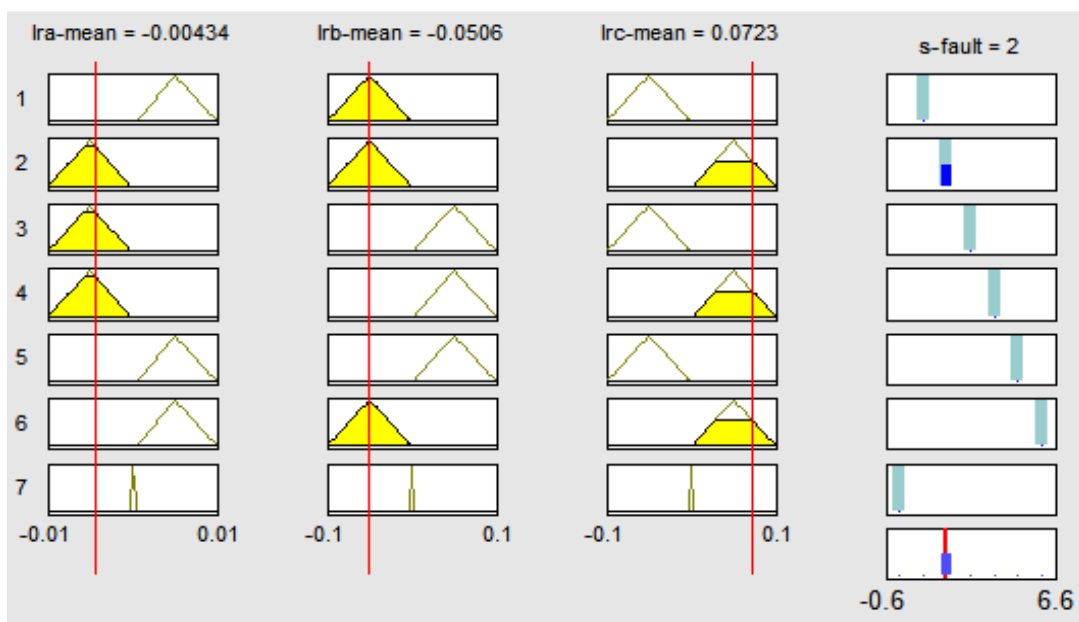
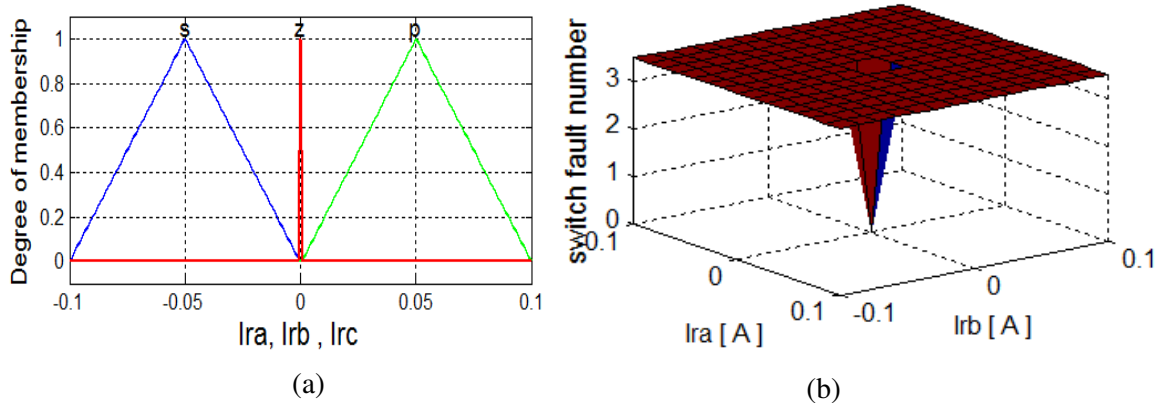


Figure 4.26. (a) Membership functions of the input variables (b) Output surface (c) Rule viewer.

4.8.3. Expert system Fault tolerant control for RSC

After the fault is detected and in order to avoid any subsequent failure in the other devices, the faulty switch must be isolated and replaced with a healthy one. As shown Figure 4.27, the converter circuit has an additional leg which contains two switches numbered S7 and S8. The redundant leg is connected to both the DC side and to the rotor side phases via a three-phase Triacs circuit (Triac1, Triac2 and Triac3).

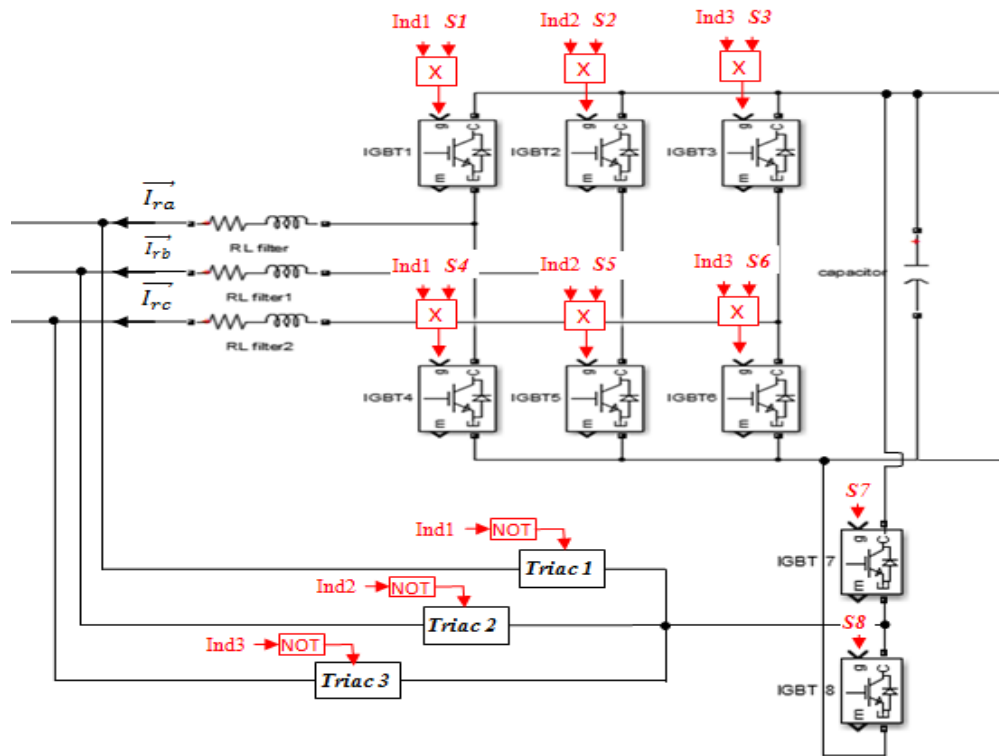


Figure 4.27. Redundancy leg of the FTC strategy.

The faulty leg is replaced by the healthy leg by changing the three indices (Ind1, Ind2 and Ind3) and the status of switches S7 and S8 based on the detected faulty switch and the status of the six switches (S1, S2, ..., S6). The three indices take the value 1 when there is no switch fault. Ind1 = 0, if the faulty switch is either the 1st or the 4th switch, Ind2 = 0 if the faulty switch is either the 2nd or 5th switch and finally, Ind3 = 0, when the faulty switch is either the 3rd or the 6th switch.

Example:

- IF (S-fault=0). THEN; (ind1=1, ind2=1, ind3=1, S7=0 and S8=0).

This means that the system works in the healthy condition, no fault has detected and the additional leg doesn't work.

- IF (S-fault=1). THEN; (ind1=0, ind2=1, ind3=1, S7=S1 and S8=S2).

This means that the faulty switch is IGBT1; in this case the first leg (which contains IGBT1 and IGBT4) must be changing by the additional leg (which contains IGBT7 and IGBT8). This step is realized by the changing of the Ind1 from 1 to 0 which permits the changing of the signals switches from the first leg to the additional leg, and so on (it's the same idea for the other cases) as shown flowchart in Figure 4.28.

Detection of the faulty leg;

- Removing the control orders of the two drivers of the faulty leg;
- Triggering the suited bidirectional switch (TRIAC) ;
- Using the control orders of the faulty leg for the redundant one;
- Stopping the fault detection algorithm.

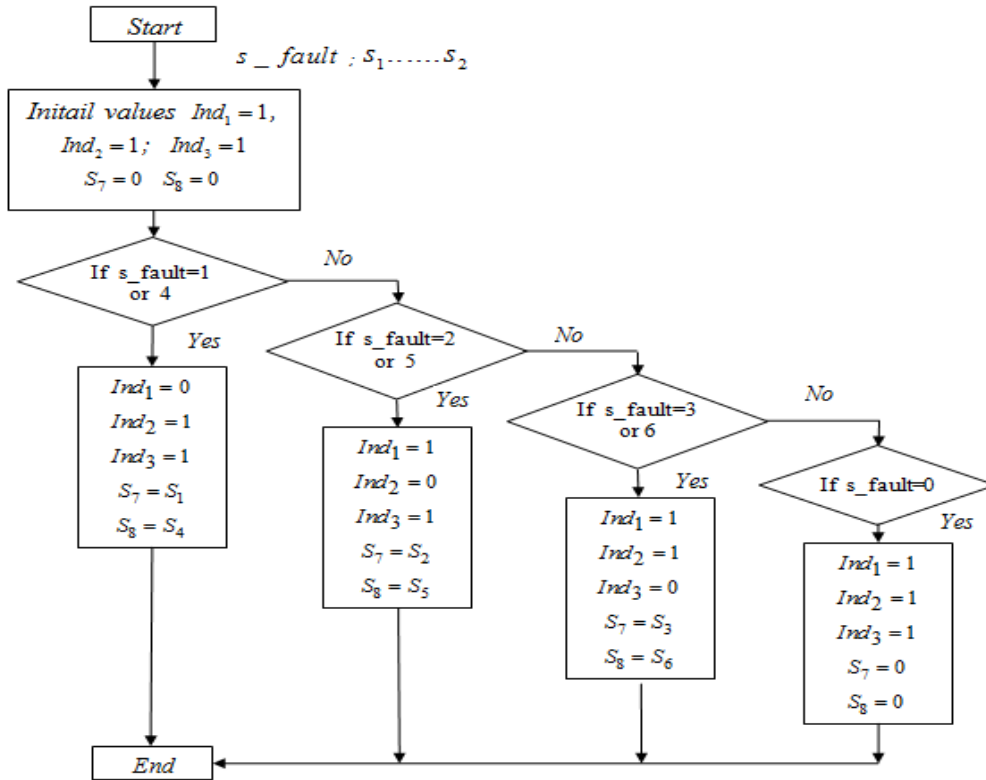


Figure 4.28. Flowchart of the FTC strategy.

4.8.4. GA-PI rotor currents controllers

A Proportional-Integrator regulator is used to control the stator active power in order to obtain the maximum power as delivered by the MPPT control strategy. The two others regulators (PI-AG) are used to control the direct and quadrature rotor currents and they are tuned using a GA-optimization technique as shown Figure 4.29.

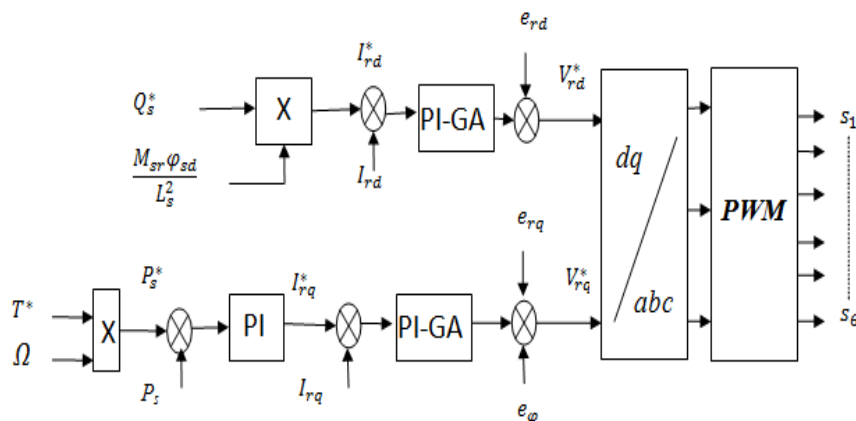


Figure 4.29. Rotor side converter control system.

The GA operations of selection, crossover and mutation are described by the flowchart as shown Figure 4.30.

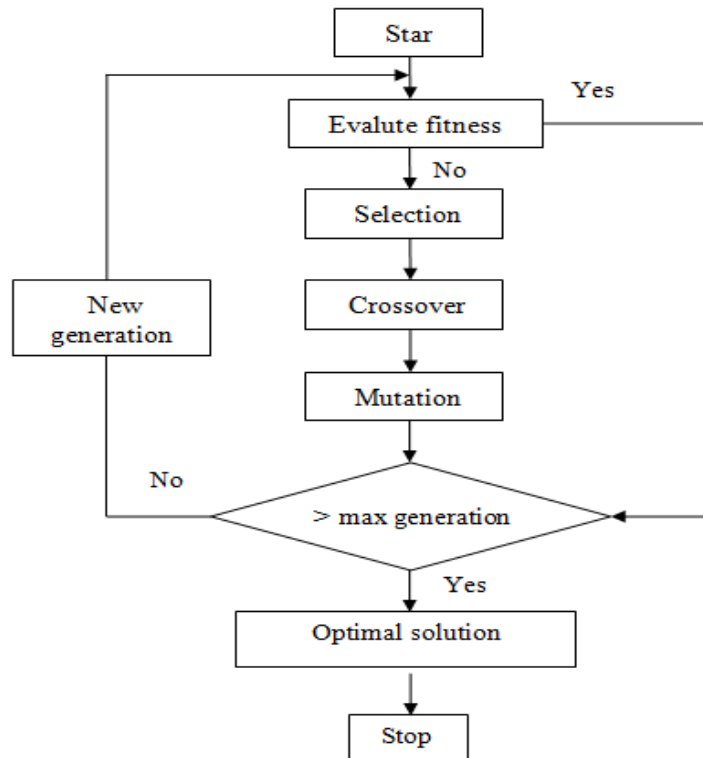


Figure 4.30. Flowchart of the GA optimization technique.

The GA parameters used in this work are listed in Table 4.3.

Table 4.3. GA parameters used in the model

Population size	80
Variable bounds	[0.40 ; 0.40]
Max no of generation	100
Tolerance	1e-6
Performance index/ fitness function	Mean square error
Probability selection	0.08
Crossover method	Arithmetic crossover
Mutation operator	Multi Non uniformly distributed
Probability of mutation	0.1%

4.9. Simulation results

The wind speed value is about 7m/s as shown Figure 4.31 (a). The wind energy must be maximum absorbed by the system to achieve a maximum power using MPPT control which delivered the reference torque from the rotor speed controller as shown Figures 4.31 (b) and 4.31 (g) respectively.

Figures 4.31 (c) and 4.31 (d) show the active and reactive powers measurements with their reference values. Figures 4.31-e and 4.31-f show the direct and quadrature rotor currents controlled by the GA-

optimized PI controllers. As we can see, the fault switch is happened at time equal to 1 second, where an impulsive is appeared for a short time in the both of rotor currents and stator powers responses as a reaction of the FTC strategy which forced the powers and currents to follow their references after the switch fault.

Figure 4.31-h shows the DC link voltage regulation at 800 V for grid side converter. As we can see, this voltage doesn't affect with the faulty switch.

Figure 4.32 and Figure 4.33 show the response of the direct and quadrature rotor currents with GA-optimized and conventional PI controllers comparison respectively. GA-based PI controllers give a better transient response than the conventional counterpart in terms of response time and overtaking.

Figure 4.34 presents GA-based PI controllers' tuned gains K_p and K_i .

Figure 4.35 shows open switch fault detection power converter response, where the fault has been detected on the second switch for detection time equal to 0.016 s.

Figure 4.36 shows the three indices responses (ind1, ind2, ind3); these indices permit to activate the Triacs to isolate the faulty leg and change it by the additional one. When the fault had occurred in the second switch; the ind1 changes from 1 status to 0 in order to isolate the second faulty leg from the system. However, the other indices state in their initial values (which are 1).

Figure 4.37 shows a succor leg switches signals (s_7 , s_8). These switches had no signals in the healthy condition once the fault occur in the converter, they takes the signals of the faulty leg and is working instead of it.

These indices and switches are changing according to the faulty switch detection via a FTC algorithm strategy to ensure service continuity.

Figure 3.39 shows the average rotor current values before the open switch fault and after the replacement of the faulty leg via the triacs circuit.

Figure 4.38 shows another switch faults detection for first, second and third switches (S1, S2, S3), the detection time is not the same for the three detection. For example, time detection in S1 fault equal to 0.013s (Figure 4.38 (a)), for the second fault switch equal to 0.015 (Figure 4.38 (b))and for the third switch fault equal to 0.005s (Figure 4.38 (c)). as, we see for the three fault switches, the detection time is less than one period.

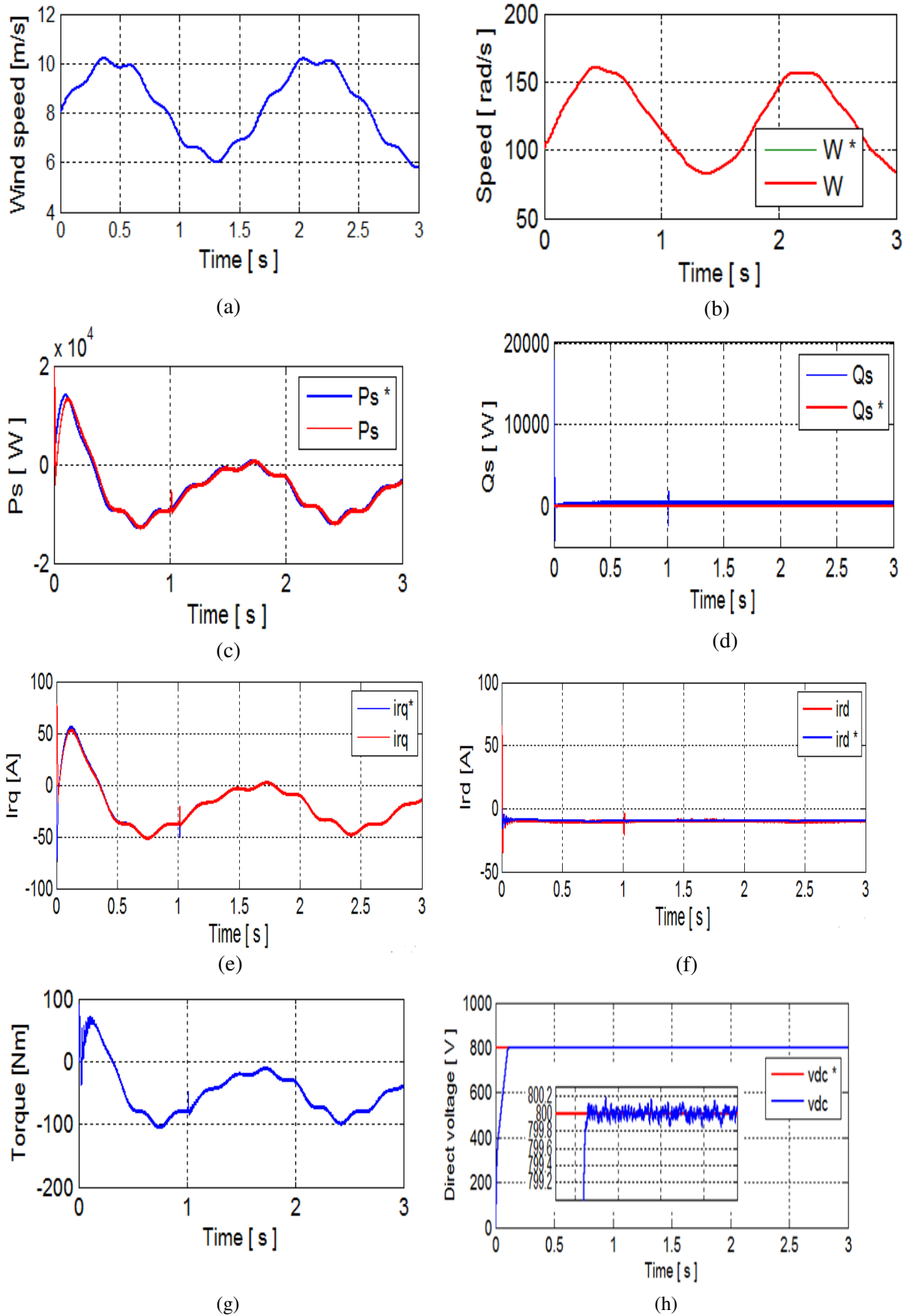


Figure 4.31. (a) Wind speed (b) Speed of DFIG with MPPT, (c) active stator power P_s (d) reactive stator power Q_s , (e) direct rotor current I_{rd} (f) quadrature rotor current I_{rq} , (g) Torque, (h) DC-link voltage V_{dc} .

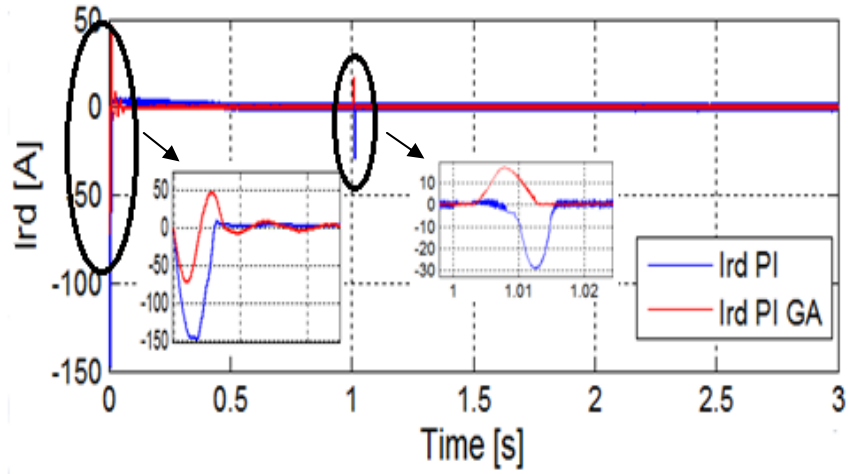


Figure 4.32. Direct rotor current: Comparison of GA-tuned PI controller and conventional PI controller.

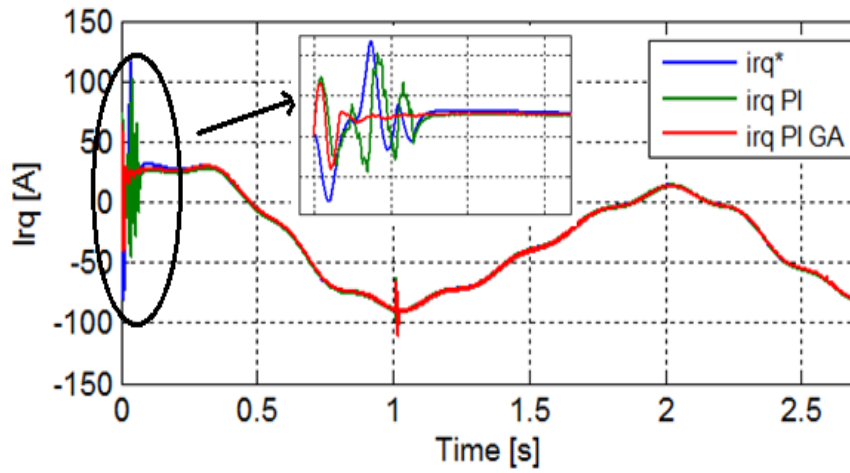


Figure 4.33. Quadrature rotor current: Comparison of GA-tuned PI controller and conventional PI controller.

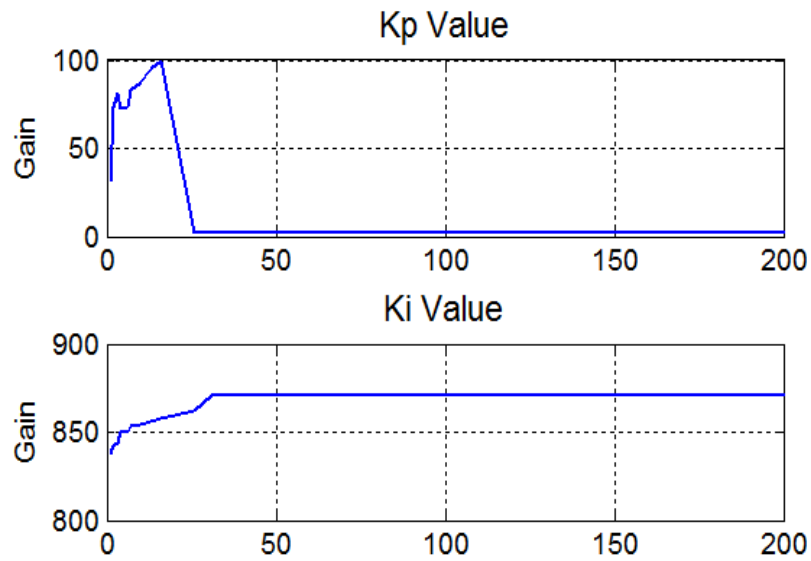


Figure 4.34. GA-based PI controllers gains K_p and K_i .

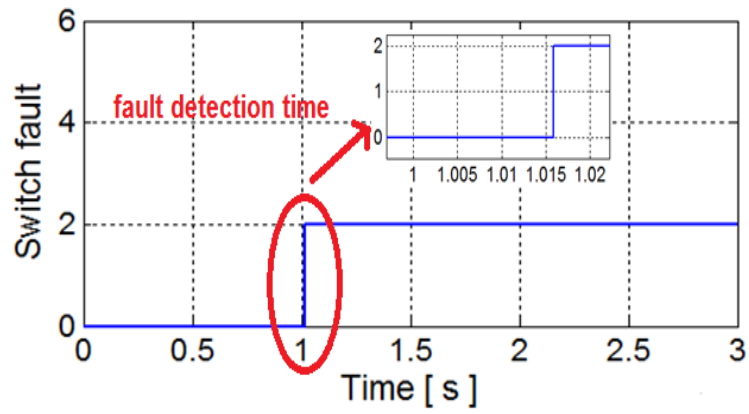


Figure 4.35. Fuzzy logic open switch fault detection (for second switch fault S_2).

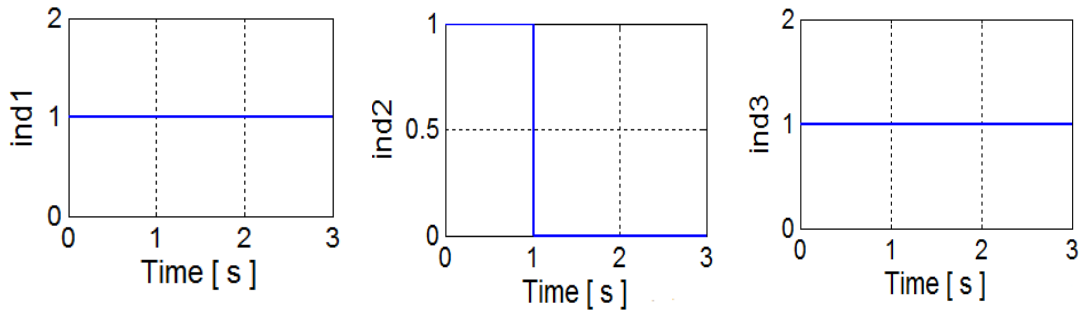


Figure 4.36. Indices $ind1$, $ind2$ and $ind3$.

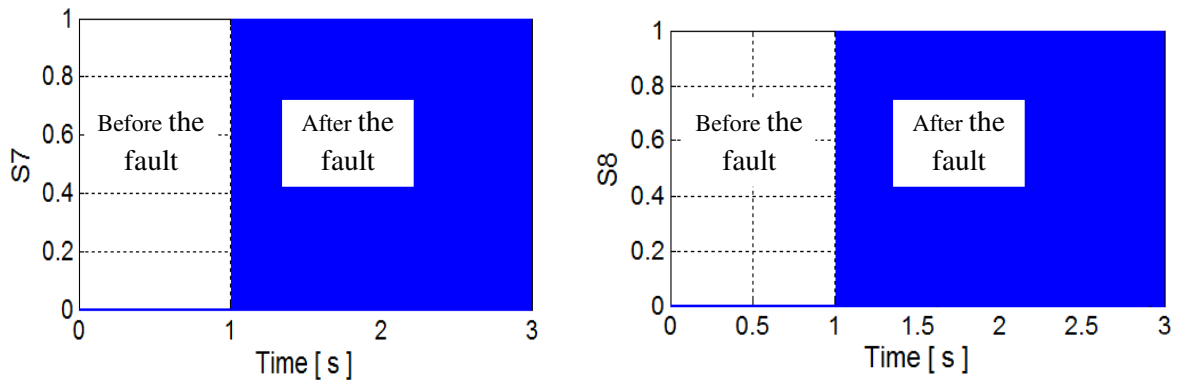


Figure 4.37. Redundant leg switching signals.

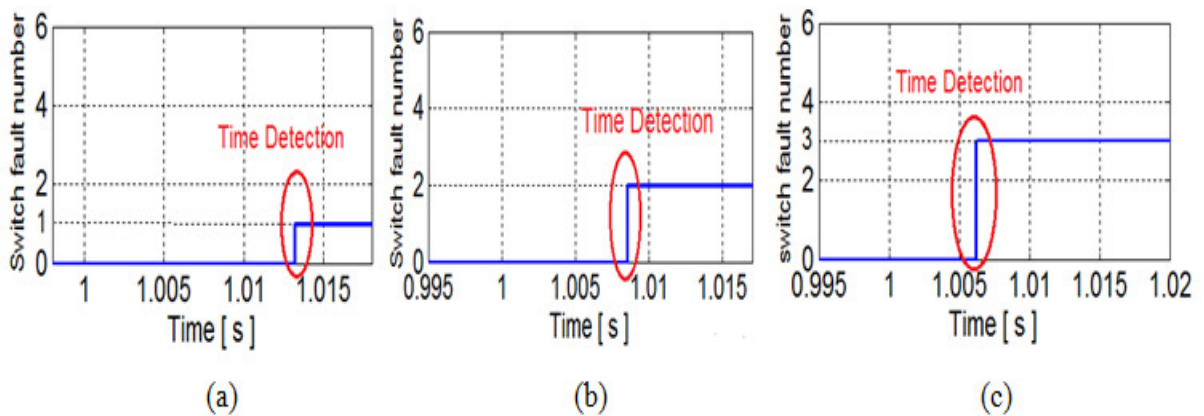


Figure 4.38. Time detection for three switches: (a) S_1 , (b) S_2 , (c) S_3 .

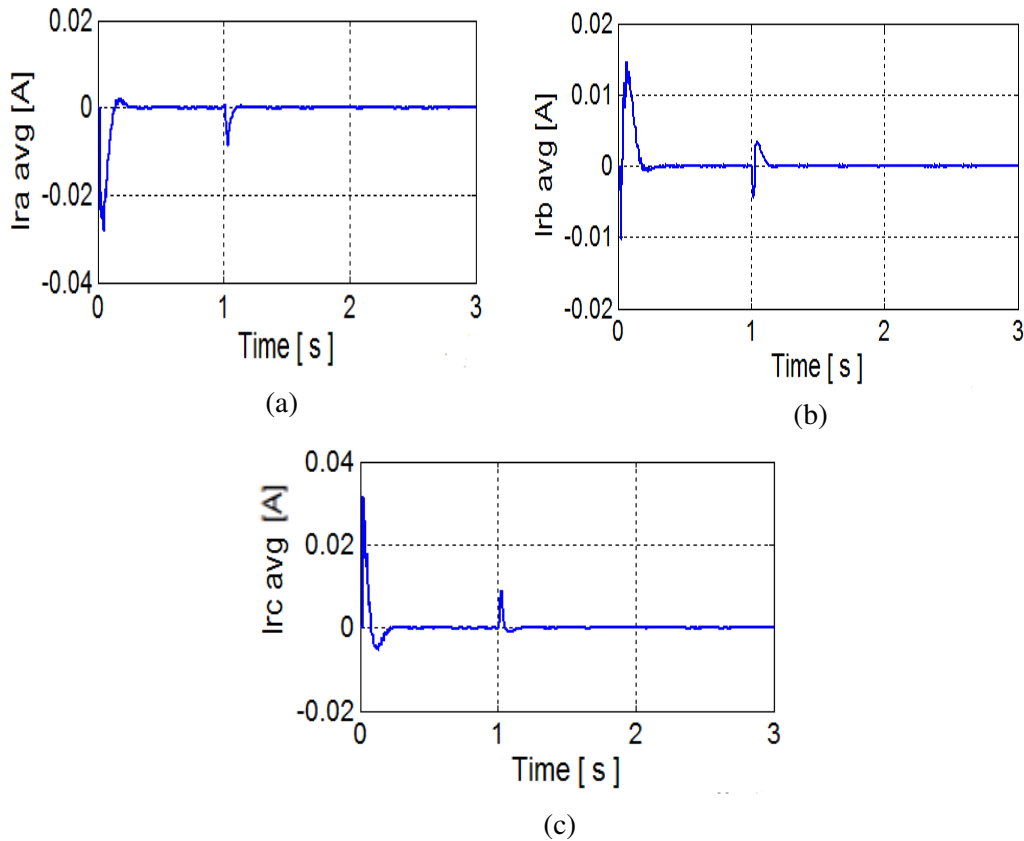


Figure 4.39. Three-phase RSC currents average values.

4.10. Conclusion

Catastrophic failure of IGBT is fairly important issues both in design phase and in operation phase of power electronic converters. In this chapter, a Fuzzy-Expert system Fault Tolerant Control strategy has been proposed for open-circuit IGBT fault switch of RSC converter in DFIG based wind turbine system.

Firstly, a brief review of the different types of power semi-conductor devices that are used in power electronic systems. The devices covered include the BJT, MOSFET and IGBT transistor. Power semi-conductor devices constitute a vast and complex subject and technology is going through continuous evolution. Within the scope the chapter, we only gave brief descriptions, characteristics and applications of IGBT used in our system.

According to a survey, semiconductor failure and soldering joints failure in power devices take up 34% of power electronic system failures. Therefore, IGBT fault has been discussed for open-circuit and short-circuit fault, and it's mainly detailed for open-circuit IGBT switch fault and its mechanism in RSC converter and their consequences in the global system.

Various detection methods have been mentioned in this chapter with a brief description about their principals with and without model-based. Among the detection methods without model-based, there are intelligent FDI methods which are: Diagnosis by Rule-Based Expert Systems, Fuzzy logic Algorithm method, neural Network Method and ANFI System method. In order to ensure service continuity, an intelligent FTC strategy with four-leg redundancy has been proposed.

The FTC proposed based on the Expert system methodology using Fuzzy logic in the fault detection method. An experienced engineer creates the algorithm detection and isolation of the faulty switch to transfer his expert to the system which can use it after by the technician easily.

This algorithm permits to change the faulty leg of the RSC converter by the additional leg (the fourth leg) and isolates the faulty leg from the system to realize the reliability and the service continuity.

The simulation results was showed that the proposed FTC strategy is very efficient and detects the faulty switch within time less than one period which allows the deterioration and prevents the deterioration and the shut-down of the production power quality.

4.11. References

- [1] Bimal K. Bose, “*Bose-Modern power electronics and AC drives*”, book, Prentice Hall PTR (2002).
- [2] Friedrich W. Fuchs, “*Some Diagnosis Methods for Voltage Source Inverters In Variable Speed Drives with Induction Machines A Survey*”, Conference: Conference: Industrial Electronics Society, 2003. IECON '03. The 29th Annual Conference of the IEEE, Volume: 2.
- [3] E. Wolfgang, “*Examples for failures in power electronics systems,*” presented at *ECPE Tutorial on Reliability Power Electronic System*, Nuremberg, Germany, Apr. 2007.
- [4] F. W. Fuchs. “*Some Diagnosis Methods for Voltage Source Inverters In Variable Speed Drives with Induction Machines A Survey*”. IEEE Industrial Electronics Conference, Roanoke, Virginia, USA, 2002. CD-ROM Paper.
- [5] B.C. Kok, M.S. Looi, H.H. Goh, “*Insulated Gate Bipolar Transistor Failure Analysis in Overvoltage Condition*”, International Conference on Renewable Energies and Power Quality (ICRE PQ'12), Santiago de Compostela (Spain), 28th to 30th March, 2012.
- [6] Authors: Alwi, Halim, Edwards, Christopher, Pin Tan, Chee, “*Fault Detection and Fault-Tolerant Control Using Sliding Modes*”, *Advances in Industrial Control*, 2011.
- [7] Afef Fekih, “*Fault Diagnosis and Fault Tolerant Control Design for Aerospace Systems: A Bibliographical Review*”, 2014 American Control Conference (ACC) June 4-6, 2014. Portland, Oregon, USA.
- [8] Leung, D., and Romagnoli, J. 2000. “*Dynamic Probabilistic Model-Based Expert System for Fault Diagnosis*”, *Computers and Chemical Engineering*, 24(11):2473-2492.
- [9] C. Angeli, “*Diagnostic Expert Systems: From Expert's Knowledge to Real-Time Systems*”, *Advanced Knowledge Based Systems: Vol. 1*, pp 50 – 73, 2010.
- [10] K. Debbe, “*Expert system for fault diagnosis of VSI AC drives*”, IEEE. pp. 369-373.
- [11] R.W. Milne, B. Chandrasekaran, « *FAULT DIAGNOSIS & EXPERT SYSTEMS* », IEEE. Pp. 603-613.
- [12] <https://www.ieee-poles.org>.
- [13] Muhammad H. Rashid, « *Power Electronics: Circuits, Devices Applications* », Pdf (4th Edition) Full eBook, 1024 pages, 2013.
- [14] Neamen, D. “*Semiconductor Physics and Devices*”, 3rd ed. New York: McGraw-Hill, 2003.
- [15] Shur M, “*Physic of semiconductor devices*”, Englewood cliffs, NJ: Prentice-Hall. Inc, 1990.
- [16] Smith R. A, “*Semiconductors*”, 2nd.ed. Combridge University press. 1979.
- [17] www.wikiwand.com/en/power.semiconductor_device.
- [18] M. Trivedi and al. “*Failure mechanisms of IGBTs under short-circuit and clamped inductive switching stress*”, *IEEE Transition on Power Electronics*, vol. 14, Issue: 1, Jan. 1999, pp: 108 – 116.
- [19] Fredrik Gustafsson, “*Fault detection terminology*”, *Adaptive Filtering and Change Detection*, 2000 John Wiley & Sons, Ltd.

- [20] Mahmoud Shahbazi , Ehsan Jamshidpour, Philippe Poure, « Open and Short-Circuit Switch Fault Diagnosis for Non-Isolated DC-DC Converters Using Field Programmable Gate Array”, IEEE by emailing pubpermissions@ieee.org.
- [21] Petr Kadaník, Prague, “*Brief survey of AC Drive Fault Diagnosis & Detection*”, The Czech Technical University Dept.of Electrical Drives & Traction, December 1998.
- [22] Adel Benmansour, Stephane Azzopardi, Jean-Christophe Martin, Eric ,Woirgard, “*A step by step methodology to analyze the IGBT failure mechanisms under short circuit and turn-o inductive conditions using 2D physically based device simulation*”, <https://hal.archives-ouvertes.fr/hal-00324010>, Submitted on 25 Sep 2008.
- [23] B.C. Kok, M.S. Looi, H.H. Goh, “*Insulated Gate Bipolar Transistor Failure Analysis in Overvoltage Condition*”, International Conference on Renewable Energies and Power Quality (ICREPQ’12), Santiago de Compostela (Spain), 28th to 30th March, 2012.
- [24] Wu, Rui; Blaabjerg, Frede; Wang, Huai; Liserre, Marco; Iannuzzo, Francesco, “*Catastrophic Failure and Fault-Tolerant Design of IGBT Power Electronic Converters -An Overview*”, In Proceedings of the 39th Annual Conference of the IEEE Industrial Electronics Society, IECON 2013 (pp. 507-513).
- [25] B. Lu and S. K. Sharma, “*A Literature Review of I BT Fault Diagnostic and Protection Methods for Power Inverters,*” IEEE Trans. on Ind. Appl., vol. 45, no. 5, pp 1770-1777, 2009.
- [26] N. S. Ismail, I. Ahmad, . usain and S. Chuah, “*Pulse Power Failure Model Of Power MOSFET Due To Electrical Overstress Using Tasca Method,*” IEEE International Conference on Semiconductor Electronics, Kuala Lumpur, Malaysia, 2006.
- [27] Christophe Delepaut, Sara Siconolfi, Olivier Mourra and Ferdinando Tonicello, “*MOSFET Gate Open Failure Analysis In Power Electronics*”, 2013 IEEE.
- [28] A. M. S. Mendes and A. J. Marques Cardoso, “*Voltage source inverter fault diagnosis in variable speed ac drives, by the average current Park’s vector approach,*” in Proc. IEMDC, 1999, pp. 704–706.
- [29] R. Peugeot, S. Courtine, and J. P. Rognon, “*Fault detection and isolation on a PWM inverter by knowledge-based model,*” IEEE Trans. Ind. Appl. vol. 34, no. 6, pp. 1318–1326, Nov./Dec. 1998.
- [30] O. S. Yu, N. J. Park, and D. S. Hyun, “*A novel fault detection scheme for voltage fed PWM inverter*”, in Proc. IEEE Ind. Electron. Conf., 2006, pp. 2654–2659.
- [31] P. Gilreath and B. N. Singh, “*A new centroid based fault detection method for 3-phase inverter-fed induction motors,*” in Proc. IEEE Power Electron. Spec. Conf., 2005, pp. 2663–2669.
- [32] K. Debebe, V. Rajagopalan, and T. S. Sankar, “*Expert systems for fault diagnosis of VSI fed ac drives,*” in Conf. Rec. IEEE IAS Annu. Meeting, 1991, pp. 368–373.
- [33] M. R. Mamat, M. Rizon, and M. S. Khanniche, “*Fault detection of 3-phase VSI using wavelet-fuzzy algorithm,*” Amer. J. Appl. Sci., vol. 3, no. 1, pp. 1642–1648, 2006.
- [34] F. Charfi, F. Sellami, and K. Al-Haddad, “*Fault diagnosis in power system using wavelet transforms and neural networks*”, in Proc. IEEE Int. Symp. Ind. Electron., 2006, pp. 1143–1148.

- [35] M. A. Awadallah and M. M. Morcos, "Diagnosis of switch open-circuit fault in PM brushless dc motor drives," in Proc. Large Eng. Syst. Conf. Power Eng., May 2003, pp. 69–73.
- [36] S. Ceballos, J. Pou, E. Robles, I. Gabiola, J. Zaragoza, J. L. Villate, and D. Boroyevich, "Three-level converter topologies with switch breakdown fault-tolerance capability," IEEE Transactions on Industrial Electronics, vol. 55, no. 3, pp. 982-995, Mar. 2008.
- [37] S. Ceballos, J. Pou, J. Zaragoza, E. Robles, J. L. Villate, and J. L. Martin, "Soft-switching topology for a fault-tolerant neutral-point clamped converter," Proceedings of IEEE International Symposium on Industrial Electronics (ISIE2007), pp. 3186-3191, Jun. 2007.
- [38] M. Shahbazi, P. Poure, S. Saadate, and M. R. Zolghadri, "Fault-tolerant five-leg converter topology with FPGA-based reconfigurable control," IEEE Transactions on Industrial Electronics, vol. 60, no. 6, pp. 2284-2294, Jun. 2013
- [39] M. Salehifar, R. S. Arashloo, M.-E. Manuel, V. Sala, and L. Romeral, "Fault tolerant operation of a five phase converter for PMSM drives," IEEE 28th Annual Applied Power Electronics Conference and Exposition (APEC2013), pp.1177-1184, Mar. 2013.
- [40] M. Shahbazi, P. Poure, S. Saadate, and M.R. Zolghadri, "FPGA-based reconfigurable control for fault-tolerant back-to-back converter without redundancy," IEEE Transactions on Industrial Electronics, vol.60, no.8, pp.3360-3371, Aug. 2013.
- [41] <https://www.quora.com/What-is-the-main-difference-between-Triac-and-thyristor-and-what-are-their-similarities>.

General Conclusion

5.1. Conclusion

In recent years, the interest in renewable energy has been increasing in an effort to overcome the environmental problems of fossil fuel and nuclear energy. Among the renewable energy sources wind power generation has especially attracted the notice of the world and many papers have been written on the subject especially inside of power quality enhancement. Therefore, this thesis was treated Hybrid algorithms for the intelligent management of a renewable production system: Power Quality Enhancement and service continuity contribution.

In the first chapter, a control strategy of wind turbine system based-on Doubly-Fed Induction Generator (DFIG) has been presented. Where, we started with a brief overview of renewable and non-renewable energies; their advantages and disadvantages, proprieties, problems and statistics. Then, we focused our studying about wind energy one's; where, we discussed about its history, construction, types and its principal work and its main expressions which mainly using in this domain. For a next step; the decoupled method was introduced for DFIG system control-based on which, the active and reactive power can be controlled independently. Where, the control strategy is divided into three blocks diagram which are: Rotor Side Converter (RSC) control, Grid Side Converter (GSC) control and Maximum Power Point Tracking (MPPT) control blocks. The simulation results showed the effectiveness of the system control, where the turbine suited efficiency the wind speed variation in order to extracts the maximum power from the wind energy.

In the second chapter, we were presented a brief review of artificial intelligence and its basic concepts and terminology including its applications, goals and various research areas. Then, we focused our studying about three research areas which we were used them in this thesis which are: Expert System, Fuzzy Logic and Algorithm Genetic.

In the third chapter, a mitigation technique of harmonics power distortion with a shunt active filter was been presented. Where, the chapter started with a brief review about Power Quality (PQ) disturbances such as: voltage variation (sag/swell), voltage interruption, voltage fluctuation, power frequency variation, current harmonic, voltage and current unbalance.

The proposed solution uses the wind turbine system's converter in goal to reduce the cost of the global control system including a new strategy named priority method technique. This priority control method permits to manage the priority among three different controls which are: the active stator power control; DC-link voltage control and suppression harmonics currents control by using the shunt active filter with Synchronous Reference Frame (SRF) harmonic extraction current method. Finally, in goal to improve the control performance; a three different controller are used to regulate the rotor currents for better filter results which are: hysteresis currents controller, conventional PI controller and PI-adaptive fuzzy logic controller regarding the harmonic currents suppression. The simulation results were showed that the proposed control scheme can effectively reduce the Total Harmonic Distortion (THD) in the grid currents where, it was decreased from 16,90% to 1,98% in the grid.

In the fourth chapter, a Fuzzy-Expert system Fault Tolerant Control strategy has been proposed for open-circuit IGBT fault switch of RSC. The FTC proposed based on the Expert system methodology using Fuzzy logic in the fault detection method. An experienced engineer creates the algorithm detection and isolation of the faulty switch to transfer his expert to the system which permits to use it easily by the non-expert person. This algorithm permits to change the faulty leg of the RSC by the additional leg (the fourth leg) and isolates the faulty leg from the system to realize the reliability and the service continuity. The simulation results were showed that the proposed FTC strategy is very efficient and permit to detect the faulty switch within time less than one period and prevents the deterioration and the shut-down of the production power quality.

5.2. Future work

In the future, it would be beneficial to feed the DFIG by matrix converter topology instead of back-to-back converter. Where, various researches have treated the comparative study between the two converters topologies for the wind turbine system based on DFIG, and they have concluded; that the topology with matrix converter one is the best in terms of THD and total power losses. In addition matrix converter has a minimal energy storage requirement, which allows to get rid of bulky and lifetime-limited energy storing capacitors. Therefore, in our future work, we will be trait the comparison study between the two topologies in terms of performance under open- and short-circuit faulty conditions as well due to the high number of switches involved in these two converters using artificial intelligent strategies and method detection. This topology has been already done and it has good results in rotor currents and stator powers controls which delivered to the grid without fault detection studied.

In the second point, we will be continued to improve the power quality and decrease or suppress the different disturbances existing or happened in the grid like: voltage variation (sag/swell), frequency variation, noise, notches...etc, by proposing a new mitigation or studying different mitigations which have been already proposed and choose best of those solutions in terms of cost reduction and simplicity using artificial intelligent technology.

The third point; we will use the Generalized Predictive Controller (GPC) therefore, I will improve my capabilities to use the artificial intelligent algorithms by learning more about Algorithms Design and Analysis (ADA) in order to use them in electrical domain control.